UNIVERSITY OF BIRMINGHAM

Cell-in-cell structures in the human liver

A Thesis by

SCOTT PHILIP DAVIES

Submitted for the degree of DOCTOR OF PHILOSOPHY

Centre for Liver Research

School of Immunity and Infection

Institute of Biomedical Research

College of Medical and Dental Sciences

University of Birmingham

Word Count: 33230

Primary Supervisor: Dr. Zania Stamataki

Secondary Supervisor: Prof. Robin May

Abstract

Hepatocytes can capture dead cells. This phenomenon is called efferocytosis. Furthermore, our lab previously observed live $CD4^+$ T cells captured by hepatocytes. This was reminiscent of entosis. This project aimed to further the understanding of the mechanisms and consequences of these processes. *In vitro* experimentation showed that efferocytosis could be modulated through cytokine treatment and using macropinocytosis inhibitors. Captured cells were also shown to associate with the uncharacterised receptor, SCARF2. Furthermore, efferocytosis was shown to cause multinucleation in hepatocytes. This was demonstrated *in vitro, in vivo* using mouse models of acute injury, and *ex vivo* with cauterised donor human tissue. Increased multinucleation was also associated with hepatocellular carcinoma and vascular invasion. Live $CD4^+$ T cell capture occurred at a lower frequency than efferocytosis and required alternative membrane rearrangements. This process also did not share defining characteristics of entosis, such as E-cadherin association or susceptibility to Rho-kinase inhibitors. Furthermore, anti-inflammatory T-regulatory cells were more likely to enter acidic compartments within their captors *in vitro*. This project has unearthed novel aspects regarding the regulation and molecular processes of hepatocyte cell-in-cell structure formation. Further understanding into the mechanisms of these processes may provide future targets for therapeutic intervention of inflammatory disease and cancer.

Acknowledgements

Professional Acknowledgements

The work described in this thesis was funded by the Medical Research Council, to whom I am incredibly thankful. Many thanks are also given to the patients of the Queen Elizabeth Hospital who gave consent, allowing their tissues to be used for many of the experiments described throughout this PhD.

Many members of the Centre for liver (and now Gastrointestinal) Research have assisted greatly in the completion of this work. Infinite thanks are given to Dr Gary Reynolds for his time, expertise and for facilitating many of the investigations conducted in this PhD. Your help has been invaluable throughout the entirety of this work and it has been greatly appreciated. I would also like to thank Dr Patricia Lalor and Dr Lozan Sheriff for their invaluable help with animal experimentation. Further thanks are given to Dr Chris Weston for enabling my long-term imaging experiments and for frequent scientific insight into the outcomes of my experiments. I would also like to thank Dr Daniel Patten for invaluable technical support and for helping me to develop ideas throughout the later parts of my PhD. Finally, I am incredibly grateful to the liver perfusion group for allowing me access to liver perfusion equipment and tissue to complete my *ex vivo* liver experiments. Particularly, thanks are given to Mr Richard Laing, Mr Ricky Bhogal, Dr Simon Afford and Miss Lorraine Wallace for their contributions to experimentation.

I have had the great privilege of working with many undergraduates and work experience students throughout the last 3 years at Birmingham. These include Biomedical Science students, Rukhsarr Ahmed and Devinderjit Sangha; visiting medical student from Cambridge

University, Colin Berry; Nuffield Foundation students Nish Rai and Sophie Rouvrey; intercalating medical student, Ratnam Gandhi; visiting PhD student from Sun Yat-sen University, Emily Li, and Biochemistry MSci student, William Porter. I enjoyed working with all of you and am very grateful for your contributions.

Many thanks are given to Dr Robert Shaw of the tech hub, as well as to both Mrs Theresa Morris and Mr Paul Stanley of the School for Metallurgy and Materials, for all their training and assistance for microscopy-related endeavours.

Of course, great thanks are given to my supervisors. I thank Professor Robin May for his invaluable input and advice throughout this PhD. Lastly, biggest thanks are given to Dr Zania Stamataki for her supervision, time, effort, advice, and continued encouragement throughout the past four years and for your continued support in years to come.

It has been a pleasure to work with all of you.

Personal Acknowledgements

I'll start by thanking you, the reader. Whether you're the very generous examiner who agreed to read this hefty piece of work, or a poor sap who has dusted this off in the future looking for the details of an antibody that may or may not exist anymore. Either way, thank you so so much for taking the time to read the fruits of my labour.

Dr. Shishir Shetty and Dr. Oliver Florey, thank you so much for agreeing to conduct my viva. Both of your works have been an inspiration throughout the course of my PhD. I look forward to a very interesting and insightful viva. For anyone else, you might want to skip to the intelligent bits – this is going to get sappy.

Big thanks to everyone in or near the lab, both past and present. To my lab brother, Ben Wiggins, thank you for all your support in lab and randomness outside of it. It has been truly appreciated. Thanks also to Kostas Aliazis for all our nerdy time! Also, Susan Liu for being amazing to work with in the lab and for being a great friend. Finally, to Dr Sudha Purswani, the original PhD student; thank you so much for all your help whilst you were here and for always being there to support me.

Dr Daniel Goncalves Cainero, I have missed you dearly throughout the time after you moved on to better things and I still miss you now. You were fantastic to work with, an inspiration to how I conduct myself and I'm so proud of how you've grown in your career.

Dr Emma Rathbone, thank you so much for putting up with all my whining and for all the coffees that we needed at the hardest of times. It always made things seem brighter. We made it. We really have got this! Emma Dutton, thank you too for always being there when I needed time to breath and for making sure I had a life outside of the lab.

I pay thanks to Dr Graham Wallace. You have been there for me throughout the entirety of my PhD, as a reviewer, an advisor and as a friend. You have supported me through very difficult times and provided help at times when I didn't think it would receive any. I will always be grateful for this.

Of course, my family have always been there for me. My parents, Philip and Dinah Davies, as well as my grandparents, John and Joyce Beech; you have all been my light throughout the busiest and darkest of times. Your support and understanding have never waved and I can't thank you enough for always being there for me, throughout everything challenge I have faced. It has been greatly appreciated and I am eternally grateful.

Lastly, but by no means least, I need to thank my future wife, Rhianne Emily May Hutchinson. I could spend most of the pages allowed here to describe every single way that you've supported me throughout this PhD and how you make my life happier than I ever thought it could be. You have made me laugh at times where I never thought I could and provided support in ways I would never have thought of. Safe to say, I would not have survived without you and I can't wait to start our married life together.

Thank you all. I hope I've made you proud.

Quotes

“There are more important things in life than a bad day at work.”

- Philip Harold Davies; my Father, my hero.

“A lot of people believe in you, and they have done for a long time.”

- Dr. Graham Wallace; our course director and my mental guardian.

“The arrogance of men is thinking nature is in our control and not the other way around.”

- Ken Watanabe as Dr. Ichiro Serizawa, Godzilla (2014). A constant reminder as to why science doesn’t always go your way.

“So basically, what you’re saying is that it’s magic?”

- Rhianne Emily May Hutchinson (Davies….almost) on several occasions where I’ve attempted to explain my research.

“Can you mention me in your thesis?”

- William “Bill” Spencer, my best friend….there you go.

Table of Contents

List of Figures

Introduction

Chapter 3 - The mechanisms of hepatocyte efferocytosis

Chapter 4 - The consequences of efferocytosis by hepatocytes

Chapter 5 - Hepatocytes engulf live $CD4^+$ T cells

Discussion

Appendix

List of Tables

List of Abbreviations

- 7-AAD - 7-Aminoactinomycin D
- ABCF1 - ATP-binding cassette subfamily F member 1
- AIH – autoimmune hepatitis
- ALT – alanine aminotransferase
- AMD – age related macular degeneration
- APAP – acetaminophen
- APC – antigen presenting cell
- ASPGR – asialoglycoprotein receptor
- APS – ammonium persulphate
- AST- aspartate aminotransferase
- ATP – adenosine triphosphate
- AV – Annexin 5
- BAI-1 – Brain-specific angiogenesis inhibitor 1
- BCL - B-cell lymphoma
- BEC – biliary epithelial cell
- BMQC – bromomethyl derivative of coumarin
- CD – Cluster of differentiation
- CICS – cell-in-cell structure
- CLEVER-1 - Common lymphatic endothelial and vascular endothelial receptor-1 (also called stabilin-1)
- CLGR – Centre for Liver and Gastrointestinal Research
- CMFDA - 5-Chloromethylfluorescein diacetate
- CMTPX – CellTracker™ Red CMTPX
- CTP – cytidine triphosphate
- DAB - 3,3’-diaminobenzidine
- DC – Dendritic cell
- DPX - distyrene, a plasticiser, and xylene
- ECL - enhanced chemiluminescence
- EDTA - Ethylenediaminetetraacetic acid
- EIPA – 5-(N-Ethyl-N-Isopropyl) amiloride
- EOMES – Eomesodermin

- FasL – Fas Ligand
- FBS – Fetal bovine serum
- FITC - Fluorescein isothiocyanate
- FOV – field of view
- FOXP3 – forkhead box P3
- FYVE - Fab 1 (yeast orthologue of PIKfyve), YOTB, Vac 1 (vesicle transport protein), and EEA
- GAP – GTPase activating protein
- GAPDH - glyceraldehyde 3-phosphate dehydrogenase
- GTP – guanosine triphosphate
- HBOC - haemoglobin-based oxygen carrier (HBOC)
- HBV – hepatitis B virus
- HCV – hepatitis C virus
- HDM – house dust mite
- HFE - haemochromatosis
- HRP – horseradish peroxidase
- HSEC – human sinusoidal endothelial cell
- Hsp72 – Heat-shock protein 72
- ICAM1/2 – intercellular adhesion molecule 1/2
- IDA - industrial denatured alcohol
- IDA – industrial denatured alcohol
- IEC – intestinal epithelial cell
- IF - immunofluorescence
- IFN – interferon
- IGF-1 – insulin-like growth factor 1
- IGFBP1 - Insulin-like growth factor binding protein
- IHC – immunohistochemistry
- IL – interleukin
- IRF3 - interferon regulatory factor 3
- IRI – ischaemia reperfusion injury
- KIM-1 – kidney injury molecule-1
- LAP – LC3-II-associated phagocytosis
- LC3 – light chain 3
- LDL – low density lipoprotein
- LGR5 - Leucine-rich repeat-containing G-protein coupled receptor 5
- LOX1/OLR1- oxidated low-density lipoprotein receptor 1

- LSEC – liver sinusoidal endothelial cells
- LXR – liver X receptor
- MAS – macrophage activation syndrome
- MCM – minichromosome maintenance
- MFGE8 - milk fat globule EGF factor 8
- MFI – mean fluorescence intensity
- MHC - major histocompatibility complex
- MIP2 - macrophage inflammatory protein 2
- NAFLD – Non-alcoholic fatty liver disease
- NASH – Non-alcoholic Steatohepatitis
- NHE1 – Na^+ - H^+ Exchanger 1
- PAMPs – pathogen associated molecular patterns
- PBMC – peripheral blood mononuclear cell
- PBMC – peripheral blood mononuclear cells
- PBS - phosphate buffered saline
- PDC-E2 - pyruvate dehydrogenase complex
- PD-L1 – programmed death ligand 1
- PHH – primary human hepatocyte
- PI3K - Phosphoinositide 3-kinase
- PS – Phosphatidylserine
- PVDF - polyvinylidene difluoride
- Rac-1 – Ras-related C3 botulinum toxin substrate 1
- RAGE - Receptor for advanced glycation end products
- RIG-1 - retinoic acid inducible gene-1
- RNF43 - Ring Finger Protein 43
- ROCK – Rho-associated protein Kinase
- RORγt - retinoic acid receptor-related orphan receptors gamma-t
- RPC – retinal pigment cell
- RT – room temperature

- S1P - sphingosine-1-phostphate
- SCARF1/2 – Scavenger Receptor Class F Member 1/2
- SDS - sodium dodecyl sulfate
- SDS-PAGE - sodium dodecyl sulfate – polyacrylamide gel electrophoresis
- SEM – standard error of the mean/scanning electon microscopy
- SIRPα - signal-regulator protein-alpha
- STING - stimulator of interferon genes (STING)
- TAM – Tyr Axl and Mer
- TBS – tris buffered saline
- TBST – tris buffered saline with Tween
- Teff – T effector cells
- TEMED - Tetramethylethylenediamine
- TGF-β – tumour growth factor beta
- TIM – T cell/transmembrane, immunoglobulin, and mucin)
- TNC – thymic nurse cell
- TNFα – tumour necrosis factor alpha
- Treg – T regulatory cells
- TULP1 – Tubby-like protein 1
- UTP – uradine triphosphate

Chapter 1: Introduction

1.1 The functions and immunology of the liver

Note that many of the themes mentioned in this introduction have been described in a review published in 'Frontiers in Immunology' (1) .

1.1.1 The structure and functions of the liver

The liver is the largest internal organ and a multitasking powerhouse, performing over 500 bodily processes. It sets itself aside from other organs through its unique blood supply (2). The portal vein supplies 75% of the livers blood content, delivering partially-deoxygenated blood received from the spleen and gastrointestinal tract. The hepatic artery provides oxygenated blood from the heart and the remaining blood supply. The liver is then tasked with absorption, metabolism and storage of the remaining nutrients found within the blood, as well as the detoxication of harmful, possibly xenobiotic products. This includes the conversion of ammonia, a by-product of protein metabolism, to urea for its later removal by the kidneys. The detoxification of alcohol is conducted through its conversion to acetate by alcohol dehydrogenase and aldehyde dehydrogenase (3). The liver is also the producer and transporter of bile. This is an alkali substance which is essential for the emulsification, and the subsequent absorption and digestion of fats. Bile is also responsible for the excretion of bilirubin, a by-product of erythrocyte breakdown in the liver.

The liver is organised into hexagon lobules, the vertices of which are composed of portal triads – branches of the bile ducts, the hepatic artery, and the portal vein (**Fig. 1Ai**). Blood perfuses centrally across these lobules through capillary-like structures called sinusoids. Blood then collects into the central vein and eventually leaves the liver, en-route to the heart. Several immune cells travel through the sinusoids, some of which constitutively inhabit the sinusoidal spaces (**Fig. 1Aii**). Immune cells wishing to enter the parenchyma of the liver can extravasate from the sinusoids in a similar manner to how they would leave the blood stream across vessel walls. The molecular mechanisms behind this recruitment have been well described by members of the Centre for Liver and Gastrointestinal Research in Birmingham (4-7). Immune cells tether to sinusoidal endothelial cells through an array of adhesion molecules which include selectins, integrins and immunoglobulin members such as Intercellular Adhesion Molecule 1 (ICAM-1) (7). Following firm adhesion to the sinusoidal endothelia, immune cells can travel paracellularly or transcellularly across the endothelial layer using mechanisms which have been reported to involve Common lymphatic endothelial and vascular endothelial receptor-1 (CLEVER-1)/stabilin-1 (8). Immune cells can then act as needed within the liver parenchyma.

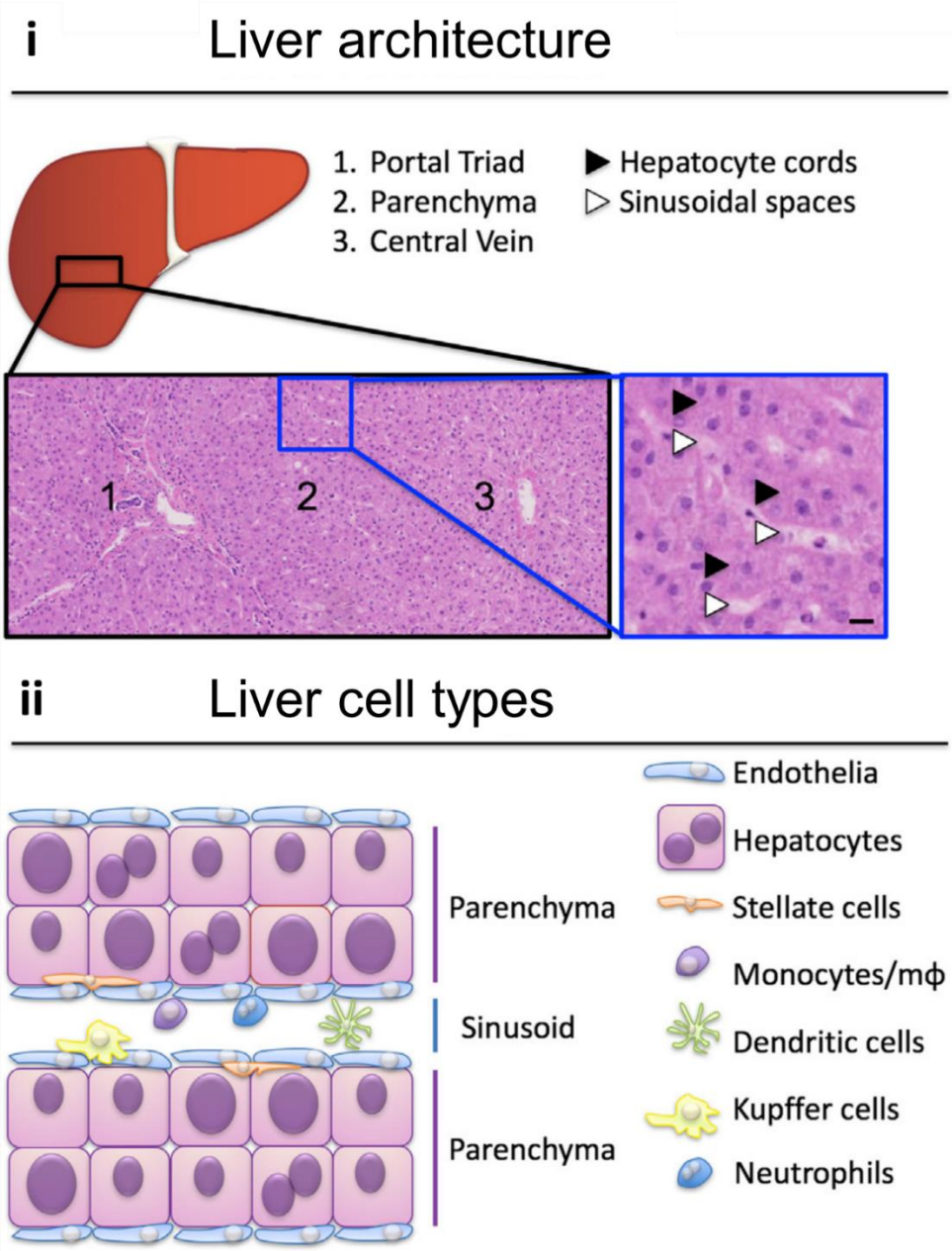

Figure 1A: Cellular architecture of the liver. **(i)** Diagram featuring haematoxylin and eosin stained tissue showing the zonation of the liver. Hepatocytes in zone 1 are situated close to the portal triad (periportal), which are formed of branches of the portal vein, hepatic artery, and bile duct. These hepatocytes have first access to incoming blood and thus have a high oxygen and nutrient supply. Zone 3 hepatocytes proximal to the central vein (pericentral) receive less nutrients and are thus less metabolically active than those in zones 1 or 2. Scale bar = 50 µm. **(ii)** Cellular organisation of sinusoids. Hepatocytes are organised into two-cell thick cords in between sinusoidal spaces, which are lined with liver sinusoidal endothelial cells (LSEC). The sinusoids are patrolled by a resident macrophage population called Kupffer cells, as well as circulating dendritic cells (DCs) and neutrophils. Stellate cells inhabit spaces between hepatocytes and LSECs, and are frequent contributors to liver fibrosis. Adapted from (1).

1.1.2 Liver immunotolerance

Most of the livers bloody supply is delivered by the hepatic portal vein, which is received from the gastrointestinal tract. As a result, the liver is perpetually exposed to antigens from commensal bacteria and food. Should the immune system recognise these bacterial and 'self' antigens, this could potentially result in prolonged immune activation and inflammation. To prevent this, the liver possesses a unique, immunotolerant environment which has been established through its cellular composition and structural arrangement (9, 10). These cells include myeloid cells, such as dendritic cells (DCs) and resident macrophages called Kupffer cells. Several studies suggest that DCs in the liver are skewed to invoke anti-inflammatory responses (10, 11). Plasmacytoid DCs (pDCs), which mature in the bone and are normally associated with high type-1 interferon (IFN) secretion, were shown to upregulate their surface expression of programmed death ligand 1 (PD-L1) in the liver via autocrine stimulation with interleukin 27 (IL-27) (12). This in turn prolongs the survival of regulatory $CD4^+$ T cells (Tregs) which promote anti-inflammatory signals. Furthermore, myeloid DCs (mDCs) which originate from bone marrow progenitor cells or monocytes, were also shown to upregulate their expression of PD-L1 in the liver and increase classic Treg survival (13). Finally, Kupffer cells are prominent agents of immunosuppression in the liver. Kupffer cells can also express PD-L1 and this is augmented in response to stimulation with the anti-inflammatory cytokine, IL-10, allowing these cells to perpetuate initial anti-inflammatory signals (14). In addition, Kupffer cells are themselves producers of anti-inflammatory cytokines – both IL-10 and tumour growth factor-beta (TGF-β) – which they secret upon capturing apoptotic cells (15). Finally, both Kupffer cells and DCs have been reported to secrete an enzyme called indoleamine 2,3-dioxygenase (IDO), which catalyses

the metabolism of tryptophan to kynurenine (16-18). This in turn binds to aryl hydrocarbon receptor on naïve T cells, promoting the development of Tregs (19).

A second method by which immune responsiveness in the liver is decreased is through lowered recruitment of immune cells associated with the adaptive immune response. This is achieved by instead promoting local activation of these cells in the liver parenchyma. Many hepatic cell types are capable of presenting antigens in complex with major histocompatibility complex molecules (MHCs) to cells of the adaptive immune response, namely T lymphocytes (20). However, many of these cells lack appropriate co-stimulatory molecules to infer long-term activation and survival of these cells. Furthermore, the potential for local activation of $CD4^+$ and $CD8^+$ lymphocytes reduces the requirement of such cells to drain into lymph nodes for activation and cross presentation. Therefore, T cells become activated rapidly in the liver, but are then quickly turned over, minimising the duration of the immune response (10, 20, 21). This turnover is augmented by the high level of Fas-ligand (FasL) expressed by hepatic immune cells, including DCs and Kupffer cells (22). This allows the liver to mount a direct and efficient immune response but with a minimal duration, swiftly returning to a steady immunotolerant state.

1.1.3 The "graveyard theory"

It is well known that the liver is a major site for the removal of defective erythrocytes (4, 23). In relation to its status as an 'immunotolerant' organ, several studies have described how many immune cells, including lymphocytes, become apoptotic more readily upon entering the liver, and are subsequently removed (24-28). These studies identified how intrahepatic T lymphocytes were susceptible to programmed cell death, partially through increased expression of Fas (26, 29). The authors suggested that these T cells were already destined for

death and succumbed in the liver. These observations gave rise to the “graveyard theory”, coined by Crispe and colleagues, which proposes that lymphocytes are prone to cell death upon entering the liver. This, in part, contributes to immune tolerance as it prevents the propagation of an unnecessary response from the adaptive immune system. Contrarily, the increased tendency of immune cells to die in the liver would create a burden for the clearance of apoptotic corpses which, if left uncleared, could further promote the risk of an immune response (discussed further in section 1.3). Still, the liver houses several cell types which can remove these dead cells (1). A largely unknown member of this group is the major cell type of the liver, the hepatocyte.

1.2 Hepatocytes

1.2.1 Physiological functions of hepatocytes

Approximately 80% of the liver is comprised of a parenchymal cell type called the hepatocyte (3). These cells form 2-cell thick cords in between the sinusoids (**Fig. 1Aii**) and they perform many of the functions of the liver. These include the storage and metabolism of nutrients (sugars, fats, proteins, etc.), bile secretion and detoxification of xenobiotics (3, 30). Hepatocytes are also responsible for converting heme, a residual compound generated from the haemoglobin of exhausted erythrocytes, to the waste product, bilirubin. They are also the main source of blood proteins including albumin, transferrin, lipoproteins, and various coagulation factors like prothrombin and fibrinogen (30). Hepatocytes also possess a wide variety of other characteristics, unseen for other parenchymal cells, which bestow the liver with its unique properties.

1.2.2 Hepatocytes zonation and liver regeneration

The liver is fascinating in being the only internal organ capable of regeneration. This ability is evolutionarily conserved and has been made evident using rodent models of partial hepatectomy, where up to 66% of the liver can be surgically removed whilst still allowing for complete restoration (31-33). Under normal physiological conditions, this quality is endowed from the hepatocytes, which have been shown to begin DNA synthesis and cell division in response to hepatectomy (34). This response is not homogeneous throughout the liver. Hepatocytes can be separated into 3 zones in relation to their proximity to central veins or portal triads (**Fig. 1Ai**). These populations differ greatly in their metabolic activity and molecular signalling rates. This is thought to be, in part, established through Wnt/β-catenin signalling (35, 36). Hepatocytes close to portal regions (periportal) are exposed to more nutrient-rich blood. As such, periportal hepatocytes are generally more metabolically active than those that are pericentral or in an intermediate zone. They are also more likely to express genes associated with the onset of regeneration, including those encoding growth factors and their regulatory proteins, such as insulin-like growth factor binding protein 1 (IGFBP1) (37). The regenerative response of hepatocytes is spatiotemporally organised in accordance with this liver lobule zonation; periportal hepatocytes are the first to proliferate, with waves of division travelling pericentrally (38). Hepatocytes closer to central vein branches divide later, relying on different targets of Wnt/β-catenin signalling to those of periportal hepatocytes, instead relying on the activity of Leucine-rich repeat-containing G-protein coupled receptor 5 (LGR5) and Ring Finger Protein 43 (RNF43) (39, 40).

Hepatocyte damage is often incurred in response to inflammation and immune infiltration. It is, therefore, intuitive that hepatocytes can be induced to divide in response to cytokine signalling. Historically, it has been known that tumour necrosis factor alpha (TNFα) could

augment the effects of growth factors for hepatocyte proliferation (41, 42). Several publications have reported the requirement of signals from Kupffer cells for the induction of hepatocyte regeneration via NFκB signalling (43, 44). More recently it was reported that STAT3 signalling in macrophages, downstream of anti-inflammatory IL-10 signalling, was concomitant with liver repair (45). These studies and others show how hepatocytes are able respond to a large variety of stimuli to proliferate, whilst allowing the liver to continue to function (46, 47). It is of note and admiration that the liver continues to provide its many homeostatic functions whilst simultaneously regenerating as necessary.

1.2.3 Hepatocytes as immune cells

As well as conducting a lot of the major functions of the liver, hepatocytes have many reported functions which directly contribute to immunity and the general immunotolerance of the liver (48, 49). In the acute phase of an immunological response, where initial inflammatory stimuli are detected by innate immune cells, hepatocytes are capable of responding to the inflammatory cytokines secreted by these cells, including TNFα, interferons alpha and gamma (IFNα/γ), as well as IL-6 and IL-1β (49-52). Stimulation with these cytokines results in subsequent secretion of additional cytokines by hepatocytes, as well other proteins which contribute to immunity, such as serum amyloid A protein, which augments bile secretion and recruitment of immune cells to the liver (48, 53, 54). Once enlisted into the immune response, hepatocytes downregulate their more-housekeeping functions such as albumin secretion (51). Hepatocytes can also recognise the same signals as innate immune cells, namely pathogen-associated molecular patterns (PAMPs) through Toll-like receptors (TLRs). Hepatocytes have been shown to respond to bacterial proteins via TLR2 (55), which can in-turn induce inflammasome secretions. Hepatocytes are also known

to bind to heat-shock protein 72 (Hsp72) via TLRs 2 and 4, which upregulates secretions of macrophage inflammatory protein 2 (MIP-2) (56).

Hepatocytes have developed intrinsic responses to viruses which commonly infect them, including hepatitis B and C viruses (HBV/HCV). Intracellular signalling receptors, retinoic acid inducible gene-1 (RIG-1) and TLR3, can bind viral RNA and dsDNA, respectively (57). Upon engagement, these receptors trigger signalling events which ultimately activate interferon regulatory factor 3 (IRF3), a transcription factor which induces type 1 interferon expression in response. Hepatocytes also express stimulator of interferon genes (STING), a signalling molecule through which many DNA-sensing proteins converge on and is thought to mediate RIG-1 signalling (58, 59). STING has recently been hypothesised to reduce HBV replication in hepatocytes (59). However, both HCV and HBV are known to have evolved various mechanism to dampen STING and IFN-related responses, which systemically reduce innate immune activity by hepatocytes (60-63).

As well as directly responding to inflammatory stimuli, some evidence exists showing that hepatocytes can perpetuate immune responses by acting as APCs. Under inflammatory conditions, hepatocytes can express major histocompatibility complex, class 2 (MHC-II), granting them the ability to activate naïve $CD4^+$ T cells (64). Hepatocytes have also been reported to express MHC class I (65). Additionally, investigations by Bertalino and colleagues suggest that hepatocytes are, thus, capable of priming $CD8^+$ T cells (66, 67). Hepatocytes were shown to activate and induce proliferation of naïve $CD8^+$ T cells. Of note, in both investigations, T cells survived for a shorter time, compared to when activated by more-dedicated APCs such as dendritic cells. This is likely due to the lack of co-stimulatory molecules, such as CD80 and CD86. Furthermore, hepatocytes have been shown to upregulate PD-L1, which can then induce programmed-cell death in pro-inflammatory T cells

(68). Overall, hepatocytes are equally dedicated to liver immunotolerance as they are perpetuating immune responses.

1.2.4 Difficulties with hepatocyte culture and alternatives

Hepatocytes present multiple problems when it comes to their study; although they possess an intrinsic ability to divide and regenerate the liver, this is not retained following their isolation from the liver for *in vitro* cell culture. Furthermore, cryopreservation of primary human hepatocytes (PHHs) is difficult to achieve. Several conditions have been published for the maintenance and temporary passage of PHH (69), although this is not efficacious for long term investigations. This drastic behavioural transformation also disparages the results obtained from *in vitro* PHH for representing their true behaviour *in vivo.* This is evidenced in how PHH respond to only a limited number of growth factors, despite expressing receptors for many more (31, 70). Due to this, alternative procedures and models are frequently exploited prior to, or instead of, experimentation with PHH. A multitude of transformed hepatocyte or hepatoma cell lines are available for *in vitro* experimentation (30). These cells retain a varying degree of physiological and genetic features of PHHs, although often have irregularities in cellular signalling and normal hepatocyte functionality (71). Examples of these include Huh-7, HepG2 and Hep3B hepatocyte cancer cells. Each of these cell lines retain a distinct level of differentiation and p53 expression from their normal counterparts (72). HepG2 cells maintain normal p53 status and polarity, forming organoid-like structures *in vitro* (73). Hep3B cells are p53-null and are highly undifferentiated cells, sustaining little activity of PHHs. Huh-7 cells possess a point mutation in the *TP53* gene (A220G) and are frequently used for studies involving viral infection due to their expression of viral entry receptors (74). These cell lines have also been further modified to suit specific investigations, such as alterations in viral permissiveness and propagation (75, 76). Cell lines, however, do

not represent the actions of PHH within the liver. Not only is this due to their tumour status, but also because of many varying conditions found in the liver which are absent from 2D cultures, such as tissue stiffness and signalling factors. Often, to obtain somewhat more physiologically relevant results, many investigations will utilise mouse models to study how hepatocytes function in the complete liver, in the presence of other hepatic cells. Overall, there are multiple methods to study the activity of hepatocytes, despite the challenges of culturing PHH and obtaining representative data.

1.3 Efferocytosis

1.3.1 The purpose of Efferocytosis

Throughout their natural lifecycle, cells eventually become exhausted and undergo regulated cell death. These cells must be removed to alleviate space and resources for their replacements. The removal of dead or dying cells is also a necessary process for the resolution of inflammation and for tissue repair (77). Without the clearance of dead cells, corpses gradually decay, and their internal components leak into the surrounding tissues. This can have many detrimental consequences. Unregulated activity of digestive enzymes, particularly those found in lysosomes like cathepsins, can result in unwanted external enzymatic activity and tissue digestion. This activity, coupled with the degeneration of cellular components, also generates a large pool of 'self-antigens'. Of note, these include the membranal components of internal organelles, whose membranes have been reported to replace portions of the cell membrane during cell death (78). Many of these self-antigens can be recognised by one's own immune cells, which can promote further immune cell recruitment, inflammation, and can increase the risk of autoimmune disease. Several cell types have therefore evolved to remove dead and dying cells which prevents this premature activation of the immune response (77). This process of clearing the dead by specialised phagocytic cells is known as efferocytosis.

1.3.2 Mechanisms of apoptotic and necrotic cell clearance

1.3.2.1 Detection of dying cells

Several mechanisms have evolved in efferocytes for the detection and engulfment of dying cells (79, 80). These are generally associated with the actions of 'find-me' signals and 'eat-me' signals (81, 82). 'Find-me' signals are generally soluble factors which direct efferocytes to the location of dying cells (82). The best example of these include free nucleotides released from dying cells as a result of nuclear breakdown (83). Binding of these to nuclear receptors, $P2X_1$ and $P2Y_2$, was shown to promote the recruitment of monocytes and macrophages. Chemotactic factors including sphingosine-1-phosphate (S1P) and CX_3CL1 (fractalkine) have also been shown to recruit phagocytes to the areas of dying cells (84, 85). Upon encountering a dead or dying cell, 'eat-me' signals assist efferocytes to identify them through direct contact. Probably the most ubiquitous of these is the phospholipid, phosphatidylserine (PS) (86). Normally only present on the inner leaf of the cell membrane, PS is flipped to the outer leaf by scramblases when a cell undergoes programmed cell-death. PS can then be recognised directly through a multitude of transmembrane receptors, triggering the internalisation of the dying cell (87). Other 'eat-me' signals include various opsonising molecules which can bind PS. These include oxidised low-density lipoproteins (oxLDLs) which can be recognised by scavenger receptors and have themselves been reported to induce apoptosis (88, 89). Intercellular adhesion molecule 3 (ICAM-3) can also act as a separate 'eat-me' signal; it is recognised by macrophages through its interactions with CD14. (90). Finally, loose nucleotides have also been shown to have dual-modality and can act as both 'find-me' and 'eat-me' signals (91).

Conversely, other molecules are tasked with preventing the engulfment of cells. These proteins, appropriately-named 'don't-eat-me' signals, include the transmembrane protein

CD47 (92). This molecule binds to the receptor, signal-regulator protein-alpha (SIRPα) on the surface of macrophages, which initiates signalling pathways that prevent the cytoskeletal contractility required for efferocytosis (93).

Efferocytes are required to make direct contact with their 'prey'. This allows for the activation of internal machinery, largely through the GTPase, Rac1, which drives the cytoskeletal rearrangements necessary for dead cell engulfment (87). How an efferocyte makes direct contact with a dying cell is normally determined by the process through which cell has died (**Fig. 1B**). Throughout steady states, cells may undergo a form of programmed cell death known as apoptosis. This is an active process, through which the dying cell induces its own death. This can occur in response to external signals received from other cells or through intracellular sensing pathways, known as the extrinsic and intrinsic apoptotic pathways respectively (94). Both pathways culminate in the activation of caspase enzymes, which proceed to digest the internal components of the cell. Although the nucleus, cytoplasm and organelles are broken down, resulting in constriction of the apoptotic cell, the cell membrane remains intact. As such, this form of cell death is generally considered to be immunologically silent, as cells are cleared without invoking an immune response. This is facilitated through the presentation of PS on the external leaf of the cell membrane at early stages in the cells death. This is recognised by efferocytes through many possible receptors (Table 1, ref 1) which allows for their swift engulfment.

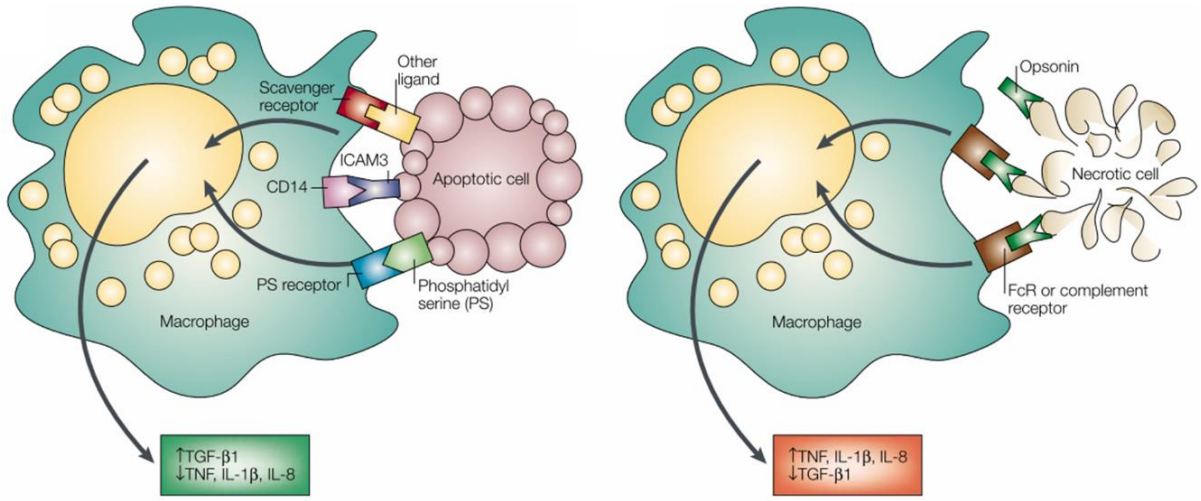

Figure 1B: Differences in recognition and consequences between apoptotic and necrotic cell capture by macrophages. Apoptotic cells are mostly recognised through phosphatidylserine (PS) receptors or by scavenger receptors. They can also be internalised through interactions between macrophage CD14 and ICAM3 on the dying cell. Capture of apoptotic cells endows a more anti-inflammatory phenotype, involving increased expression of TGF-β, and decreases in TNF, IL-1β and IL-8. The opposite phenotype is induced following necrotic cell capture, which is conducted using receptors that ordinarily are used to initiate an inflammatory response, such as those which recognise Fc regions of antibodies and members of the complement pathway. TGF-β – tumour growth factor-β; TNF – Tumour necrosis factor; IL – interleukin. Taken, with permission, from (95).

Another frequent form of cell death is a passive process called necrosis. In contrast with apoptosis, necrosis is unprogrammed and there is no uniform molecular process for its induction. It is generally defined by the loss of integrity of the cell membrane, which can be caused by numerous methods including physical rupturing, pH alterations or biochemical toxicity (96). Necrosis can also be induced by the depletion of ATP within a cell. This often occurs in apoptotic cells that are unable to continue with the programmed pathway of cell death, instead undergoing 'secondary necrosis'. Unlike with apoptotic cell recognition, no dedicated receptors exist for the detection of necrotic cells. Although some reports have suggested that necrotic cells can also be identified through PS-recognition (97-99), it is generally accepted that their recognition by efferocytes is improvisational; many receptors used are normally tasked with immune response activation and bacterial sensing (80, 95). These include receptors for components of the complement system and for Fc regions of

antibodies, respectively. This is due to the level of degradation associated with necrotic cells, whereas apoptotic cells constrict but remain intact. As such, apoptotic and necrotic cell capture can be distinguished by the receptors that are used for their recognition.

1.3.2.2 Molecular mechanisms of efferocytosis and cargo processing

Several components of internal molecular machinery have been identified which are required for the intracellular processing of corpses engulfed by phagocytes. Homologs of these genes were initially identified in *Caenorhabditis elegans* (100, 101). It was shown how mutations in genes encoded CED-1/2/5/6/7/8/10 and NUC-1 prevented efficient clearance of dying cells within these nematode worms. The roles of human homologs for some of these genes, in the context of phagocytosis, were later elucidated (102, 103). CED-2, CED-5 and CED-10 was shown to resemble the adaptor protein, CrkII, the guanine exchange factor (GEF), DOCK180 and the Rho GTPase, Rac1, respectively. A later investigation by Ravichandran and colleagues also confirmed the activity CED-12 and its mammalian homolog, Engulfment and cell motility 1 (ELMO-1), in macrophage phagocytosis (104). These investigations lead to further understanding of the downstream events that incurred once a phagocyte recognises a dying cell. Downstream of PS-receptors, such as brain-specific angiogenesis inhibitor 1 (BAI1) (105), adaptor proteins, CrkII and ELMO1 are recruited to the site of dead cell-recognition. These protein further recruit Dock180. The GEF activity of this protein activates Rac1, which drives the actin cytoskeleton arrangements required for dead cell engulfment.

Other early investigations implicated Phosphoinositide 3-kinase (PI3K) in the completion of efferocytosis (106). Although normally concerned with growth factor signalling, early reports showed that macrophages treated with the broad, potent PI3K inhibitor, wortmannin, showed inhibition of FcR-mediated phagocytosis, due to failure to close the phagosome

(107). Vieira and colleagues later confirmed that specifically type I PI3Ks, responsible for the creation of phosphatidylinositol 3, 4, 5-phosphate [PI(3,4,5)P] were necessary for the actin remodelling required for phagosome formation (108). More recently, it was shown that PI(3,4,5)P formation was required to recruit Rho GTPase activating proteins (GAPs) capable of inhibiting GEFs involved in actin assembly, including cdc42 and Rac1 (109). This permitted actin disassembly required for phagosome completion. Conversely, PI(3)P-forming type III PI3Ks such as autophagy-related kinase, VPS34, were shown to be involved in phagosome maturation and lysosomal fusion. The activity of these kinases were thought to involve the recruitment of endosomal trafficking proteins, including Rab GTPases (110). Relating to this function, many reports now imply the role of non-canonical autophagy within the ultimate processing steps for internalised dying cells. It has been observed that LC3, one of the major directing components of the autophagy pathway, would become lipidated to single-membrane intracellular structures containing engulfed apoptotic corpses (111, 112). This so-called LC3-associated phagocytosis (LAP), requires the activity of VPS34 and is thought to assist the fusion of these structures with lysosomes, allowing for the breakdown of its contents (113).

1.3.3 Non-professional phagocytes

Cells which have been reported to clear dead cells are commonly divided into 2 distinct categories; professional and non-professional phagocytes (114). Much of the studies regarding efferocytosis focus on circulatory cells which are recruited to sites of dying cells, whose primary function is efferocytosis. These include macrophages and monocytes, as well as DCs and neutrophils. However, a large number of non-circulatory, tissue-forming cells are capable of engulfing dying cells (97, 114). These cells are critical for relinquishing the burden of dead cell clearance when professional phagocytes are unavailable (97, 115). Best

characterised of these are the epithelial cells which line the airway (116, 117). As the first responders to airborne toxins and pathogens, these cells have a high rate of turnover. This is augmented by the subsequent recruitment of immune cells, including lymphocytes, and allergy-related cells such as basophils, eosinophils, and mast cells. Dying epithelial and immune cells must be speedily removed to prevent persisting inflammation which could disrupt the airway. Efferocytic alveolar and bronchial epithelial cells can clear these cells, reducing the time required for professional phagocyte recruitment. However, their ability to clear dead cells is still ultimately regulated by airway macrophages activities (118).

Another class of non-professional phagocytes are retinal pigment cells (RPCs). During the development of the retina, these cells engulf neighbouring cells of the same lineage that undergo autophagy-related death (119-121). Of note, both airway and retinal cells have been shown to recognise dying cells using receptors that are also expressed by professional phagocytes, including CD36, αvβ5 integrins and TAM receptors such as MerTK (119, 122-124). Similar preservation of macrophage efferocytic machinery was also observed in colonic epithelial cells; they possess the PS-receptor, BAI1, but also the same downstream intracellular machinery used by macrophages to induce the Rac1-driven cytoskeletal rearrangements required for efferocytosis (125).

As with the activity of retinal pigment cells, other non-professional phagocytes have evolved the ability to clear dead cells for developmental reasons. Mesenchymal cells have been shown to clear apoptotic cells generated in foot limb development in macrophage-depleted mice (115). Similarly, neuronal progenitor cells engulf their apoptotic neighbours, which aids the process of developing neural networks (126). This exemplifies the evolutionary conservation of this activity due to its necessity in early stages of development. This is the likely origin of many non-professional phagocytes. This behaviour was subsequently

preserved for the prevention of premature inflammatory responses and to supplement the activity of professional phagocytes.

1.3.4 Efferocytosis in health and disease

Although the clearance of dying cells is often integral to the resolution of disease, efferocytosis is in some cases related to actual disease pathogenesis. As explained earlier, this discrepancy is inferred from whether apoptotic cells or necrotic cells are captured. The clearance of apoptotic cells is generally associated with the resolution of inflammation and disease; efficient and early clearance of dying cells reduces the risk of inducing inflammation and generally infers anti-inflammatory phenotypes to efferocytes (127). The prevention of apoptotic cell clearance is often implicated with inflammatory disease, especially for autoimmune disorders (128). The loss of scavenger receptors associated with efferocytosis, including axl and scavenger receptor family F member 1 (SCARF1), have been linked to autoimmune diseases, such as autoimmune encephalitis and lupus (129, 130). Similarly, mice which lacked the scavenger receptor, Mer, and its ligand, Gas6, showed exasperated inflammation which was associated with an increase of tumorigenesis (131). More recently, mice whose macrophages lacked the PS-receptor, CD300f, were also shown to express a lupus-like phenotype (132). Of interest, an upregulation of CD300f on DCs, instead of macrophages, resulted in a similar outcome (133). This was also the result of reduced efferocytosis in these mice, showing certain PS-receptors can have alternative functions in different cells.

The importance of efferocytosis in the airway, by both professional and non-professional efferocytes, has been made evident in numerous investigations into lung and bronchial-related diseases. Reduced activity of airway macrophages has been linked to the

pathogenesis of pulmonary obstruction disease, cystic fibrosis and bronchiectasis (134, 135). Furthermore, the promotion of efferocytosis by anti-inflammatory cytokine stimulation was shown to reduce inflammation associated with asthma (117).

A common cause of pathogenesis associated with reduced efferocytosis is the activity of the 'don't-eat-me' signal, CD47. The ability of this molecule to promote the longevity of cells has been exploited by many varieties of tumour (92, 136, 137). Its expression has also been attributed to the aberrant clearance of apoptotic cells that normally comprise the vasculature, which can increase in the risk of atherosclerosis (138). In each of these studies, blockade of CD47 showed therapeutic potential by restoring efferocytosis.

Although efferocytosis is generally a pro-resolution process, it can also cause the opposite effect under certain circumstances. This is mostly associated with the clearance of necrotic cells. As these cells are detected using receptors normally associated with initiating the immune response, the downstream consequences are normally pro-inflammatory (79, 139). As such, engagement of these receptors by necrotic cell fragments can cause efferocytes to enhance localised inflammation. This effect can be synergistically enhanced by increased immune cell influx which are recruited by dying cells. In support of such possibilities, the removal of scavenger receptor, TIM4, was shown to reduce immune cell infiltration to the liver in a model of ischaemia reperfusion injury (IRI) (140). As this mouse model commonly presents with localised areas of necrosis, it is likely the efferocytosis of these cells which contributes to inflammation. The inflammatory consequences of such incidents may, however, be lessened if necrotic cells can be recognised through PS recognition as some investigations would suggest (98, 99). Non-professional phagocytes have been shown not to develop such a pro-inflammatory phenotype in response to engulfing necrotic cells, potentially for this reason (97). Taken together, although efferocytosis is generally necessary

for preventing disease pathogenesis, it must still be regulated to reduce the risk of indirect inflammatory fallout.

1.3.5 Hepatic Efferocytosis

The burden of dying cell removal is particularly palpable in the liver. Frequent cell turnover is required in the liver, both of apoptotic immune cells and of dying cells resulting from frequent exposure to xenobiotic substances. In relation to its requirement for maintaining an immunotolerant environment, the liver possesses many cell types which are capable of efferocytosis (1). Many of these are commonly described circulatory cells, including DCs, monocytes, and neutrophils. Most investigations concerning this, however, focus on the resident macrophage population of the liver, the Kupffer cell (141). Although these cells frequently patrol the sinusoidal endothelium, they are also capable of clearing corpses which form within the parenchyma. As with most phagocytes, Kupffer cells can respond to 'find-me' signals and clear dying cells from the parenchyma.

As a further distinctive feature which separates it from other internal organs, most tissue-forming cells in the liver are non-professional phagocytes (1). Stellate cells, which ordinarily contribute to liver fibrosis, have been reported to engulf apoptotic hepatocytes (142). Cells which line the bile ducts, biliary epithelial cells (BECs) are also capable of internalising blebs exuded from apoptotic cells (143). Liver sinusoidal endothelial cells (LSECs) are also capable of apoptotic cell clearance, through the expression of scavenger receptors, SCARF1 and stabilin-1/2 (144, 145). Of importance, the major cell type which comprises the liver, the hepatocyte, is also capable of efferocytosis. This was originally described in 1944 by Dini and colleagues, where erythrocytes were observed within cytoplasmic spaces of rat hepatocytes (23). However, further elaborations on this observation were not made until almost 50 years

later (146). Hepatocytes are known to express a carbohydrate scavenger receptor called asialoglycoprotein receptor (ASGPR). This has been shown to facilitate the capture of apoptotic lymphocytes by other efferocytes by sequestering them in the parenchyma (147). This potentially crucial aspect of liver biology has been largely confined to history. With hepatocytes providing 80% of the livers mass and with the importance of efferocytosis in other organs in preventing premature inflammation, it is imperative that this process should be further elucidated and understood.

The occurrence of efferocytosis for the prevention of unwarranted inflammatory responses is likely a contributor to liver immunotolerance. In support of this, the activity of MerTK-expressing professional phagocytes was recently shown to promote resolution in mouse models of acute liver injury (148). Mice which lacked MerTK displayed more persistent fibrosis and a reduced number of Kupffer cells. Similarly, the PS-opsonising protein, milk fat globule-EGF factor 8 (MFG-E8), was shown to be downregulated in liver macrophages that were exposed to alcohol (149). In relation to this, expression levels of ASGPR1 were also decreased in response to ethanol (150). This is likely to reduce the efficiency of apoptotic cell clearance in the liver parenchyma. Overall, it appears that alcohol damage in the liver is partially induced by preventing the removal of dying cells.

The overall contribution of efferocytosis reduction to different forms of liver disease is likely to be under-represented in the literature. Several autoimmune disorders are known for the liver, including autoimmune hepatitis (AIH), primary biliary cholangitis (PBC) and primary sclerosing cholangitis (PSC) (151, 152). Although the exact mechanisms of pathogenesis for these diseases are uncertain, they are synonymous with an upregulation of apoptosis, particularly for BECs and hepatocytes (153). As mentioned before, failure to clear apoptotic cells, allowing their progression to secondary necrosis, can increase the risk of immune

system overactivation and autoantibody development (154, 155). It is therefore likely that efferocytosis is defective in these diseases. In support of this, PBC patients possess autoantibodies raised against pyruvate dehydrogenase complex (PDC-E2), which is preserved and exposed in blebs derived from apoptotic BECs (156). Autoantibodies targeting ASGPR are also thought to be raised in AIH patients, which are likely to be derived from dying hepatocytes (157). This is also likely to contribute further to disease progression by disrupting later efforts to clear dying cells. Further understanding into the pathogenesis of these diseases is needed to identify a possible reduction in efferocytosis, as well as to which efferocytic cell this deficiency is attributed to.

1.4 $CD4^+$ T-lymphocytes and their interactions

1.4.1 $CD4^+$ T cell functions and subtypes

T helper lymphocytes, identified by the surface expression of CD4, denote a major component of the adaptive immune system. In cooperation with T cytotoxic cells ($CD8^+$ cells), they perpetuate signals derived from innate immune cells and antigen presenting cells (APCs), allowing for swifter, more targeted and long-lived responses (158, 159). $CD4^+$ T cells invoke different and sometimes contrasting responses, depending on their predominately active transcription factors (**Fig. 1C**). Pro-inflammatory cells can be broadly grouped in to T_H1, T_H2 and T_H17 cells, based on their expression of transcription factors Tbet, GATA3 and RORγ, respectively (158). T_H1 cells are frequently found in the liver during inflammation and are the major sources of pro-inflammatory cytokines, including IFN-γ and TNF-α. These cells are generally recruited and activated in response to bacterial antigens. T_H2 cells are more associated with responses to helminth infections and allergy, together with IL-4 secretions. Such cells are less frequently found in the liver. T_H17 cells, characterised by IL-17 secretions,

are variable and versatile in immunity, behaving either pro-inflammatory or anti-inflammatory. Their activity is determined by their stimulation with cytokines of the same overall function (IL-6 and TGF-β, respectively) (160).

$CD4^+$ T cells can also respond to inflammatory signals and act to dampen immune responses. The major cells responsible for this are called T-regulatory cells (Tregs). These cells can be identified in mice by their expression of the transcription factor, FOXP3, which is necessary for their development and immunosuppressive activity (161). However, in humans, FOXP3 can also be transiently expressed by non-Treg subtypes (162). Consequently, normal human Tregs are instead identified by high expression of CD25 and CD11a, and low expression of CD127. Tregs secrete anti-inflammatory cytokines like IL-10 and TGF-β which promotes resolution of inflammation. As such, some clinical trials have endeavoured to expand Tregs isolated from patients and then re-introduce them as a form of therapeutic intervention (163). Although these trials have experienced some success, they run the risk of immunocompromising the patient by preventing *de novo* inflammatory responses. Additionally, reports suggest that Tregs can be influenced by pro-inflammatory cytokines to acquire more pro-inflammatory characteristics, such as through Tbet expression for example (164). Bearing this in mind, it should be noted that $CD4^+$ subsets, although possessing identifiable markers, are versatile cells and often do not have terminal functionality. As such, controlling the population of $CD4^+$ T cell subtypes within a tissue represents a delicate balance in regulating infection whilst limiting inflammatory stimuli.

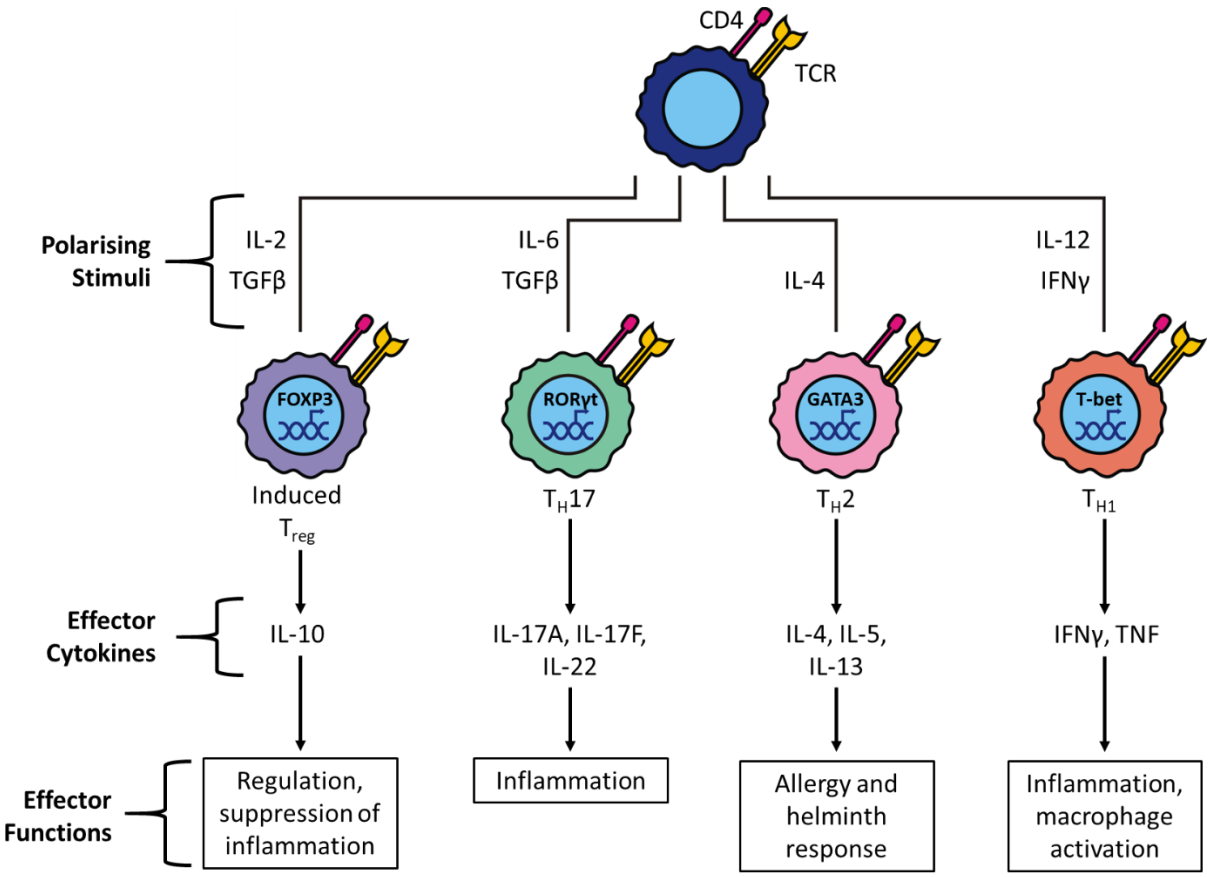

Figure 1C: Development and activities of CD4⁺ T cells. Naïve CD4⁺ T cells are committed towards a specific subset lineage after activation by T-cell receptor (TCR) engagement with an antigen presenting cell (APC). Specific extracellular signals dictate the expression of transcription factors which determine the subset which the cell will become. Each subset produces a distinct (although not fixed) set of effector mediators which are associated with their specific mode of action. CD – cluster of differentiation; TGF-β – tumour growth factor-β; TNF – Tumour necrosis factor; IL – interleukin; IFN-γ – interferon-γ; FOXP3 – forkhead box P3; RORγt - retinoic acid receptor-related orphan receptors gamma-t; Treg – T regulatory cell. Information adapted from (165).

1.4.2 How epithelial cells alter $CD4^+$ T cell behaviour

Although largely determined by other members of the immune system, mostly including APCs like DCs, T cell activity can also be altered through interactions with epithelial cells, especially in the lung and gut (166). This is mostly achieved through inflammatory signalling; several epithelial cell types are capable of cytokine secretion. Airway epithelial cells are integral to T_H2 cell functionality associated with allergic responses. This is done through the production of cytokines such as interleukins 1, 25 and 33, which in-turn alter the behaviours of DCs and $CD4^+$ T cells (167). In addition, these barrier epithelial cells are capable of producing T_H2-related active molecules which are thought to contribute to asthma, including periostin and serpinB2 (168).

Some epithelial cells are capable of influencing T cell behaviour through direct cell-cell interactions. Kidney epithelial cells have been shown to upregulate MHC-II molecules in response to pro-inflammatory cytokine stimulation, allowing for them to activate $CD4^+$ T cells. However, this was shown not to promote their proliferation; a similar situation to T cell stimulation in the liver (169). RPCs also express and interact with $CD4^+$ T cells using MHC-II, although this was also shown to induce a state of anergy within these cells (170). Similar outcomes have been described for colonic epithelial cells, which were hypothesised to prevent inappropriate T cell activation (171). Intestinal epithelial cells (IECs) were additionally reported to activate $CD4^+$ T cells in the gut, skewing them to more T_H17-like lineages (172). This was induced through direct interactions with T cells via the MHC-I-like molecule, thymus leukaemia antigen. IECs can also promote T_H17 activity in response to sensing bacterial DNA, although this is altered to more anti-inflammatory responses when sensing DNA from commensal strains (173). Of note, retinal, airway and intestinal epithelial

cells are capable of phagocytosing apoptotic cells (as mentioned earlier in section 1.3.3), which in turn promotes anti-inflammatory response and Treg activity (116, 120, 174).

1.4.3 Live T cell capture by other cells

As the initiators of the immune response, T cells represent key targets in controlling the overall activity of the immune system. Although many soluble factors and cytokines have been described to alter their activity, some investigations have reported certain situations when other cells capture live T cells, providing a mechanism of disease and immunity modulation. Under certain circumstances, it has been described how macrophages can capture live T cells, a process known as haemophagocytosis (175). This is commonly observed in cases of chronic inflammation and hyperactivation of the immune system, such as in autoimmunity. In xenograft mouse models of graft vs host disease, both $CD8^+$ and $CD4^+$ T cells from donated tissues have been reported to be engulfed by recipient macrophages and DCs (176). Additionally, haemophagocytosis is often concurrent with macrophage-activation syndrome (MAS) (177). In the liver, MAS has been shown to coincide with a large influx of inflammatory T cells, both $CD4^+$ and $CD8^+$ varieties, as well as haemophagocytic macrophages (178, 179). This results in a large local increase in pro-inflammatory cytokine secretion, as well as the inability of engulfed cells to target and eliminate possibly infected cells. Under these conditions, despite the outnumbering of $CD4^+$ helper T lymphocytes by $CD8^+$ cytotoxic T cells, macrophages can still be observed engulfing $CD4^+$ T cells (178). Aside from situations of chronic inflammation, macrophages have also been reported to engulf live $CD4^+$ T cells infected with HIV-1, which was shown to be a method of viral transfection of the engulfing macrophages (180).

Although several situations of live T cell capture have been described, most of these involved macrophages as the predatory cell. Minimal examples have been described for other, non-circulatory cells, especially for live $CD4^+$ T cells specifically. However, it was reported that hepatocytes were able to engulf and remove live, autoreactive $CD8^+$ T cells (181). This was proposed as another method in which hepatocytes contribute to maintaining a steady immune state by removing autoreactive cells from the environment. Additionally, metastatic melanoma cells have also been reported to capture $CD8^+$ T cells, as a likely mechanism of avoiding immune surveillance (182).

1.5 Cell-in-cell structures

1.5.1 The mechanisms of cell-in-cell structures

In recent years, a new and ever-expanding field of research has emerged concerning cell-in-cell structures (CICSs). This literally concerns the presence of whole, undamaged live cells within other host cells. The mechanisms and consequences of CICSs have proven to be of great interest in a growing number of biological systems. Their formation has been most efficiently described by Overholtzer and colleagues. They initially observed how primary and immortalised breast cancer cells were able to internalise live neighbouring cells of the same lineage (183). They named this process as "entosis". From this, the molecular requisites of CICSs and their methods of formation were elucidated (184, 185). They describe how this homotypic capture of one cell by another was reliant on Rho GTPase and Rho Kinase (ROCK) activity (**Fig. 1D**). The resulting vesicle containing this live cell would associate strongly with E-cadherin and β-catenin, which are well known to interact in the formation of adhesion junctions under normal circumstances (185, 186). Some evidence also suggests that entosis can be modulated by androgen receptor via the Rho-ROCK pathway in prostate cancer (187). Later reports have linked these associations to the establishment of the cell-cell junctions following the completion of mitosis (188); "rounder" cells with less-established adherence junctions, which is often a state associated with actively dividing cells, were more prone internalisation by a neighbouring cell which possessed better-established junctions. This was exemplified whereby cells deficient in cdc42, and could therefore not enter the cell cycle, were less likely to be engulfed. These collective data thus summarised the molecular dynamics of entosis. Although described as form of "non-apoptotic cell death", the internalised cell does not always suffer this fate; investigations have described the

proliferation of captured cells, as well as their release from the host cell (183, 184) (**Fig. 1D**). These examples suggest that the purpose and consequences of CICSs are specific to the tissue and cells in which they occur.

1.5.2 Examples and consequences of cell-in-cell structures

Since the initial definitive markers and mechanisms for entosis were established, other cells or tissues which have exhibited similar characteristics have now been described. Historically, it has been observed that thymic nurse cells (TNCs) were capable of internalising multiple live thymocytes, potentially as process of immature cell elimination (190). It has now been shown that the thymocytes take a more active role in the internalisation process than initially thought by interacting with cytoskeletal components of the TNC, similar circumstances as to those described for entosis (191). Li Y *et al*, presented a highly convincing case for the involvement of entosis in embryo implantation (192). This was a paradigm-shifting investigation which demonstrated that blastocyst trophoblasts internalised and cleared live uterine epithelial cells. This was an early example of heterotypic live-cell capture and showed the absence of apoptosis during blastocyst implantation. Other investigations described entosis-like phenomena in keratinocytes, mesenchymal cells, and in specialised testicular cells as a mechanism of eliminating spermatozoa (193-195).

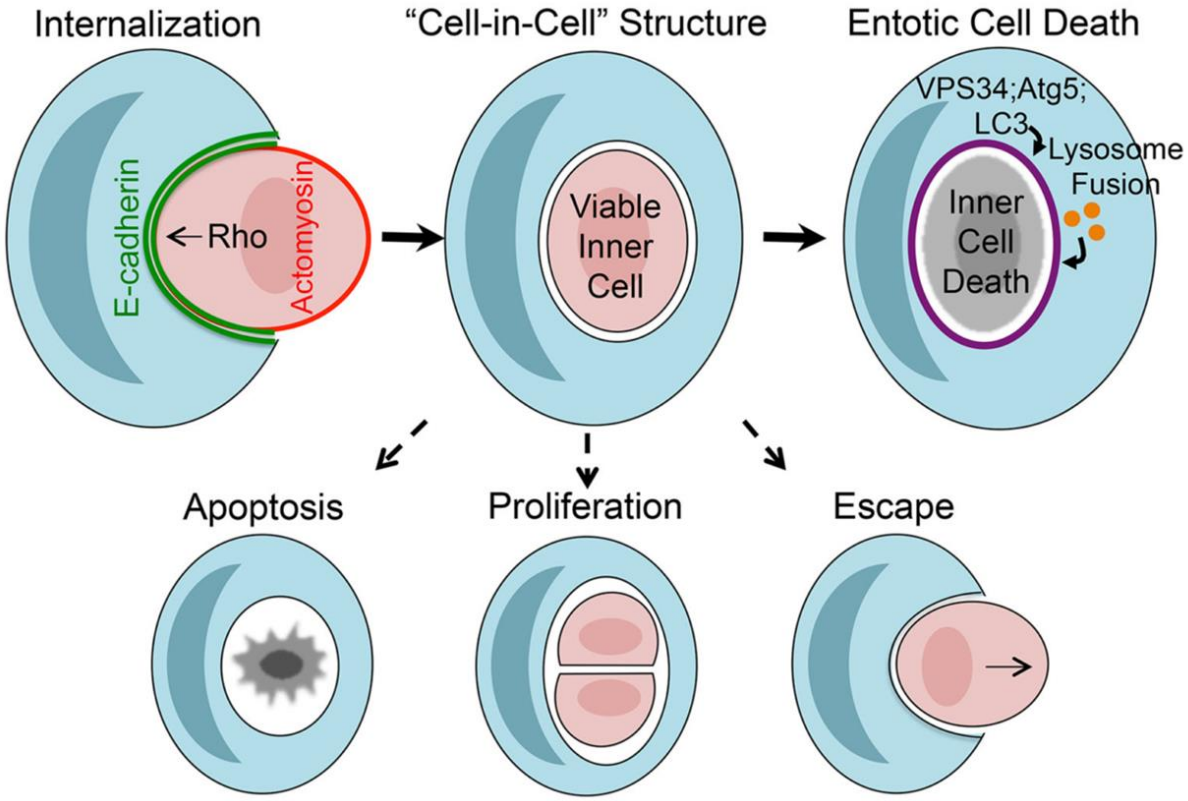

Figure 1D: The formation and fates of cell-in-cell structures formed via entosis. A cell invades into a neighbouring cell. This required Rho kinase-dependent actomyosin contractile activity and cell-cell junction formation involving E-cadherin. A cell-in-cell structure is then created following complete internalisation of the captured cell. Reports have shown that cells internalised via Entosis can be digested upon lysosomal fusion, which requires the activation of the non-canonical autophagy pathway, via VPS34, a class-III phosphatidylinositol-3-kinase. Internalised cells can also die via apoptosis, they can persist within the cell and proliferate, or can be released from the host. Taken, with permission, from (189).

Aside from entosis, other situations and processes which lead to CICS formation have been described in the literature, often referred to as 'emperipolesis' (184). Many of these are heterotypic and frequently involve the capture of immune cells, frequently playing pivotal roles in immune responses. It has been widely reported, for example, that live neutrophils can be found within megakaryocytes in the bone marrow (184, 196-199). It is thought that neutrophils eventually pass through megakaryocytes as a form of transcellular migration and enter circulation (199). More recently, some reports have described CICS formation through a process known as suicidal emperipolesis (181, 200). This term was used to describe the capture and deletion of one live cell by another. As previously mentioned, it was described in the liver, whereby autoreactive $CD8^+$ T cells were engulfed and deleted by hepatocytes (181), further contributing to liver immunotolerance and homeostasis.

Each cell type for which entosis has been described has displayed specific requirements for, and consequences of this process. Many of these have been related to development and cell population control, akin to induced programmed cell death via apoptosis. Additionally, as many of these cells have been transformed or are tumour cells, entosis has been suggested as a method of intercellular competition (201-203). It was postulated by Sun *et al*, in 2014 that during homotypic entosis between cancers, there is 'winning' and 'losing' cell (203). This nomenclature presents a predator-prey-like scenario whereby one cell provides sustenance for another, but also relates entosis to a form of Darwinian selection within a tumour that maintains more-transformed, oncogenic cells, whilst eliminating less-transformed cells. Sun and colleagues evidenced this with experiments whereby transformed cells were observed to engulf their normal counterparts (203). The authors also showed that the ability to 'entose' other cells is linked to their oncogenicity and potentially with their capacity for metastasis. Cells with higher expression of *kras*, a well-known oncogene, were shown to

engulf their neighbours more frequently. This was concurrent with increased expression of Rac1, the Rho GTPase linked to cytoskeletal rearrangement and, by extension, metastasis.

Aside from providing nutritional support and a mechanism of cell elimination, CICSs were shown in early stages of their study to induce genetic alterations to the host cell (185, 204). The CICS is an incredibly large internal structure, relative to the size of the host cell, which can impose a physical block on the cleavage furrow during cytokinesis. Cells containing CICSs were, consequently, more likely to fail cell division, becoming multinucleate and polyploid. This can create difficulty in resolving the increased number chromosomes across metaphase plates during later cell divisions (205). This leads to further genetic alterations through the loss or gain of, so-called "lagging chromosomes". As such, CICSs can also force cells to become aneuploid, as well as polyploid. The increased likelihood of genetic instability represents another advantage of Entosis for cancers, as it promotes the accumulation of potentially transformative and proliferative mutations. These investigations show that CICSs can be a method of controlling cell populations, but are also linked with genetic manipulation, particularly in transformed, oncogenic cells.

1.5.3 Similarities and differences between cell-in-cell structures and efferosomes

The induction of CICSs and their cellular organisation have obtained their own distinct field of research in recent years. Many key techniques utilised to investigate CICSs have been modified from those used to study the capture of dead cells and efferosomes. As such, the capture of live and dead cells shares several molecular and consequential parallels. The clearest molecular link described is through the sharing of molecular machinery associated with autophagy (206). Reports have shown how both entotic vesicles and efferosomes initially associate with the lipidated version of autophagy initiating protein, Light chain 3

(LC3-II) and that their internal processing is regulated by the starvation-sensing protein, mTOR (111, 207). This was shown, in breast cancer cells, to be initialised by vacuolar-type ATPase (V-ATPase) in response to osmotic alterations in endolysosomal compartments that were induced following live or dead cell engulfment (208). Efferosomes were also reported to associate with the autophagic molecularly machinery which assists in the lysosomal fusion (121, 209). As this is not evident in all phagocytes, this process has received its own nomenclature, called LC3-II-associated phagocytosis (LAP) (112, 210). Entotic vesicle membranes were shown to be transiently enriched with LC3-II (111). Consequently, these cells are engaged by the autophagy pathway, but do not necessarily perish because of this. Overall, efferosomes (or at least so-called LAPosomes) share the same association with LC3-II as entotic vesicles, but not necessarily for the same length of time. This similarity thus may also be a factor which distinguishes these processes.

Aims

The mechanisms and consequences of dead cell capture and live $CD4^+$ T cell capture by hepatocytes are poorly understood. I hypothesise that they are phenotypically and molecularly distinct processes. To investigate this, the work conducted in this thesis endeavoured to accomplish the following aims.

1. To understand the molecular processes behind hepatocyte efferocytosis.
2. To outline the consequences of efferocytosis for the engulfing hepatocyte.
3. To compare the capture of live $CD4^+$ T cells to efferocytosis and entosis.

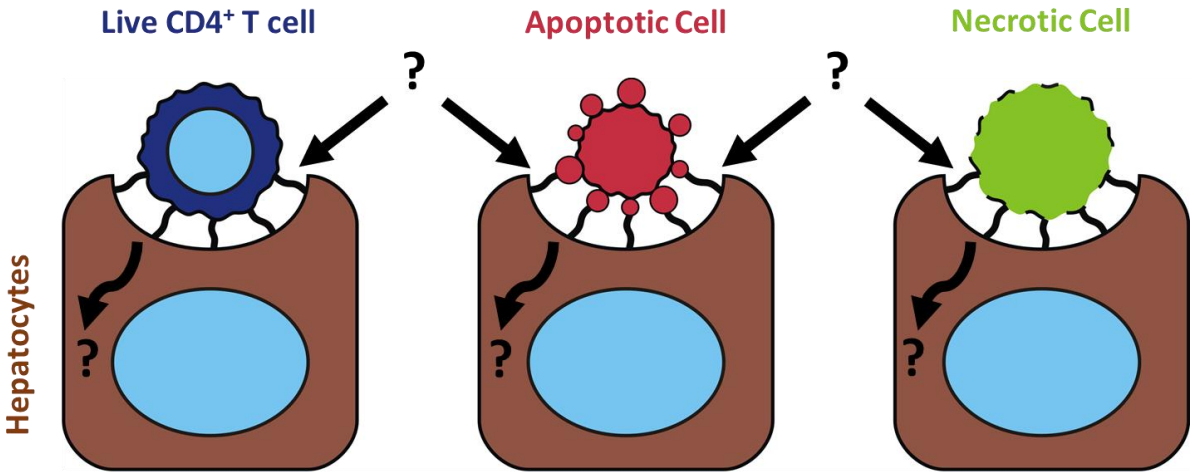

Figure 1E: Problems to be addressed in this PhD project. Previous data in the Stamataki lab has demonstrated that hepatocytes (brown) can engulf live $CD4^+$ T cells (blue). Previous reports have shown that hepatocytes can also capture apoptotic (red) and necrotic (green) cells. Question marks represent the lacking details behind the receptors of cell-cell interactions involved in each of these processes, for the molecular processes involved with intracellular trafficking of the captured cell, and the consequences for the internalising hepatocytes.

Chapter 2: Materials and Methods

2.1 Antibodies

Table 1, below, details all antibodies used throughout the duration of this project, as well as their source, purpose, and their working concentrations.

Table 1: List of antibodies used throughout this project and their purpose

Antibody	Host	Clone	Supplier	Primary/ Secondary	Purpose(s)	Concentration
Anti-Beta catenin 1	Mouse	IgG1	Biolegend (clone 12F7, cat. 844602)	Primary	Immunofluorescence and immunohistochemistry	2.5 µg/ml (1/200)
Anti- Cofilin	Rabbit	IgG	Cell signalling technologies (D3F9, Ab 5175)	Primary	Western blotting primary	(1/1000)
Anti- E-cadherin	Mouse	IgG2a	BD Biosciences (Clone 36RUO, Cat. 610182)	Primary	Immunofluorescence primary	1.25 µg/ml (1/200)
Anti- FOXP3	Mouse	IgG1	Abcam (clone 236A/E7, ab20034)	Primary	Immunohistochemistry	20 µg/ml (1/50)
Anti- FOXP3	Rabbit	IgG	Abcam (ab4728)	Primary	Immunohistochemistry	40 µg/ml (1/25)
Anti- GAPDH	Rabbit	IgG	Cell signalling technologies (Ab 2118)	Primary	Western blotting primary	1/1000
Anti- HNF4α	Mouse	IgG2a	Abcam (clone K9218;	Primary	Immunohistochemistry	10 µg/ml (1\100)

			ab41898)			
Anti- ICAM-1	Mouse	IgG1	R&D Systems (Clone BBIG – I1, Cat: 11C81)	Primary	Immunofluorescence	10 µg/ml (1/50)
Anti- ICAM-2	Goat	IgG Polycloncal	R&D Systems (Poly clonal, Cat: AF244)	Primary	Immunofluorescence	10 µg/ml (1/50)
Anti- Ki67 (human)	Mouse	IgG1	Agilent/Dako (clone MIB-1, cat. M7240)	Primary	Immunohistochemistry	0.92 ug/ml (1/50)
Anti- Ki67 (mouse)	Rabbit	IgG monoclonal	Abcam (clone SP6, Cat. ab16667)	Primary	Immunohistochemistry	(1/100)
Anti- LOX1	Goat	IgG	R&D Systems (1798-LX)	Primary	Immunohistochemistry	10 µg/ml (1/50)
Anti-Phospho-Cofilin	Rabbit	IgG	Cell signalling technologies (Ser3, mAb 3313)	Primary	Western blotting primary	(1/1000)
Anti- Tbet	Rabbit	IgG	Santa Cruz Biotechnology (H-210, sc-21003)	Primary	Immunohistochemistry	1 µg/ml (1/200)
Anti-p21 (human)	Rabbit	IgG Monoclonal	Invitrogen	Primary	Immunohistochemistry	(1/50; concentration not provided)
Anti-p21 (mouse)	Rabbit	IgG Monoclonal	Abcam (Clone [EPR18021], Cat: ab188224)	Primary	Immunohistochemistry	0.487 µg/ml (1/1000)
Anti-rabbit IgG1 HRP conjugated	Goat	IgG	Cell signalling technologies (7074)	Secondary	Western blotting secondary	(1/15000)
Anti-SCARF2	Rabbit	IgG Polycloncal	Atlas Antibodies (HPA035079)	Primary	Immunofluorescence and immunohistochemistry	2 µg/ml (1/100)

Donkey Anti-goat Alexafluor 568 conjµgated	Donkey	IgG Polycloncal	Thermo (Polyclonal, Cat. A-11057)	Secondary	Immunofluorescence	2 µg/ml (1/1000)
Goat Anti-mouse Alexafluor 594 conjµgated	Goat	IgG Polycloncal	Thermo (Cat. A-11005)	Secondary	Immunofluorescence	2 µg/ml (1/1000)
IgG Goat IMC	Goat	IgG Polycloncal	R&D Systems (Polyclonal, AB-108C)	Isotype matched control	Immunofluorescence	Matched to primary
IgG LEAF Mouse IMC	Mouse	IgG1	Biolegend (Clone MG1-45, Cat 401404)	Isotype matched control	Immunofluorescence	Matched to primary
IgG Rabbit polyclonal IMC	Rabbit	IgG Polycloncal	Biolegend (Poly29108), Cat 910801	Isotype matched control	Immunofluorescence and immunohistochemistry	Matched to primary
IgG2a Mouse IMC	Mouse	IgG2a	Biolegend (Clone MG2a-53, Cat 401302)	Isotype matched control	Immunofluorescence	Matched to primary

2.2 Reagents and buffers

Table 2 and table 3, below, details all reagents and buffers, respectively, used throughout the duration of this project, as well as their source, purpose, and their working concentrations if available. The components, and their concentrations, of all buffers are listed.

Table 2: List of reagents used throughout this project.

Category/procedure	Reagent	Supplier	Purpose	Working concentration if applicable
All	Phosphate Buffered Saline (PBS)	GIBCO/Life Technologies™ (20012019)	Washing/diluent	N/A
Apoptotic cell induction	FITC Annexin V Apoptosis Detection Kit with 7-AAD	Biolegend (640922)	Detection of apoptotic and necrotic cells	Used as per manufacturer's instructions
Apoptotic cell induction	Staurosporine (STS)	Sigma (S6942)	Induction of apoptosis	1 µM
Cell culture	Dulbeccos modified eagles medium (DMEM), high glucose, high pyruvate	Life Technologies™ (11995065)	Culture of adherent cells	N/A
Cell culture	Roswell Park Memorial Institute Medium 1640, high glutamine (RPMI 1640)	GIBCO/ Life Technologies™ (11875-085)	Culture of suspension cells	N/A
Cell culture	0.05% Trypsin-EDTA	GIBCO/ Life Technologies™ (H3570)	Detachment of adherent cells for passage	N/A
Cell culture	Fetal Bovine Serum	Sigma-Aldrich (F4135)	Culture media supplement	10% in media
Cell culture	Non-essential Amino acids (NEAA)	GIBCO/ Life Technologies™ (11140-035)	Culture media supplement	1% in media
Cell culture	Penicillin-Streptomycin (Pen/Strep)	GIBCO/ Life Technologies™ (15140122)	Bacteriostatic antibiotic for culture medium	1% in media

Cell labelling	Celltracker green CMDFA	Thermofisher (C2925)	Immunofluorescence labelling	5 µM
Cell labelling	Celltracker red CMTPX	Thermofisher (C34552)	Immunofluorescence labelling	5 µM
Cell labelling	Celltracker violet BMQC	Thermofisher (C10094)	Immunofluorescence labelling	5 µM
Cell labelling	HCS CellMask Deep Red	Thermofisher (H32721)	Immunofluorescence labelling	5 µM
Cell labelling	pHrodo red dextran	Thermofisher (P10361)	Immunofluorescence detection of low pH	10 ug/ml
Hepatocyte/hepatoma treatment	Interferon-γ (IFN-γ)	PeproTech (300-02)	Analysing the effects of cytokines efferocytosis of necrotic cells	100 ng/ml
Hepatocyte/hepatoma treatment	Interleukin-2 (IL-2)	PeproTech (200-02)	Primary $CD4^+$ T cell media supplement	500 IU
Hepatocyte/hepatoma treatment	Tumour necrosis factor alpha (TNFα)	PeproTech (300-01A)	Analysing the effects of cytokines efferocytosis of necrotic cells	100 ng/ml
Hepatocyte/hepatoma treatment	Tumour growth factor beta (TGF-β)	PeproTech (100-21)	Analysing the effects of cytokines efferocytosis of necrotic cells	100 ng/ml
Hepatocyte/hepatoma treatment	Interleukin-6 (IL-6)	PeproTech (200-06)	Analysing the effects of cytokines efferocytosis of necrotic cells	100 ng/ml
Hepatocyte/hepatoma treatment	IL-10	PeproTech (200-10)	Analysing the effects of cytokines efferocytosis of necrotic cells	100 ng/ml
Hepatocyte/hepatoma treatment	IL-1β	PeproTech (200-01B)	Analysing the effects of cytokines efferocytosis of necrotic cells	100 ng/ml
Hepatocyte/hepatoma treatment	Dexamethasone	Sigma (D2915)	Analysing the effects of corticosteroids efferocytosis of necrotic cells	10 µg/ml
Hepatocyte/hepatoma treatment	Insulin-like growth factor 1 (IGF-1)	Peprotech (100-11)	Growth factor previously described for altering efferocytosis by non-professional phagocytes	1 µg/ml
Immunofluorescence	Paraformaldehyde (PFA)	Sigma-Aldrich (P6148-500G)	Fixative for immunofluoresence staining of cells	1% (w/v)

Immunofluorescence	Formaldehyde solution	Sigma-Aldrich (F8775)	Fixative for immunofluoresence staining of cells	3.7% (w/v)
Immunofluorescence	Hoechst 33342	Life Technologies™ (H3570)	Fluorescent labelling of nuclei	1 µg/ml
Immunohistochemistry	ImmPRESS™ HRP Universal Antibody (Anti-Mouse IgG/Anti-Rabbit IgG, Peroxidase) Polymer Detection Kit	Vectorlabs (SK-4105)	Immunohistochemistry (secondary detection)	Used as per manufacturers instructions
Immunohistochemistry	ImmPACT DAB Peroxidase (HRP) Substrate	Vectorlabs (MP-7500)	Immunohistochemistry chromagen	Used as per manufacturers instructions
Immunohistochemistry	Antigen Unmasking Solution, Tris-Based (10X)	Vectorlabs (H-3301)	Immunohistochemistry	Used at 2X diluted in TBST
Immunohistochemistry	StayGreen/AP Plus	Abcam (ab156428)	Immunohistochemistry (secondary detection)	Used as per manufacturers instructions
Immunohistochemistry	Mayers haematoxylin	Pioneer Research Chemicals (PRC/R/42)	Immunohistochemistry (Counterstain)	Filtered and stained for 30-40 sec
Immunohistochemistry	Harris' haematoxylin	Pioneer Research Chemicals (PRC/R/51)	H&E Staining	N/A
Immunohistochemistry	Distyrene, a plasticiser, and xylene mountant (DPX)	CellPath (SEA-1304-00Y)	Immunohistochemistry mounting medium	N/A
Immunohistochemistry	XTF mountant	CellPath (SEA-1904-00A)	Immunohistochemistry mounting medium (for xylene incompatible chromagens)	N/A
Immunohistochemistry	Xylene	Pioneer Research Chemicals (PRC/R/201)	Tissue clearing	N/A
Immunohistochemistry	Industrial denatured alcohol (IDA) (99%)	Pioneer Research Chemicals (PRC/R/101)	Tissue dehydration	N/A
Immunohistochemistry	Peroxidase-Blocking Solution	Dako™ REAL (S2023)	Blocking intrinsic peroxidase activity of tissues	N/A
Immunohistochemistry	Casein Solution 10X	Vectorlabs (SP-5020)	Blocking non-specific binding of antibodies	2X

Immunohistochemistry	EnVision FLEX wash buffer (Tris-buffered saline with Tween - TBST)	Dako (K8007)	Tissue washing	N/A
Immunohistochemistry	Prolong Gold Fluorescent mounting medium	Life Technologies™ (P36930)	Mounting medium for fluorescently stained tissues and cells	N/A
Inhibitor	5-(N-Ethyl-N-isopropyl amiloride) (EIPA)	Sigma (A3085)	Macropinocytosis inhibitor used for blocking efferocytosis and live T cell capture	Experiment-specific
Inhibitor	H-1152	Tocris (2414)	Inhibitor of Rho Kinase (ROCK)	10 µM
Inhibitor	Blebbistatin	Sigma (B0560)	Macropinocytosis inhibitor used for blocking efferocytosis and live T cell capture	50 µM
T cell isolation	Lympholyte	Cedarlane Labs (CL5020)	Gradient solution for isolating live human lymphocytes	N/A
T cell isolation	EasySep™ Human $CD4^+$ T Cell Enrichment kit	Stem cell (19058)	Negative selection kit for isolation of $CD4^+$ T cells	N/A
Western blotting	Clarity ECL blotting substrate	Biorad (17050)	ECL substrate for western blotting exposure	Used as per manufacturers instructions
Western blotting	40% acrylamide	Biorad (1610140)	Acrylamide Gel ingredient	See section 2.14
Western blotting	2% BIS-acrylamide	Biorad (1610143)	Acrylamide Gel ingredient	See section 2.14
Western blotting	10% SDS	Biorad (1610416)	Acrylamide Gel ingredient	See section 2.14
Western blotting	Tetramethylethylenediamine (TEMED)	Sigma (T9281)	Acrylamide Gel ingredient	See section 2.14
Western blotting	Ammonium persulphate (APS)	Sigma (A3678)	Acrylamide Gel ingredient	See section 2.14

Table 3: List of buffers used throughout this project and their ingredients.

Buffer	Compenents	Component Concentrations
Isolation Buffer	PBS	Diluent
	FBS	2% (w/v)
	EDTA	1 mM
FACS Buffer	PBS	Diluent
	FBS	1% (w/v)
	EDTA	2 mM
SDS Running Buffer (10x)	ddH20	Diluent
	Tris-base	248 mM
	SDS	1% (w/v)
	Glycine	1.92 M
Transfer Buffer 10x stock	ddH20	Diluent
	Tris-base	250 mM
	Glycine	1.92 M
Transfer Buffer 1x working solution	ddH20	Diluent
	Transfer Buffer 10x stock	10%
	MeOH	20%
TBS (pH 7.6) X10	ddH20	Diluent
	Tris-base	200 mM
	NaCl	1.37 M
TBST	TBS	Diluent
	Tween20	0.01% (v/v)
Staining buffer	PBS	Diluent
	BSA	1% (w/v)
	FBS	1% (w/v)
Laemelli Buffer	Tris-base	120mM
	SDS	4% (w/v)
	Glycerol	20% (w/v)
	Bromophenol Blue	0.02% (w/v)

2.3. Cell culture

Huh-7, HepG2 and Hep3B cells were used for models of primary hepatocytes and were kind gifts from Prof. Jane McKeating. All hepatic cell types were cultured in DMEM containing sodium pyruvate. For continued passage and for seeding, adherent cells were washed with PBS and treated with 0.25% trypsin-EDTA for 3 min, 37°C. Cultures were agitated to ensure that all cells were dislodged. Trypsin-EDTA was then quenched with an equal volume - minimum – of serum-containing media. Cells were then centrifuged for 5 min, g at room temperature. Supernatants were discarded and then cells were used for seeding. Part of the culture was retained and replaced into new flasks for continued passage.

Primary T cells and Jurkat T cell lymphomas were cultured in RPMI. All media was supplemented 1% PenStrep, 1% NEAA, 1% L-Glutamine and 10% FBS (hereon known as 'complete media'). Media of primary T cells was supplemented with 500 IU Interleukin 2 (IL-2). All cells were cultured in incubators at 37°C, 5% CO_2.

2.4 Primary T cell isolation and Regulatory T cell separation

All primary lymphocytes were isolated from blood samples of fully consented haemochromatosis patients at the Queen Elizabeth Hospital. Blood was layered was on top of Lympholyte cell separation media at a blood:Lymphocyte ratio of 8:3 (commonly 35 ml blood was layered on top of 15 ml lympholyte) in 50 ml centrifuge tubes. Tubes were then centrifuged for 20 min, 423 g at room temperature, with no brake. Peripheral blood mononuclear cells (PBMCs) were then extracted from the subsequent buffy coat. PMBCs were then washed in PBS and diluted to a concentration of $5x10^7$ in isolation media (see table 2). Primary $CD4^+$ T-cells were then isolated using a STEMCELL negative selection kit,

according to manufacturer's instructions (Cat. 17952). Isolated cells were then cultured in media supplemented with 500 IU IL-2. $CD127^{lo}$ $CD25^{+}$ Treg cells were separated from total $CD4^{+}$ T cells using a different STEMCELL negative selection kit (Cat.18063). Non-Tregs were salvaged from these isolations and allowed time for the magnetic beads to detach prior to their use within experiments.

2.5 Induction of apoptosis in primary $CD4^{+}$ T cells and Annexin V/7AAD labelling

Isolated primary $CD4^{+}$ T cells were briefly washed in PBS before resuspending in serum-free RPMI containing 1 µM staurosporine (STS) or volume-matched vehicle control of DMSO. Cells were resuspended at a concentration of $4x10^{6}$/ml and incubated for a varying period at 37°C (4 hr was eventually selected). Incubation times were staggered to ensure each were completed at the same time. Cells were then washed in PBS and staining using a Biolegend FITC-Annexin V Apoptosis Detection Kit with 7-AAD according to manufacturer's instructions. Cells were then analysed by flow cytometry using a Beckman Coulter Cyan ADP9.

2.6 Cell Tracker labelling

For most *in vitro* experiments with an output of fluorescence microscopy, cells were initially fluorescently labelled with CellTracker dyes (CMFDA green, CMTPX red or BMQV violet). Cells were initially washed with PBS and then incubated with each label, 5 µM in serum-free media for 45 min, 37°C. Cells were then washed again in PBS and then rested in serum-containing media for 1 hr, prior to experimentation, to avoid leaching and cross-labelling.

2.7 T-cell and Jurkat lymphoma preparation for co-culture assays

Co-culture experiments were conducted between hepatoma cell lines and primary $CD4^+$ T cells or Jurkat lymphomas. The latter cells were either live, apoptotic or heat-killed cells. For live cell co-cultures, the lymphocytes or lymphomas were layered on Lympholyte separation medium and centrifuged according manufacturers to instructions. This step was required to remove dead cells from the culture, which was later confirmed by trypan blue staining. Apoptotic cells were compared through treatments with 1 µM STS, with cells at a concentration of $4x10^6$/ml. The development of this protocol and its variations is discussed in section 3.2. For heat-killing, cells were placed in a heat block at 60°C for 30 min.

2.8 Co-culture assays

For all co-culture assays, hepatocyte cell lines were seeded in polypropylene plates (24 or 96 wells) for 80% confluence the following day. 13 mm glass coverslips were placed into wells prior to seeding for all confocal experiments. Cells were allowed 24 hr to adhere prior to experimentation. Cells were then labelled and pre-treated as necessary. All pre-treatments were conducted for 1 hr, unless stated otherwise, in 250 ul complete DMEM. Following this, the appropriate concentration of either primary $CD4^+$ T cells or Jurkat lymphomas were added on top of the Huh-7 cells, dropwise in complete RPMI. Unless stated otherwise, $5x10^5$ cells were added to each well, giving a rough Huh-7:lymphocyte/lymphoma ratio of 1:2 for most experiments, and co-cultured for 3 hr. These suspension cells were either live, apoptotic or heat-killed. For most experiments, cells were fixed in -20°C, 100% methanol (MeOH) for 5 min and then washed with PBS. Glass coverslips, if used, were then mounted onto microscope slides using Prolong Gold antifade mountant. These coverslips were then

imaged using a Zeiss 780 or 880 confocal microscope. 5 fields of view were taken for each coverslip. Total Huh-7s were determined using Bitplane IMARIS cell rendering tools. Internalised cells were determined by eye and assisted using the 'cell counting' plugin for ImageJ.

2.9 *In vitro* multinucleation experiments

For *in vitro* induction of multinucleation through efferocytosis, Huh-7 hepatomas were seeded as described in section 2.3, but at a density of $2.5x10^5$ in 24-well plates. Huh-7s were then incubated with heat-killed Jurkat T cell lymphomas at a ratio of 1:1. Excess Jurkat cells were removed following 24 hr co-culture. Cells were then washed with PBS and normal culture media was replaced. Huh-7s were permitted to conduct efferocytosis until they became confluent, indicating that they had completed efferocytosis (they do not divide when conducting efferocytosis). Huh-7s were then trypsinised as described in section 2.3 and divided between 2 wells of separate 24-well plates. Unfed control wells were passaged as needed but seeded at the same time and density as the co-cultured cells for analysis. Huh-7s from one well were 're-fed' with heat-killed Jurkat cells as described earlier and the experiment as repeated. Huh-7s in the other plate were labelled with Hoechst 33342 and CellMask Orange. The mean percentage of multinucleate cells was then determined from the total population of cells. Manual counting of these was facilitated by the counting tool within Image J. Numbers were generated from 5 fields of view (FOV), taken from 3 technical replicates. Means were acquired from 3, staggered experimental replicates.

Experiments which involved single repeats were conducted as above but were instead terminated after a single round of co-culture. The Huh-7:heat-killed Jurkat ratio was altered for one experiment which assessed the effect of increased efferocytosis for multinucleation.

For experiments requiring 5-(N-Ethyl-N-isopropyl-amiloride) (EIPA), Huh-7s were pre-treated with 10 µM EIPA for 1 hour. This concentration was maintained following the addition of heat-killed Jurkat cells, which were added at a 1:1 ratio.

2.10 Animal Experiments

Observations taken from mouse models of ischemia reperfusion injury (IRI) and paracetamol overdose (acetaminophen [APAP] alone with no EIPA treatment) were made from haematoxylin and eosin (H&E)-stained paraffin-embedded liver tissues. Ischemia reperfusion injury was conducted with 8-week old C57BL/6 mice and induced as previously described (211). Mice were reperfused for 6 hr or 24 hr. N=5 per condition. Mr. Ricky Bhogal conducted these experiments. Paraffin-embedded tissues from these experiments were stained or reanalysed for the purposes of this project. APAP-injury was induced in C57BL/6 mice through intraperitoneal injections (IP) of 300 mg/kg APAP. For all *de novo* animal experimentation, 20 male, 8-week old C57BL/6 mice were used across 2 individual experiments. 16 mice received 300 mg/kg acetaminophen (APAP), in 200 ul PBS, via IP. Half of these mice received 2.5 mg/kg EIPA via the same method 1 hour later, whereas the others received an equal volume of vehicle (0.001% DMSO). 4 mice received EIPA alone. 20 mice were used in total. Mice were sacrificed 24 hr later and their livers were removed. The largest lobes were prepped for paraffin wax embedment. Other lobes were snap frozen in liquid N_2 for later experimentation. Cardiac punctures were also performed for blood extraction. Blood samples were then analysed for measurements of liver damage at the Birmingham Women's Hospital: aspartate transaminase (AST) alanine transaminase (ALT), alkaline phosphatase (ALP) and bile acid. Mouse handing was performed by post-doctoral researcher, Dr. Lozan Sheriff.

2.11 Normothermic machine liver perfusion and cauterisation model of liver injury

Livers that underwent normothermic machine perfusion were donor livers, from consented patients, which had been rejected for transplantation (n=3, Centre for Liver research numbers: CLR1500, CLR1691 and CLR2519). Livers had undergone a 6 hr perfusion with an acellular haemoglobin-based oxygen carrier (HBOC), Hemapure™ or blood, using an Organ Assist™, Liver Assist perfusion system, prior to my involvement. Physiological oxygen and temperature levels were maintained throughout the perfusion. Livers were sat within the same perfusate of which they were perfused with and the entire liver was perfused roughly every 2 min. The volume of perfusate was lowered to 1.6 L to limit the mass of EIPA required and increase the recycling rate of the entire perfusate volume. A concentrated 500 mM stock of EIPA was prepared prior to perfusion to limit the volume of DMSO added to the perfusate. 160µl DMSO was added to the perfusate and wedge samples were taken after 5 min as vehicle-treated controls. 160 µl, 500 mM EIPA was then added to the perfusate (final concentration 50 µM) and allowed to perfuse around the liver for 30 min. Further wedges were then sampled after this period. All wedges were stored in pre-warmed, DMEM throughout all incubation and transportation periods. A blunt surgical needle (14 mm) was then heated using a Bunsen burner and immediately bored entirely through each tissue wedge. The needle was left in the wedge for at least 1 min before removing it. The wedges were then replaced into at least 100 ml DMEM in tin foil-covered beakers and incubated overnight at 37°C. Wedges were then fixed in Formalin for at least 3 days and underwent preparations for Paraffin embedding. For this, fixed liver tissues were cut down the centre of the cauterisation wound and both sides were placed face down in tissue cassettes. This was

to ensure that both the wound aperture and the surrounding parenchyma could be seen on one tissue section.

2.12 Assessment of hepatocyte multinucleation in mouse and human injury models

Hepatocyte multinucleation was determined on tissues stained either by H&E or for hepatocyte nuclear factor 4-alpha (HNF4α) by immunohistochemistry (IHC). For mouse tissues, necrotic lesions were outlined and 3 concentric shapes of 2-3 hepatocytes thick were also drawn out. Only suitably isolated lesions were only selected, as the counts may be influenced by other nearby lesions. At least 3 lesions were assessed per mouse. 5 random fields of view (FOVs) from WT, untreated mice containing at least 100 hepatocytes were also analysed for controls. For human tissue with cauterisation injury, 5 FOVs were taken at random positions along the length of the wound at 10x magnification, using Zen software. The boundary between healthy and dying cell was outlined on each FOV and then areas 5 hepatocytes thick there outlined. Both total and multinucleate hepatocytes were counted in outlined areas using the 'cell counting' plugin for ImageJ.

2.13 Paraffin Tissue Sample Preparation

Primary liver samples from both consented human patients and mice with APAP injury were used for paraffin-embedded samples. All human sections were cut from liver tissue, obtained from surgical procedures carried out at the Queen Elizabeth Hospital, Birmingham, UK. Ethical approval for the study was granted by the Local Research Ethics Committee (LREC) (reference number 06/Q702/61). All tissues were fixed in 100% formalin (4%

formaldehyde) for at least 24 hr and placed in tissue cassettes. Tissues were then embedded in wax and allowed 24 hr to set. 3 µm-thick sections were then cut using a rotary microtome and then floated on 35°C water to remove undesired tissue folding. Tissue sections were then mounted onto charged glass slides. Sections were then loaded into metal racks and set at 60°C. These sections were then used for IHC.

2.14 Immunohistochemistry (IHC)

Paraffin-embedded tissue samples were initially dewaxed and rehydrated using the following treatment procedure:

- 3 x 3 min incubations in xylene
- 3 x 3 min incubations in 99% industrial denatured alcohol (IDA)
- 2 x 3 min ddH20 in order to wash off excess alcohol and keep tissue sections hydrated.

1 L, 1% tris-based (high-pH) unmasking solution (2X overall) was prepared and preheated in a microwave oven at max. temperature for 10 min. Rehydrated tissue sections were submerged in pre-warmed unmasking solution and microwaved for 30 min for antigen retrieval. Tissues were cooled for 10 min following microwave proteolysis. Humidified chambers were prepared using plastic slide boxes lined with damp paper towels. Broken, parallel glass stripettes were placed inside to act as slide racks. Slides were removed from the cooled unmasking solution and tissue samples were outlined using an ImmEDGE Hydrophobic Barrier PAP pen. Slides were then washed in TBST for 5 min. For chromogen-based detection stains, tissues were then blocked for 10 min with Dako Peroxidase blocking solution or Vectorlabs Bloxall solution to prevent endogenous peroxidase/alkaline

phosphatase activity. Slides were then washed again for 5 min and blocked for a further 10 min with 2X casein solution. All primary antibodies were diluted in TBST, pH 7.6. Working concentrations were optimised on a single tissue cases before batch staining of samples from multiple patients. After blocking, tissues were incubated with primary antibody for 1 hr, RT. Tissues were then washed as before in TBST and then incubated with an appropriate secondary antigen solution as per manufacturers instructors; HRP, ALP or fluorophore conjugated solutions (See table 2). Tissues were then washed twice with TBST. For fluorescent staining, tissues were then immediately mounted using Prolong gold antifade mounting reagent and glass coverslips. After the mountant had solidified, tissues were then imaged using a Zeiss 780 or 880 confocal microscope. For chromogen-based staining, tissues were then incubated with an appropriate chromogen, prepared according to manufacturer's instructions (e.g. IMMpact DAB). Chromogens were washed off with dH_20 and then counterstained with filtered Mayers haematoxylin for 30-40 sec. The counterstain was developed with hot water for 30 sec and then tissues underwent the following dehydration and clearing procedure:

- 2 x 3 min ddH20 in order to wash off excess alcohol and keep tissue sections hydrated.
- 3 x 3 min incubations in 99% industrial denatured alcohol (IDA)
- 3 x 3 min incubations in xylene

Tissues were then mounted with DPX mountant and glass coverslips. For non-xylene tolerant chromogens (e.g. StayGreen), xylene substitutes were used for 2 x 3 min and tissues were mounted with XTF in place of DPX. Once mountants had set, slides were imaged using a Zeiss AxioScan Z.1 slide scanner and then analysed using Zen and ImageJ software.

2.15 Quantification of multinucleation in tissue samples from HCC patients

Assessment of hepatocyte multinucleation was performed for tissues within a cohort of tissue samples from 43 consented patients with hepatocellular carcinoma (HCC) at the Queen Elizabeth Hospital, Birmingham, as part of the Birmingham, NHS trust. Tumour and normal tissues were available for 12 of these patients. Tissue sections from these patients were used to assess differences in multinucleation between tumour and non-tumour areas. Tissues were stained for hepatocyte nuclear factor 4 alpha (HNF4α) by IHC and were scanned using a Zeiss Axio SCAN.Z1 slide scanner. Random fields of view (FOVs) were captured at 20x magnification and a minimum of 1000 cells were assessed for multinucleation for each tissues section. The mean percentage of multinucleate cells was determined for each patient. Analysis and staining was performed by biomedical science undergraduate, Rukhsarr Ahmed.

Out of this same cohort of patients, 16 samples presented with interface hepatitis. This information was received from pathology reports. Areas of interface hepatitis were identified in HNF4α-stained section. Areas 5-hepatocytes thick were then outlined with increasing distance from the margin of the inflammatory infiltrate. The percentage of multinucleate hepatocytes was determined for each area. This analysis was performed by biomedical science undergraduate, Devinderjit Sangha.

All studies conducted using primary human liver sections were ethical approved by the Local Research Ethics Committee (LREC).

2.16 Gel electrophoresis and Western blotting

For polyacrylamide gel electrophoresis (PAGE), cells were lysed in 1x Lamelli buffer and frozen for storage. Acrylamide gels were made using the following 10 ml recipe:

Resolving (10%)		**Stacking (5%)**	
Reagent	**Volume (ml)**	**Reagent**	**Volume (ml)**
40% acrylamide	2.43	40% acrylamide	0.61
2% BIS-acrylamide	1.34	2% BIS-acrylamide	0.33
1M Tris pH 8.8	3.75	1M Tris pH 8.8	0.63
10% SDS	0.10	10% SDS	0.05
Distilled water	2.34	Distilled water	3.35
TEMED	0.01	TEMED	0.01
10% w/v APS	0.03	10% w/v APS	0.03

Samples were denatured at 95°C for 5 min and then loaded into the gel. Samples were resolved by SDS-PAGE; samples were run at a current of 40 mA and voltage of 100 V for enough time for samples to run through the gel (1.5 hr). Proteins were then transferred to (polyvinylidene difluoride) PVDF membranes using a Biorad semi-dry transfer system. A constant voltage of 25 V and current of 2.5 mA was used for 25 min. Membranes were then blocked in TBST containing 5% BSA (w/v) for 30 min. Membranes were then incubated with primary antibodies within the same blocking buffer. Incubations were contained within a 50 ml tube and placed on tube roller overnight at 4°C. Membranes were then washed 3 times with TBST and incubated with HRP-conjugated rabbit anti-mouse secondary antibody for 90 min at RT. Membranes were then treated with Clarity Western enhanced chemiluminescence (ECL) substrate according to manufacturer's guidelines and exposed to autoradiographic film.

2.17 Immunofluorescence staining

All cells were seeded on 13 mm glass cover slips for immunofluorescence staining. Preparation of cells was specific to individual antigens to be detected. In most cases, cells were labelled live with Celltracker Dyes prior to fixation. In these cases, nuclei were also labelled with Hoechst 33342 simultaneously with these cytoplasmic labels, at a concentration of 1 µg/ml. Cells were fixed prior to immunostaining in one of the following ways; the optimal fixation strategy was determined for each antigen/antibody, based on the largest and most representative signal achieved, prior to experimentation:

- -20°C, 100% MeOH – 5 min
- RT 3.7% formaldehyde – 10 min
- RT 1% paraformaldehyde

Cells were then washed in PBS and blocked for 30 min in staining buffer. Cells that were not fixed in MeOH, and therefore not permeabilised, were blocked in staining buffer containing 0.1% saponin. Primary antibodies were prepared in the same staining buffer at a previously optimised concentration (see section 2.1/table 1). Cells were incubated with primary antibody for 1 hr at RT, or 24 hr at -20°C. Cells were washed again in staining buffer and then incubated with secondary, fluorophore-conjugated antibodies in the same buffer at the appropriate dilution. Cells were then washed twice in PBS and mounted on to glass microscope slides using Prolong gold antifade mounting reagent. Coverslips were then imaged using a Zeiss 780 or 880 confocal microscope. Images requiring greater resolution or clarity were imaged using Airyscan technology available on the Zeiss 880 and were 3D volume rendered using bitplane IMARIS cell biology software.

2.18 Quantification of SCARF2 vesicles and SCARF2 vesicle MFI

Confocal images of Huh-7 cells, previously stained for SCARF2 by immunofluorescence, acquired using a Zeiss 880 confocal microscopy were uploaded into Bitplane IMARIS. The 'spots' tool was then used to analyse the total and nuclear populations of SCARF2 positive vesicles and obtain information regarding their number and mean fluorescence intensity (MFI). 10 cells were analysed from images taken across three individual experiments.

2.19 Scanning electron microscopy

Huh-7 hepatomas were seeded at a density of $5x10^4$ in 24-well plates on 12mm glass coverslips and allowed 24 hr to adhere. Huh-7s were then co-cultured with primary $CD4^+$ T cells, as described in section 2.8. T cells were either live, apoptotic, or heat-killed and prepared as described in section 2.7. Huh-7s received $2.5x10^5$ T cells/well. Cells were co-cultured for 4 hr to ensure a selection of cells at different stages of internalisation at the point for fixation. Cells were washed with PBS to removed excess, uncaptured T cells and then fixed in 2.5% glutaraldehyde for 24 hr. Cells were then imaged using a JSM-7000F (JEOL) SEM fitted with an Oxford Instruments Inca Energy Dispersive Spectroscopy (EDS) system.

2.20 Live, apoptotic and heat-kill cell kinetic comparison and long-term imaging

Huh-7 hepatomas were seeded at a density of $2.5x10^5$ in 24-well plates and allowed 24 hr to adhere. Huh-7 cells and primary $CD4^+$ T cells were labelled as described in section 2.6. All medias were replaced with prewarmed Iscove's Modified Dulbecco's Medium (IMDM)

containing ordinary media supplements (FBS, LG, NEAA, PS), as well as 25 mM (4-(2-hydroxyethyl)-1-piperazineethanesulfonic acid (HEPES). Spaces between wells were filled with 500 µl PBS as form of insulation and to maintain a humid environment throughout the culture period. $2.5x10^5$ live, apoptotic or heat-killed $CD4^+$ T cells were added on top of Huh-7s and co-cultured under normal conditions for an initial 1.5 hr. Cells were then transferred to a Cell-IQ time-lapse fluorescence imager. Images were taken every 30 min for 18 hr for 5 FOVs. For each timepoint, the number of internalised cells per 100 Huh-7 cells were determined by eye, which was assisted using the 'cell counting' plugin for ImageJ. Images were also combined to form movies and analysed to observe the activity of co-cultured cells over time.

2.21 Treg vs. Non-Treg experiments and live confocal imaging

For live confocal imaging of co-cultures, Huh-7 hepatomas were initially seeded at $1x10^5$ cells/well in glass-bottomed culture plates and allowed to adhere for 24 hr. The following day, $CD4^+$ T cells were isolated from HFE patients and separated into Treg and non-Treg cells, as described in section 2.4. Cells were then labelled with BMQC as described in section 2.6. A minimum of $2.5x10^5$ Tregs or non-Tregs were then added in wells on top of Huh-7s. Cells were co-cultured for 24 hr under normal culture conditions, in the presence of 10 µg/ml pHrodo red dextran in the media. Prior to imaging, normal culture conditions were established in the Zeiss 780/880 confocal microscope's incubation chamber. Cells were also labelled with 5 µM Cell Mask Deep Red as per manufacturer's instructions prior to imaging. Up to 5 z-stacks were taken per well at x63 magnification using the least possible digital zoom. The mean number of internalised, acidified T cells/ Huh-7 cell was then determined by eye, using the 'cell counting' plugin for ImageJ.

2.22 Statistics

All data was statistically analysed using (GraphPad) Prism software. All *in vitro* phagocytosis and live-cell capture assays were analysed using unpaired, two-tailed Students t tests. Numbers were obtained from 3 experimental replicates. Assessment of experimental parameters associated with NMLP and animal experiments (multinucleation, p21 and Ki67 stains, etc) were assessed using paired, two-tailed Students t tests. Standard error of the mean (SEM) was calculated for most experiments (unless stated otherwise) and expressed as error bars on plots.

Chapter 3: The mechanisms of hepatocyte efferocytosis

3.1 Introduction

As described previously, many epithelial cell types clear apoptotic and necrotic cells from the parenchyma (77, 80, 114). Amongst the studies concerning these non-professional phagocytes, historical publications describe the potential capacity for hepatocytes to engulf other cells (23, 147). In 1944, Rosin and Doljanski noticed the presence of erythrocytes within rat hepatocytes (23). Almost 50 years later, Dini and colleagues further described the presence of vesicles containing apoptotic cells in association with a collection of rat liver cells, including hepatocytes (147). This association was partially mediated through the asialoglycoprotein receptor 1 (ASGPR1), expressed by hepatocytes. The authors postulated that these vesicles contained the corpses of dying hepatocytes, which would be later consumed by neighbouring cells. The identity of these engulfing cells, however, remained elusive. Besides these studies, the primary focus of the literature for efferocytosis in the liver has laid with Kupffer cells (77, 212). Although the role of hepatocytes in the regulation of efferocytosis by Kupffer cells has been studied in depth (49), including the secretion of complement factors (213), their direct engagement of the process has been largely overlooked. As such, the molecular mechanisms, and consequences of hepatocyte efferocytosis are poorly understood.

It is likely that the ability of hepatocytes to capture dead cells is regulated by cytokines. In most tissues, efferocytosis is an intrinsic, necessary part of immunity. Dead cells must be removed from the environment to prevent the activation of an immune response and to

maintain the steady state. As such, the capacity of efferocytes to clear dead cells is commonly influenced by cytokine stimulation. Apoptotic cell clearance is generally augmented by stimulation with anti-inflammatory cytokines such as IL-10 and TGF-β (214, 215). Furthermore, it is frequently reported that engulfment of apoptotic cells alters the behaviour of efferocytosing cells, switching them more anti-inflammatory phenotypes (1, 216). As they are integral members of liver immunity, the capacity of hepatocytes to clear dead cells is likely to be altered by contrasting cytokine cues.

Another step towards understanding hepatocyte efferocytosis is to determine the receptors which are used by them to recognise dying cells. One possibility is ASGPR1, whose expression has already been reported on hepatocytes (147). ASPGR1 is a scavenger receptor which binds carbohydrates and has been reported to facilitate the trapping of T cells within the liver, which allows for their capture by Kupffer cells (147, 217). However, it's role in efferocytosis conducted directly by hepatocytes has not yet been explored. Several other scavenger receptors have been reported to bind dead cells and assist with their internalisation (87, 130, 218). Many of these receptors are expressed by hepatic cells, although their expression is largely limited, confined to Kupffer cells and LSECs, with very few of them shared with hepatocytes. A member of these is scavenger receptor family F, member 1 (SCARF1). This receptor is mostly composed of EGF and EGF-like domains. SCARF1 is expressed on HSEC and has also been shown to recognise apoptotic cells (130, 145). Although the absence of SCARF1 expression on hepatocytes was shown by Patten *et al*, 2017, the same authors described, in supplementary data, that they're able to express a close family member, SCARF2. Overall, the functions of SCARF2 are not fully understood, as previous studies regarding this scavenger receptor are limited. SCARF2 has been shown to scavenge acetylated low-density lipoproteins (ac-LDLs) and potentially interact directly with

SCARF1 (219). Additionally, mutations in *scarf2* have been linked to Van Den Ende-Gupta syndrome, although the reason for this is unknown (220, 221). No investigations have suggested that SCARF2 is a scavenger of dying cells. Work from Ramirez-Ortiz and colleagues even suggest that SCARF2 is incapable of recognising dead cells (130). However, these conclusions were drawn from cytokine reporter assays and not those directly assessing phagocytosis of dead cells. Such findings do not dismiss the possibility that SCARF2 could facility efferocytosis.

In this chapter, I will describe and discuss the investigations I undertook to understand how hepatocytes internalise dead cells.

3.2 Assay development for investigating hepatocyte efferocytosis

3.2.1 Development of apoptosis induction protocol

Efferocytosis encompasses all processes which involve the clearance of dying cells by other. However, not all cells are recognised and engulfed in the same manner. As previously described in section 1.3.2, different receptors on phagocytes are used to recognised apoptotic cells than those which recognise necrotic cells (79). The downstream consequences of each process are also often contrasting (1, 79, 139). As such, all observations made for hepatocyte capture of apoptotic cells cannot be extrapolated to necrotic cell engulfment. Therefore, it was necessary to study efferocytosis of both apoptotic and necrotic cells, as it would be likely that these would be alternatively regulated processes. A strategy was therefore required with which to induce these states in 'prey' cells. Necrosis is generally defined by a compromised cellular membrane, which can be replicated by heat-treatment (222, 223). This also ensures that all cells receive the same

level of damage. Various treatments are available with which to induce apoptosis in target cells (224). However, as apoptotic cells can progress to secondary necrosis, it was necessary to select a treatment which limits this progression. Staurosporine (STS) has been reported to be such a treatment (225); although its mode of action is not thoroughly understood, STS is known to act as a broad kinase inhibitor which induces apoptosis, whilst also limiting the progression of treated cells to secondary necrosis. Furthermore, effective strategies for apoptosis induction using STS have been published for T cell lymphomas called Jurkat cells (226). As previously mentioned in section 1.1.3, lymphocytes are frequently induced to undergo apoptosis upon entering the liver (24). T cells therefore represent a physiologically relevant candidate to be used as 'prey' cells within these assays. With this, I aimed to verify the use of STS to induce apoptosis in lymphocytes isolated from PBMCs (**Fig. 3A)**.

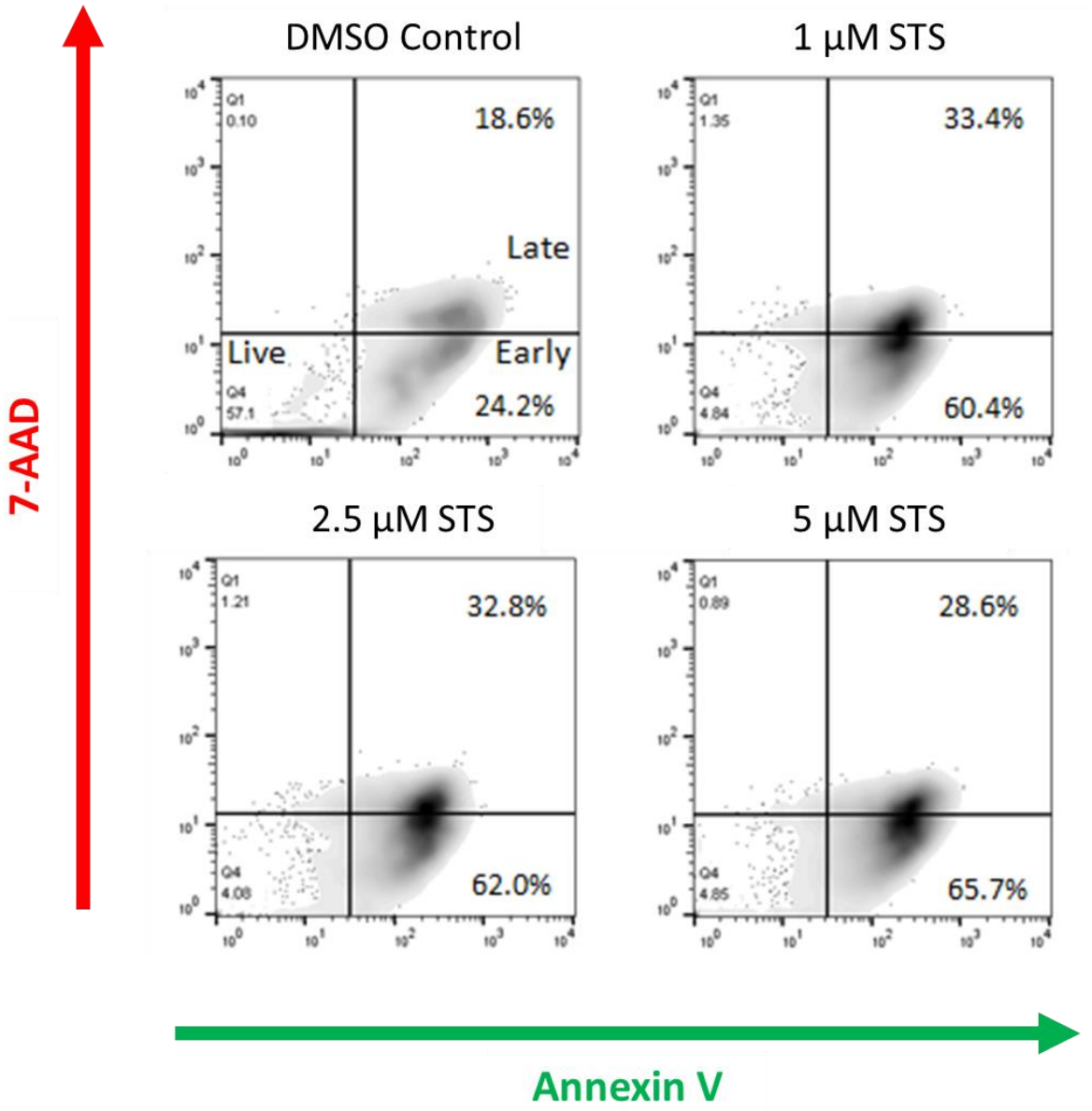

Figure 3A: Optimisation of Staurosporine (STS) treatment of primary CD4⁺ T cells for apoptosis induction. Primary human CD4⁺ T cells were treated with varying concentrations of Staurosporine (STS) for 4 hr. Cells were then labelled using the Biolegend apoptosis detection kit; Annexin V-Fluorescein isothiocyanate (FITC) and 7-Aminoactinomycin D (7-AAD). Cells were the analysed by flow cytometry using a Beckman Coulter Cyan ADP9 flow cytometer. Single positive cells for Annexin V represent apoptotic cells. Double positive cells represent secondary necrotic cells. N=1.

Human primary CD4⁺ lymphocytes were treated with varying concentrations of STS for 4 hr, as previously described (226). The proportion of apoptotic and secondarily necrotic cells after treatment was then determined by labelling cells with Fluorescein isothiocyanate (FITC)-labelled Annexin V (AV) and 7-Aminoactinomycin D (7-AAD). AV binds to PS on the

outer leaf of cell membranes, which is indicative of apoptotic cells. 7AAD is cell-impermeable and only labels necrotic cells which have a compromised membrane. It is thus possible to identify the stages of cell death amongst a population of cells by combining these two stains. All treatments induced comparable levels of apoptotic and secondary-necrotic cells. As such, the smallest concentration used, 1 μM, was selected for the induction of apoptosis in later experiments.

3.2.2 Selection of hepatocyte cell line for efferocytosis assays

To study the mechanisms and outcomes of hepatocyte efferocytosis, it was necessary to first select an *in vitro* assay for both quantification and molecular probing of efferocytosis. To select the most appropriate cell to use for future experiments, I observed the ability of 3 commonly-used hepatic cell lines to engulf dead cells; Huh-7s, HepG2s and Hep3Bs (227-229) . These were then co-cultured with apoptotic or heat-killed primary human T cells. All cell lines were cultured in multi-welled plates and were fluorescently labelled. Cells were then imaged using confocal microscopy (**Fig. 3B**). Complete internalisation of cells was confirmed through acquisition of confocal Z-stacks. All cell lines were capable of efferocytosis, which further establishes the ubiquitous nature of this phenomenon for hepatocytes. Huh-7s and Hep3Bs formed monolayers in culture, which assisted with confirming complete internalisation of dead cells. Reports have shown that Hep3Bs divide less frequently in culture due to reduced cyclin D1 expression and possess very few response pathways for common signalling pathways (230, 231), partially due to overactive NFκB activity and downregulated TGFβ-R (232). As such, Huh-7 cells were selected for *in vitro* representation of hepatocytes for this thesis.

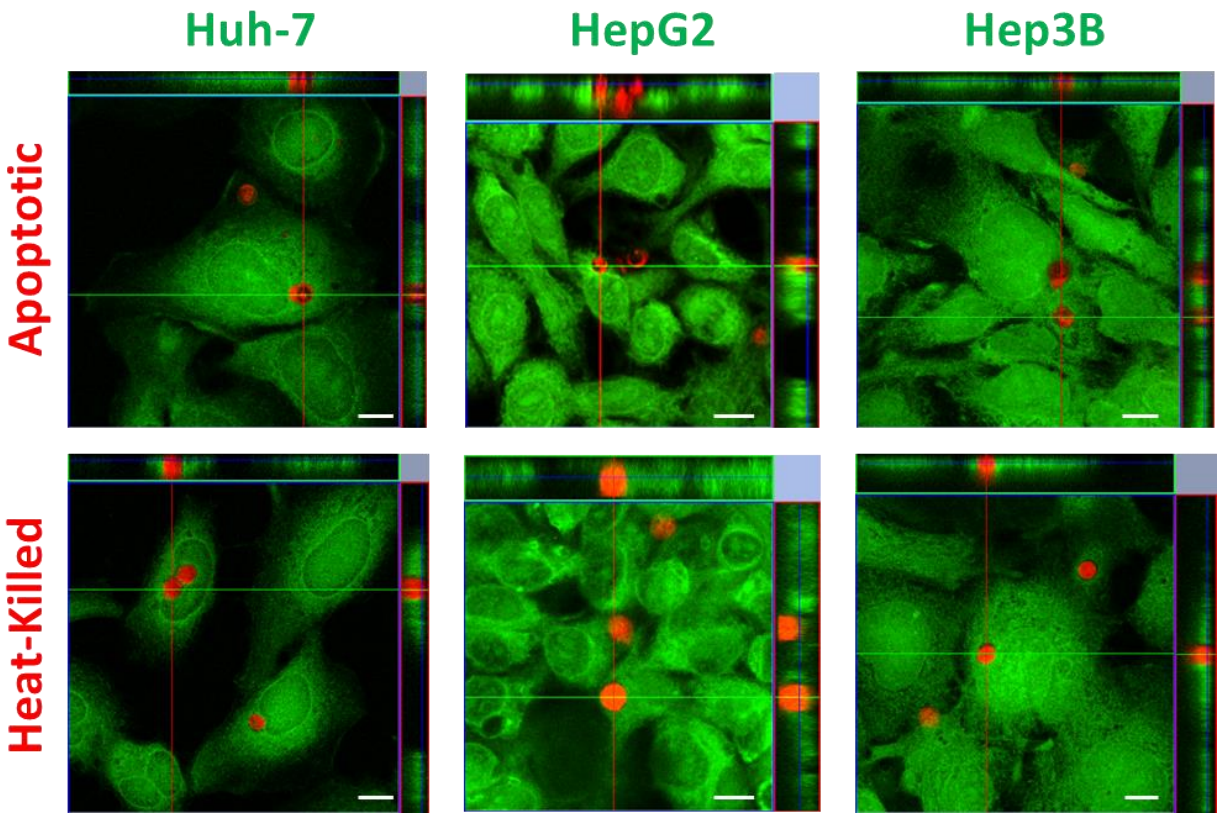

Figure 3B: Capture of apoptotic and heat-killed cells was conserved in three hepatocyte cancer cell lines. Orthographical images of hepatoma cell lines containing apoptotic or heat-killed $CD4^+$ T cells. Huh-7, HepG2 and Hep3B hepatomas were seeded in 24-well plates on glass coverslips and fluorescently labelled with Cell Tracker Green (CTG)/ Chloromethylfluorescein diacetate (CMFDA). Hepatomas were then co-cultured with primary $CD4^+$ T cells, labelled with Cell Tracker Red (CTR)/CMTPX, which were either apoptotic via staurosporine (STS) treatment or heat-killed (necrotic), for 3 hr. Cells were then fixed with MeOH and then imaged by confocal microscopy using a Zeiss LSM Zeiss 880. Z-stacks were acquired to confirm complete internalisation of T cells. Scale bars represent 10 µm.

3.3 The mechanisms of efferocytosis by hepatocytes

3.3.1 Hepatocyte efferocytosis was modulated by cytokines

To investigate the effect of cytokines on hepatocyte efferocytosis, Huh-7 cells were pre-treated for 1 hr with cytokines known to be relevant in the establishment and resolution of liver inflammation. These cells were then co-cultured with apoptotic or heat-killed (necrotic) cells (**Fig. 3C**). Cells were also treated with insulin-like growth factor-1 (IGF-1) which, when secreted by actively efferocytosing macrophages, was reported to reduce the capacity of neighbouring airway epithelial cells to engulf apoptotic cells (118). Huh-7s were initially serum starved to reverse effects induced by FBS-derived cytokines. Cells were then imaged using confocal microscopy and the frequency of efferosomes found within hepatomas was quantified. Apoptotic cell capture was significantly increased by TGF-β treatment and decreased by the pro-inflammatory cytokine, IL-1β. However, contrary to this, IL-10 also caused a decrease in apoptotic cell capture. Other cytokines did not alter apoptotic cell capture. Heat-killed cell capture was augmented by cytokines with contrasting immunological functions. The pro-inflammatory cytokine, interferon-gamma (IFN-γ) increased the capture of heat-killed cells by 50%. Similar increases were not seen in response to cytokines with related functions, like tumour necrosis factor-alpha (TNF-α) and IL-1β. Contradictory to this, heat-killed cell capture was also augmented by anti-inflammatory cytokines IL-10 and TGF-β, although not to the same degree as IFN-γ-treated Huh-7s. IGF-1 treatment had no effect of hepatocyte efferocytosis. Together, these data suggest show that apoptotic cell capture was altered by alternative cytokines compared to necrotic cell capture, the exception being TGF-β, which augmented both apoptotic and necrotic cell capture.

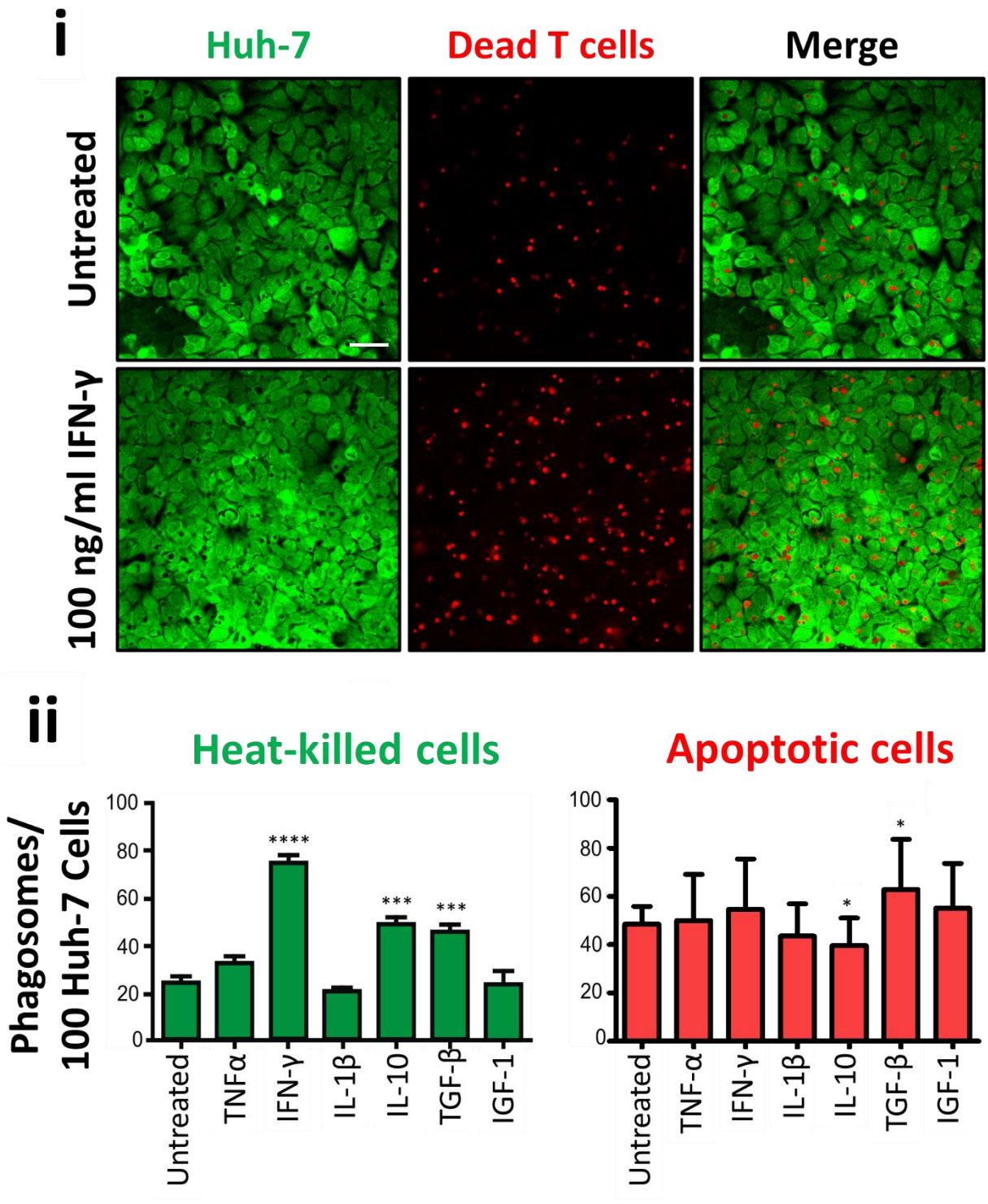
i
Huh-7
Dead T cells
Merge
Untreated
100 ng/ml IFN-γ
ii
Heat-killed cells
Apoptotic cells
Phagosomes/
100 Huh-7 Cells
100
80
60
40
20
0
****
***
***
*
*
Untreated
TNFα
IFN-γ
IL-1β
IL-10
TGF-β
IGF-1
TNF-α

Figure 3C: Capture of apoptotic and heat-killed CD4$^+$ T cells by hepatomas was modulated by cytokines. Huh-7 hepatomas seeded in 24-well plates on glass coverslips were fluorescently labelled with Cell Tracker Green (CTG)(CMFDA. Huh-7s were then serum starved and treated with 100 ng/ml cytokines for 1 hr. Huh-7s were then co-cultured with Celltracker Red (CTR)/CMTPX-labelled primary human CD4$^+$ T cells. T cells were either made apoptotic, via staurosporine (STS) treatment, or were heat-killed (necrotic) prior to co-culture. Cells were cultured in the presence of cytokines, for 3 hr, fixed with MeOH, and then imaged by confocal microscopy using a Zeiss LSM 880 microscope. **(i)** Confocal micrographs of untreated and IFN-γ-treated Huh-7s conducting efferocytosis. **(ii)** Quantification of the number of phagosomes per 100 Huh-7 cells for each cytokine treatment. Numbers were obtained using 5 fields of view (FOV), taken from three independent experiments (N=3). Statistics were derived from a two-tailed, unpaired Student's t-test when comparing other treatments to the control. * - ≤0.05, *** - p≤0.001, **** - p≤0.0001. Scale bars represent 50 µm. Error bars represent the standard error of the mean (SEM). IFN-γ – interferon-gamma; IL – interleukin; TGF-β – tumour growth factor-beta. Data set was partially acquired from work conducted by intercalating medical student, Nick Weight, and Nuffield Foundation work experience student, Nish Rai.

3.3.2 Hepatocyte efferocytosis was reduced by molecular inhibitors of actin polymerisation and macropinocytosis

The molecular mechanisms regarding the cytoskeletal rearrangements associated with efferocytosis have been well characterised for professional phagocytes (233). Such details are not known for efferocytosis conducted by hepatocytes. To gain an initial understanding as to how hepatocytes perform efferocytosis, Huh-7 hepatoma cells were treated with commonly-used inhibitors of similar forms of endocytosis (**Fig. 3D**). These included verified inhibitors of macropinocytosis (234, 235), blebbistatin (234, 236, 237) and 5-(N-Ethyl-N-Isopropyl) amiloride (EIPA) (234, 236, 238, 239). Huh-7 cells were also treated with the Phosphoinositide 3-kinase (PI3K) inhibitor, Wortmannin, as well as an inhibitor of Rho-associated protein kinase (ROCK), H-1152, which have both been reported to inhibit Fc-receptor (FcR) mediated phagocytosis by preventing phagosome sealing in macrophages (240, 241). These inhibitors were only given to Huh-7s receiving heat-killed cells, as apoptotic cells are not normally detected using FcRs (see section 1.3). Cytochalasin D was used as a positive control as it is a known global inhibitor of *de novo* actin polymerisation

and cytoskeletal movement (242). As expected, capture of apoptotic and heat-killed cells was significantly reduced in response to cytochalasin D treatment (**Fig. 3Dii**). Wortmannin and H-1152 induced no significant alteration to heat-killed cell efferocytosis. In contrast, macropinocytosis inhibitors caused significant reductions to both heat-killed and apoptotic cell capture by Huh-7s. EIPA was particularly effective in blocking heat-killed cell capture, ablating efferocytosis more efficiently that cytochalasin D treatment. Together, these data showed that total hepatocyte efferocytosis was susceptible to global inhibitors of macropinocytosis.

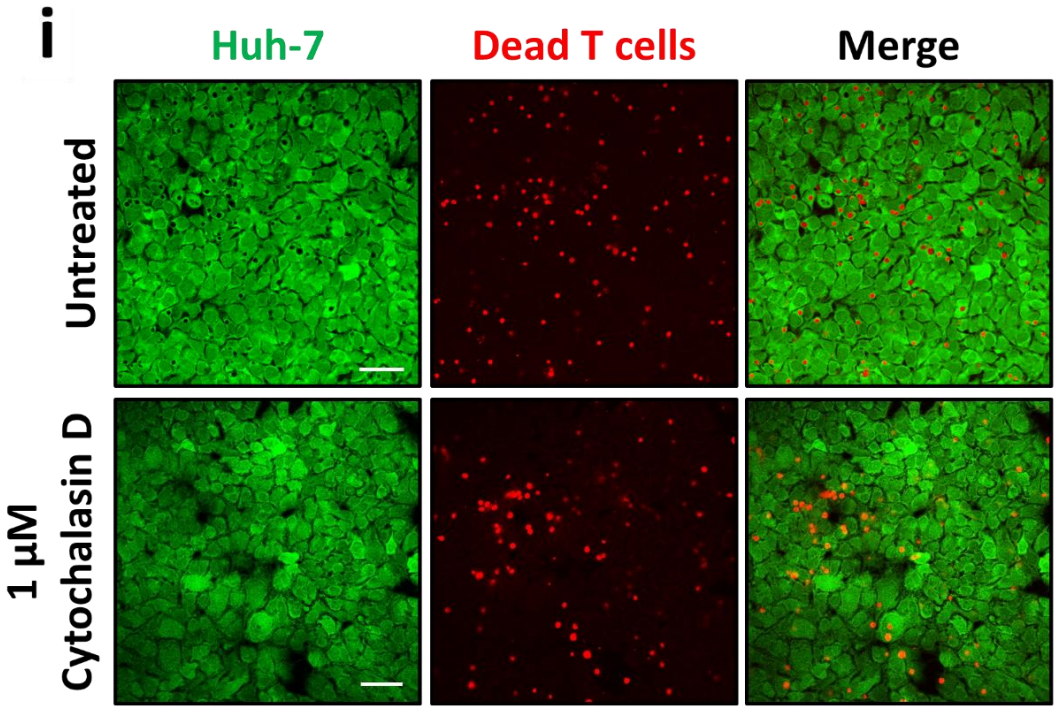
i
Huh-7
Dead T cells
Merge
Untreated
1 µM Cytochalasin D

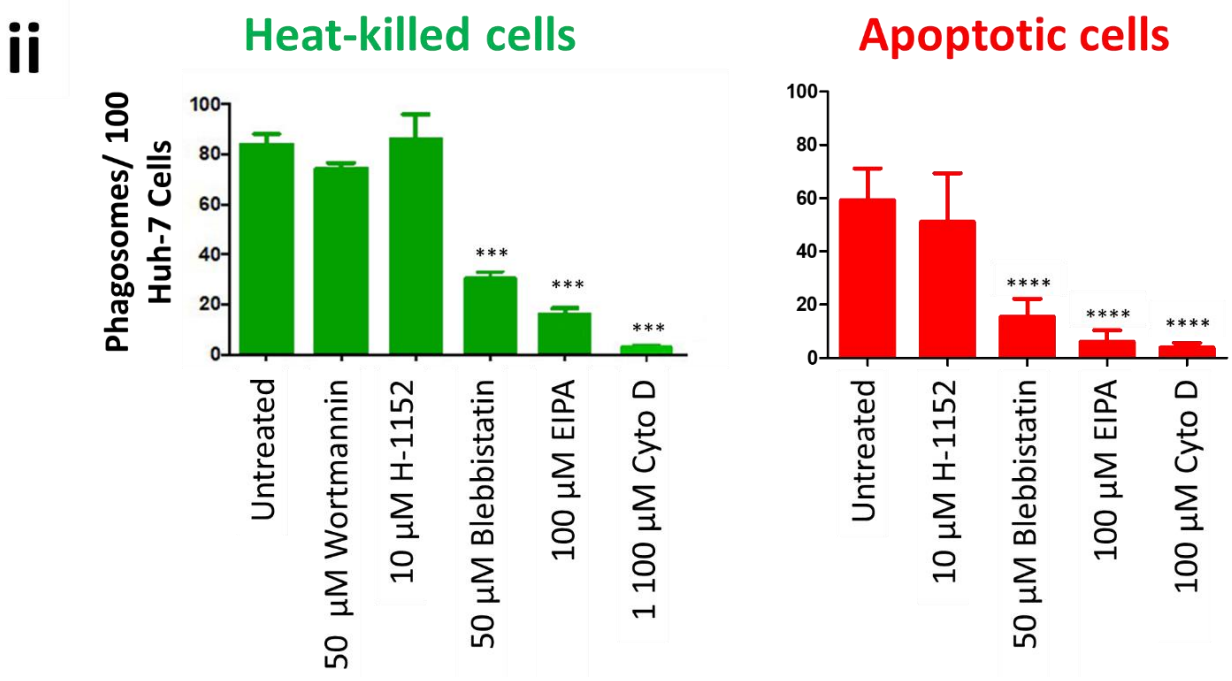
ii
Heat-killed cells
Apoptotic cells
Phagosomes/ 100 Huh-7 Cells
100
80
60
40
20
0
***
***
***
****
****
****
Untreated
50 µM Wortmannin
10 µM H-1152
50 µM Blebbistatin
100 µM EIPA
1 100 µM Cyto D
Untreated
10 µM H-1152
50 µM Blebbistatin
100 µM EIPA
100 µM Cyto D

Figure 3D: Capture of apoptotic and heat-killed CD4$^+$ T cells by hepatomas was modulated molecular inhibitors. Huh-7 hepatomas seeded in 24-well plates on glass coverslips were fluorescently labelled with Cell Tracker Green (CTG)/ CMFDA. Huh-7s were then serum starved and treated with molecular inhibitors, at concentrations indicated, for 1 hr. Huh-7s were then co-cultured with Celltracker Red (CTR)/CMTPX-labelled primary human CD4$^+$ T cells. T cells were either made apoptotic, via staurosporine (STS) treatment, or were heat-killed (necrotic) prior to co-culture. Cells were cultured in the presence of cytokines, for 3 hr, fixed with MeOH, and then imaged by confocal microscopy using a Zeiss LSM 880 microscope. **(i)** Confocal micrographs of untreated and cytochalasin D-treated Huh-7s conducting efferocytosis. **(ii)** Quantification of the number of phagosomes per 100 Huh-7 cells for each cytokine treatment. Numbers were obtained using 5 fields of view (FOV), taken from three independent experiments (N=3). Statistics were derived from a two-tailed, unpaired Student's t-test when comparing other treatments to the control. * - ≤0.05, *** - p≤0.001, **** - p≤0.0001 **i)** confocal micrographs of untreated and IFN-γ-treated Huh-7s undergoing efferocytosis. Scale bars represent 50 µm. Error bars represent the SEM. Cyto D – cytochalasin D; EIPA - 5-(N-Ethyl-N-Isopropyl) amiloride.

3.4 Recognition of dead cells by hepatocytes

3.4.1 Screening of possible receptors for dead cells

The number of candidate receptors which may be responsible for recognition of dead cells by hepatocytes is limited. Several receptors with varying primary functions can often recognise dead cells as a secondary function (87). These include adhesion molecules, which are normally concerned with leukocyte recruitment, as well as scavenger receptors that often bind dead cells via PS opsonising molecules (243). I hypothesised that molecules within these categories that are expressed by hepatocytes could play roles in efferocytosis. To test this, immunofluorescence staining of efferocytosing Huh-7 cells was performed for adhesion molecules or scavenger receptors whose expression had previously been reported for hepatocytes (**Fig. 3E-F**). These included ICAM-1 (28, 244, 245) and ASGPR1 (147, 217). Cells were fixed with the permeabilising fixative, MeOH, and imaged by confocal microscopy, using Z-stacks to confirm complete internalisation of dead cell. Images were also 3D volume rendered to show to distribution of the molecule that was stained for, in relation to internalised cells. ICAM-1 staining was enriched around the base of adhered apoptotic cells

forming a cup-like structure (**Fig. 3Eiii**). However, vesicles containing fully internalised apoptotic cells were not enriched for ICAM-1 (**Fig. 3Ei-iii**). Necrotic cells showed no enrichment with ICAM-1(**Fig. 3Eiv-vi**). Similar localisation observed for ICAM-1 was also observed for ASGPR1 in relation to captured heat-killed cells (**Fig. 3F**). Partially engulfed heat-killed Jurkat cells possessed halos/cup-like structures which stained positively for ASGPR1. This highlights a potential role of ICAM-1 and ASPGR1 in the initial adhesion step of dead cell capture.

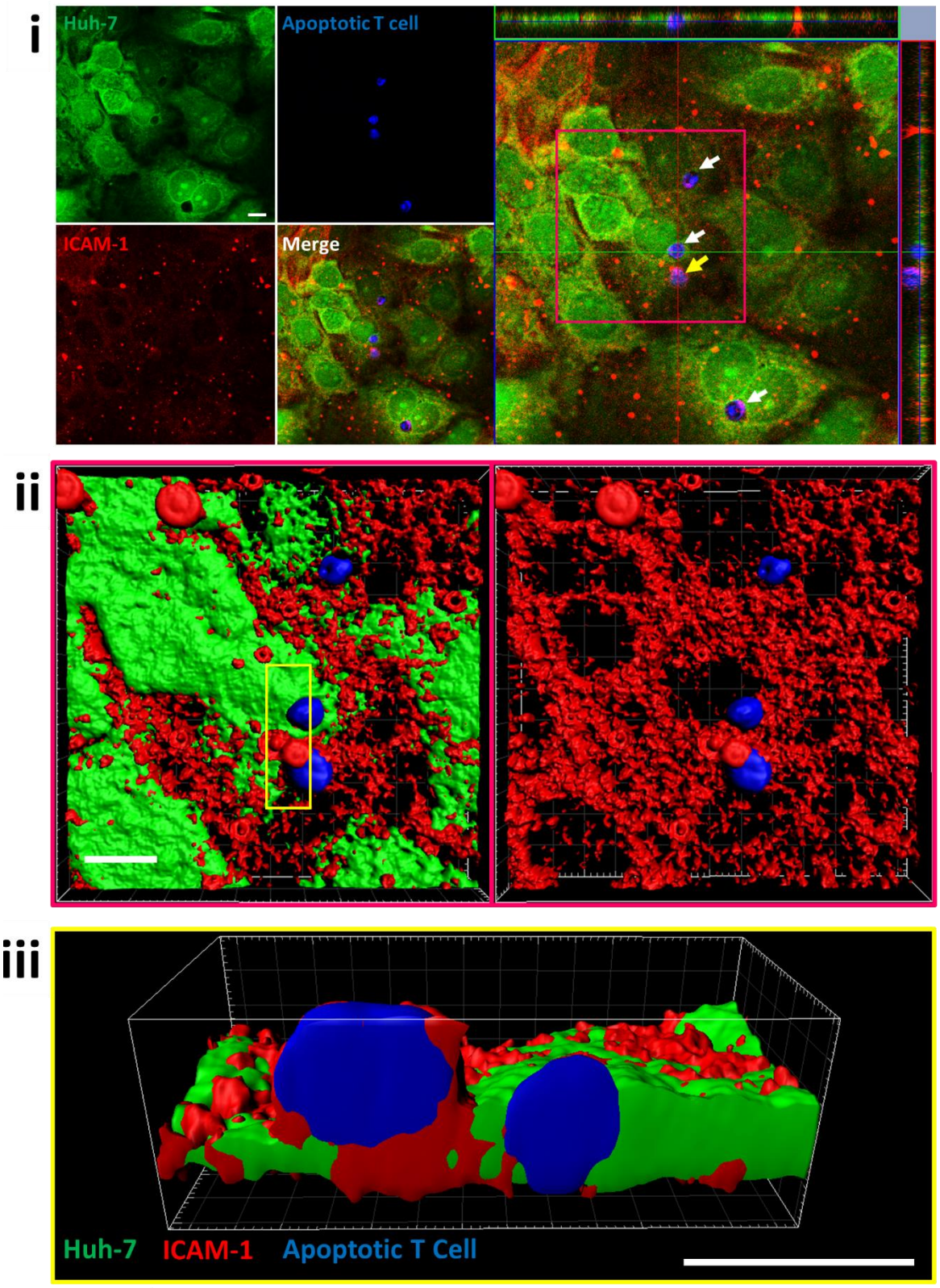
i
Huh-7
Apoptotic T cell
ICAM-1
Merge
ii
iii
Huh-7
ICAM-1
Apoptotic T Cell

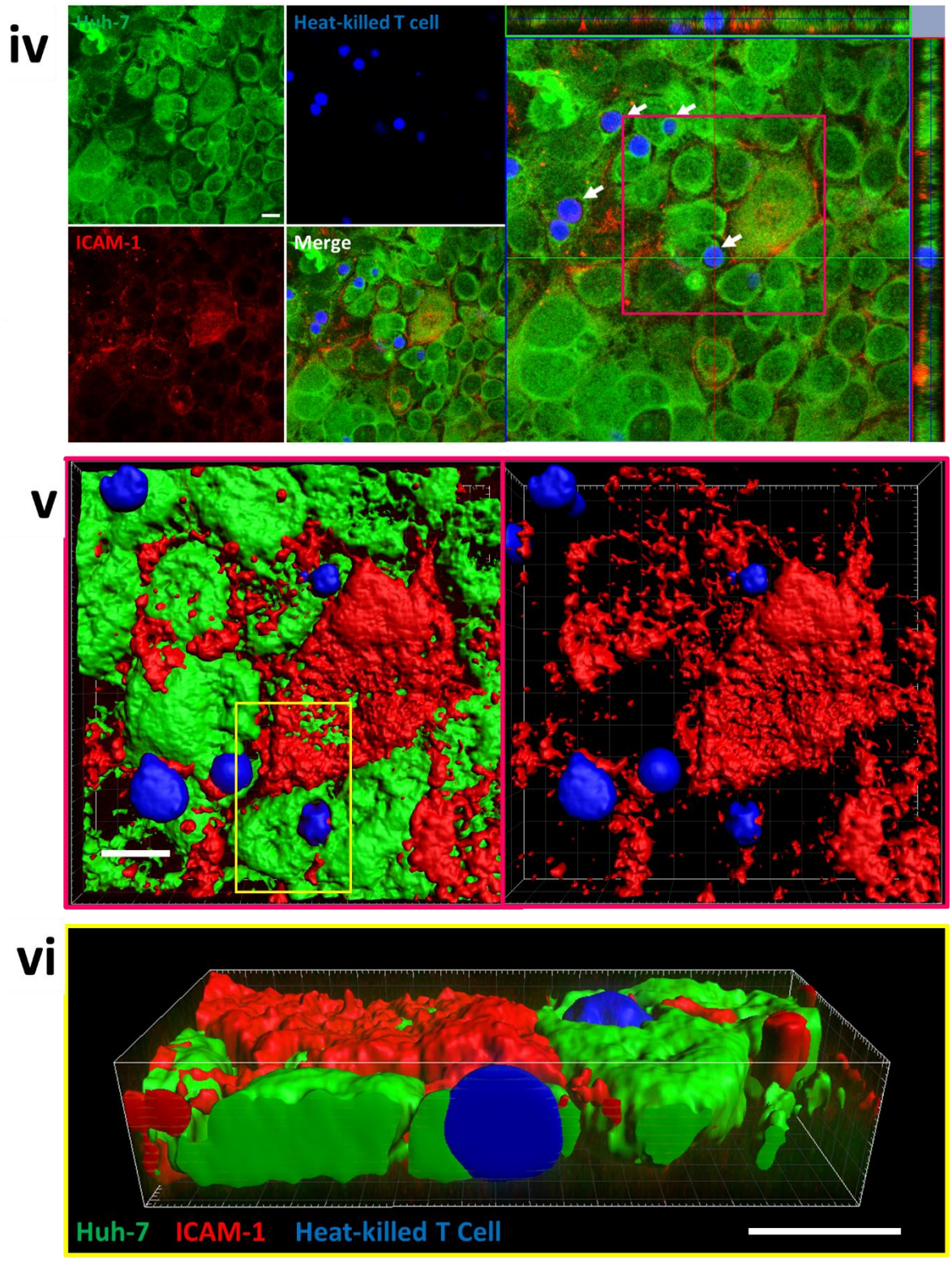
iv
Huh-7
Heat-killed T cell
ICAM-1
Merge
v
vi
Huh-7
ICAM-1
Heat-killed T Cell

Figure 3E: Apoptotic and heat-killed CD4$^+$ T cells captured by Huh-7 hepatomas did not associate with ICAM-1. Huh-7 hepatomas seeded in 24-well plates on glass coverslips were fluorescently labelled with Cell Tracker Green (CTG)/CMFDA. Huh-7s were then co-cultured with primary human CD4$^+$ T cells, labelled with Cell Tracker Violet (CTV)/ bromomethyl derivative of coumarin (BMQC). T cells were either apoptotic **(i-iii)** via staurosporine (STS) treatment, or heat-killed (necrotic) **(iv-vi)**. Cells were co-cultured for 3 hr, fixed with MeOH and stained for intercellular adhesion molecule 1 (ICAM-1) via immunofluorescence (shown in red). Cells were then imaged by confocal microscopy using a Zeiss LSM 880 microscope. Z-stacks were acquired to confirm complete internalisation of T cells. **(i$^+$iv)** Confocal micrographs of Huh-7 hepatomas (green) efferocytosing dead T cells (blue). Orthographical image (right) shows complete internalisation of cells. White arrows show fully internalised cells. Yellow arrows show adhered cells. **(ii$^+$v)** 3D renderings, generated with Bitplane IMARIS, of selected regions shown in previous images (indicated by pink box in **i/iv**). **(iii$^+$vi)** Cross-section of 3D-rendered image made using a plane which cuts through internalised T cells, indicated by yellow box in middle panels. Images are representative of 3 independent experiments. All scale bars represent 10 µm. Stains using mouse IgG1 isotype-matched control (IMC) can be found in the appendix, **Figure A1**.

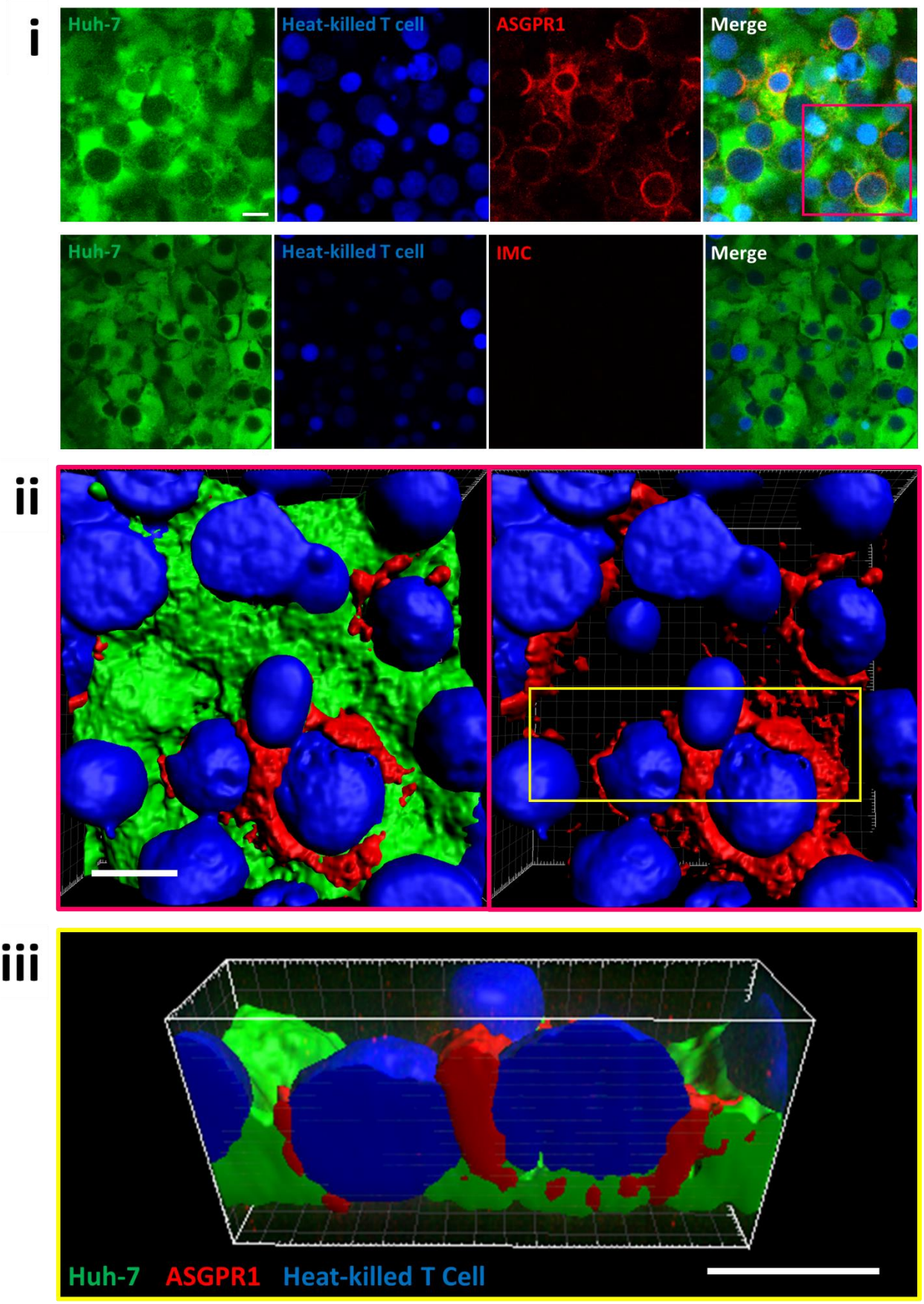
i
Huh-7
Heat-killed T cell
ASGPR1
Merge
Huh-7
Heat-killed T cell
IMC
Merge
ii
iii
Huh-7
ASGPR1
Heat-killed T Cell

Figure 3F: – Adhered heat-killed $CD4^+$ T cells associated with ASGPR1 on Huh-7 hepatomas. Huh-7 hepatomas seeded in 24-well plates on glass coverslips were fluorescently labelled with Cell Tracker Green (CTG)/ Chloromethylfluorescein diacetate (CMFDA). Huh-7s were then co-cultured with heat-killed (necrotic) Jurkat T cell lymphomas, labelled with Cell Tracker Violet (CTV)/ bromomethyl derivative of coumarin (BMQC). Cells were co-cultured for 3 hr, fixed with MeOH and stained for asialoglycoprotein receptor 1 (ASGPR1) via immunofluorescence (shown in red). Cells were then imaged by confocal microscopy using a Zeiss LSM 880 microscope. Z-stacks were acquired to confirm complete internalisation of T cells. **(i)** Confocal micrographs of Huh-7 hepatomas (green) efferocytosing dead T cells (blue), stained using anti- ASGPR1 antibody or a Rabbit IgG isotype-matched control (IMC). **(ii$^+$v)** 3D renderings, generated with Bitplane IMARIS, of selected regions shown in previous images (indicated by pink box in **i/iv**). **(iii$^+$vi)** Cross-section of 3D-rendered image made using a plane which cuts through internalised T cells, indicated by yellow box in middle panels. Images are representative of 3 independent experiments. All scale bars represent 10 µm. Non-rendered images were contributed by intercalated medical student, Ratnam Gandhi.

3.4.2 Scavenger receptor family F, member 2 (SCARF2) associates with engulfed dead cells in hepatocytes

Previous reports have suggested that hepatocytes express the scavenger receptor, SCARF2 (145). Details in this report regarding its distribution were limited. Additionally, the function of SCARF2 in hepatocytes has never been investigated. As such, I set out to examine the localisation of SCARF2 on hepatocytes and hepatomas alike. Immunohistochemistry staining of donor liver tissue revealed consistent expression of SCARF2 across hepatocytes (**Fig. 3G**). Its expression was often enriched at junctions between hepatocytes. Furthermore, several hepatocytes possessed large SCARF2-positive intracellular structures adjacent to their negatively-stained nucleus. This confirmed the expression of SCARF2 on hepatocytes *in vivo*.

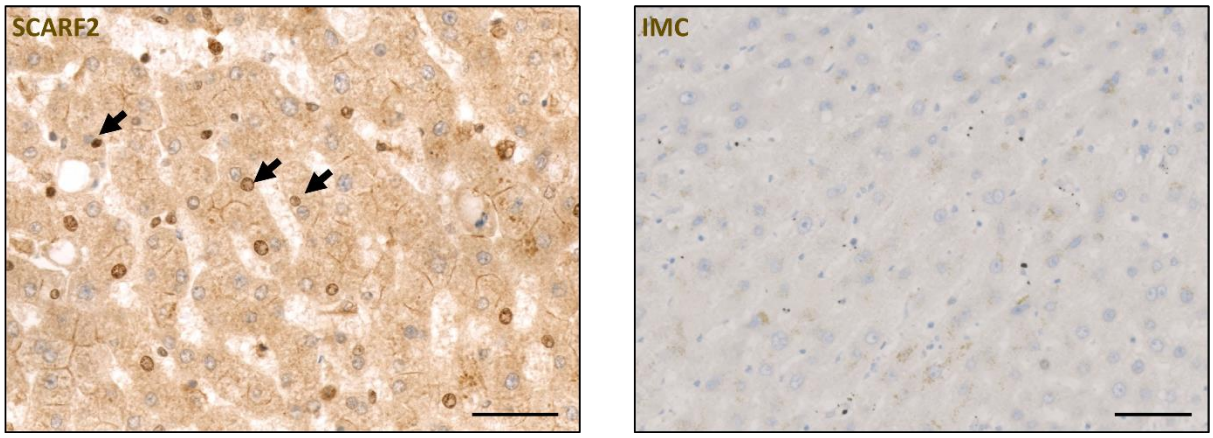

Figure 3G: Hepatocytes expressed SCARF2 *in vivo* in donor liver tissue. Immunohistochemistry (IHC) staining of paraffin-embedded donor liver tissue scavenger receptor family f, member 2 (SCARF2), shown in in brown. Tissues were also stained using a Rabbit IgG, isotype-matched control (IMC). Tissues were counterstained with Mayers haematoxylin nuclear stain (blue). Black arrows indicate SCARF2-positive structures within hepatocytes that also possess SCARF2-negative nuclei. Scale bars represent 50 µm.

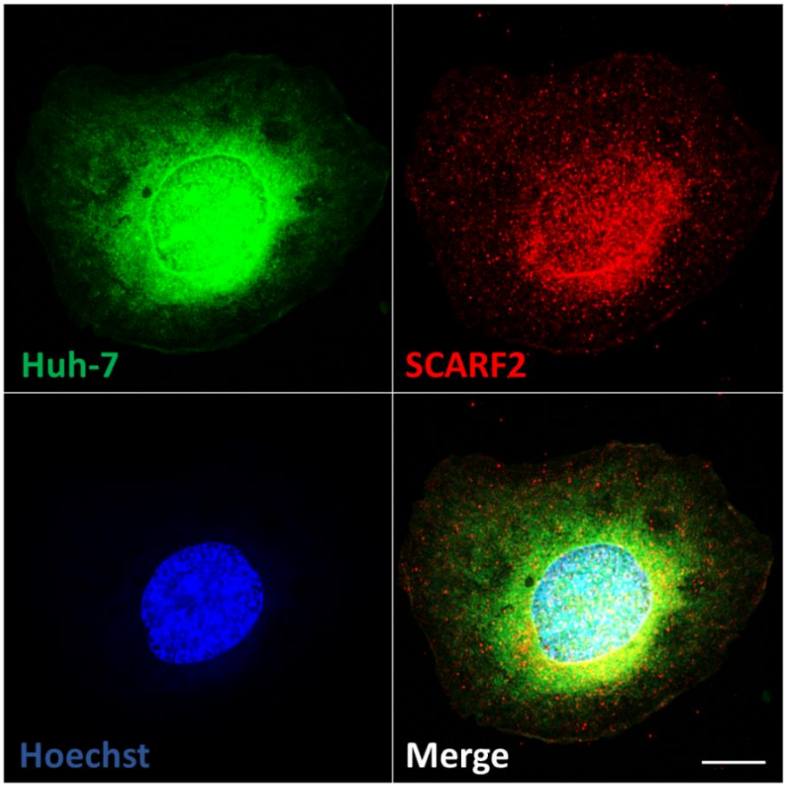

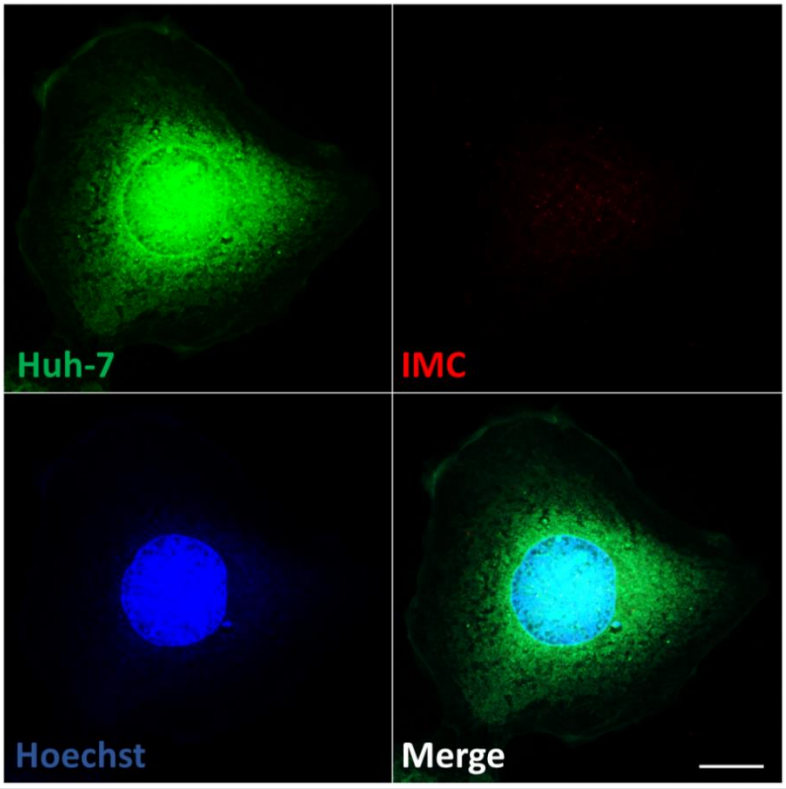

Figure 3H: Huh-7 hepatomas expressed SCARF2 in vesicles within the nucleus and perinuclear spaces. Huh-7 hepatomas seeded in 24-well plates on glass coverslips were fluorescently labelled with Cell Tracker Green (CTG)/ CMDFAand Hoechst 33342 (blue). Cells were then fixed with MeOH and stained for scavenger receptor family f, member 2 (SCARF2) or a Rabbit IgG isotype-matched control (IMC) via immunofluorescence (shown in red). Cells were then imaged by confocal microscopy using a Zeiss LSM 880 microscope. Scale bars represent 10 µm.

To confirm whether the expression and distribution of SCARF2 was conserved in hepatocyte cell lines, immunofluorescence staining was performed of labelled Huh-7 hepatomas (**Fig. 3H**). Positive staining was seen mostly in the nucleus and perinuclear compartments. Vesicular-like staining was also seen in cytoplasmic spaces. The vesicles ranged from 0.2-1.3 μm^2 in area, which was consistent both within and outside of the nucleus. I next stained Huh-7 hepatomas which had been previously co-cultured with heat-killed or apoptotic primary T cells, which had been fluorescently labelled (**Fig. 3I**). These cells were then imaged by confocal microscopy, whilst acquiring Z-stacks. It was frequently observed that SCARF2 expression was enriched at areas surrounding both internalised heat-killed and apoptotic cells (**Fig. 3Ii**). 3D volume rendering of immunofluorescence stains further revealed that internalised apoptotic and necrotic $CD4^+$ T cells within hepatomas were fully enclosed in SCARF2-positive vesicles (**Fig. 3Ii**). Non-internalised T cells were not positively stained for SCARF2. Aggregation of SCARF2 around the phagosome was also seen in apoptotic cells adhered to HepG2 cells (**Fig. 3Iii**), which shows the conservation of this interaction across different hepatocyte cell lines. Together, these observations suggest that SCARF2 may play a role in hepatocyte efferocytosis.

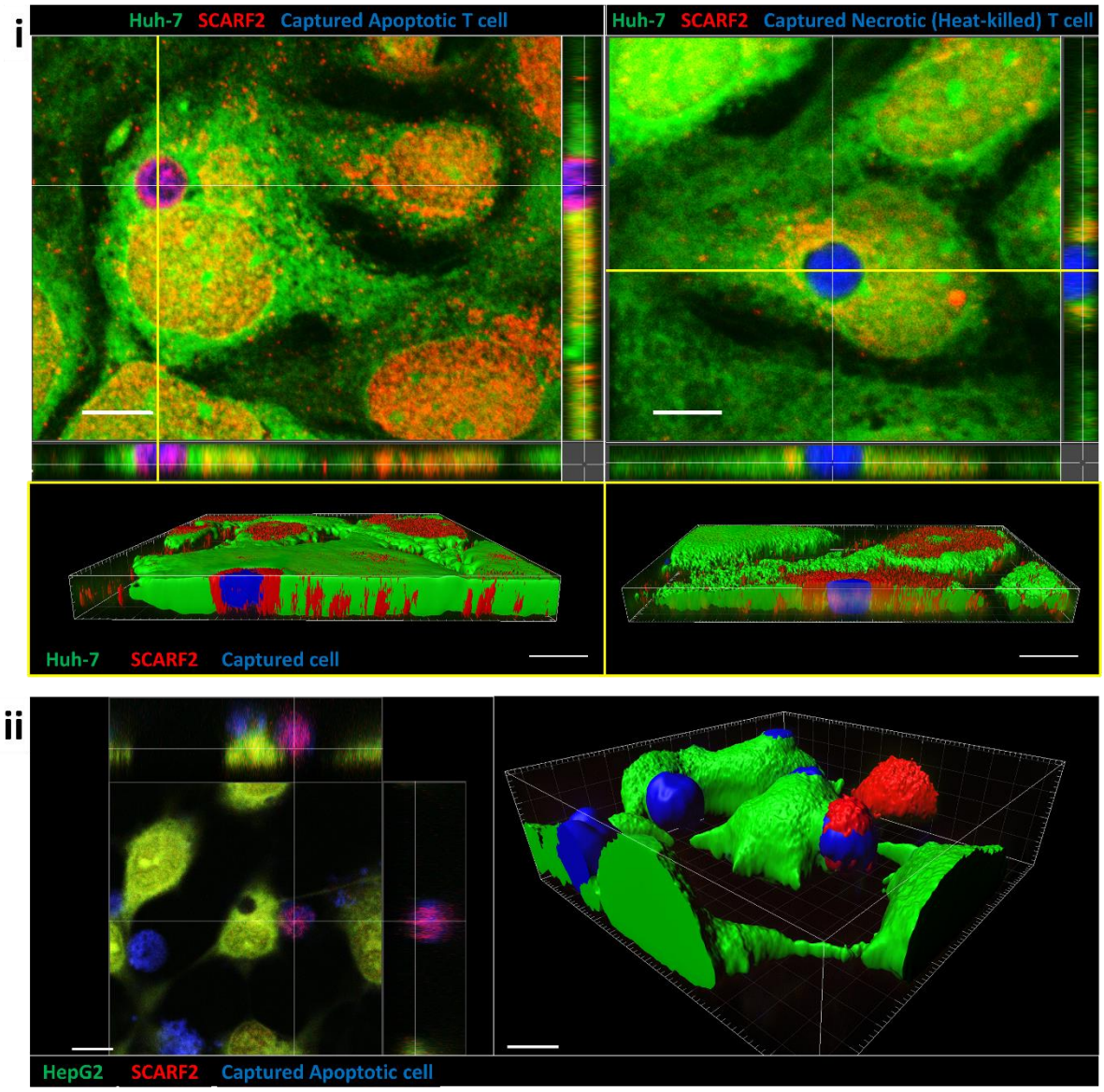

Figure 3I: Phagosomes containing apoptotic or heat-killed CD4⁺ T cells associated with SCARF2 in Huh-7 and HepG2 cells. Huh-7 **(i)** or HepG2 cells **(ii)** seeded in 24-well plates on glass coverslips were fluorescently labelled with Cell Tracker Green (CTG)/ Chloromethylfluorescein diacetate (CMFDA). Huh-7s were then co-cultured with primary human CD4⁺ T cells, labelled with Cell Tracker Violet (CTV)/ bromomethyl derivative of coumarin (BMQC). T cells were either apoptotic via staurosporine (STS) treatment, or heat-killed (necrotic). Cells were co-cultured for 3 hr. Cells were then fixed with MeOH and stained for scavenger receptor family f, member 2 (SCARF2) via immunofluorescence (shown in red). Cells were then imaged by confocal microscopy using a Zeiss LSM 880, in which Z-stacks were acquired. Images were also 3D volume rendered using Bitplane IMARIS software. **(i)** Top: orthographical image showing SCARF2-stained Huh-7 cells (green) possessing fully internalised apoptotic or heat-killed T cells (blue). Bottom: cross-sections made using a plane which cuts through the internalised T cell, indicated by yellow line on top panels. **(ii)** Orthographical and 3D-rendered images of SCARF2-stained HepG2 cells cultured with apoptotic T cells. Images are representative of 3 independent experiments. All scale bars represent 10 µm.

3.4.3 The cellular distribution of SCARF2 was altered in hepatomas in response to cytokine stimulation

Immunofluorescence staining of actively efferocytosing hepatomas revealed that SCARF2 relocates to the perimeter of efferosomes. This suggests an active role for SCARF2 in hepatocyte efferocytosis. To investigate the regulation of this vesicular relocation, immunofluorescence staining was performed of Huh-7 cells following a 1 hr treatment with cytokines that were used in previous sections to study their effect on the frequency of efferocytosis (**Fig. 3J**). Huh-7s were also treated with EIPA, as this was previously shown to significantly inhibit efferocytosis in hepatomas. Cells were stained for SCARF2 and imaged using confocal microscopy. The proportion of SCARF2-positive vesicles found in cytoplasmic regions appeared to increase in response to treatments, aside from TNF-α. To confirm this, the distribution of SCARF2-positive vesicles was then analysed using Bitplane IMARIS software (**Fig. 3Jii**)**.** The percentage of non-nuclear SCARF2 vesicles was significantly increased by IFN-γ and IL-10 treatments. The latter cells also displayed increased expression of SCARF2 at the perimeter of their membranes. These results showed that SCARF2 localisation could be influenced by certain cytokines expression and can be altered through cytokine stimulation.

To determine if this shift in the distribution of SCARF2 vesicles was concurrent with an alteration in expression, the mean fluorescent intensities (MFI) of vesicles within previously-treated Huh-7 cells were acquired using Bitplane IMARIS software (**Fig. 3K**). These values were used to approximate SCARF2 expression. Highly significant increases in SCARF2 vesicles MFIs were observed in EIPA-treated cells (**Fig. 3Ki**). A more modest increase was also induced in response to IFN-γ. Other treatments did not affect SCARF2 vesicle MFI. Further, the cytoplasmic:nuclear ratio of vesicle MFI was not altered in response to any treatment.

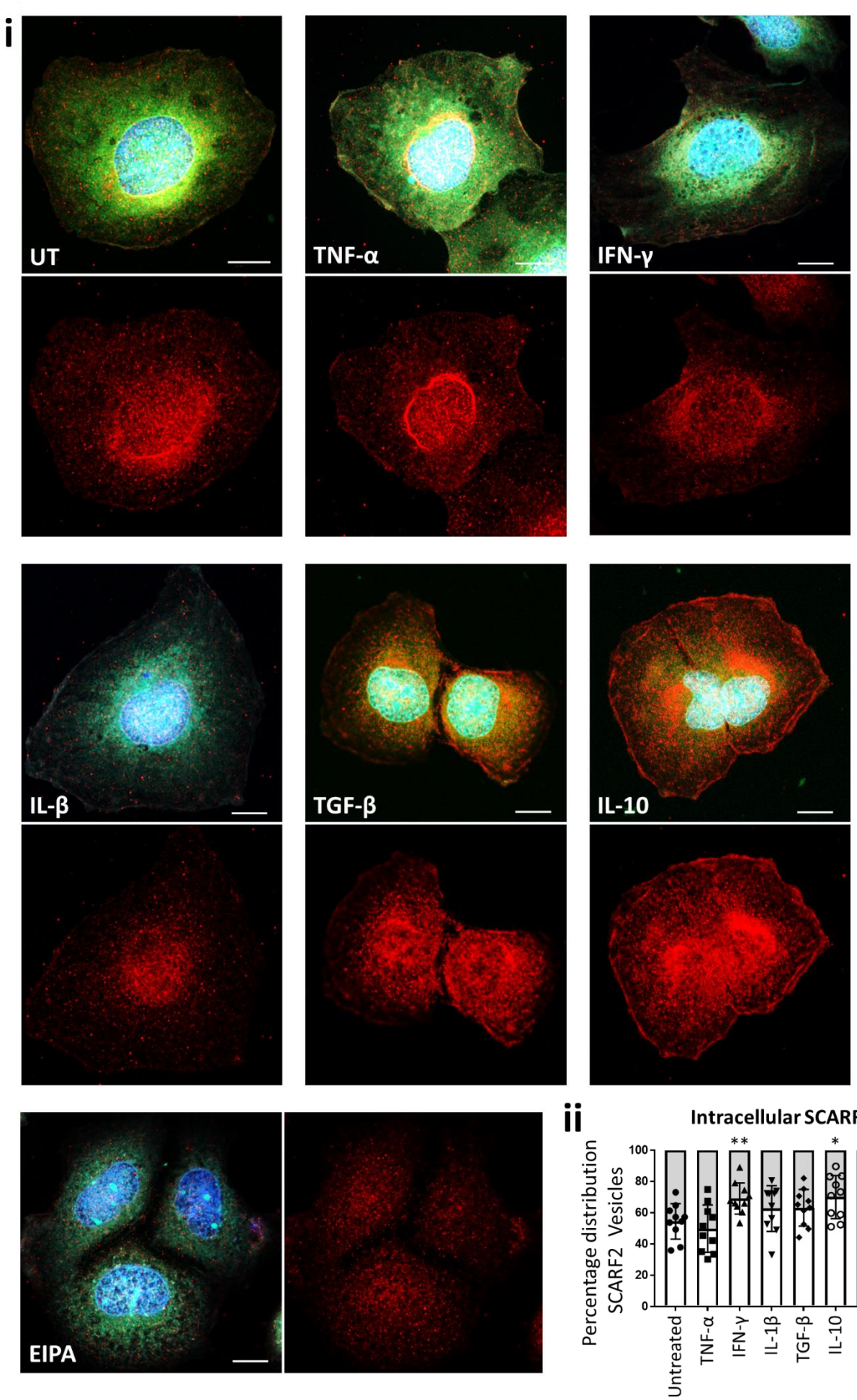
i
UT
TNF-α
IFN-γ
IL-β
TGF-β
IL-10
EIPA
ii
Intracellular SCARF2
Percentage distribution SCARF2 Vesicles
100
80
60
40
20
0
**
*
Untreated
TNF-α
IFN-γ
IL-1β
TGF-β
IL-10
EIPA

Figure 3J: The distribution of SCARF2-positive vesicles in hepatomas was altered in response to cytokine treatment. Huh-7 hepatomas seeded in 24-well plates on glass coverslips were fluorescently labelled with Cell Tracker Green (CTG)/ CMDFA and Hoechst 33342 (blue). Huh-7s were then serum starved and treated with 100 ng/ml cytokines or 5-(N-Ethyl-N-Isopropyl) amiloride (EIPA) for 1 hr. Cells were then fixed with MeOH and stained for scavenger receptor family f, member 2 (SCARF2) via immunofluorescence (shown in red). Cells were then imaged by confocal microscopy. **(i)** Confocal micrographs of labelled Huh-7 cells (green), stained for SCARF2 (red) following cytokine/EIPA treatments. Scale bars represent 10 μm. Images are representative of 3 independent experiments. **(ii)** Percentage of SCARF2-positive vesicles found within the nucleus (grey bar) or outside of it (white bar) in cytokine-treated hepatomas. Numbers were obtained from 10 cells imaged across 3 independent experiments (N=3), using Bitplane IMARIS for cell biologists software. Statistics were derived from a two-tailed, unpaired Student's t-test when comparing cytoplasmic values of treatments to the control. Data points represent mean value obtained for individual cells. Error bars represent the SEM. * - ≤0.05, ** - p≤0.01. TNF-α – Tumour necrosis factor-alpha; IFN-γ – interferon-gamma; IL – interleukin; TGF-β – tumour growth factor-beta.

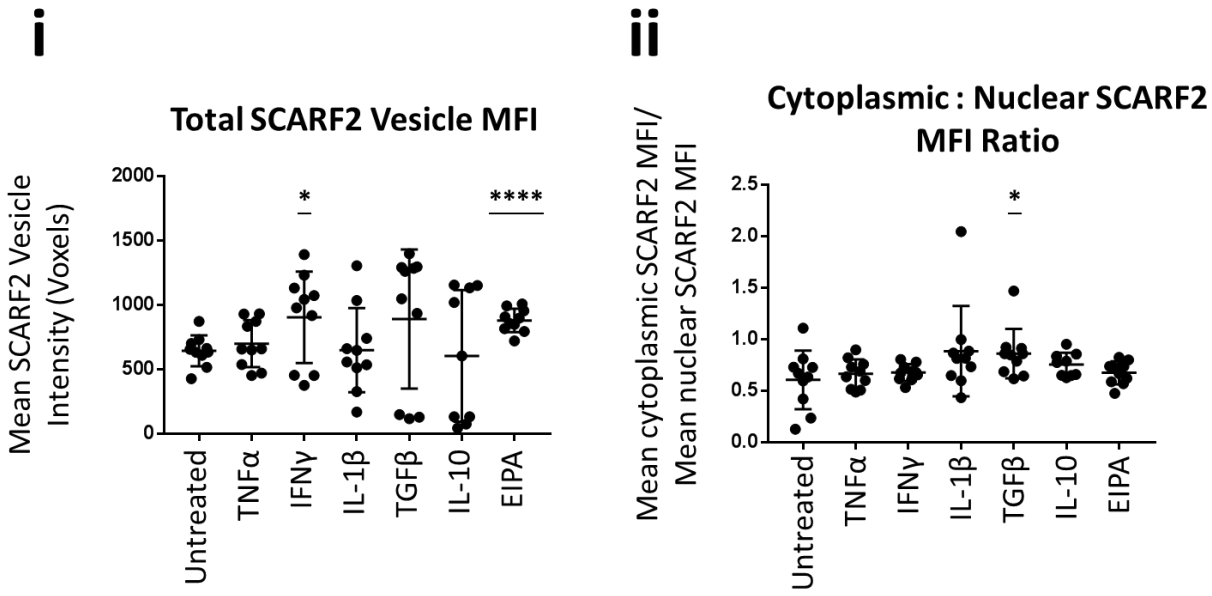

Figure 3K: Effect of cytokine stimulation of hepatomas on mean fluorescent intensity (MFI) of SCARF2-postive vesicles. Huh-7 hepatomas seeded in 24-well plates on glass coverslips were fluorescently labelled with Cell Tracker Green (CTG)/ CMDFA and Hoechst 33342 (as shown in **Fig. 3J**). Huh-7s were then serum starved and treated with 100 ng/ml cytokines or 5-(N-Ethyl-N-Isopropyl) amiloride (EIPA) for 1 hr. Cells were then fixed with MeOH and stained for scavenger receptor family f, member 2 (SCARF2) via immunofluorescence. Cells were then imaged by confocal microscopy. The mean fluorescent intensity (MFI) of SCARF2-positive vesicles found within each cell were then obtained from images using Bitplane IMARIS software. Numbers were obtained from 10 cells imaged across 3 independent experiments. **(i)** MFI values for the total population of SCARF2 vesicles. **(ii)** MFI ratio of cytoplasmic vesicles to nuclear vesicles. Statistics were derived from a two-tailed, unpaired Student's t-test when comparing other treatments to the control. * - ≤0.05, **** - p≤0.0001. Data points represent mean value obtained for individual cells. Middle line represents mean and error bars represent the SEM. TNF-α – Tumour necrosis factor-alpha; IFN-γ – interferon-gamma; IL – interleukin; TGF-β – tumour growth factor-beta.

3.4.4 The distribution of SCARF2 is altered under inflammatory conditions *in vivo*

Cells do not necessarily attain the same polarity in 2D cultures that they would in the setting of a tissue. As such, the expression and distribution of SCARF2 may differ *in vivo* to what was seen in cell lines. Further, its activity may be altered under inflammatory conditions associated with disease that are difficult to simulate *in vitro*. To investigate whether the behaviour of SCARF2 in the liver is comparable to observations made *in vitro*, IHC staining was performed on tissues from patients with a variety of liver diseases (**Fig. 3L**). Tissues from donor livers which were rejected for transplantation were used as 'normal' (fatty) controls. In these livers, SCARF2 was largely located at nuclear membranes as previously seen in IF stains of cell lines. This provides some validation for the antibody used to accurately represent SCARF2, as well as for Huh-7 cells to authentically represent its activity. Again, large, round structures with positive staining were frequently observed within hepatocytes. In contrast, nuclear expression of SCARF2 was reduced in hepatocytes within diseased livers. Furthermore, hepatocyte cytoplasm was largely occupied with irregularly sized intracellular vesicles with strong positive staining. Taken together, it appears that SCARF2 expression and intracellular location within hepatocytes is altered in response to cytokines both *in vitro* and *in vivo*.

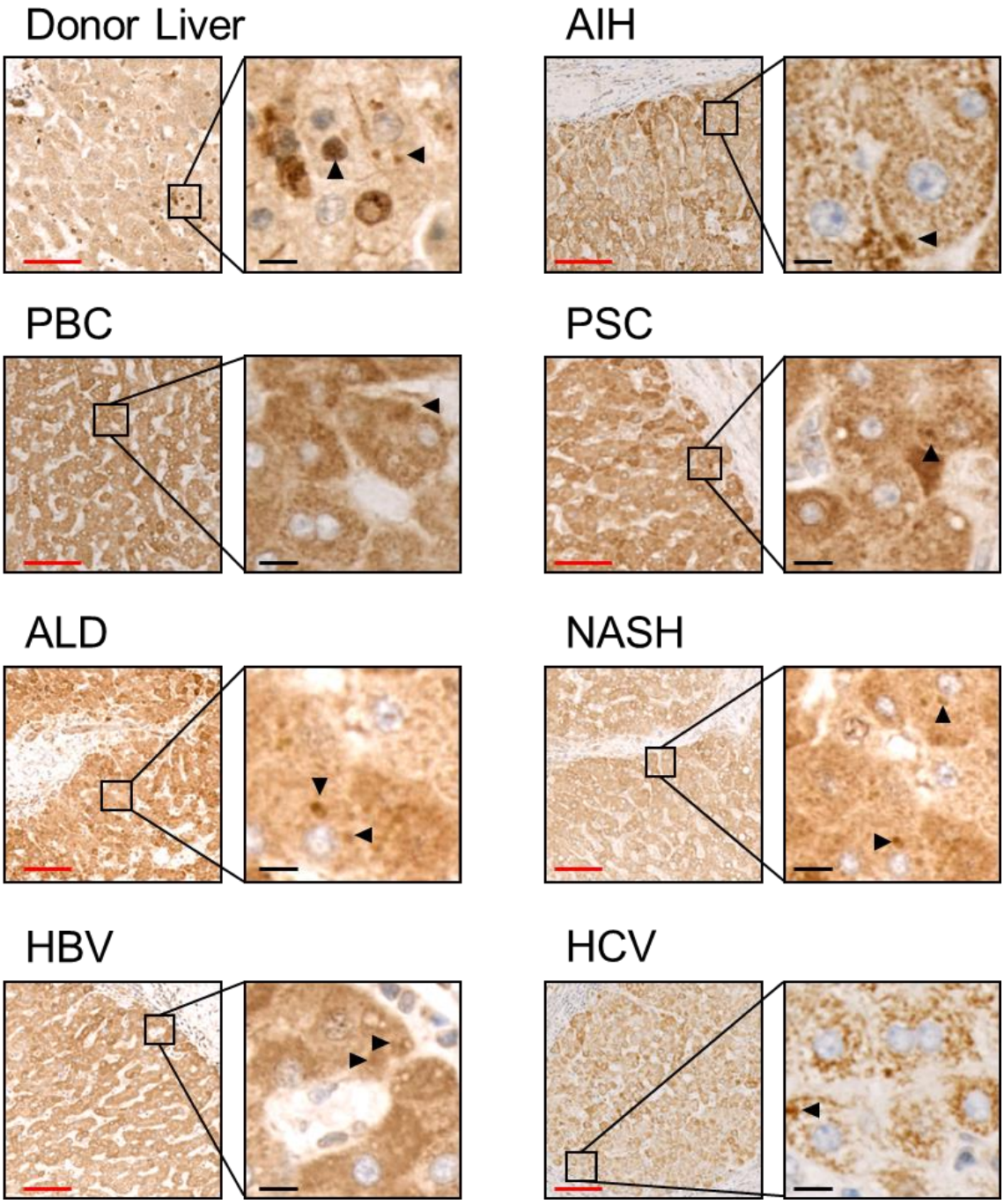

Figure 3L: The distribution of SCARF2 was altered under inflammatory conditions *in vivo*. Immunohistochemistry (IHC) staining of explanted liver tissue from patients with different chronic disease for Scavenger receptor family F, member 2 (SCARF2 - brown). Tissues were counterstained with Mayers haematoxylin nuclear stain (blue). Inset boxes highlight positive structures within hepatocytes which are likely to represent efferosomes. Red scale cars represent 100 µm. Black scale bars represent 10 µm. AIH – Autoimmune hepatitis; PBC – primary biliary cholangitis; PSC – primary sclerosing cholangitis; ALD – Alcoholic liver disease; NASH – Non-alcoholic steatohepatitis; HBV – hepatitis B virus; HCV – hepatitis C virus. Images were provided from work conducted by MSci student, William Porter.

3.5 Chapter Summary

Table 4: Summary of all new discoveries presented in chapter 3.

1. Hepatocytes and hepatocyte tumour cell lines are adept at the engulfment of apoptotic and heat-killed cells.
2. Necrotic cell capture by hepatocytes was augmented by both pro-inflammatory cytokine, IFN-γ and anti-inflammatory cytokines, TGF-β and IL-10.
3. Apoptotic cell capture was augmented by TGF-β, as described for other efferocytes, but was reduced by IL-10.
4. Hepatocyte efferocytosis was susceptible to inhibitors of macropinocytosis, blebbistatin and EIPA, and actin-remodelling inhibitor, cytochalasin D.
5. Sites of adhered dead cells were enriched with ICAM-1 and ASGPR1. This association was lost upon complete internalisation.
6. SCARF2 associated with vesicles containing apoptotic and heat-killed cells in hepatomas and hepatocellular carcinoma cells *in vitro* and hepatocytes *in vivo.*
7. The distribution of SCARF2-positive vesicles significantly shifted to the cytoplasm in hepatomas following stimulation with IL-10 and IFN-γ *in vitro* and in hepatocytes in chronically diseased livers *in vivo*.
8. SCARF2 was enriched in the cytoplasm in patients with chronic diseases and liver cancer.

3.6 Discussion

3.6.1 Hepatocytes as non-professional phagocytes

3.6.1.1 Hepatomas as *in vitro* models of hepatocyte efferocytosis

Hepatocyte efferocytosis was originally described in 1944, where their capacity to engulf erythrocytes was described (23). Since then, this novel ability of hepatocytes has been largely ignored. The work described here begins to decipher some of the regulatory and

mechanistic attributes of this process. This was initially achieved using an *in vitro* model of hepatocyte efferocytosis. Combining the *in vitro* culture of these cells with fluorescent-labelling, together with confocal microscopy, allowed for the complete internalisation of apoptotic or dying cells to be confirmed following the acquisition of Z-stacks. Similar techniques have been used to monitor and enumerate efferocytosis in other non-professional phagocytes (97). Other groups have supplemented these analyses with reporter assays which measure the downstream genetic alterations in the predatory phagocyte (130). However, this was not possible for hepatomas as these details regarding the downstream consequences of efferocytosis were lacking.

Using this system, it was confirmed that the capacity for efferocytosis was conserved within 3 different hepatocyte cancer cell lines **(Fig. 3B)**. This would suggest that efferocytosis is still a necessary part of the hepatocyte biology, even upon oncogenic transformation and isolation from the setting of a complete liver. Furthermore, this model allowed for the enumeration of efferocytosis in response cytokine and molecular inhibitors. The validity of such findings may be limited by how representative Huh-7 cells are of PHH activity. Huh-7 cells were selected for the studies presented here, as efferosomes were easily identified in the monolayers that they form, following immunofluorescence labelling. However, as with other dedifferentiated hepatomas, they lack certain responses to cytokines and growth factors (30). Despite this, their capacity for efferocytosis and their expression of SCARF2 was notably altered by cytokines in experiments described this chapter. As the latter was also confirmed for hepatocytes in diseased human tissues, Huh-7 cells appear to accurately represent hepatocytes in the context of efferocytosis.

There are consistent limitations in the conclusions drawn from 2D *in vitro* culture systems. These predominantly arise from differences in polarity and stiffness between these cells

cultured on plastic and those found in tissues. They also eliminate the effects exerted by other cells found in tissues, as well as the influences of extracellular matrices (246). As such, the molecular activity, as well as the distribution and surface availability of receptors of hepatocytes *in vivo* may differ from these aspects in 2D-cultured cells. This is evident from the inability to grow PHHs *in vitro* and their loss of polarisation following their isolation from the liver (69). For these reasons, the capacity for efferocytosis by hepatomas may be misrepresented in 2D cultures. 3D *in vitro* culture models may represent a more representative method for culturing hepatocytes and their related cell lines. PHHs grow in 3D cultures were reported to retain APAP-sensitivity that was lost in 2D cultures (247). Notably, Huh-7 cells grown in 3D cultures were shown to obtain a more differentiated phenotype and were more permissive to HCV infection (248). As the latter characteristic is likely related to availability of HCV entry receptors, including scavenger receptor class B type 1, Huh-7 cells grown in 3D cultures may also provide more accurate model in studying efferocytosis.

3.6.1.2 Heat-killing as method for creating necrotic cells

Throughout these experiments, heat-killed cells were used as a representation of necrotic cells. Although this is accepted as general method for inducing necrosis in cells (223), results obtained whilst using them are not always consistent with those acquired when using necrotic cells formed using an alternative method. Hirt and Leist showed that secondary necrotic (ATP-depleted) cells induced anti-inflammatory responses in macrophages when engulfed (99). This was not recapitulated in macrophages that engulfed heat-killed cells. This discrepancy is possibly due to the differences in molecules released from heat-killed cells following heat-treatment, compared with alternatively-induced necrotic cells. Levels of heat-shock protein 72 (HSP-72) have been shown to increase in heat-treated cells (56). Of note, HSP-72 has been reported to induce pro-inflammatory phenotypes in hepatocytes (56).

Furthermore, heat treatment is likely to denature certain ligands of dead cell-receptors on their surfaces which might be preserved in necrotic cells produce by alternative means. Overall, observations made using heat-killed cells to assess necrotic cell capture require confirmation using different methods for inducing necrosis, such as ATP depletion and H_20_2 treatment (249).

3.6.1.3 The mechanisms and regulation of hepatocyte efferocytosis; differences between apoptotic and necrotic cell capture

Different cytokine treatments elicited varied effects on apoptotic and heat-killed cell capture by hepatomas (**Fig. 3C**). These results provided potential similarities and differences to efferocytosis conducted by other cells. In general, efferocytosis of apoptotic cells is inhibited by pro-inflammatory stimulation and promoted by anti-inflammatory stimulation (1, 127, 139). The opposite is normally true for the uptake of necrotic cells (95). In hepatomas, anti-inflammatory cytokine, TGF-β increased apoptotic cell capture. Additionally, pro-inflammatory cytokines, IFN-γ and IL-1β promoted the capture of heat-killed necrotic cells. These observations were consistent with how efferocytosis is regulated in both professional and non-professional phagocytes (79). In contrast to these findings, TGF-β and IL-10, another anti-inflammatory cytokine that has been reported to promote apoptotic cell capture in macrophages (214), also augmented heat-killed cell capture by Huh-7 cells. Surprisingly, IL-10 significantly reduced apoptotic cell capture in hepatomas. The mechanisms for these differences are unclear. Overall, the results displayed here suggest that hepatocyte capture of apoptotic cells is alternatively regulated to their capture of necrotic cells, which is akin to the behaviour other efferocytes. However, they also suggest that hepatocyte efferocytosis bears some situational and regulatory differences to other efferocytes. This is likely due to adaptations to the immunotolerant environment of the liver. As such, responses to both

pro- and anti-inflammatory stimuli may be skewed towards the clearance of dying cells in the liver and promoting resolution. Further elucidation into hepatocyte inflammasome beyond the scope of this project may be required in future to explain the effects of cytokines on hepatocyte efferocytosis.

Although the effects of cytokines were varied between apoptotic and heat-killed cell capture, the effects of molecular inhibitors were comparable for both processes (**Fig. 3D**). Inhibition of these processes by cytochalasin D was expected as *de novo* actin polymerisation is necessary for all forms of endocytosis (250). Of interest, both processes were susceptible to blebbistatin and EIPA. Both molecules inhibit macropinocytosis, albeit through different mechanisms. This would suggest that hepatocyte efferocytosis is mechanistically similar to macropinocytosis. Taken together, these data suggest apoptotic and necrotic cell capture by hepatocytes may be regulated through distinct mechanisms, but their effects may converge to regulate similar intracellular contractile machinery.

3.6.1.4 How do hepatocytes recognise and internalise dying cells?

Immunofluorescence staining of efferocytosing Huh-7 cells combined with 3D volume rendering allowed for visualising the distribution of candidate dead cell-receptors in relation to fully and partially internalised cell corpses. These combined technologies revealed possible roles for ICAM-1 and ASGPR1 in hepatocyte efferocytosis. ICAM-1 associated with apoptotic cells that were adhered to the surface of hepatomas (**Fig. 3Ei-iii**). This association was lost on vesicles containing fully internalised apoptotic cells. Heat-killed cells did not associate with ICAM-1 during any stage of their capture by hepatomas. The denaturation of its ligands, like CD11a, by heat treatment may have contributed to this. Such ligands are more likely to be retained on early apoptotic cells. As such, ICAM-1 may provide similar assistance to efferocytosis as they do for lymphocyte recruitment (251), by binding apoptotic

cells to allow for other receptors to interact with their ligands, initiating internalisation of the dying cells. In contrast to this, ICAM-1 expression was shown to be inversely proportional to efferocytosis by M2 macrophages (252). This presents another difference between efferocytosis by hepatocytes and professional phagocytes. However, immunofluorescence staining does not distinguish the ownership of the specific antigen that has been probed. ICAM-1 expression has also been reported for $CD4^+$ T cells that were used in these assays (253). Furthermore, this association may only be present with apoptotic cells that previously expressed ICAM-1 ligands. Overall, it is uncertain as to whether ICAM-1 is necessary for the hepatocyte efferocytosis.

ASGPR1 was shown to associate with partially engulfed necrotic cells (**Fig 3F**). This carbohydrate scavenger receptor was already reported to be expressed by hepatocytes and to bind apoptotic T cells in the liver (147). The data shown in this chapter mark the first report of its capacity to bind necrotic cells. As with ICAM-1 however, not all adhered necrotic cells were enriched for ASGPR1. As such, ASGPR1 may facilitate efferocytosis but not be required. It is likely that the molecules investigated in this chapter do not act in isolation; there are likely other receptors that facilitate hepatocyte efferocytosis that were not investigated in this project, as well as redundancy in between them; macrophages express multiple receptors which recognise dying cells (87, 254). Treating actively efferocytosing hepatomas with functionally blocking antibodies to these molecules or performing siRNA-mediated knockdowns would be needed to determine their specific functions and necessity for hepatocyte efferocytosis.

3.6.2 An important new role for SCARF2 in the liver?

3.6.2.1 Evidence supporting SCARF2 as a hepatocyte dead cell receptor

Although the molecular mechanism of hepatocyte efferocytosis still remains uncertain, these investigations have unearthed a potential novel role for SCARF2 in this process. Little is known regarding the functions of this scavenger receptor. Mutations in its gene have been attributed to the development of the rare autosomal-recessive development disorder called Van Den Ende-Gupta syndrome (220, 221). The contribution of mutated SCARF2 to the pathogenesis of this disease is still unknown. Interest in the activity of SCARF2 has largely stayed in relation to this disorder, or in comparison with SCARF1 activity (145). With regards to the latter, one report disregarded SCARF2 for an involvement with efferocytosis when comparing its activity to SCARF1 (130). However, observations described in this chapter have shown that SCARF2 associated with efferosomes containing both apoptotic and necrotic cells (**Fig. 3I**). Furthermore, the percentage of SCARF2-postive vesicles found outside of the nucleus was increased in Huh-7 cells in response to treatment with cytokines that were also shown to increase efferocytosis these cells (**Fig. 3J**). This redistribution of vesicular SCARF2 was also recapitulated *in vivo* (**Fig. 3L)** in hepatocytes within livers plagued with chronic liver disease. These hepatocytes would be frequently exposed to cytokines (49). The latter observation suggests that the activity of SCARF2 in hepatomas is representative of its *in vivo* activity in hepatocytes. These data collectively suggest that SCARF2 may form part of the molecular machinery associated within hepatocyte efferocytosis. This represents the first candidate receptor involved in how hepatocytes recognise dying cells since ASGPR1.

In support of its potential role in hepatocyte efferocytosis, the distribution of SCARF2-positive vesicles was altered in response to cytokine treatment, with significant differences observed in response to IFN-γ and IL-10 (**Fig. 3J**). These cytokines were also shown to

augment heat-killed cell capture (**Fig. 3C**). This increase may therefore be linked with the observed alteration in SCARF2 vesicle localisation. The exact mechanism as to how this occurs is unclear. The MFI of SCARF2 vesicles in Huh-7 cells was used as a proxy to investigate if these cytokines increase the expression of SCARF2 in the cytoplasm (**Fig. 3K**). Although IFN-γ increased SCARF2 vesicle MFI, this was not seen with other cytokine treatments. Furthermore, IFN-γ, nor IL-10 altered the MFI of cytoplasmic SCARF2 vesicles relative to nuclear population. Therefore, it is more likely that SCARF2 is mobilised towards the cytoplasm in response to cytokines. In support of this, the activity of vesicle trafficking proteins, Rho GTPases, have been shown to influenced but NFκB activation by various cytokines (255). In further support of this, EIPA treatment caused the most significant increase in SCARF2 vesicle MFI, despite significantly inhibiting hepatocyte efferocytosis. This increase in MFI may be the result of SCARF2-postivie vesicles arresting in the hepatocyte, preventing its trafficking to the cell membrane, which in turn would reduce the cells capacity to capture dead cells. This observation may also provide insight into the exact mode of action for how EIPA inhibits hepatocyte efferocytosis. More accurate methods to assess protein expression, such as western blotting, as well as live tracking of SCARF2 vesicles will be required to validate these theories.

3.6.2.2 How does SCARF2 function?

Exactly what SCARF2 binds to remains uncertain, as does the modality through which it acts; whether it is involved in dead cell binding, internalisation, or intracellular trafficking. As SCARF2 associated with both necrotic and apoptotic cells, it is likely to recognise a component shared between both forms of dead cell. It is likely to be an opsonising molecule that may bind PS. One possibility is that the SCARF2 can recognise dead cells through modified low-density lipoproteins (LDLs). Similar activity has been reported for the receptor Lectin-like oxidized low-density lipoprotein receptor 1 (LOX-1), and SCARF2 has been

reported to bind to acetylated and oxidised LDLs (ac-LDLs/ox-LDLs) (219, 256). However, SCARF2 expression was shown not to increase LDL internalisation. As such, this protein may instead act as an adhesion molecule to initiate the internalisation of dead cells. We also saw that SCARF2 could be found at intercellular junctions between hepatocytes (**Fig. 3G**). Coupled with its likelihood to denote efferosomes, this appears to be reminiscent of the dual modality of certain integrins. Certain combinations like αvβ3/β5 can recognise PS but also form a part of adhesion junctions (257). Despite its difference in structure, SCARF2 may also act in a similar manner. Its expression has been linked to increased clumping of cells through homophilic interactions (219). This further exemplifies its role as an adhesion molecule, rather than a scavenger receptor, and illustrates its likely importance in the liver. Further experimentation is necessary to further understand the functionality of SCARF2 in the liver.

The observations made in this study do possess the drawbacks of relying on antibody staining. Only a single antibody which recognises SCARF2 is commercially available. Although the use of this rabbit polyclonal antibody has been described before in the literature (145), it has not undergone extensive validation. Furthermore, polyclonal antibodies possess drawbacks of recognising multiple epitopes, creating batch variability. As such, it is not entirely certain if it specifically and correctly recognises SCARF2. This casts doubt on its distribution observed in hepatocytes and related cell lines within the experiments described here. As such, further verification of this antibody would be required to validate these findings. This could be achieved by using the antibody to stain cells which have been confirmed not to express SCARF2. Furthermore, the Fc region of the antibody could be tagged in a way to allow its use within pull-down assays or purification columns. The proteins which are pulled out from hepatocyte lysates by the antibody could then be identified by mass spectrometry to confirm the presence of SCARF2 amongst them.

The activity of SCARF2 could also be tested in future experiments by performing efferocytosis assays in the presence of molecules which mask its candidate ligands. Efferocytosis by both professional and non-professional phagocytes is frequently inhibited experimentally by masking PS with soluble Annexin V (AV) (97, 258, 259). In addition, modified LDLs have also been used to inhibit the activity of scavenger receptors which assist the capture of dead cells, such as LOX-1 (89, 260) and kidney injury molecule-1 (KIM-1) (261). Similar treatments have been previously shown to interrupt SCARF2 interactions with SCARF1 (219). Treatment of hepatocytes or hepatomas with modified LDLs may therefore reduce efferocytosis. Contrastingly, coating of dying cells with LDLs may increase efferocytosis by providing more targets for SCARF2. Such experiments would provide some information as to the ligands of SCARF2 and its role in hepatocyte efferocytosis. Genetic silencing of SCARF2 would also shed further light on its global role both in the liver. This will highlight the importance of SCARF2 in the future.

3.6.3 Do hepatocytes control liver immunotolerance?

Several aspects of the biological activity of hepatocytes can be attributed to the general immune-unresponsiveness in the liver (48). They're able to prematurely activate lymphocytes under inflammatory circumstances, thus reducing their longevity (21). The work discussed here now exemplifies a further role for hepatocytes in promoting immunotolerance in the liver by clearing dying cells. Efferocytosis is generally considered an anti-inflammatory process, as preventing the accumulation of dying cells in the parenchyma is vital for avoiding further tissue damage and leukocyte recruitment (77, 127). As the liver frequently accumulates apoptotic cells, both tissue-forming and circulating, hepatocytes now possess another primary immune function with removing these cells. What's more, hepatocytes can also clear necrotic cells as well as apoptotic cells. Although necrotic cell

capture can impose a pro-inflammatory phenotype on phagocytes, this is not thought to happen with non-professional phagocytes (97). Furthermore, capture of necrotic cells by hepatomas was augmented by anti-inflammatory cytokines, suggesting that hepatocyte efferocytosis may not incur the same inflammatory consequences as other phagocytes. As such, efferocytosis conducted by hepatocytes may reduce the likelihood of further immune activation in the liver.

The ability of the major liver cell type to clear dying cells gives a greater protection from premature immune responses than if professional phagocytes were working alone. Although Kupffer cells (212) and infiltrating phagocytes (262) effectively contribute to clearing dying cells in the liver , it may not be advantageous to increase the number of these cells in the parenchyma as they have the potential to acquire pro-inflammatory phenotypes in a disease setting. It is therefore more efficient for hepatocytes to largely control the burden of removing dead cells, as they are less likely to contribute to liver inflammation and fibrosis. They are also most likely to be the cell to first encounter a dead cell within the liver, which limits the time between cell death and its clearance. A similar hierarchy is established in the airways, another series of tissues with frequent exposure to potentially toxic substances (116, 117, 263). In these tissues, epithelial cells can efferocytose which alleviates the burden of this for macrophages and prevents further inflammatory cell recruitment. It would now appear that a similar system has been established in the liver.

Chapter 4: The consequences of efferocytosis by hepatocytes

4.1 Introduction

4.1.1 Cell-in-cell structures can cause multinucleation in the host

As a field that is generally in it's infancy, multiple aspects of CICSs are available for further study. Although a lot of pioneering work has focussed on the molecular mechanisms and signalling pathways which are involved in live cell capture, other investigations have focussed on the impact for the predatory cell (185, 204, 264). The original authors who described entosis observed that breast cancer cells who engulfed their live neighbours were prone to failing cytokinesis (204); the large internal vesicle containing the "prey cell" served as a physical impediment to the cytokinetic cleavage furrow (**Fig. 4Ai**). As such, the host cell would fail cytokinesis and become multinucleate. This has been hypothesised to increase the accumulation of genetic abnormalities in these cancers, potentially incurring greater levels of survival for the tumour (202, 204). In support of this, cytokinesis failure and binucleate cell formation in tumours has been previously linked to tumorigenesis (265). Furthermore, breast cancers with higher ploidy levels have been associated with poor prognosis (266). CICS formation can therefore bestow profound genetic changes to the predatory cell.

Similar mechanisms have been reported whereby an intracellular physical impediment can result in the failure of cytokinesis. Macrophages infected with *Chlamydia trachomatis* have been reported to have their cleavage furrows perturbed by the infections inclusion bodies, resulting in multinucleation (267). The same authors recapitulated this same cytokinetic failure using latex beads, a common tool used to model phagocytosis in macrophages (268).

This would suggest that phagocytosis also has the potential to induce cytokinetic failure, as a similar physical impediment is created by a phagosome.

4.1.2 Hepatocyte ploidy

Alterations in ploidy are more frequently associated with pathological and oncogenic transformations and are often the result of cell cycle dysregulation (269-272). Physiologically normal cases of polyploidy, however, have been described and are often the result of cell fusion. These phenomena are generally associated which terminal stages of cell differentiation, including the development of muscle fibres and the formation of osteoclasts in the bone (273, 274). They can also occur under chronic inflammatory conditions, as seen with the formation of multinucleate giant macrophages (274). Hepatocytes, however, are unique in that a percentage of these cells have a propensity to be multinucleate and polyploid under homeostasis (205). Approximately 50% of human hepatocytes are polyploid and this percentage is higher in mice (205). Marcus Grompe and colleagues have reported several observations regarding the potential of hepatocytes to gain multiple chromosome sets. They have described how polyploidy in mouse hepatocytes was increased with age (275, 276). This change was predominantly the result of cytokinetic failure. The authors also reported that hepatocytes in mice could also lose whole sets of chromosomes through reductive cell divisions, a process known as 'ploidy reversal'. However, this process was less frequent than cytokinesis failure. These observations lead to the creation of their "ploidy conveyor" model, which describes the gradual increase in hepatocyte polyploidy over time as cytokinesis failure overfrequents ploidy reversal (**Fig. 4Aii**).

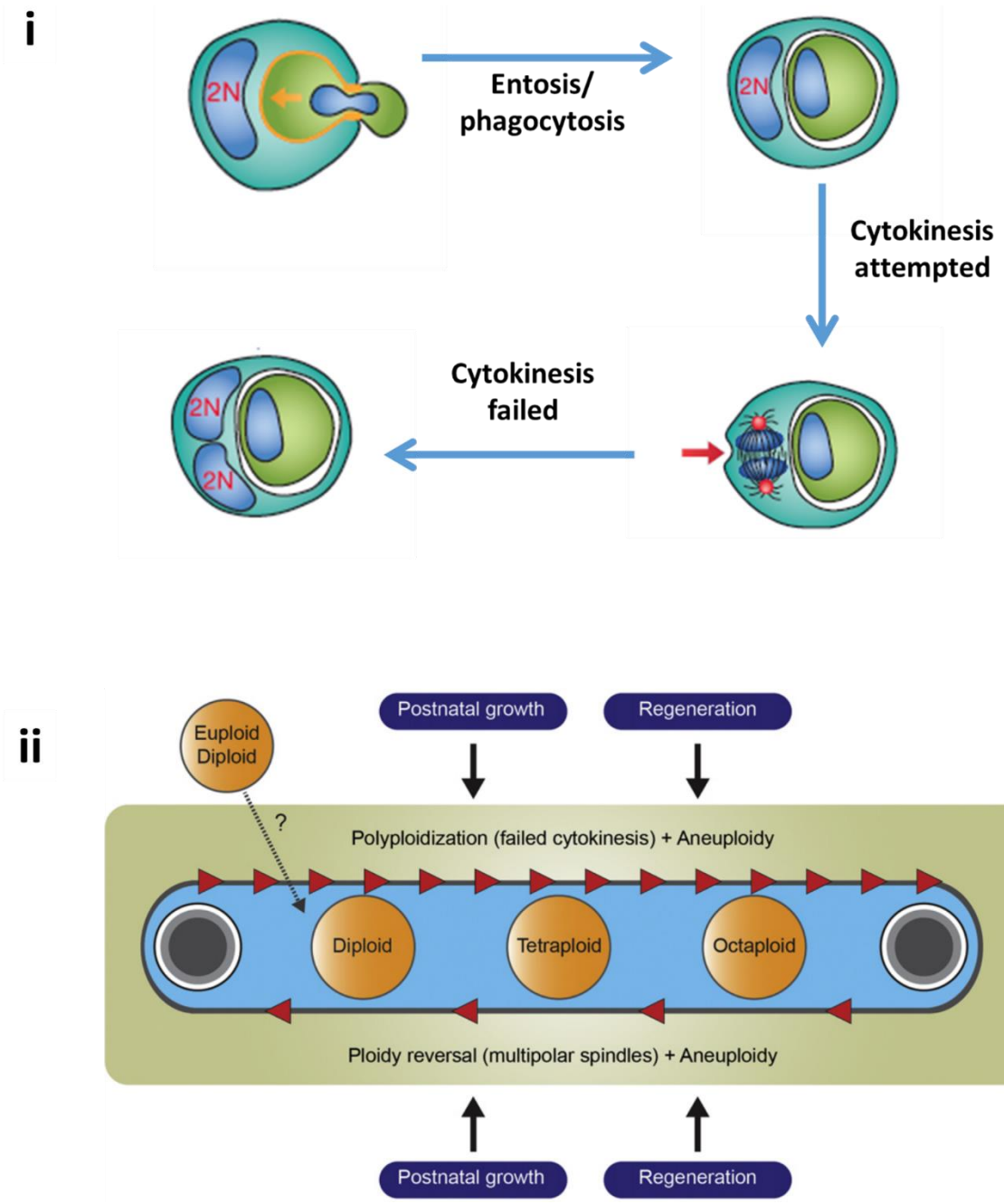

Figure 4A: Sources of multinucleation and ploidy increases through cell-in-cell structures and cytokinesis failure in the liver. (i) Mechanism of cytokinesis failure induced by cell-in-cell structures. The large vesicle formed through the engulfment of a live or dead cell imposes a physical block on the cytokinetic cleavage furrow. This causes the cell to abandon cell division, despite having replicated its genome. Two nuclei form, resulting in binucleation of the host cell. Modified, with permission, from (204). **(ii)** The ploidy conveyor model of hepatocyte polyploidisation established by Marcus Grompe and colleagues. During liver regeneration, increases in ploidy are frequent in the liver (depicted by larger number of red arrows) caused by failed cytokinesis. During the same periods, the less frequent event of multipolar mitotic spindle formation (depicted by fewer red arrows) results in the loss of chromosome sets, a process known as 'ploidy reversal'. Hepatocytes thus cycle through increases and decreases in ploidy, skewing more to the gain of whole chromosome sets. The origin of initial diploid cells within the cycle is not known. Taken, with permission, from (205)

How hepatocytes polyploidisation is induced is not thoroughly understood. Cytokinesis failure was originally observed to be the major source of polyploidisation in the liver, which is concurrent with multinucleation. This is not always the case in patients with Non-alcoholic Fatty Liver Disease (NAFLD) or Non-alcoholic Steatohepatitis (NASH). It was shown that polyploidy was induced by cell cycle arrest in phases prior to cytokinesis due to oxidative stress (277). This would result in polyploid, mononucleate cells in contrast to the binucleate cells generated from cytokinesis failure. The exact reasons or mechanisms for cytokinesis failure in hepatocytes are, to this point, uncertain. Recent evidence in mice has suggested that the microRNA, miRNA-122, regulates polyploidisation by antagonising the expression of cytokinetic machinery (276). Mice possessing no miRNA-122 exhibited significantly reduced binucleation, yet some binucleate hepatocytes were still recorded. Although it has been reported that hepatocytes conduct efferocytosis, the consequences of this for hepatocyte ploidy have not been examined. I therefore set out to interrogate the effects of efferocytosis on hepatocyte multinucleation using *in vitro, in vivo* and *ex vivo* models.

4.2 Efferocytosis increased multinucleation in hepatomas *in vitro*.

When CICSs are created via entosis, they create a large internal structure which has the potential to prevent cytokinesis and induce multinucleation in the host cell. During efferocytosis, dying cells are also compartmentalised into large intracellular vesicles. I hypothesised that efferosomes could induce multinucleation via cytokinetic failure in hepatomas, as they readily divide when cultured *in vitro*. To test this, Huh-7 hepatomas were labelled with Hoechst 33342 following co-culture with heat-killed Jurkat lymphoma cells (**Fig. 4B**). Huh-7 cells that underwent consecutive feeds exhibited cumulative increases in multinucleation with each round of efferocytosis (**Fig. 4Bi**). Large hepatocytes possessing

up to 8 nuclei were observed in cultures at the end of this experiment (**Fig. 4Bii**). Furthermore, a dose-dependent increase in hepatocyte multinucleation was observed with increasing ratios of Huh-7:Jurkats after only 24 hours of co-culture (**Fig. 4Biii**). To ensure that increases in multinucleation were not the result of factors exuded from the Jurkat cell corpses, Huh-7s were co-cultured with heat-killed Jurkat cells for 24 hours in the presence or absence of 10 uM EIPA (**Fig. 4Biv**). This inhibitor was previously shown to inhibit hepatocyte efferocytosis (**Fig. 3D**). The concentration was lowered compared to previous experiments as not to severely perturb macropinocytosis and induce apoptosis. There was no observable increase in multinucleation in the presence of EIPA compared to untreated cells (**Fig. 4Biv, left**). The number of Huh-7 cells present at the end of the experiment rose when co-cultured with dead cells (**Fig. 4Biv, right**). This increase was not affected by EIPA treatment. Overall, these data show that efferocytosis could induce multinucleation in hepatocytes.

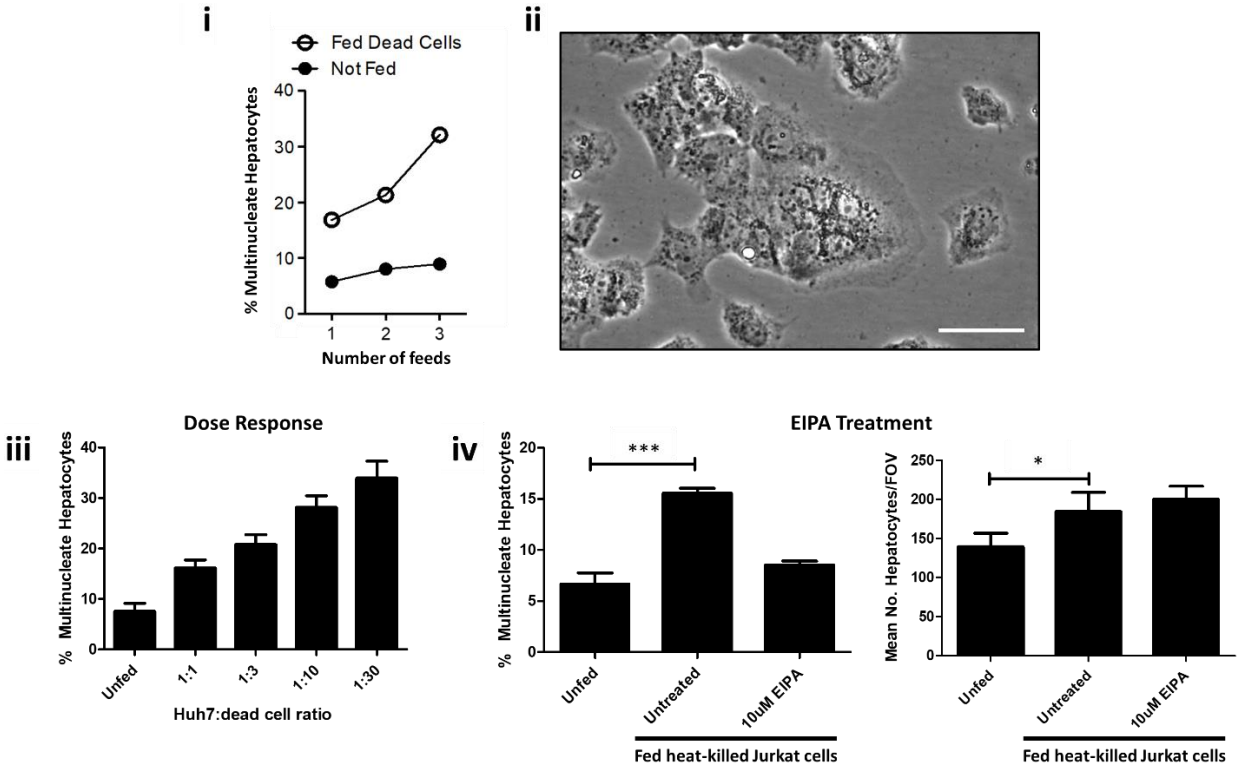

Figure 4B: Efferocytosis increased multinucleation in hepatomas *in vitro*. **(i)** cumulative co-cultures with dead cells caused cumulative increases in multinucleation in hepatomas. Huh-7 cells were then incubated with heat-killed Jurkat T cell lymphomas at a ratio of 1:1. Excess Jurkat cells were removed following 24 hr co-culture. Cells were then washed with PBS and normal culture media was replaced. Huh-7s were permitted to conduct efferocytosis until they became confluent, indicating that they had completed efferocytosis (they do not divide when conducting efferocytosis). Huh-7s were then trypsinised and divided between 2 wells of separate 24-well plates. Unfed control wells were passaged as needed but seeded at the same time and density as the co-cultured cells for analysis. Huh-7s from one well were 're-fed' with heat-killed Jurkat cells and the experiment was repeated. The mean percentage of multinucleate cells were determined from cells seeded in the other well. These cells were labelled with Hoechst 33342 and CellMask Orange to facilitate the counting of nuclei ownership **(ii)** Phase contrast image of multinucleate Huh-7 following 3 consecutive feeds with heat-killed cells. Scale bar = 50 µm. **(iii)** Dose response of increasing Huh-7:heat-killed cell ratios on Huh-7 multinucleation. Experiment conducted as in part (**i)** but only for a single feed. N=1. *** - p≤0.001. **(iv)** Effect of 5-(N-Ethyl-N-isopropyl)amiloride (EIPA) treatment on Huh-7 multinucleation over a single co-culture at a ratio of 1:1. . Means for all experiments were determined from 5 FOVs obtained across 3 technical replicates. N=1. * - p≤0.05. Statistics were derived from a two-tailed, unpaired Students t-test. Error bars represent SEM.

4.3 Hepatocyte efferocytosis induced multinucleation in mouse models of acute liver injury

To investigate if efferocytosis could cause multinucleation in hepatocytes *in vivo*, Haematoxylin and Eosin (H&E)- stained liver tissues from mice modelling ischemia reperfusion injury (IRI) [described in reference (211)] were examined. In this model, the portal vein and hepatic artery of the mouse is clamped for the 30 min, causing ischaemia to part of the mouse liver (**Fig. 4Ci**). The clamp is then released, allowing the blood to re-perfuse. This creates a time-dependent increase in necrotic lesions in the liver. I hypothesised that the live hepatocytes surrounding these areas of necrosis would be actively efferocytosing. As such, these cells should be more multinucleate than hepatocytes further from the necrotic lesions. H&E-stained tissues from mice with 6 hr and 24 hr reperfusion injury were examined for discreet, localised areas of necrosis (**Fig. 4Cii**). Up to three, 2-hepatocyte thick, concentric zones were outlined from the necrotic lesions (**Fig. 4Ciii**). The level of multinucleation for each concentric layer was then determined (**Fig. 4Civ**). Hepatocytes were significantly more multinucleate when proximal to necrotic lesions, both at 6 and 24 hr reperfusion (N=4 per experimental group).

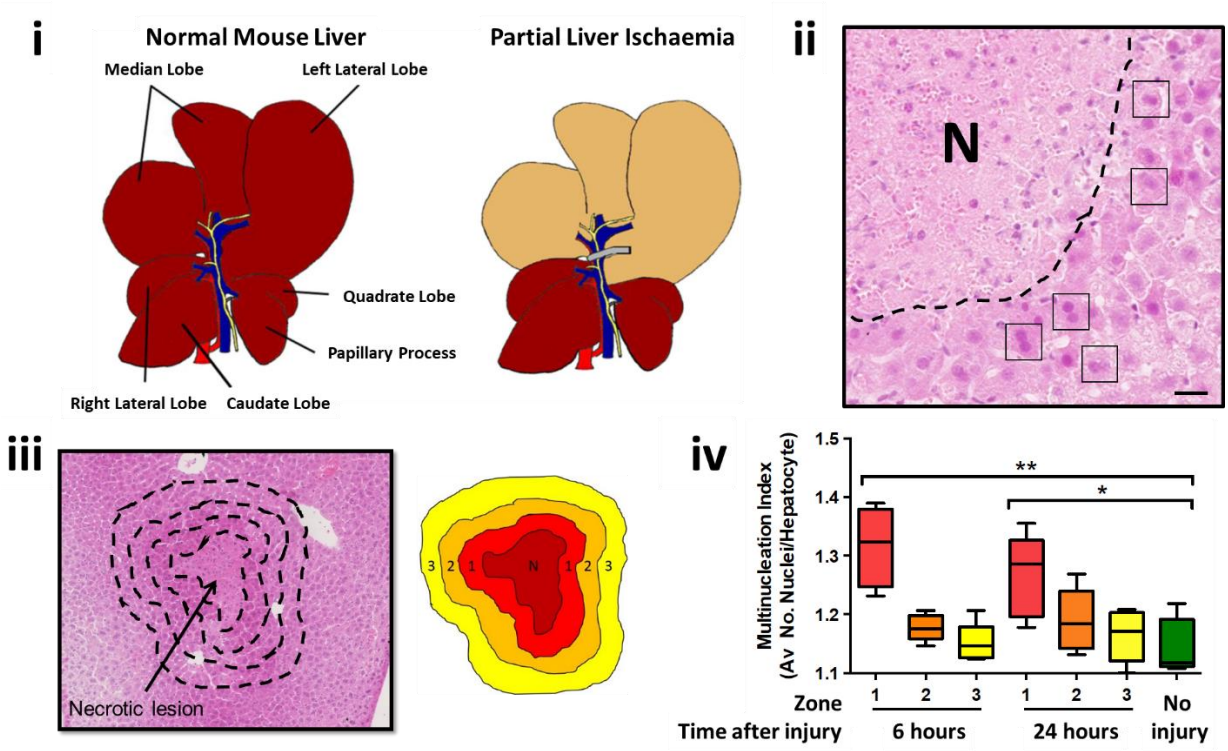

Figure 4C: Efferocytosis induced multinucleation *in vivo* in a mouse model of ischaemia reperfusion injury (IRI). (i) Diagram describing the IRI mouse model. The portal vein and hepatic artery in the livers of 8-week old male C57BL/6 mice were clamped for the 0.5 hr, obstructing the blood supply to the median and left lateral lobe. The clamp was then released to allow the blood to perfuse for 6 or 24 hr, causing a time-dependent increase in necrotic lesions in the liver. Adapted, with permission, from (211). **(ii)** Haematoxylin and eosin stain of IRI mouse liver, showing area of necrosis (N) and proximal multinucleate hepatocytes (highlighted in black boxes). Scale bare represents 20 µm. **(iii)** Hepatocyte zonation around necrotic lesions used for assessing increased multinucleation. Areas of necrosis (N) were identified by Haematoxylin and Eosin (H&E) staining. Concentric zones, 2 hepatocytes-thick were then outlined. **(iv)** Quantification of multinucleate hepatocytes in areas surrounding IRI-induced necrotic lesion. Multinucleate hepatocytes were recorded in zones moving proximal to distal from areas of necrosis in IRI mice. Lesions were identified and collectively analysed from 4 animals per group (8 total). Hepatocytes within random fields of view (FOVs) were also analysed from 4 uninjured mice as controls. Numbers were used to determine the multinucleation index (mean no. counted nuclei/no. hepatocytes counted per zone). * - $p<0.05$, ** - $p<0.01$. Statistics were derived from a two-tailed, paired Student t-test when comparing multinucleation values in concentric zones to values obtained from uninjured mice.

To show that this observation was not specific to this acute injury model, tissues were also examined from mice modelling paracetamol overdose [described in reference (278)] (**Fig. 4D**). These 8-week old, male C57BL/6 mice had received 300 mg/kg acetaminophen (APAP) and were then taken after 24 hr. Similar, discreet areas of necrosis were identified and then analysed as previously done for IRI mice (N=4). Again, there was a significant increase in multinucleation in live hepatocytes at the circumference of the necrotic lesions (**Fig. 4Dii**). Furthermore, immunohistochemistry staining of these tissues for SCARF2 revealed live hepatocytes at the circumference of necrotic legions that contained positively-stained intracellular structures resembling phagosomes (**Fig. 4Diii**).

It was not clear as to whether the observed increases in hepatocyte multinucleation were the result of efferocytosis-induced cytokinesis failure. The ability of EIPA to inhibit Na^+-H^+ exchanger 1 (NHE1) and diminish macropinocytosis is conserved in mice liver (279). Therefore, to confirm that multinucleation was induced by efferocytosis, mice who had received APAP-induced injury were given a dose of 2.5 mg/kg EIPA, or an equal volume of DMSO (vehicle) (**Fig. 4E**). Four mice were used per experimental group. Although other studies have described the use of 25 mg/kg for inhibiting macropinocytosis in mice (279), a smaller dose was used to lower the required volume of DMSO for control animals. H&E staining was performed for liver tissue from these mice. Discreet areas of necrosis were again identified, and the proximal regions were assessed for multinucleation (**Fig. 4Eii-iv**). Hepatocytes in proximity to the necrotic lesion were more multinucleate than hepatocytes situated further away as previously observed. In contrast, this increase in multinucleation was not seen in mice treated with EIPA. Blood samples from mice were also examined for prognostic markers of liver injury (280) (**Fig. 4Ev**). Increases of detectable alanine aminotransferase (ALT) and aspartate aminotransferase (AST) and were recorded in APAP

treated mice compared to untreated. This damage was not significantly altered by the addition of EIPA treatment. These data provide more evidence that efferocytosis may induce multinucleation in hepatocytes *in vivo*.

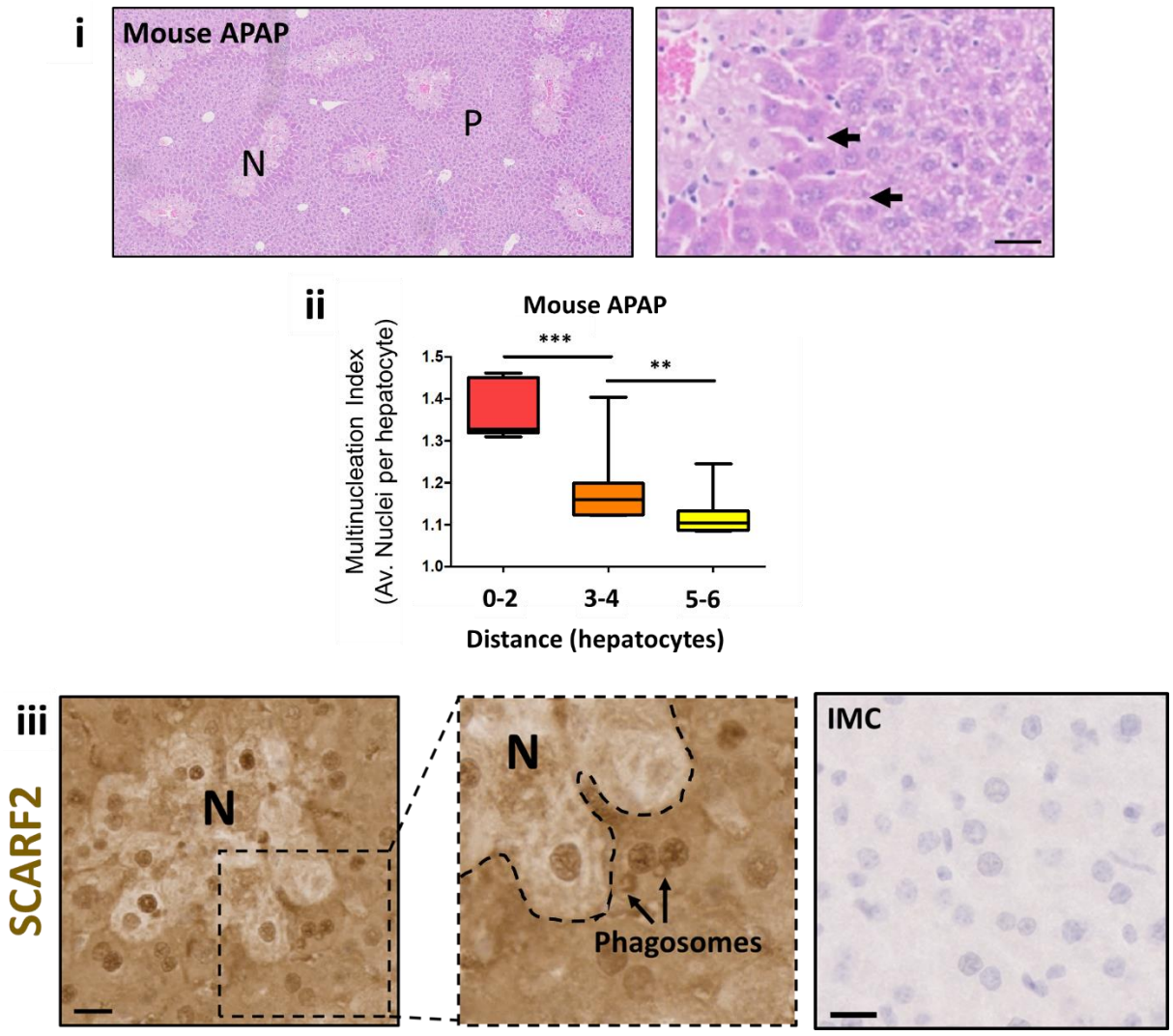

Figure 4D: Hepatocytes were more multinucleate proximal to areas of acetaminophen (APAP)-induced injury in mice. Eight-week old male C57BL/6 mice which received 300 mg/kg APAP in saline by intraperitoneal injection were then sacrificed after 24 hr. Tissues were harvested, fixed and paraffin-embedded for staining. **(i)** Areas of necrosis (N) and portal triads (P) in mouse livers which received an APAP-induced chemical injury, as shown by Haematoxylin and Eosin (H&E) staining. Arrows indicate hepatocytes containing small, dark-stained efferosomes. Scale bars represent 100 µm. **(ii)** Quantification of multinucleate hepatocytes in areas surrounding APAP-induced necrotic lesions in mouse livers. Numbers were derived from tissue analysis and did not required new experimentation. A minimum of 5 lesions were assessed each from 4 animals (N=4). ** - $p<0.01$, *** - $p\leq0.001$. Statistics were derived from a two-tailed, paired Student t-test when comparing multinucleation values in concentric zones to values obtained from the most distal zone identified. **(iii)** Immunohistochemistry staining for Scavenger receptor family F, member 2 (SCARF2 - brown) of liver tissue from mice treated with APAP alone. Tissues were counterstained with Mayers haematoxylin nuclear stain (blue). Black arrows indicate positively-stained intracellular structures resembling phagosomes. Dotted black line outlines necrotic lesion. Scale bars represent 20 µm.

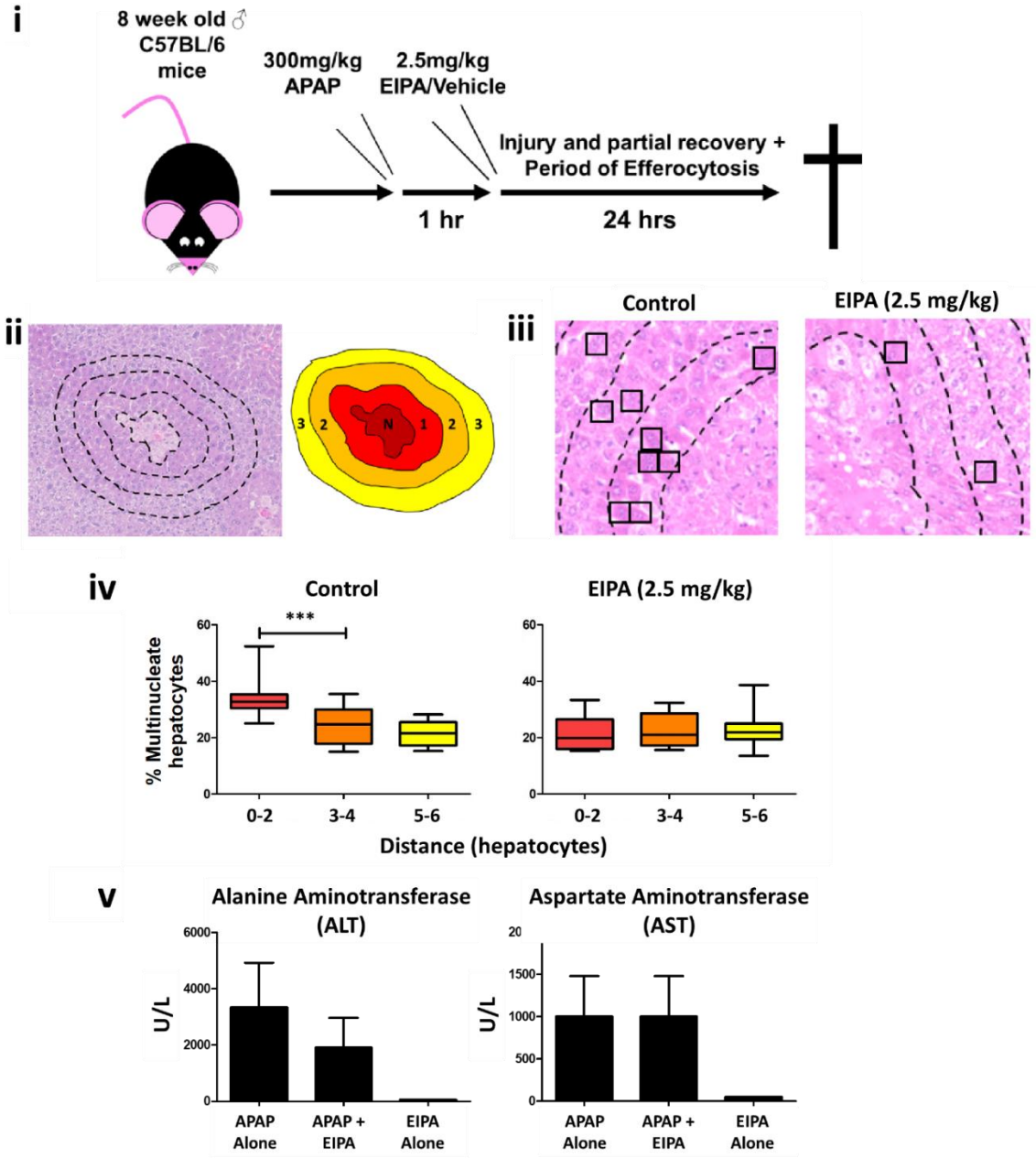

Figure 4E: Increases in hepatocyte multinucleation in response to injury were abolished following treatment with EIPA in mice with APAP-induced injury. (i) Diagram of experiment design. 8-week old male C57BL/6 mice received 300 mg/kg APAP in saline by intraperitoneal injection. Then they received 2.5 mg/kg 5-(N-Ethyl-N-isopropyl) amiloride (EIPA) through the same method. Mice were sacrificed after 24 hr and livers were collected for fixation, paraffin-embedding and staining. **(ii)** Example of Haematoxylin and Eosin (H&E) staining used to identify necrotic lesions (N), with outlined 2-hepatocyte thick concentric zones, moving proximal to distal. **(iii)** Identification of multinucleate cells (shown within black boxes) in areas surrounding necrotic lesions. **(iv)** Quantification of multinucleate hepatocytes with increased distance from the necrotic lesions. A minimum of 5 lesions were assessed per animal. N=8/experimental group. *** - $p \leq 0.001$. **(v)** Levels of alanine aminotransferase (ALT) and aspartate aminotransferase (AST) recorded from mice subjected to each condition. Error bars represent SEM. Statistics were derived from a two-tailed, paired Student t-test when comparing multinucleation values in concentric zones to values obtained from the most distal zone identified. Mouse handling, culling and liver harvesting were performed by Dr. Lozan Sheriff.

4.4 Hepatocytes proximal to necrotic lesions were more multinucleate than distal hepatocytes in tissues of paracetamol overdose patients.

Based on previous observations made *in vitro* and in mice *in vivo*, I hypothesised that efferocytosis could also induce multinucleation in human hepatocytes. To obtain an initial indication for the validity of this, I analysed tissues of both explants and biopsies from patients who required a transplant due to paracetamol overdose injury (POD) (**Fig. 4F**). This is the form of acute livery injury that is by simulated in mice by direct APAP administration. Giant hepatocytes possessing multiple nuclei were observed (**Fig. 4Fii**) that were reminiscent of cumulatively fed Huh-7 cells previously observed *in vitro* (**Fig. 3Bii**). However, the coverage of blanket necrosis is often much greater in human POD than in APAP-treated mice. As such, discreet necrotic lesions with enough viable surrounding tissue with which to assess for multinucleation were limited. Nevertheless, in one patient, I was able to assess a limited number of lesions were assessed as previously performed for mouse models (**Fig. 4Fiii**). Hepatocytes proximal to the necrotic lesions were again more multinucleate than those situated further way.

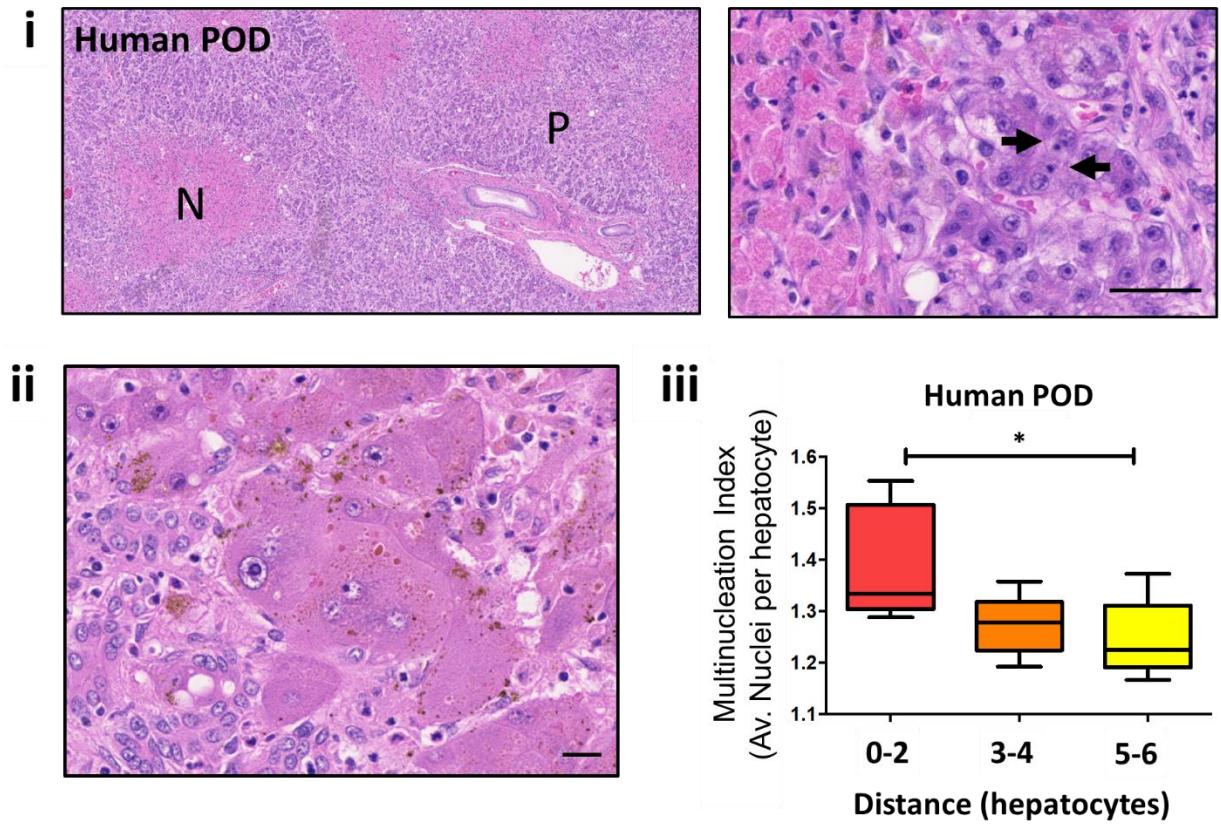

Figure 4F: Hepatocytes were more multinucleate proximal to areas of acetaminophen (APAP)-induced injury in paracetamol overdose patients. Staining and analysis of liver tissue explanted from a patient who suffered with paracetamol overdose (POD). **(i)** Areas of necrosis (N) and portal triads (P) as shown by Haematoxylin and Eosin (H&E) staining. Arrows indicate hepatocytes containing small, dark-stained efferosomes. Scale bars represent 100 µm. **(ii)** H&E stain showing larger multinucleate hepatocyte observed in the paracetamol overdose patient. **(iii)** Quantification of multinucleate hepatocytes in areas surrounding APAP-induced necrotic lesions in human liver. 5 lesions were assessed. N=1. * - $p<0.05$. Statistics were derived from a two-tailed, paired Student t-test when comparing multinucleation values in concentric zones to values obtained from the most distal zone identified.

4.5 Cauterisation model of injury in *ex vivo* human livers recapitulated consequences of hepatocyte efferocytosis in mouse models

Several clinical trials are currently underway at the Queen Elizabeth hospital which involve using normothermic machine liver perfusion (NMLP) (281, 282). The primary goal of these trials is to improve liver viability pre-transplantation by promoting normal metabolic activity of the liver, thus increasing the likelihood of successful transplantation. Many livers are perfused with blood or substitutes designed to improved oxygen delivery, such as the

acellular hemoglobin-based oxygen carrier (HBOC), Hemapure (281). Livers which do not meet the criteria required for transplantation are available for experimentation.

NMLP presented a unique opportunity for the delivery of drugs throughout the entirety of a human liver, *ex vivo*. It was reasoned that this setup could be used to assess whether efferocytosis specifically induces multinucleation in human hepatocytes under near-normal physiological conditions. Henceforth, NMLP was used to deliver 50 µM EIPA to donor livers which had previously under long-term perfusion with blood or Hemapure (**Fig. 4G**) (N=3). Livers were perfused for 30 min with EIPA-containing perfusates before wedge samples were taken. Livers were also perfused with DMSO and sampled prior to EIPA perfusions for use as controls. Wedges then received a cauterisation wound from a heated needle (**Fig. 4Gi, right**) to create a localised injury as a source of dying cells. The wedges were then incubated in DMEM for 24 hr to allow hepatocytes to efferocytose. Liver tissues were then fixed and paraffin-embedded for staining, whilst preserving the area of cauterisation. I hypothesised that these hepatocytes should be more multinucleate than those situated further away from the cauterisation wound, in a similar manner to the hepatocytes close to necrotic lesions in the previously used mouse models. To show this, H&E staining was performed on these tissues, which aided the identification of the "crush-like" cauterisation wound (**Fig. 4Gii**). Possible phagosomes, and multinucleate hepatocytes, were observable in these tissues (**Fig. 4Giii-iv**). Five-hepatocyte thick zones radiating from the wound were outlined and assessed for multinucleation (**Fig. 4Gv**). Hepatocytes were more multinucleate when situated closer to the cauterisation wound. This increase was abolished in tissues which were sampled post-perfusion with EIPA. In addition, the percentage of multinucleate hepatocytes was further augmented in liver tissue incubated with IFN-γ. This showed that efferocytosis could be both boosted and inhibited in *ex vivo* human tissues.

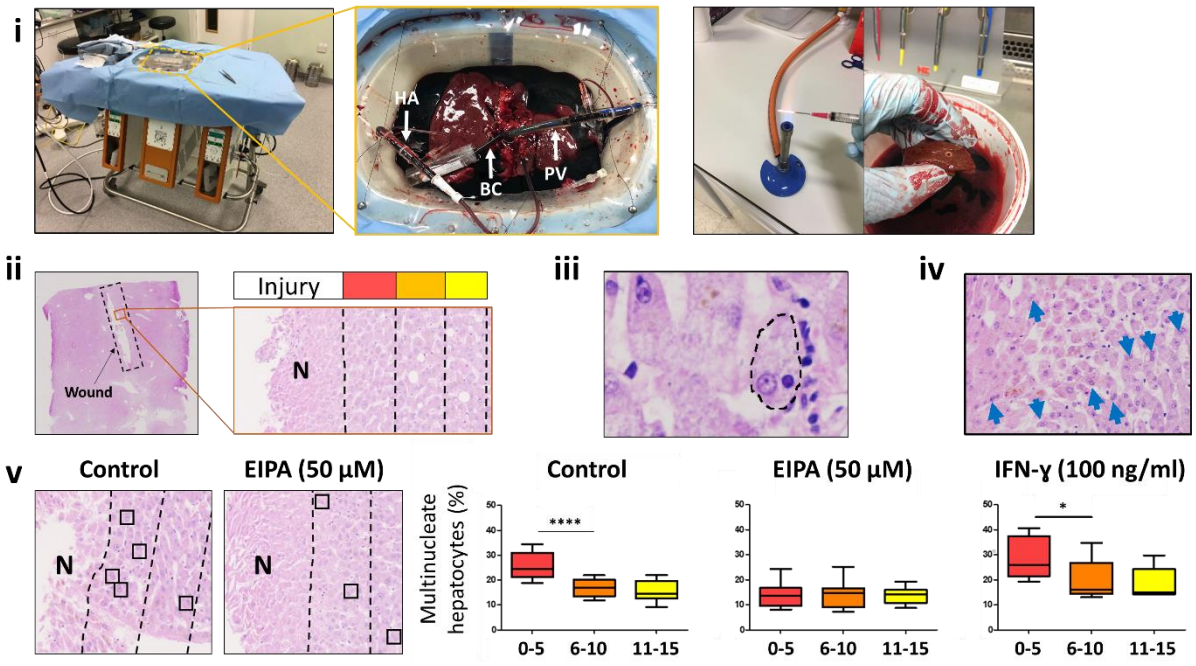

Figure 4G: Cauterisation injury in normothermic machine perfused, preserved human livers induced multinucleation to injury-proximal hepatocytes. Donor livers which had undergone 6 hr perfusion using normothermic machine perfusion (NMP) with blood or blood-substitutes, using a Liver Assist perfusion system, were sampled both before and after a 0.5 hr perfusion with 5-(N-Ethyl-N-isopropyl) amiloride (EIPA). Samples then received a localised cauterisation injury using a hot needle and were then incubated in media at 37°C for 24 hr to allow for hepatocyte efferocytosis and regeneration. Some samples were also incubated with media containing interferon-gamma (IFN-ɣ). Tissues were then fixed and stained with Haematoxylin and Eosin (H&E) and hepatocyte multinucleation was assessed compared to distance from the cauterisation wound. **(i)** Photographs of a Liver Assist perfusion machine (Left) containing a donor liver (middle) attached by the hepatic artery (HA) and portal vein (PV) and containing a bile collection (BC) tube, and of a heated syringe needle (right) used to create the cauterisation injury. **(ii)** H&E stained tissue identified the cauterisation would and the layout for analysing hepatocyte multinucleation, moving from proximal to distal from the site of necrosis (N). **(iii)** hepatocyte potentially containing an efferosome. **(iv)** Multinucleate cells present in cauterised tissue, as shown by blue arrows. **(v)** Percentage of multinucleate hepatocytes (shown in black boxes) with increased distance from the cauterisation wound. A minimum of 5 fields of view (FOV) were assessed per sample. N=3. * - $p<0.05$, *** - $p\leq0.001$, **** - $p\leq0.0001$. Statistics were derived from a two-tailed, paired Student t-test when comparing multinucleation values in concentric zones to each other.

4.6 Expression of proliferation and cell-cycle arrest markers was altered in hepatocytes proximal to sites of necrotic injury

This section details experiments which assessed the effect of hepatocyte efferocytosis on the expression of markers related to the continuity or arrest of the cell cycle.

4.6.1 Ki67 expression was increased in hepatocytes proximal to injury compared to distal hepatocytes in APAP-treated mice *in vivo* and cauterised human tissue *ex vivo*.

Previous reports regarding changes in polyploid in hepatocytes, either full sets or single chromosomes (aneuploidy), have been linked to the onset of liver regeneration (205, 275, 276, 283, 284). In addition, a recent report linked increases in macrophage efferocytosis with liver tissue repair and hepatocyte division (45). To investigate whether similar mechanisms could be incurred from hepatocyte efferocytosis, untreated and EIPA-treated liver tissues from APAP-treated mice and previously perfused, cauterised *ex vivo* human tissue, previously assessed for multinucleation at proximal regions to necrosis were stained for the proliferation marker, Ki67 (285), using immunohistochemistry (**Figs. 4H+I**). Ki67 has been previously validated as a marker for regenerating hepatocytes (276). An increase in Ki67 positive cells was observed in hepatocytes proximal to necrotic lesions in mice (**Fig. 4Ii**). An increase in Ki67 expression was also detected in hepatocytes close to the site of injury than those situated further away in cauterised human tissue (**Fig. 4Iii**). No change in Ki67 expression was seen in EIPA-treated tissues with increasing distance from the site injury. These data suggest that hepatocyte proliferation may be promoted in areas where these cells are actively conducting efferocytosis.

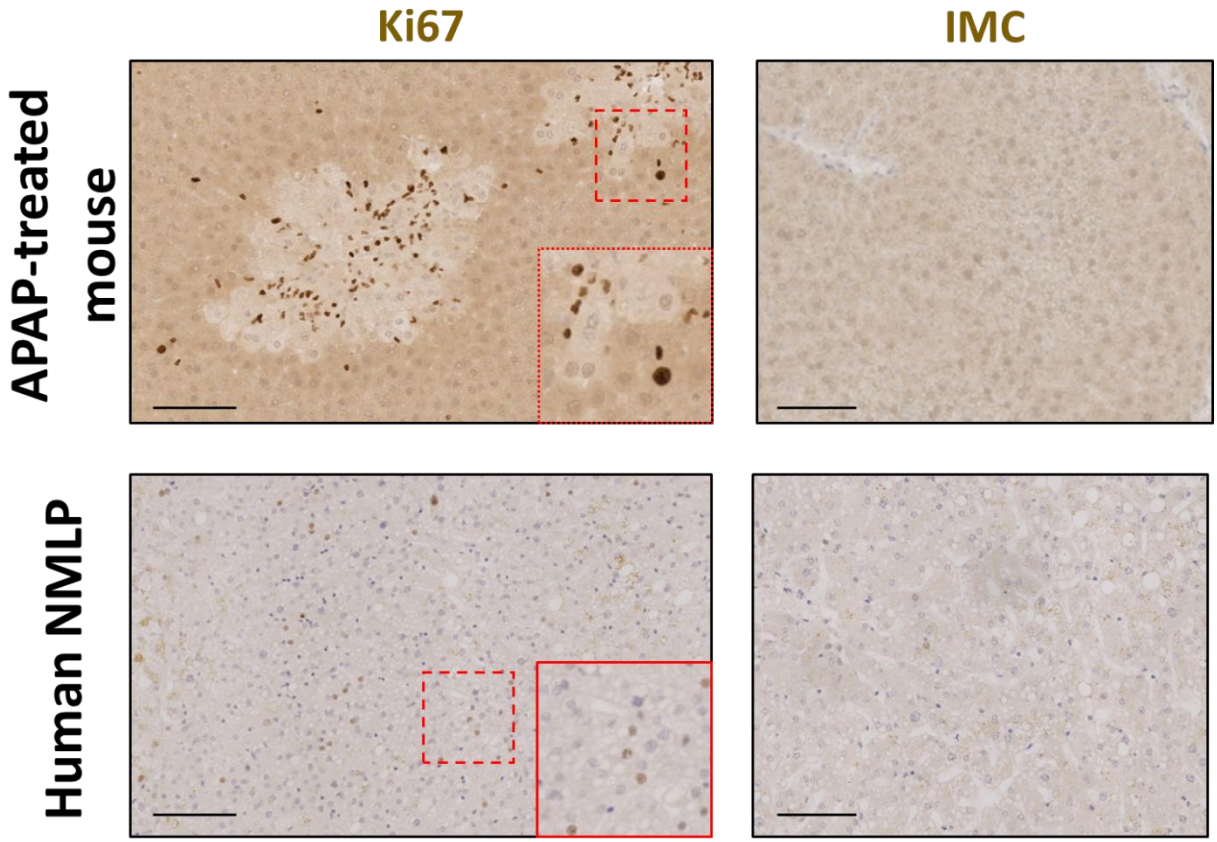

Figure 4H: Immunohistochemistry staining for Ki67 of liver tissues from mouse *in vivo* model and human *ex vivo* model of acute liver injury Paraffin-embedded tissues from mouse *in vivo* models and human *ex vivo* of acute liver injury were stained by immunohistochemistry for Ki67 (brown) or using an appropriate isotype-matched control (IMC; Goat IgG for mice, mouse IgG1 for human). Tissues were counterstained with Mayers haematoxylin (blue). Black scale bars represent 100 µm. Mouse tissues were derived from 8-week old male C57BL/6 mice which had received 300 mg/kg APAP in saline by intraperitoneal injection. Mice were sacrificed after 24 hr and their livers were collected for fixation and staining. Mouse handling, culling and liver harvesting were performed by Dr. Lozan Sheriff. Human tissue was supplied by donor livers which had undergone 6 hr perfusion using normothermic machine perfusion (NMP) with blood or blood-substitutes. IMC – isotype-matched control.

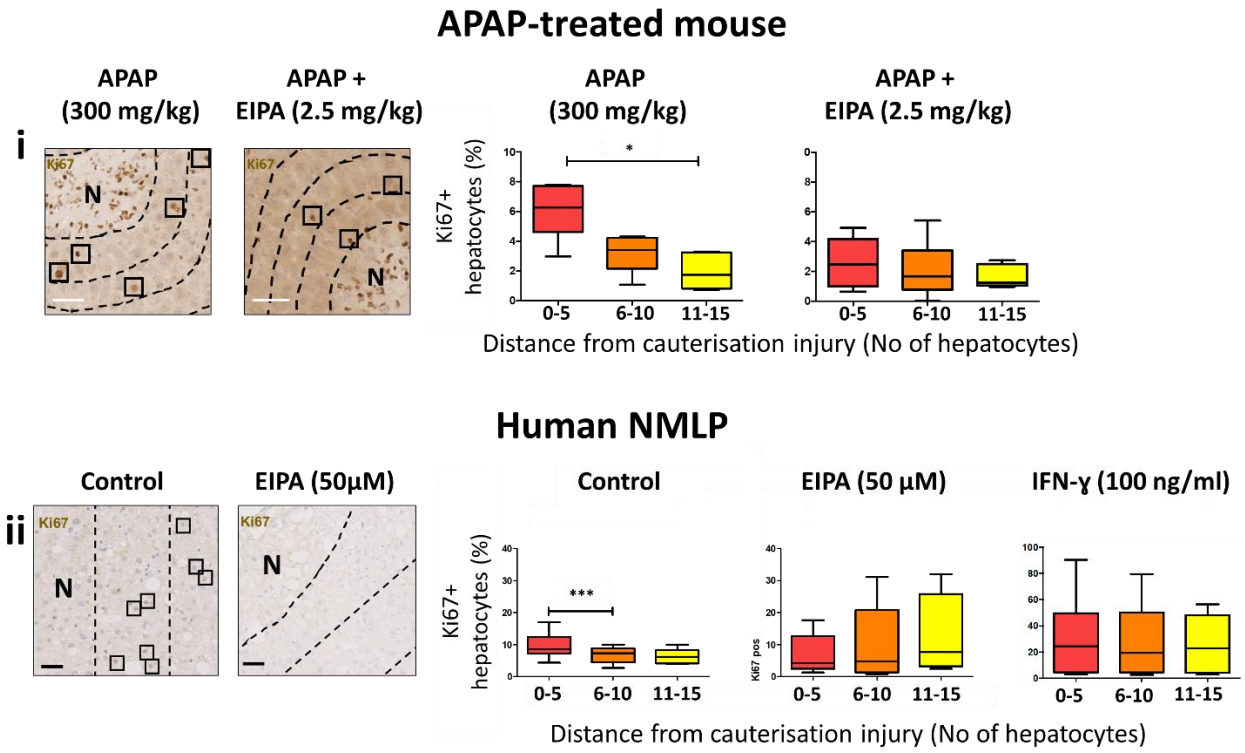

Figure 4I: Hepatocytes proximal to injury displayed EIPA-sensitive increases in Ki67 expression compared to distal hepatocytes in APAP-treated mice *in vivo* and cauterised human tissue *ex vivo.* Paraffin-embedded tissues from **(i)** mouse *in vivo* models and **(ii)** human *ex vivo* of acute liver injury were stained for Ki67 (brown) by immunohistochemistry and counterstained with Mayers haematoxylin (blue) (left panels). The percentage of positive hepatocytes (right panels) were then scored in proximal and distal areas relative to areas of necrotic injury (N). White and black scale bars represent 50 µm. * - $p<0.05$, *** - $p\leq0.001$. Statistics were derived from a two-tailed, paired Student t-test when comparing multinucleation values in concentric zones to each other. Black boxes indicate positively stained hepatocytes. **(i)** 8-week old male C57BL/6 mice received 300 mg/kg APAP in saline by intraperitoneal injection. They then received 2.5 mg/kg 5-(N-Ethyl-N-isopropyl) amiloride (EIPA) through the same method. Mice were sacrificed after 24 hr and their livers were collected for fixation and staining. A minimum of 5 lesions were assessed per animal. Eight animals were used per experimental group (N=8). Mouse handling, culling and liver harvesting were performed by Dr. Lozan Sheriff. **(ii)** Donor livers which had undergone 6 hr perfusion using normothermic machine perfusion (NMP) with blood or blood-substitutes were sampled both before and after a 0.5 hr perfusion EIPA. Samples then received a localised cauterisation injury using a hot needle and were then incubated in media at 37°C for 24 hr. Some samples were also incubated with media containing interferon-gamma (IFN-ɣ). Tissues were then fixed and stained. A minimum of 5 fields of view (FOV) were assessed per sample. Numbers are indicative of three experimental repeats (N=3).

4.6.2 Expression of p21 in hepatocytes proximal to injury increased in APAP-treated mice *in vivo*, compared to distal hepatocytes, but decreased in cauterised human tissue *ex vivo*

To provide further evidence that efferocytosis by hepatocytes could promote liver regeneration, tissues that were previously stained for Ki67 were also stained on serial sections for p21, a regulator of the G_1-S phase checkpoint and marker of cellular senescence (**Fig. 4J+Ki**) (286, 287). Significant increases in p21 expression were also observed at proximal regions compared to distal hepatocytes, in relation to necrotic lesions in APAP-treated mice (**Fig. 4Ki**). However, this increase was also observed in mice also treated with EIPA. Stains performed on cauterised human liver tissue showed collectively more p21-positive cells in tissues perfused with EIPA than in untreated tissues (**Fig. 4Kii**). Additionally, the median of p21-postive cells in these EIPA-treated human tissues was over double that of their mouse counterpart. Finally, a decrease in p21 expression was detected in hepatocytes proximal to the cauterisation injury in untreated and IFN-γ-treated tissues which was not observed in EIPA-treated tissues (**Fig. 4Kii**).

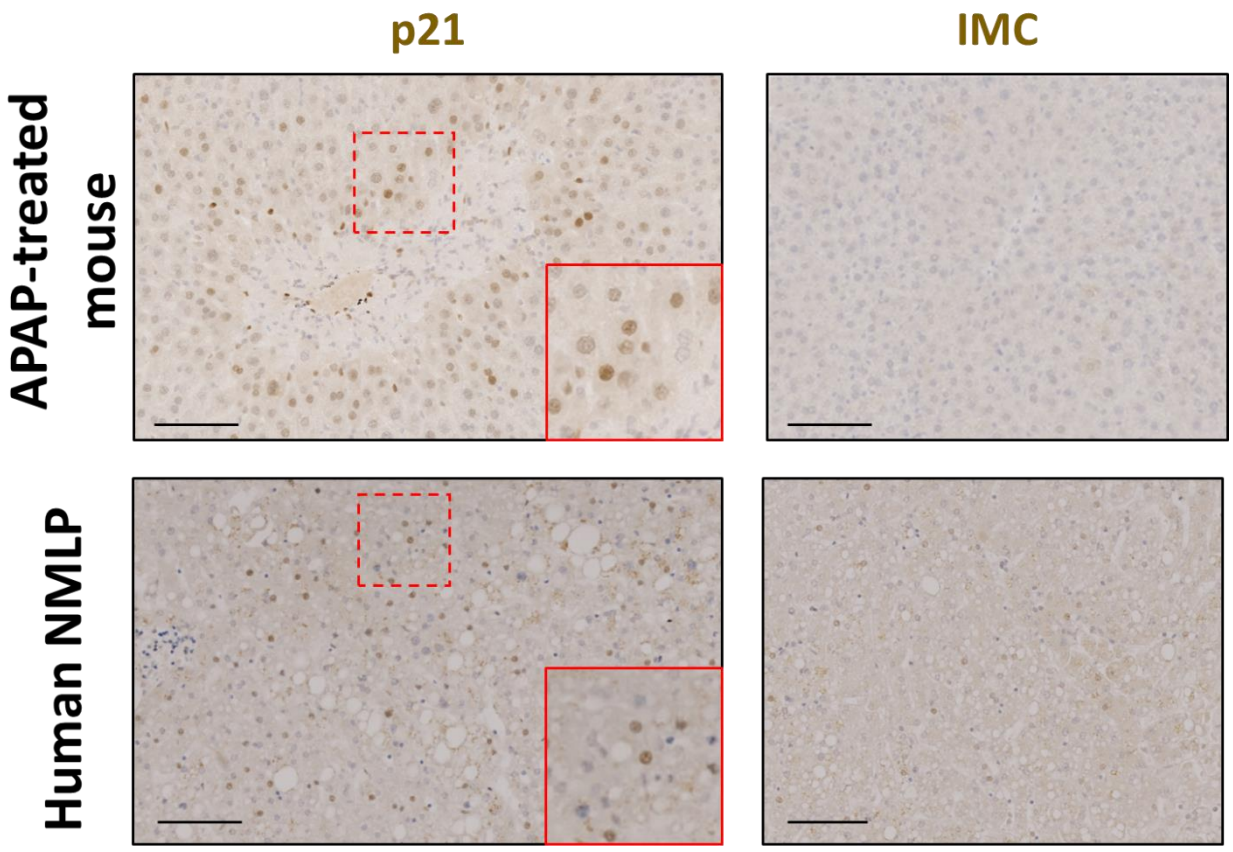

Figure 4J: Immunohistochemistry staining for p21 of liver tissues from mouse *in vivo* model and human *ex vivo* model of acute liver injury Paraffin-embedded tissues from mouse *in vivo* models and human *ex vivo* of acute liver injury were stained by immunohistochemistry for p21 (brown) or using a rabbit IgG isotype-matched control (IMC). Tissues were counterstained with Mayers haematoxylin (blue). Black scale bars represent 100 µm. Mouse tissues were derived from 8-week old male C57BL/6 mice which had received 300 mg/kg APAP in saline by intraperitoneal injection. Mice were sacrificed after 24 hr and their livers were collected for fixation and staining. Mouse handling, culling and liver harvesting were performed by Dr. Lozan Sheriff. Human tissue was supplied by donor livers which had undergone 6 hr perfusion using normothermic machine perfusion (NMP) with blood or blood-substitutes. IMC – isotype-matched control.

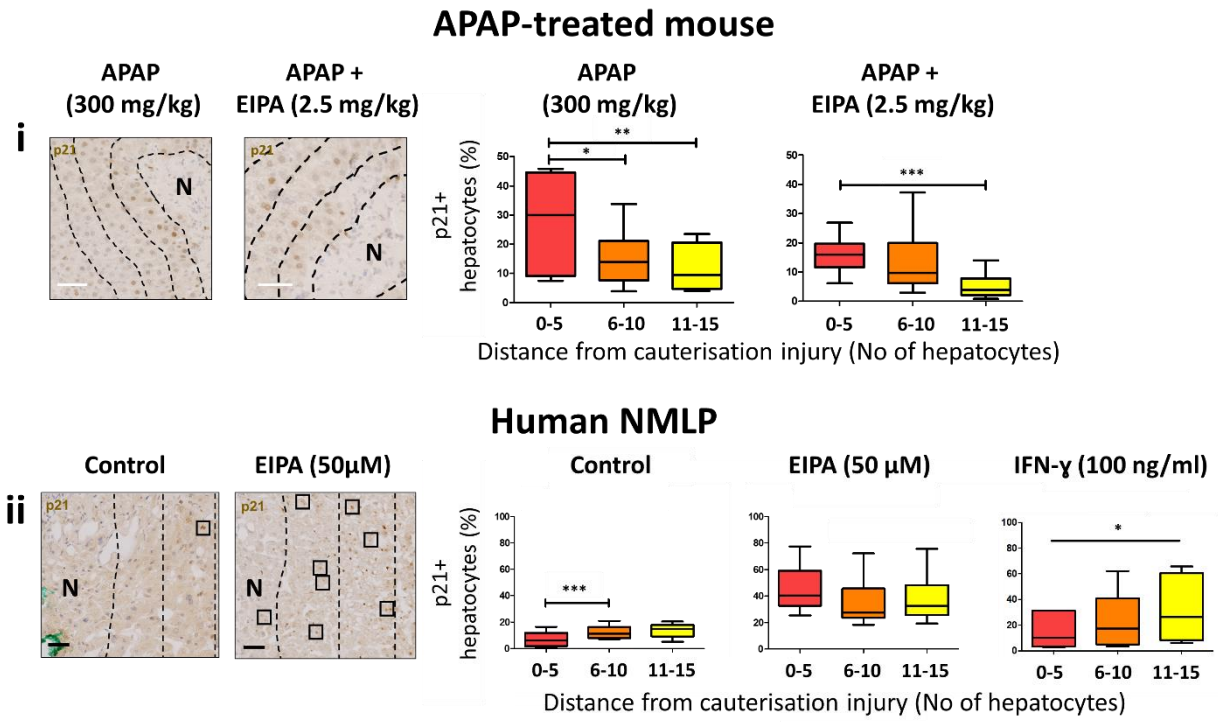

Figure 4K: p21 expression in hepatocytes proximal to injury increased in APAP-treated mice *in vivo,* compared to distal hepatocytes, but decreased in an EIPA-sensitve manner in cauterised human tissue *ex vivo.* Paraffin-embedded tissues from **(i)** mouse *in vivo* models and **(ii)** human *ex vivo* models of acute liver injury were stained for p21 (brown) by immunohistochemistry and counterstained with Mayers haematoxylin (blue) (left panels). The percentage of positive hepatocytes (right panels) were then scored in proximal and distal areas relative to areas of necrotic injury (N). White and black scale bars represent 50 µm. * - p<0.05, ** - p≤0.01, *** - p≤0.001. Statistics were derived from a two-tailed, paired Student t-test when comparing multinucleation values in concentric zones to each other. Black boxes indicate positively stained hepatocytes. **(i)** 8-week old male C57BL/6 mice received 300 mg/kg APAP in saline by intraperitoneal injection. They then received 2.5 mg/kg 5-(N-Ethyl-N-isopropyl) amiloride (EIPA) through the same method. Mice were sacrificed after 24 hr and their livers were collected for fixation and staining. A minimum of 5 lesions were assessed per animal. Eight animals were used per experimental group (N=8). Mouse handling, culling and liver harvesting were performed by Dr. Lozan Sheriff. **(ii)** Donor livers which had undergone 6 hr perfusion using normothermic machine perfusion (NMP) with blood or blood-substitutes were sampled both before and after a 0.5 hr perfusion EIPA. Samples then received a localised cauterisation injury using a hot needle and were then incubated in media at 37°C for 24 hr. Some samples were also incubated with media containing interferon-gamma (IFN-γ). Tissues were then fixed and stained. A minimum of 5 fields of view (FOV) were assessed per sample. Numbers are indicative of three experimental repeats (N=3).

4.7 Hepatocyte multinucleation in hepatocellular carcinoma

Changes in ploidy have been a frequently remarked feature of epithelial tumours (265, 269, 270, 272). Furthermore, multinucleation is often associated with the most prominent form of liver cancer, hepatocellular carcinoma (HCC) (288), and has also been noted to promote survival of in HepG2 cells (289). This section will address multinucleation in a cohort of HCC patients from the Birmingham NHS trust.

4.7.1 Hepatocyte nuclear factor 4α (HNF4α) staining facilitated hepatocyte multinucleation counts in normal liver and hepatocellular carcinoma

The relationship between multinucleation/ploidy increases and hepatocellular carcinoma (HCC), the most prominent form of liver cancer, has not been fully characterised. Liver cancer cells are much smaller and irregularly shaped, whilst often associated with other infiltrating cells (**Fig. 4Li**). This makes the task of attributing nuclei to specific cells difficult in these tumours. To overcome this, a method was developed to highlight hepatocyte-specific nuclei by staining tissues from HCC patients for hepatocyte nuclear factor 4 alpha (HNF4α) by immunohistochemistry (**Fig. 4Lii**). The antibody that was used has been to reported to selectively stain hepatocyte nuclei and exclude those of other hepatocyte cell types such as BEC (290). Hepatocyte nuclei could be identified in both normal and tumour tissue using HNF4α staining. Furthermore, non-hepatocytes could be identified as cells which were haematoxylin stained only, such as BECs, LSECs and lymphocytes. Negative staining of lymphocytes allowed them to be identified as CICSs or artefacts of tissue slicing, and thus not be included in multinucleation counts. This reduced the likelihood of confusing hepatocytes containing internalised cells with binucleates. Overall, HNF4α staining allowed

for the identification of hepatocyte-specific nuclei and their allocation to individual hepatocytes or tumour cells.

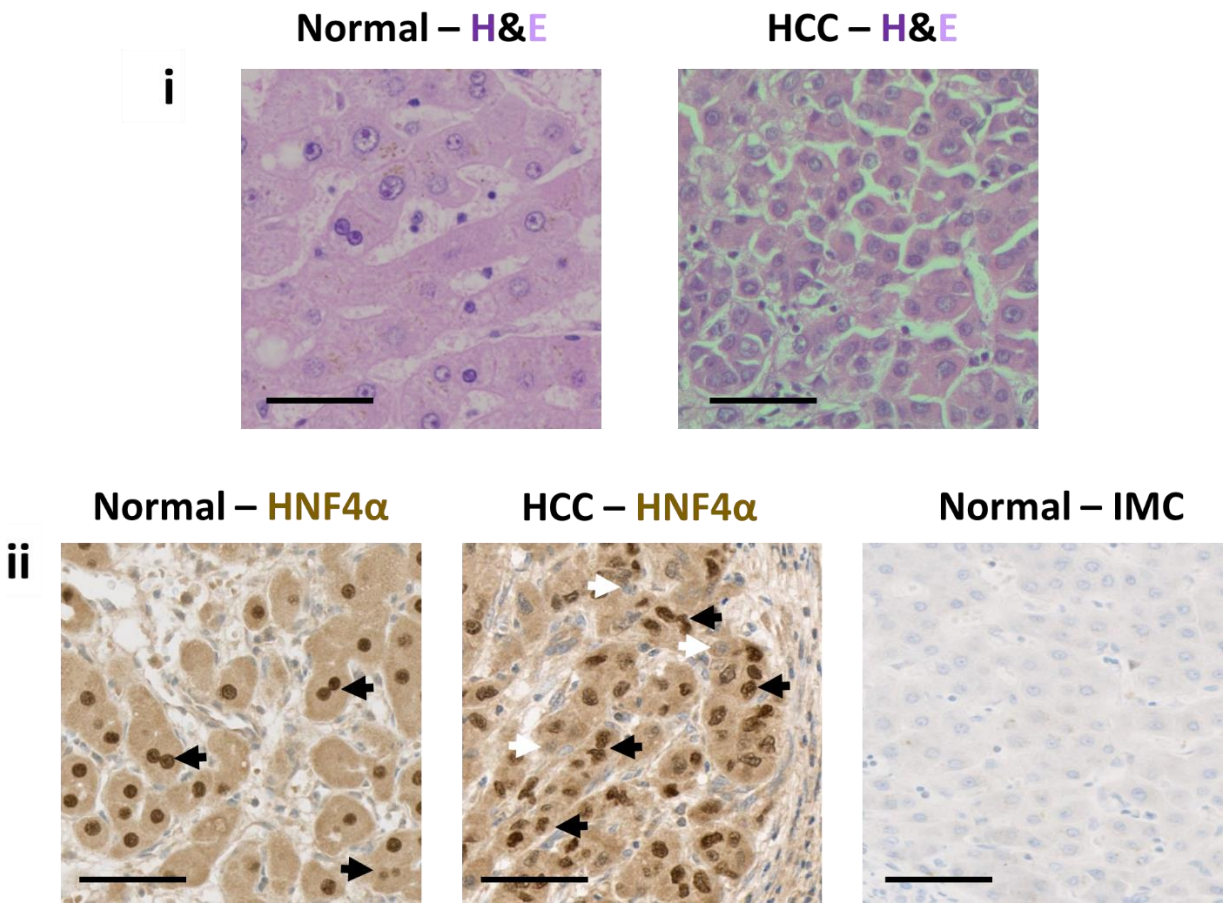

Figure 4L: Immunohistochemistry staining of HNF4α accurately and specifically identified the nuclei of hepatomas in patients with Hepatocellular carcinoma (HCC). (i) Haematoxylin and Eosin (H&E) staining of normal liver tissue and HCC. **(ii)** Normal and HCC tissues stained for hepatocyte nuclei factor 4-alpha (HNF4α) by immunohistochemistry (brown) and counterstained with Mayers haematoxylin (blue). Normal tissues from the same patient were also stained using a mouse IgG2a isotype-matched control (IMC). Black arrows identify HNF4α $^{+}$ve, binucleate hepatocytes. White arrows identify HNF4α -ve cells in hepatocyte cytoplasmic. Scale bars represent 50 µm.

4.7.2 Hepatocytes were more multinucleate near regions of interface hepatitis

Several patients with liver disease, particularly those which are autoimmune, often present with interface hepatitis, a process of parenchyma erosion is periportal areas, which correlate with a large mononuclear lymphocytic infiltration (291-293). Many of these areas are rich in dying, apoptotic cells, both of lymphocytic and hepatic origin. I hypothesised that hepatocytes in these regions would clearing these apoptotic cells and be more multinucleate than those further away from areas of interface hepatitis. To address this, IHC staining for HNF4α was performed on liver tissues from HCC patients presenting with interface hepatitis, as determined by the resident pathologist (n=16, **Fig. 4M**). This staining facilitated the accurate determination of hepatocyte nuclei in these parenchymal areas with heavy inflammatory cell infiltration. Five hepatocyte-thick 'zones' were then outlined, radiating from the border of the hepatic infiltrate (**Fig. 4Mi**). The percentage of multinucleate hepatocytes within each of these zones was then determined. Significantly more hepatocytes were multinucleate in zones proximal to the region of interface hepatitis than those situated further away (**Fig. 4Mii**). Out of 16 patients analysed, 14 displayed a decrease in hepatocyte multinucleation when moving proximal to distal from the area of interface hepatitis (**Fig. 4Miii**).

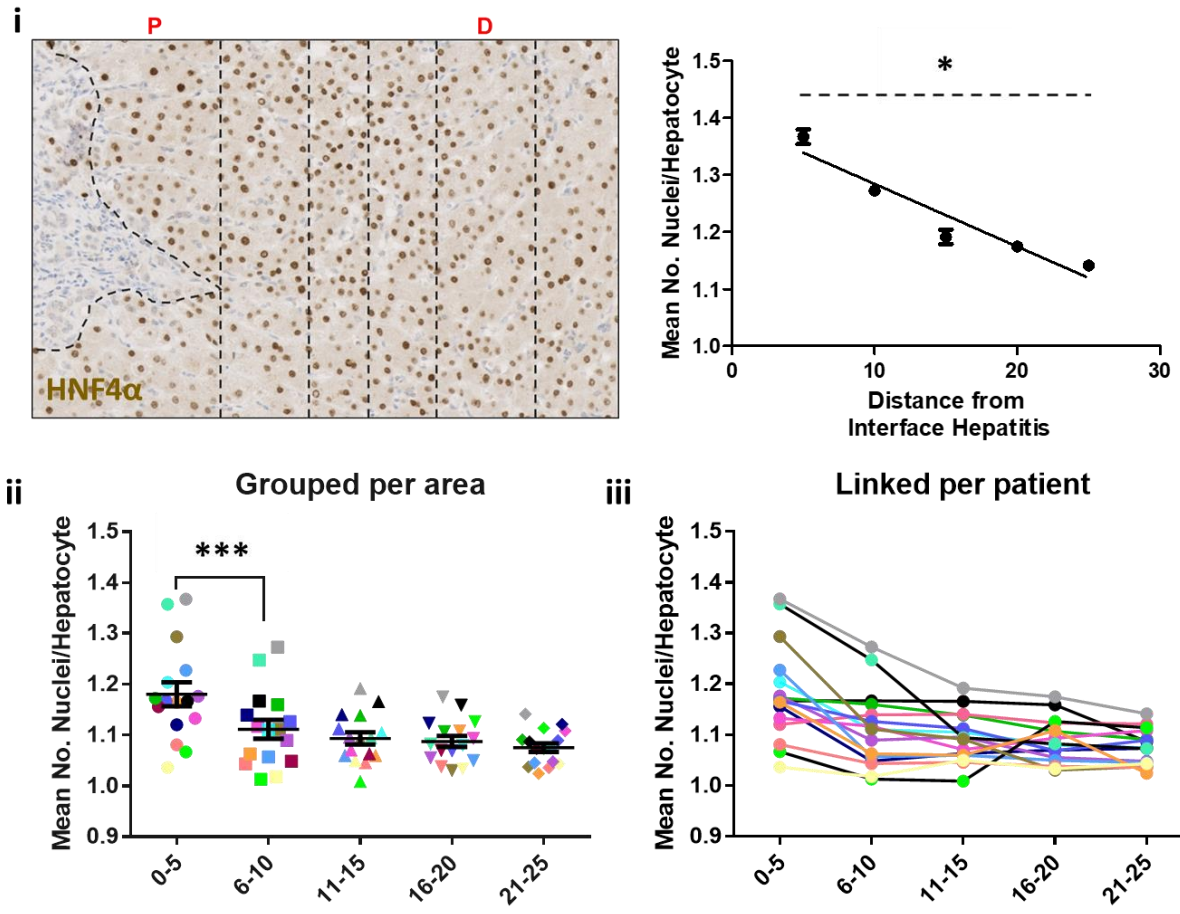

Figure 4M: Proximity to areas of high efferocytosis linked to inflammation, correlated with more multinucleate hepatocytes. Paraffin-embedded liver tissues from patients presenting with chronic liver disease, hepatocellular carcinoma and interface hepatitis were stained for hepatocyte nuclear factor 4α (HNF4α) and counterstained with Mayers haematoxylin. The mean number of nuclei/hepatocyte was then determined in five-hepatocyte-thick areas with increasing distance from areas of inflammatory infiltrate. **(i)** Left: Example area of HNF4α staining (brown) and sectioning of parenchymal areas with distance from inflammatory infiltrate (large areas of smaller blue cells), moving from proximal (P) to distal (D) areas; Right: corresponding quantification of mean no. of nuclei/hepatocyte with increasing distance from inflammatory infiltrate. *- $p<0.05$ as determined by Pearsons correlation coefficient. **(ii-iii)** Collective quantification of mean no. of nuclei/hepatocyte in hepatocyte areas with increasing distance from inflammatory infiltrate. Data are plotted both **(ii)** grouped per hepatocyte areas and **(iii)** linked per patient sample. Each colour represents an individual patient. *** - $p<0.001$. Middle line represents mean and error bars represent the SEM. Statistics were derived from a two-tailed, paired Student t-test when comparing multinucleation values in concentric zones to each other. These analyses were partially performed by Biomedical Science undergraduate, Devinderjit Sangha.

4.7.3 Tumours Increased hepatocyte multinucleation was associated with tumours

To demonstrate whether tumour cells were more multinucleate than their corresponding non-neoplastic hepatocytes, HNF4α IHC staining was performed for HCC tissue samples, both from liver resections and biopsies, of tumour, distal, and marginal regions within the same patient (**Fig. 4N**). Normal and tumour regions in tissues were easily identifiable in HNF4α-stained tissues (**Fig. 4Ni**). This staining also allowed for the identification of CICSs within hepatocyte cancer cells (**Fig. 4Nii).** The percentages of multinucleation within normal hepatocytes and tumours were then assessed (**Fig. 4Niii-iv**). In all cases analysed, tumour cells were more multinucleate than their non-neoplastic counterparts. These observations suggest that HCC may correlate with increased multinucleation and, therefore, ploidy.

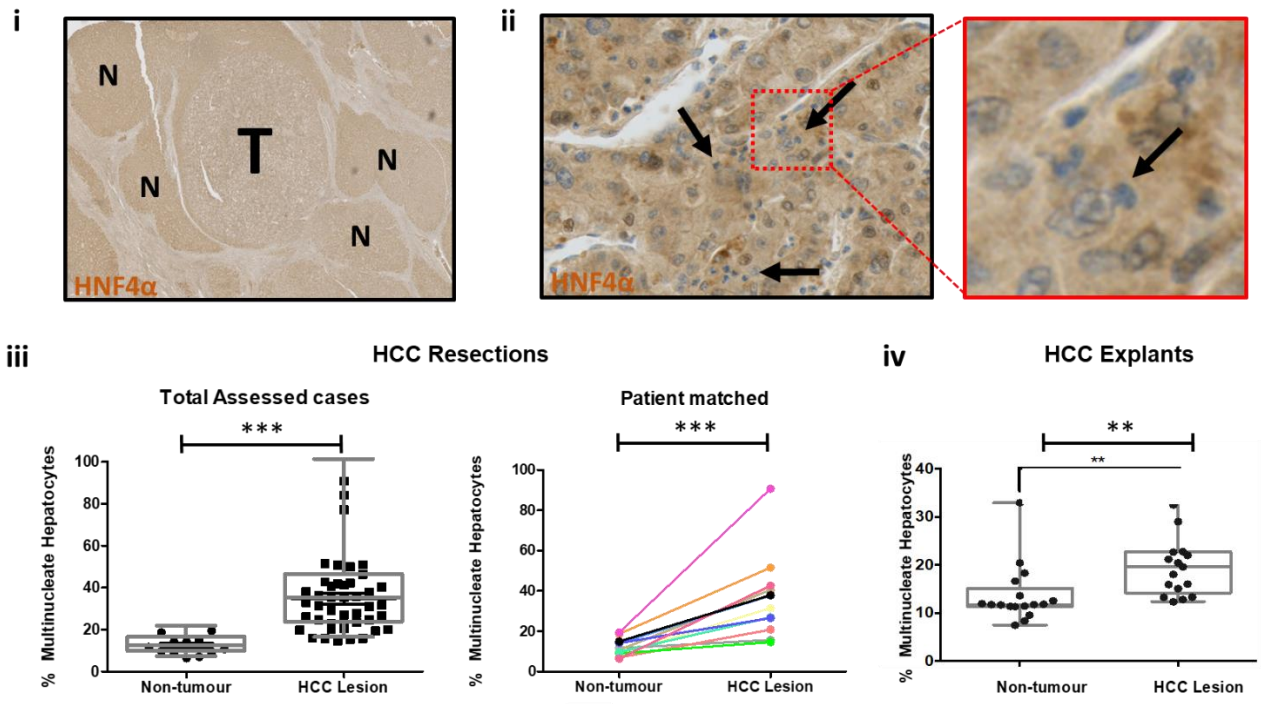

Figure 4N: Hepatomas displayed more frequent multinucleation compared to marginal and distal hepatocytes in hepatocellular carcinoma (HCC) explants and resection specimens. Paraffin-embedded liver tissues from patients with HCC were stained for hepatocyte nuclear factor 4α (HNF4α) by immunohistochemistry and counterstained with Mayers haematoxylin to allow for the confident identification of hepatocyte/hepatoma nuclei, as well as neoplastic areas. **(i)** Example tissue stained for HNF4α (brown) with identifiable areas of HCC tumour lesion surrounded by a fibrous capsule (T) and adjacent non-cancer liver lobules (N). **(ii)** *Left;* Area of tissue exhibiting efferocytosis by neoplastic hepatocytes. Arrows show small dark blue nuclei seen inside the cytoplasm of hepatic tumour cells. Hepatoma nuclei were large and oval. *Right;* Red box displaying zoomed image of an efferocytosing neoplastic hepatocyte. **(iii-iv)** Mean values of hepatocyte multinucleation for HCC patients, comparing tumour to distal/margin areas where available. Each data point represents mean values for an individual patient where over 1,000 hepatocytes were scored per patient. **(iii)** Comparison of hepatocyte multinucleation in tumour and non-tumour regions in resected tumours. *Left;* total available tumour and non-tumours. *Right*; matched comparison within the same patient. **(iv)** Comparison of hepatocyte multinucleation in tumour and non-tumour regions in tumours explants. ** - $p<0.01$, *** - $p<0.001$ based on an unpaired two-tailed Students t-test comparing tumour and non-tumour values. These stains and analyses were partially performed by Biomedical Science undergraduate, Rukhsarr Ahmed.

4.7.4 Tumours with vasculature invasion possessed more multinucleate hepatocytes

Increases in ploidy have been linked to more aggression and an increased risk of metastasis in cancers (294). It is likely that increased multinucleation may have similar implications for HCC. An unexpected benefit to HNF4α staining of HCC tissues was that it was possible to identify tumour cells that were invading into vessels (**Fig. 4Oi**). With this, the percentage of multinucleate hepatocytes (both normal and neoplastic) was compared between samples from patients with or without evidence of vascular invasion by cancer cells **(Fig. 4Oii).** More multinucleate hepatocytes were seen in tumours that also presented evidence of tumour invasion. This provides evidence that multinucleation may also be associated with increased aggression in HCC.

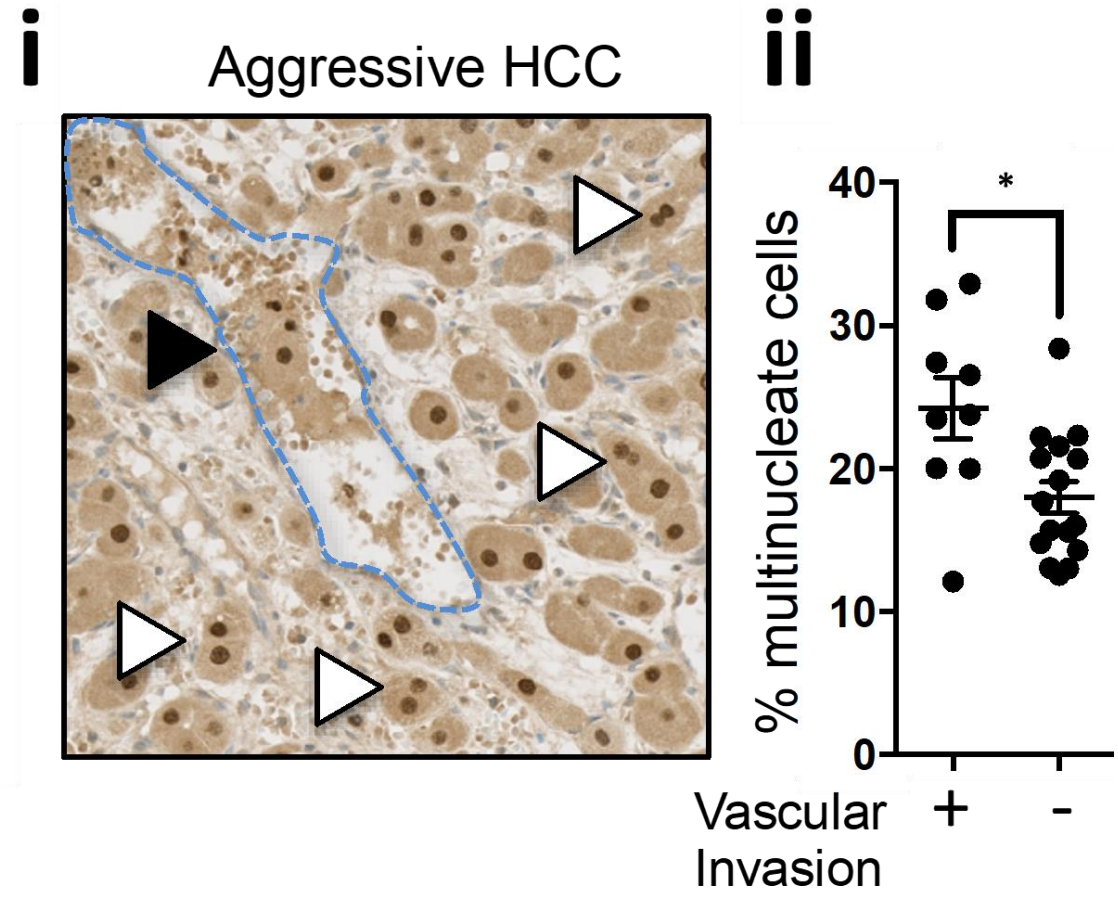

Figure 4O: Patients with evidence of vascular invasion possessed a higher incidence of multinucleate hepatocytes. Paraffin-embedded liver tissues from patients with hepatocellular carcinoma (HCC) were stained for hepatocyte nuclear factor 4α (HNF4α -brown) by immunohistochemistry and counterstained with Mayers haematoxylin (blue) to allow for the confident identification of hepatocyte/hepatoma nuclei, as well as neoplastic areas. **(i)** Area of HCC tumour metastasis. White arrows indicate binucleate cells. Black arrow indicates outlined region of vascular invasion. **(ii)** Percentages of multinucleate normal and neoplastic hepatocytes in tissues with and without evidence of vascular invasion of tumours. Middle line represents mean and error bars represent the SEM.* - $p<0.05$. Statistics were derived from an unpaired, two-tailed Student-test comparing patients with and without evidence of vascular invasion.

4.8 Chapter Summary

Table 5: Summary of all new discoveries presented in chapter 4.

1. Efferocytosis induced cumulative increases in multinucleation in hepatomas *in vitro.*
2. Hepatocytes were more multinucleate when proximal to necrotic lesions, both in mouse models of acute liver injury and in human livers with APAP-induced injury.
3. The hepatocyte efferocytosis inhibitor EIPA abolished the increase of multinucleation in hepatocytes proximal to sites of injury in mouse and human tissue with acute injury.
4. Hepatocytes proximal to necrotic lesions in mice expressed Ki67 more frequently than distal cells. This was abolished in EIPA-treated mice.
5. Hepatocytes proximal to necrotic lesions in cauterised *ex vivo* donor liver tissue from NMLP-treated livers expressed p21 less frequently than distal cells. This was not observed in EIPA-treated mouse livers.
6. Hepatocytes proximal to areas of interface hepatitis with high efferocytosis rates were consistently more multinucleate than distally situated hepatocytes in patients with chronic inflammation.
7. Tumour cells were more multinucleate than non-neoplastic hepatocytes in patients with the hepatocellular carcinoma.
8. Increased multinucleation was associated with increased vascular invasion in hepatocellular carcinoma.

4.9 Discussion

4.9.1 Hepatocyte efferocytosis induced multinucleation in three different experimental models

Experimentation using a variety of differently biological models has provided robust evidence that efferocytosis can induce multinucleation in hepatocytes. Initial evidence for this came from *in vitro* experiments, whereby the frequency of multinucleate Huh-7 cells was increase following their 'feeding' with heat-killed Jurkat lymphomas. Heat-killed cells were used over apoptotic cells as they create generally larger efferosomes which are more likely to impede cytokinesis. In isolation, these experiments did not reflect the likelihood of efferocytosis to increase multinucleation *in vivo*; Huh-7 cells are cancerous cells and may have different propensities for efferocytosis. The liver is also occupied by other efferocytes, such as Kupffer cells, which would partial relieve the burden of clearing dead cells in the liver (1). However, increases in multinucleation were observable *in vivo* in hepatocytes proximal to necrotic lesions in different mouse models of acute liver injury, but also in cauterised *ex vivo* human tissue. Collectively, using *in vitro, in vivo* and *ex vivo* provided robust evidence that efferocytosis could cause multinucleation in hepatocytes.

Cytokinesis failure was never observed in actively efferocytosing cells. However, this phenomenon was implied by the ubiquitous effect of the previously validated inhibitor of hepatocyte efferocytosis, EIPA, to prevent multinucleation in all three experimental models. Another explanation for the abolishment of increased hepatocyte multinucleation following EIPA-treatment would be if hepatocytes were prevented from proliferating; cells must enter

the cell cycle and complete DNA synthesis to become binucleate following failure of cytokinesis. However, EIPA treatment did not prevent Huh-7 cells from dividing *in vitro* (**Fig. 4Biv**). Additionally, treatment of mice and *ex vivo* human tissue with EIPA did not reduce the overall expression of Ki67 in hepatocytes in the liver when compared to controls (**Fig. 4I**). These data suggest that efferocytosis is more likely to induce multinucleation by cytokinesis failure in similar fashion to CICSs (185, 204).

4.9.2 Advantages of normothermic machine liver perfusion for research investigations

The work described in section 4.5 exemplifies, for the first time, a novel use of NMLP as an investigative tool for answering a research question. This provided an effective drug delivery tool which allowed for the studying the effects of EIPA on hepatocytes in the setting of a complete liver. This model of using human *ex vivo* tissue provides numerous advantages over commonly used tools. The foremost of which is the opportunity to work directly with human tissue. All findings made using this system can thus be directly applied to human liver biology. This removes the requirement for validation or stratification of results produced from mouse models. Furthermore, as there are numerous differences in the immune system and liver transcriptome, between mice and humans, mouse models do not accurately represent human disease pathology (295, 296). As such, NMLP and human *ex vivo* tissue may represent a more biologically relevant model than mice. Adapting the use of NMLP, or potentially related, downscaled technologies, for use with diseased liver tissues may alleviate the requirement for representative mouse models for each aetiology of chronic liver disease.

Direct experimentation using *ex vivo* human liver also reduces the complications associated with using primary human hepatocytes (PHH) for experimentation. PHH are difficult to

isolate and culture *in vitro.* Furthermore, they do not maintain many of their functions when isolated from the liver; many signalling pathways are silenced, their polarity is altered, and they fail to proliferate (247). Studying hepatocytes in the context of an intact human liver removes the requirement to isolate them and maintains their correct functionality and polarity. As such, it is likely that results achieved with this model are more representative of authentic hepatocyte behaviour.

The validity of the results derived from NMLP tissue was made apparent by its ability to recapitulate results derived from *in vivo* mouse models (**Fig. 4G**). Cauterisation of human tissue was able to able to mimic the induction of hepatocyte efferocytosis which was achieved by APAP treatment in mice. Equally, the capacity of EIPA to prevent efferocytosis in the liver was achieved in both models. Importantly, this would suggest that the ability of hepatocytes to clear dead cells, as well as its susceptibility to EIPA, is conserved between mice and humans. As such, evolutionary conservation of efferocytosis in hepatocytes is made evident by comparing data received from both mouse and human, which demonstrates the physiological importance of this process for the liver.

4.9.3 Ploidy alterations in the liver – a complex system for adaptation

Changes in the quantity of chromosomes within hepatocytes presents a complex and intricate system for intercellular adaptation. It is known that increased genetic diversity within the liver grants aspects of increased survival, such as the ability to adapt to more detrimental mutations by gaining others which compensate for them (297, 298). Additionally, increased multinucleation in normal hepatocytes is thought to decrease the risk of tumorigenesis by preserving tumour-suppressing genes (299). Although this was initially thought to be caused by cytokinetic failure, based on expression of the cytokinetic

machinery (276, 300, 301), the data presented in this chapter now show a new phenomenon where hepatocytes can intrinsically promote their own multinucleation. Due to the higher degree of potential variation between hepatocytes in ploidy, coupled to the unique role of certain hepatocytes caused by lobular positioning, it is conceivable that multiple subtypes of hepatocytes may develop over a lifespan. Understanding how and when ploidy alterations are generated, and to which of these persist in the liver, may improve our understanding as to how the liver changes over time. Furthermore, this may also yield useful insights into risk factors of HCC, particularly for patients already suffering with end-stage liver disease with a high burden of necrosis.

4.9.4 Is efferocytosis the primary signal of liver regeneration?

The ability for hepatocytes to proliferate and regeneration large portions of the liver in response to damage has set them aside from other parenchymal cell types. However, although signalling events and molecular alterations are involved in liver regeneration, many of the signals which stimulate hepatocytes to proliferate are not well understood (31). Hepatocytes rarely divide under homeostasis and lose the ability to divide once isolated from the liver (69). A greater insight into the initiation mechanisms of hepatocytes would be of benefit for both physiological and experimental reasons. A recent publication described evidence for infiltrating, efferocytosing macrophages in promoting liver regeneration through STAT3 signalling (45). However, in response to parenchymal liver injury, it would be hepatocytes who would initially respond and engulf their necrotic or apoptotic brethren. It is logical that hepatocytes would proliferate in response to signals from dying cells, as they would be required to replace cells which were lost.

Using cauterised *ex vivo* human tissue, it was shown that in parenchymal areas proximal to injury, hepatocytes were more likely to express Ki67 and less likely to express p21 (**Fig. 4K+4I**). These observations were lost in EIPA-treated tissue, suggesting that these changes in expression were consequences of hepatocyte efferocytosis. EIPA-sensitive increases in Ki67 expression in injury-proximal hepatocytes were also observed in APAP-treated mice (**Fig. 4K**). Contradictory to this, p21 expression in hepatocytes was also higher in these areas (**Fig. 4I**). However, the same increases were also seen in EIPA-treated animals, suggesting that efferocytosis stimulated by injury did not influence p21 expression. This was logical as the livers of these mice were otherwise healthy prior to APAP delivery. As such, these mice would only possess a minimal quantity of senescent hepatocytes, which may have been in acutely increased next to areas of metabolic injury. Collectively, these data suggest that hepatocytes can be induced to divide through signals derived from dying cells, or hepatocytes which are actively engulfing them. Further understanding as to the identity of these signals may prove useful in promoting liver generation in patients. The same information may also prove effective in extending the *in vitro* culture time of PHH isolated from the liver, as they do not proliferative under currently used culture conditions.

The observed decreases in p21 expression in hepatocytes proximal to cauterisation injury suggests that efferocytosis may rescue hepatocytes from senescence and become available for liver regeneration. Under chronic inflammatory conditions, often associated with fatty diets or increased alcohol consumption, hepatocytes can lose the ability to regenerate the liver because of decreased intracellular signalling in response to inflammatory stimuli (302, 303). Coupled to the limited capacity of hepatocytes to regenerate, due to nodular fibrotic scarring, liver regeneration is often compromised during end-stage liver disease. As such, patients with chronic liver disease have difficulty in recovering damage which occurs to their

liver. This may be coupled with a reduced capacity either of hepatocytes to conduct efferocytosis or for them to recover from senescence in response to dying cells. With further understanding into the exact mechanisms involved with hepatocytes responses to internalising dying cells, such mechanisms could be exploited to reduce senescence within patients with chronic liver disease.

4.9.5 Hepatocyte efferocytosis and multinucleation – balance of good and evil?

Many reports have shown how multinucleation in hepatocytes can be of great benefit to the hepatic 'cellular ecosystem'. As to whether changes in ploidy in hepatocytes are solely beneficial or detrimental to the liver is currently in dispute. Duncan *et al,* 2012, used both single and double knockout mouse models for members of the tyrosine metabolism pathway to illustrate how genetic instability could promote Darwinian survival of adapted hepatocytes (298). The production of a hepatotoxic substance in the single knockouts, caused by the incomplete metabolism of tyrosine, created widespread liver damage and weight-loss. After these mice recovered, all hepatocytes had the same genotype as the double knockout mouse. The hepatocytes which had gained genetic alterations were able to adapt to the toxic insult. This demonstrates how the liver is designed to establish genetic diversity at the cellular level. The capacity of hepatocytes to engulf apoptotic cells in homeostasis may represent a catalyst for this by promoting multinucleation and increasing the incidence of aneuploidy by 'lagging chromosomes'.

It is often described that end-stage chronic liver disease, regardless of the aetiology, is tantamount to onset of HCC (304). This would imply that different chronic liver diseases share the same oncogenic process, even if they arise under different circumstances. One aspect associated with all liver diseases is the increase of cell corpses in the liver, both of

hepatocytes and infiltrating immune cells. Given the capacity of hepatocytes to efferocytose dying cells, this would also suggest that all forms of liver disease are concurrent with increases in hepatocyte multinucleation. Several large multinucleate cells were previously observed in patients with POD (**Fig. 4F**).

Though this is a form of acute liver injury, it typifies the possibility of increased multinucleation and dysregulated cells in response to necrotic injury. On these grounds, despite the inherent advantage of efferocytosis for hepatocytes to improve their survival through genetic alteration, unregulated efferocytosis in disease states may increase the risk of acquiring unwanted, potentially oncogenic mutations.

In conclusion, the influence of efferocytosis on hepatocyte ploidy exists a tenuous balance (**Fig. 4P**); in the steady state, ploidy increases which arise from random cytokinetic failure or hepatocyte efferocytosis in homeostasis are most likely to be of benefit as they provide genetic adaptions at the cellular level. This would ensure that some hepatocytes would be adapted to specific inflammatory insults or injuries, as shown by Duncan *et al.* Initially this would provide a source of genetic variation throughout the liver and increase the likelihood that a population of hepatocytes could adapt to certain toxic or inflammatory insults. However, in liver disease hepatocyte efferocytosis is increased by the larger incidence of cell death. Although this is initially still beneficial to the liver by limiting inflammatory responses and potentially promoting regeneration, high volumes of efferocytosing cells may eventually become detrimental; not only will hepatocytes frequently fail to divide when actively efferocytosing, but they will continue to gain whole chromosome sets and genetic alterations. Eventually, a 'point of no return' may be reached in which efferocytosing hepatocytes eventually acquire oncogenic alterations and develop HCC. Cancer cells may also continue to efferocytose and gain further genetic abnormalities. Overall, efferocytosis in the liver is a process that is necessary to ensure immunotolerance and provide genetic variation to the liver but must be controlled to reduce the risk of acquiring undesirable mutations.

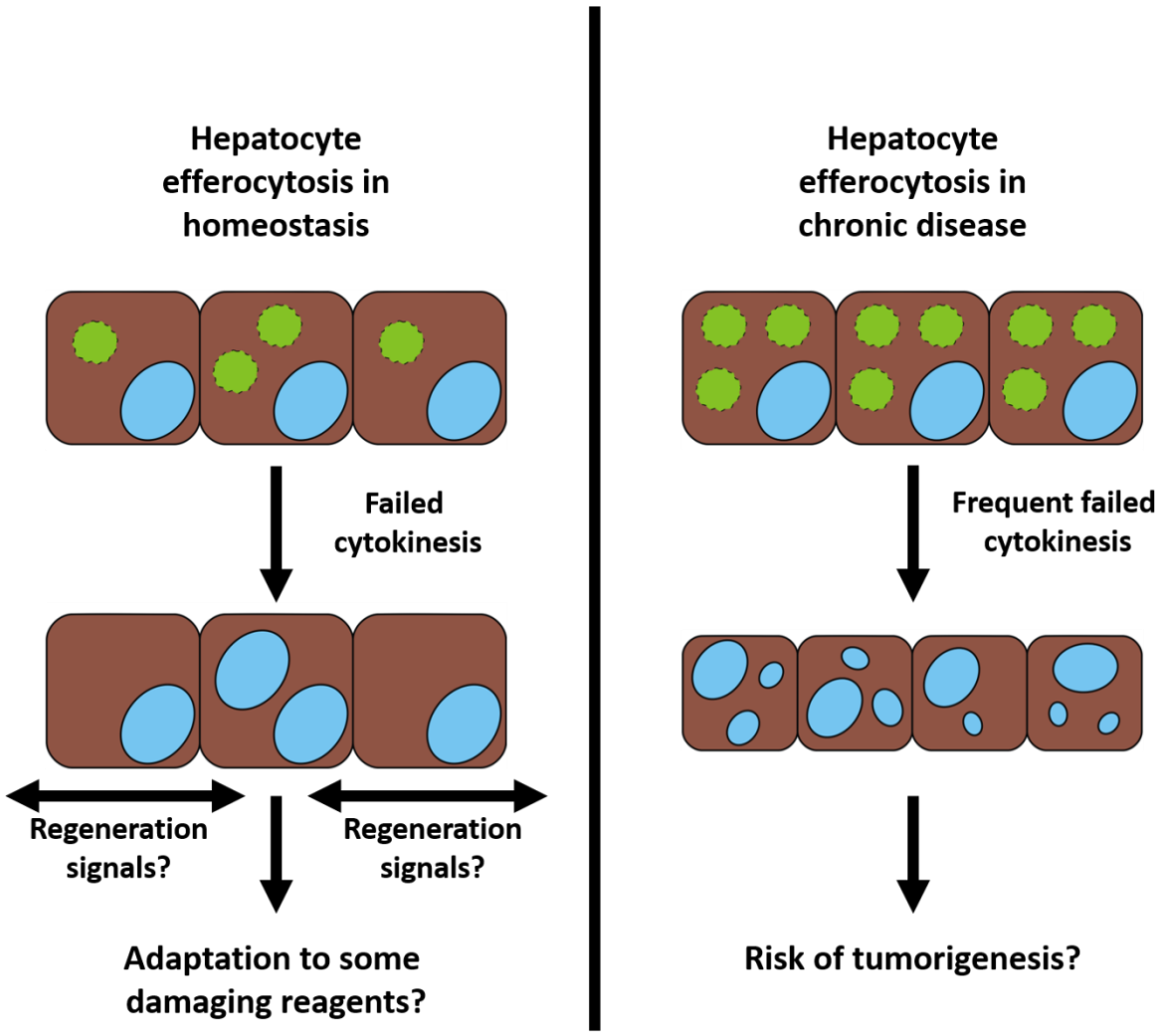

Figure 4P: The balance of hepatocyte efferocytosis in the liver. Left: moderate efferocytosis of dead cells (green) by hepatocytes (brown) during homeostasis promotes cytokinesis failure in a limited number of hepatocytes. These cells may gain adaptations as a consequence of obtaining a second nucleus (blue). These could include the ability to survive specific insults to the liver and provide potential protection from tumorigenesis. Efferocytosing cells may also promote hepatocyte proliferation and regeneration through currently unknown signals. **Right:** uncontrolled efferocytosis, caused by frequent cell death associated with chronic liver disease causes many hepatocytes to fail cytokinesis. Continuous failure of cytokinesis could increase the risk of asymmetric cell division and further genetic dysregulation. This would further increase the risk of developing hepatocellular carcinoma throughout the duration of chronic liver disease.

4.9.6 Targeting hepatocyte efferocytosis in hepatocellular carcinoma

Many types of tumours have been reported to display increased aggressiveness and poorer prognosis in association with ploidy increases (265, 270, 272, 294). Data described in this chapter now show the potential of a similar aspect for HCC. Tumour cells in HCC patients were consistently more multinucleate than their distal or marginal counterparts (**Fig. 4N**). Furthermore, increased multinucleation in tumour cells and hepatocytes in these patients correlated with the appearance of tumour invasion (**Fig. 40**). Although increased ploidy can reduce the risk of hepatocellular carcinoma (299), this does not discredit the advantages of higher ploidy for cancer cells which maintain the capacity to efferocytose. Such cells would also not be in short supply of corpses; many lymphocytes are recruited to tumours and then subsequently induced to apoptose (67), which is already a frequent event in normal liver (9). Furthermore, HCC shares a trait of many solid tumours in which the high oxygen demand of tumours causes the core of the tumour to become necrotic, providing more dying cells in which to clear (305, 306). These tumours therefore have multiple opportunities to clear dead cells throughout their development, providing a source of both cellular nutrition and a pathway for genetic alteration. Therapeutic targeting of tumour efferocytosis may therefore be of benefit for reducing tumour progression. This would lower the survivability of tumours by removing the nutritional benefit of efferocytosis but also by reducing the potential of them obtaining further mutations that promote growth, invasion, or metastasis.

Candidate treatments for specific targeting of tumour cell efferocytosis are still lacking. Although EIPA was shown to be significantly effective in preventing hepatocyte efferocytosis *in vivo*, it may not represent an ideal targeted therapeutic. EIPA specifically inhibits sodium-proton exchanger 1 (NHE1), but also indirectly inhibits macropinocytosis by lowering the submembranous pH. This pH change inhibits the activity of Pak1, thereby preventing

downstream signalling associated with macropinocytosis (307). As this pathway is largely conserved across different cell types, it would not be possible to specifically inhibit tumour efferocytosis. Furthermore, long-term inhibition of macropinocytosis throughout the liver is likely to induce undesired cell exhaustion. Further understanding of how hepatocytes recognise dying cells may yield receptors that could prove to be more appropriate therapeutic targets. Such candidates may include SCARF2 which was previously identified as a likely contributor to hepatocyte efferocytosis. As SCARF2 is not expressed on other hepatic efferocytes, blocking this receptor specifically would still allow for other efferocytes in the liver to compensate, at least partially, for reduced hepatocyte efferocytosis.

Chapter 5: Hepatocytes engulf live $CD4^+$ T cells

5.1 Introduction

In earlier chapters I have discussed the adept capacity of hepatocytes to engulf dead cells and its links to multinucleation and liver regeneration. These observations also provide novel insights into the contribution of hepatocytes to immune regulation in the liver; the swift and efficient clearance of dying cells is required to prevent an immune response (148). Like with their capacity for efferocytosis efferocytosis, other aspects of hepatocyte contribution to liver immunology are poorly understood. One major aspect of this entails interactions between hepatocytes and immune cells. The series of events involved in immune cell migration from the sinusoids to the liver parenchyma have been efficiently elucidated by members of the Centre for Liver and Gastrointestinal Research (CLGR) at the University of Birmingham (4, 6-8, 308). Less details are available for the activities of lymphocytes in the parenchyma where they come into contact with hepatocytes.

Previous co-culture experiments in the Stamataki lab have yielded novel findings regarding interactions between hepatocytes and different types of lymphocyte. It was found that $CD4^+$ T helper cells were frequently, and reproducibly, engulfed by hepatocytes, whilst still alive (**Fig. 5Ai**). The same observations were not seen with $CD8^+$ T cytotoxic cells or B cells. This phenomenon bore resemblance to the formation of the previously described cell-in-cell structures (CICSs), whereby a live cell is engulfed by another (184). Several processes have been attributed to CICS creation, including entosis and emperipolesis (184). A similar process in the liver was previously reported in the literature whereby hepatocytes were shown to

selectively engulf and delete autoreactive $CD8^+$ cells, through a process termed as “suicidal emperipolesis” (181). However, our lab has shown that $CD4^+$ T cells entry into hepatocytes does not require self-reactivity, nor does this always result in the deletion of the T cell (**Fig. 5Aii**). It is also not known as to whether this process bears molecular similarities to other mechanisms of live cell capture.

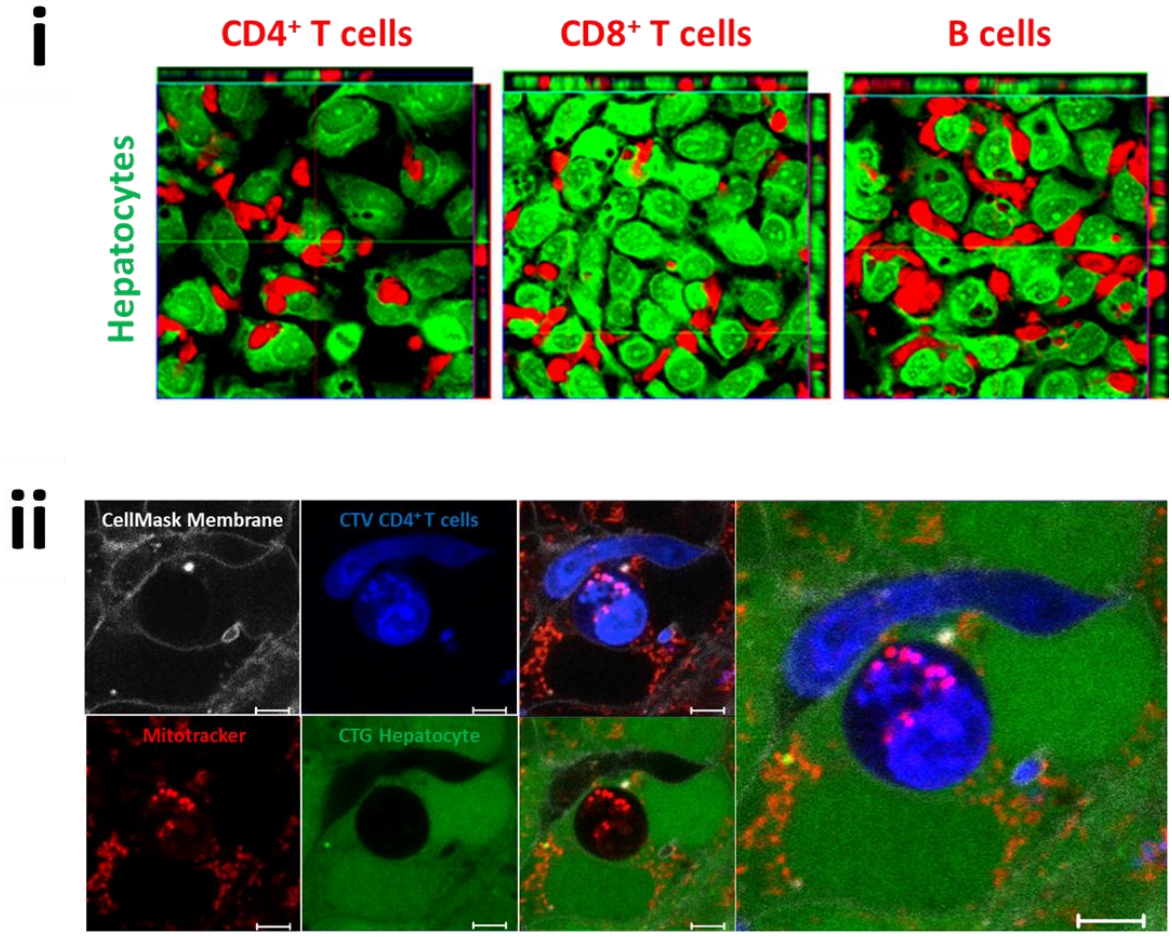

Figure 5A: Previous work in the Stamataki lab showing the capture of live CD4$^+$ T cells *in vitro*. (i) Confocal micrographs with Z-stacks showing fluorescent-labelled hepatocytes (green) co-cultured with lymphocytes (red), separated into CD4$^+$ T cells, CD8$^+$ T cells or B cells. CD8$^+$ T cells and B cells travel in between hepatocytes within the monolayer whereas CD4$^+$ T cells become completely internalised by them. **(ii)** Confocal micrograph of a captured and uncaptured CD4$^+$ T cell. Hepatocytes were labelled with Cell Tracker green (CTG) and T cells were labelled with Cell Tracker Violet (CTV) prior to co-culture. Prior to imaging, cells were labelled with CellMask membrane (grey) to show complete T cell internalisation and mitochondria were labelled with Mitotracker (red) to show cell viability. Scale bars represent 10 µm.

When our lab initially observed that live $CD4^+$ T cells were engulfed by hepatocytes, two possible explanations came to the forefront; transcellular migration or efferocytosis. As the initial data was acquired from imaging fixed cells from a single timepoint, one possibility was that these images represented T cells undergoing transcellular migration. Previous work published by the CLGR has exemplified how T cells can enter the liver by travelling through the cytoplasm of HSECs (8). However, long-term imaging of T cells co-cultured with hepatocytes revealed that internalised cells do not exit hepatocytes over periods of several hours. Therefore, it is unlikely that the process witnessed was as a form of transcellular migration.

It is also conceivable that live $CD4^+$ cell capture by hepatocytes is related to their previously discussed ability for efferocytosis. Validating this possibility, however, presents several challenges. Although much of the molecular machinery used by efferocytosing cells has been identified, especially in macrophages (233, 243), it is still uncertain as to whether the same molecules are involved in hepatocyte efferocytosis. As such there was no obvious pathway with which to target for inhibition to investigate whether live $CD4^+$ T cell capture by hepatocytes is molecularly similar or distinct to efferocytosis.

This final results chapter will aim to describe and discuss the experiments undertaken to compare $CD4^+$ T cell capture to efferocytosis and to understand its requirement in the liver.

5.2 Hepatocyte internalisation of CD4$^+$ T cells is not the same process as efferocytosis

5.2.1 Hepatocyte capture of CD4$^+$ T cells was phenotypically different to efferocytosis

A conceivable explanation for the presence CD4$^+$ T cells within hepatocytes is that they have been mistaken for dying cells. Although both processes are poorly understood, it is possible to assess them by comparing observable phenotypic differences between these two processes. Many distinct membranal structures have been described for different forms of endocytosis, including macropinocytosis and phagocytosis (234, 309). To image these structures on hepatomas, scanning electron microscopy (SEM) was used because it provided a greater resolution than confocal microscopy. Huh-7 hepatomas were co-cultured with live, apoptotic or heat-killed (necrotic) primary human CD4$^+$ T cells. Cells were co-cultured for 4 hr in order to image cells at several stages of capture. The cells were then fixed and imaged using SEM to observe the initial tethering of lymphocytes to hepatomas, through to complete internalisation of a cell (**Fig. 5B**). The formation of membrane ruffles was frequently observed on hepatocytes which were actively engulfing heat-killed or apoptotic cells. This is also characteristic of professional phagocytes, including macrophages (310). In contrast, hepatocytes that were in the process of capturing live T cells were frequented with membrane blebs. These observations showed that live CD4$^+$ T cell capture employed different membrane structures than those used for efferocytosis.

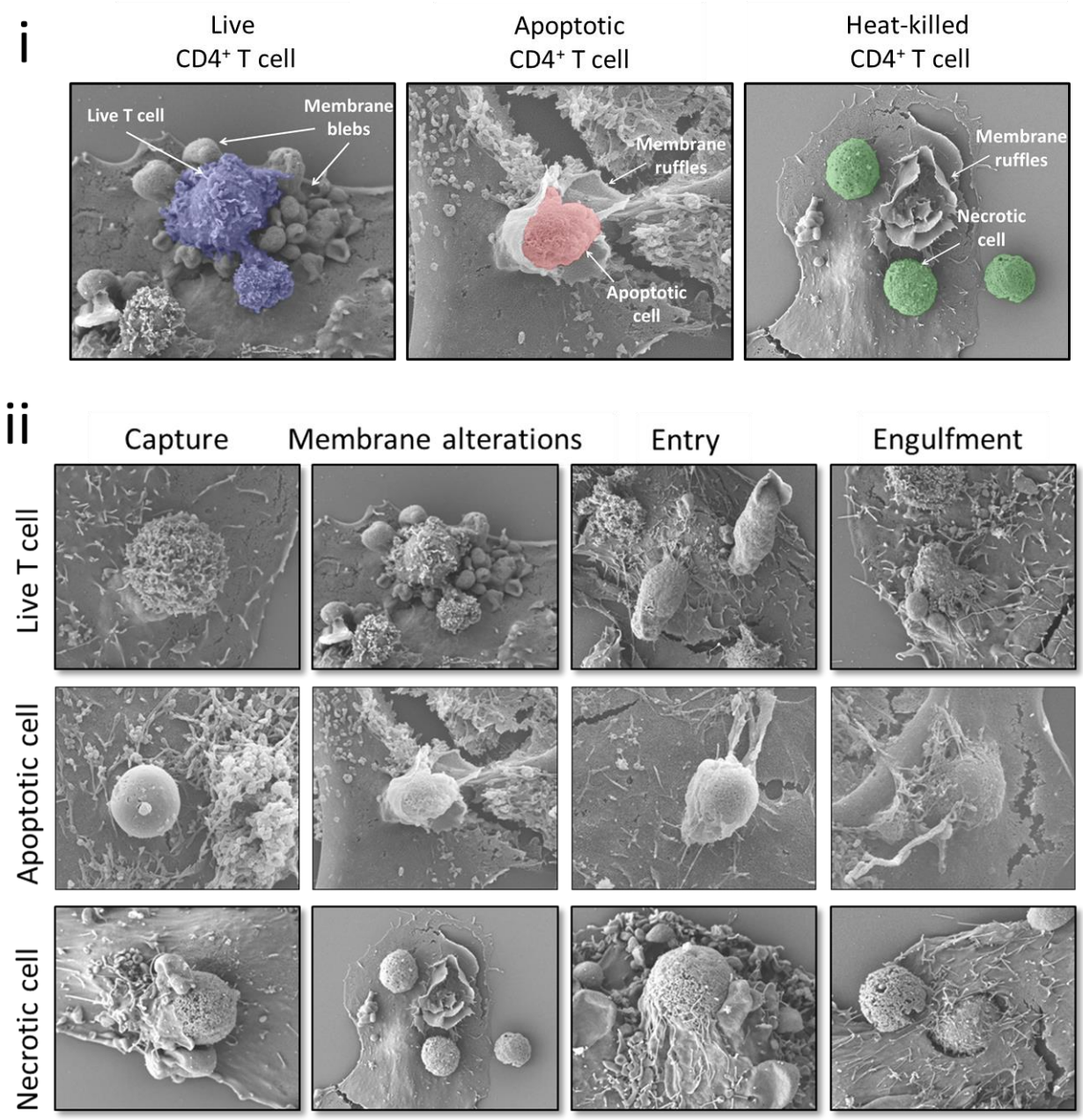

Figure 5B: Hepatomas used different membrane structures to capture live CD4⁺ T cells compared to those used for efferocytosis. Huh-7 hepatomas seeded on glass coverslips were co-cultured with primary CD4⁺ T cells, which were either live, apoptotic via staurosporine (STS) treatment or heat-killed (necrotic), for 24 hr. Cells were then fixed in 2.5% glutaraldehyde and imaged by scanning electron microscopy (SEM) using a JSM-7000F (JEOL) SEM. **i)** Pseudocoloured SEM micrographs showing the membranal blebs formed by the Huh-7 cells during live CD4⁺ T cell (blue) capture, as well as the membrane ruffles formed when capturing apoptotic (red) or heat-killed/necrotic (green) cells. **ii)** SEM micrographs detailing the membranal structures formed throughout the capture of live, apoptotic, and heat-killed CD4⁺ T cells by Huh-7 cells.

5.2.2 The kinetic of live CD4$^+$ T cell capture by hepatomas was slower to that of dead cells

Scanning electron microscopy revealed that different membranal structures on the surface of the hepatocytes are used for capturing live CD4$^+$ T cells compared to those used for efferocytosis. This could imply that these processes also possess contrasting kinetics. To test this, fluorescently-labelled Huh-7 cells were co-cultured with alternatively-labelled live, apoptotic or heat-killed primary human CD4$^+$ T cells. Cultures were preincubated for 90 min and were then imaged overnight at 30 min intervals using time-lapse fluorescence microscopy. The number of internalised cells at each time point was then assessed (**Fig. 5C**). At the beginning of the imaging period, more apoptotic and heat-killed cells were internalised than live cells; only 20% of Huh-7 cells contained vesicles, whereas twice as many cells contained heat-killed cells (**Fig. 5Ci**). Throughout the experiment, the number of vesicles containing apoptotic cells gradually increased (**Fig5Cii**). The number of internalised heat-killed cells within hepatocytes did not alter throughout the duration of the experiment. In contrast, the number of Huh-7s containing live cells was fewer than those containing apoptotic cells and half the number which contained heat-killed. What's more, this number only increased modestly over the course of the experiment, peaking at 9 hr post-incubation. Interestingly, the number of hepatomas containing live cells gradually decreased following 9 hr incubation. Overall, it appears that the kinetic of live cell capture is a slower than efferocytosis in hepatocytes.

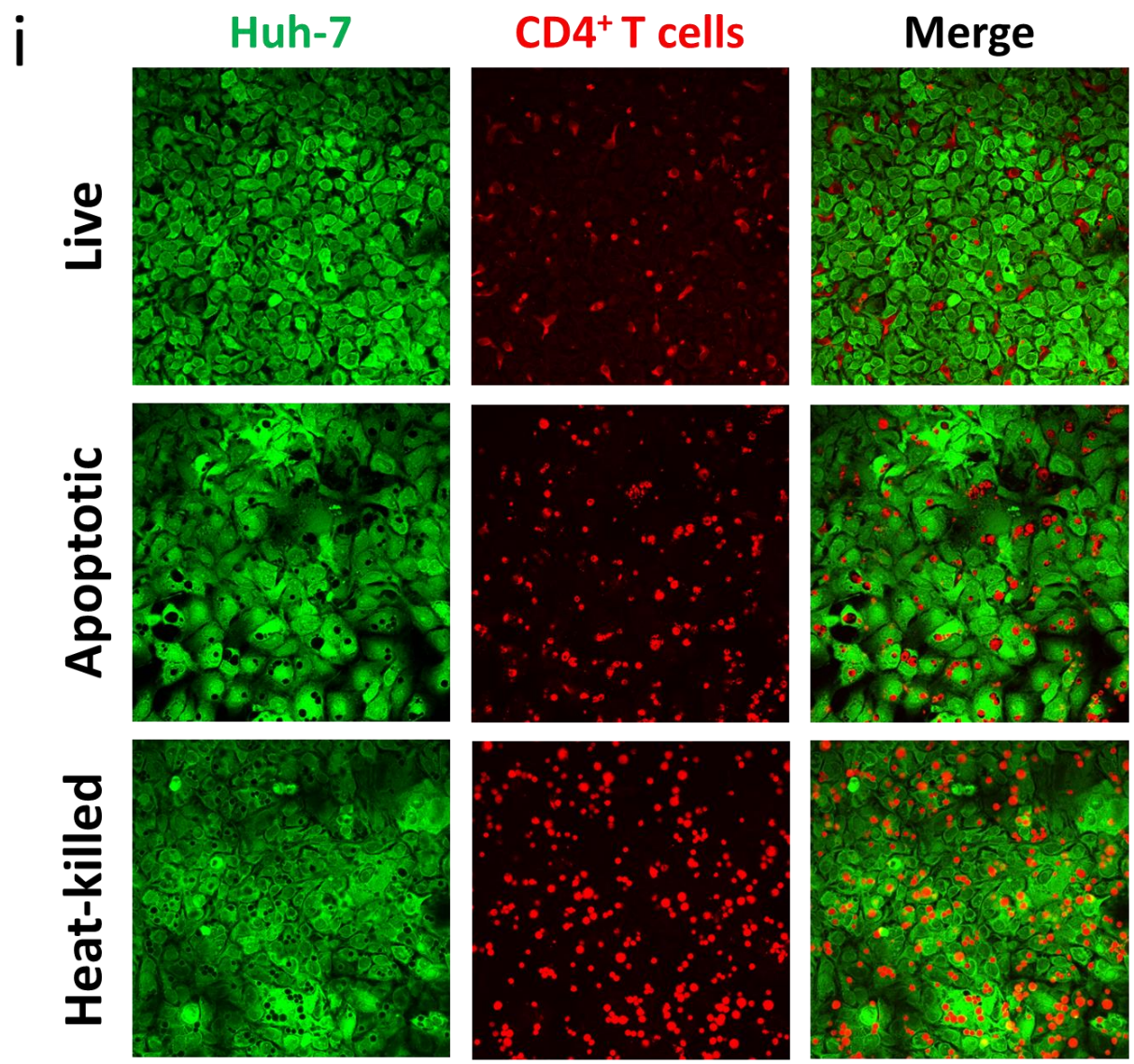
i
Huh-7
CD4+ T cells
Merge
Live
Apoptotic
Heat-killed

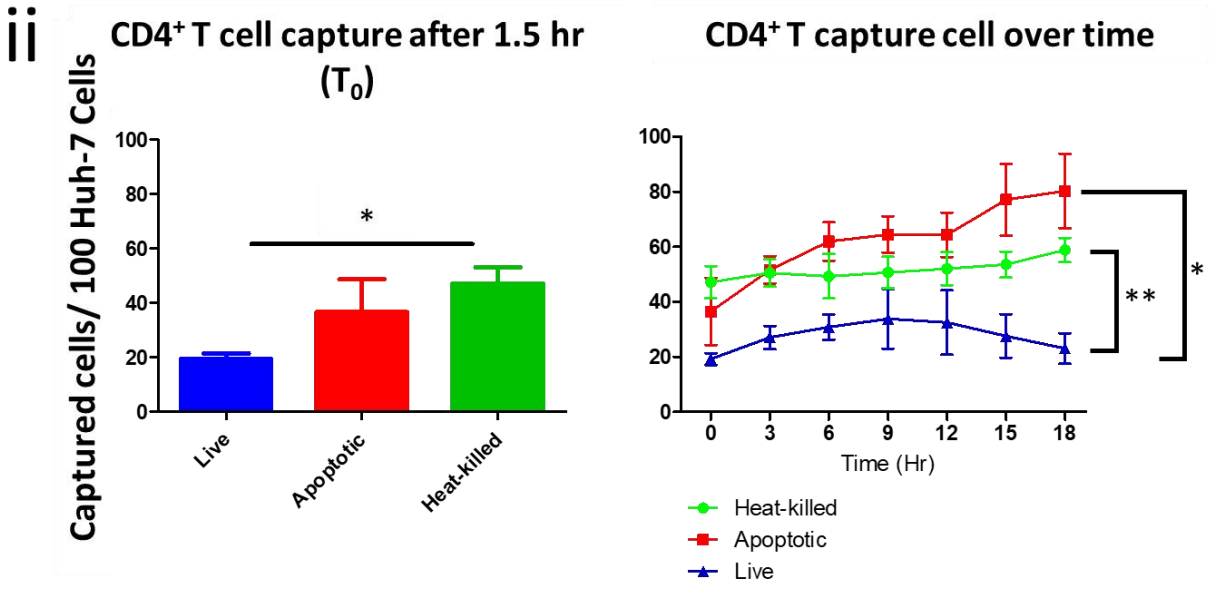
ii
CD4+ T cell capture after 1.5 hr (T0)
Captured cells/ 100 Huh-7 Cells
100
80
60
40
20
0
*
Live
Apoptotic
Heat-killed
CD4+ T capture cell over time
100
80
60
40
20
0
0
3
6
9
12
15
18
Time (Hr)
*
**
*
Heat-killed
Apoptotic
Live

Figure 5C: The kinetic of live CD4$^+$ T cell capture by Huh-7 hepatomas was slower to that of apoptotic and heat-killed cells. Huh-7 hepatomas seeded in 24-well plates (some on glass coverslips for confocal microscopy [i]) were labelled with Cell Tracker Green (CTG)/ Chloromethylfluorescein diacetate (CMFDA). Huh-7s were then co-cultured with primary CD4$^+$ T cells, which were labelled with Cell Tracker Violet (CTV)/bromomethyl derivative of coumarin (BMQC and either live, apoptotic via staurosporine (STS) treatment or heat-killed (necrotic), for 1.5 hr. Plates were then transferred to a Cell-IQ time-lapse, fluorescence imager and imaged for a futher 18 hr. **(i)** Confocal microphaphs of Huh-7 – T cell co-cultures following 1.5 hr co-culture (time point zero [T_0]). **(ii)** Quantification of captured CD4$^+$ T cells per 100 Huh-7 cells after the initial 1.5 hr co-culture period (Left, T_0), and throughout the 18 hr culture period at 3 hr intervals. Numbers were derived from 3 technical repeats, using 5 fields of view (FOV) per repeat. * - p≤0.05, ** - p≤0.01. Statistics were derived from a two-tailed, unpaired Students t-test when comparing capture of each cell condition to each other. Error bars represent the SEM.

5.2.3 Vesicles containing captured live CD4$^+$ T cells did not associate with SCARF2

It was uncertain as to whether captured live CD4$^+$ T cells were internally trafficked by hepatomas through the same processes as apoptotic or heat-killed cells. It was revealed earlier (**section 3.4.2**) that hepatocyte efferosomes frequently associated with the scavenger receptor, SCARF2. I hypothesised that if live CD4$^+$ T cells were engulfed and trafficked intracellularly through the same processes as dead cells, it would be expected that SCARF2 would also associate with captured live cells. To investigate this, I co-cultured Huh-7 cells with live, primary human CD4$^+$ T cells. These were the fixed, permeabilised and stained for SCARF2 by immunofluorescence. Cells were the imaged by confocal microscopy (**Fig. 5D**). Images were also 3D volume rendered to provide more accurate information regarding the distribution of SCARF2 in relation to the internalised T cell**.** Vesicles containing fully internalised live CD4$^+$ T cells showed no association with SCARF2. As such, the capture of live CD4$^+$ T cells does not share this aspect of intracellular processing that was seen with efferosomes.

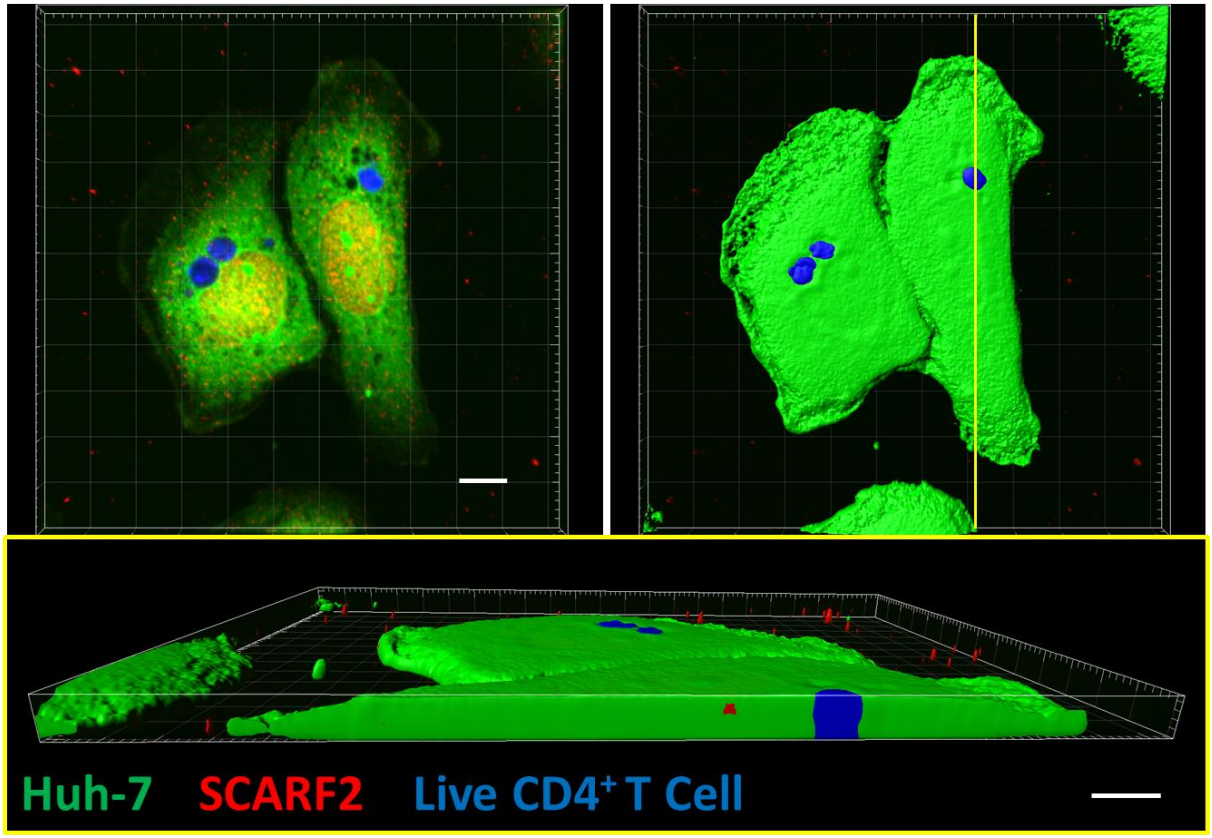

Figure 5D: Captured live CD4$^+$ T cells did not associate with SCARF2 within Huh-7 hepatomas. Huh-7 hepatomas were seeded in 24-well plates on glass coverslips were fluorescently labelled with Cell Tracker Green (CTG)/ Chloromethylfluorescein diacetate (CMFDA). Huh-7s were then co-cultured with live, primary human CD4$^+$ T cells, labelled with Cell Tracker Violet (CTV)/ bromomethyl derivative of coumarin (BMQC). Cells were co-cultured for 3 hr. Cells were then fixed with MeOH and stained for scavenger receptor family f, member 2 (SCARF2), shown in red. Cells were then imaged by confocal microscopy using a Zeiss LSM 880, in which Z-stacks were acquired. Images were also 3D volume rendered using Bitplane IMARIS software. Bottom panels show cross-sections made using a plane which cuts through the internalised T cell, as indicated by yellow line on top-right panel. Scale bars represent 10 µm.

5.2.4 Live $CD4^+$ capture by hepatocytes was unaffected by cytokine treatment

Both hepatocytes and lymphocytes can take cues from cytokines in the liver (9, 49, 55). Cytokines have also been shown to trigger or influence processes of live cell internalisation, including macrophage capture of live T cells (178). It is thus prospective that such stimulation may alter the ability of hepatocytes to capture live $CD4^+$ T cells. To test this, Huh-7 hepatomas were pre-treated with cytokines and then co-cultured with live, primary human $CD4^+$ T cells in the presence of both pro- and anti-inflammatory cytokines (**Fig. 5E**). The number of internalised T cells per hepatocytes was determined after 3 hr co-culture. There was no significant alteration in the capacity of Huh-7 cells to internalise live cells in response any cytokine stimulation.

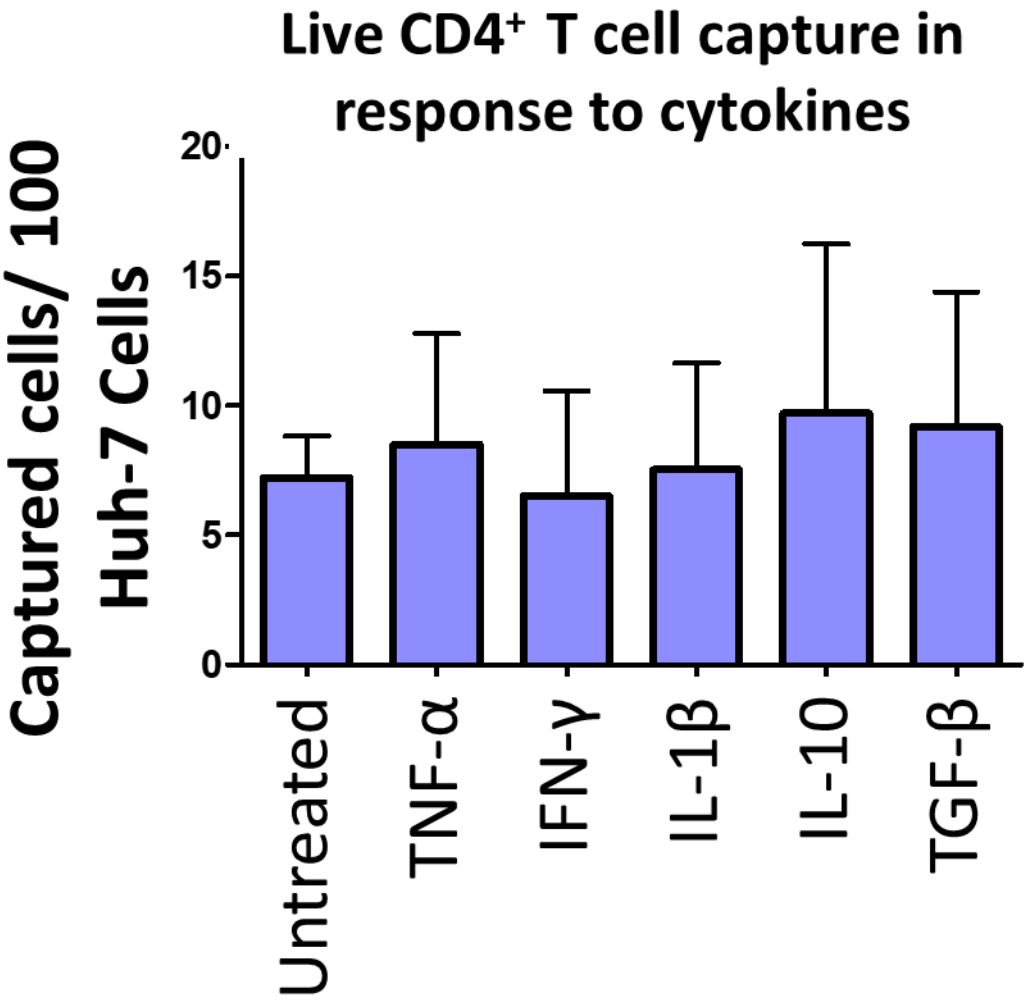

Figure 5E: Capture of live CD4$^+$ T cells by hepatomas was unaffected by cytokines. Huh-7 hepatomas seeded in 24-well plates on glass coverslips were fluorescently labelled with Cell Tracker Green (CTG)/ Chloromethylfluorescein diacetate (CMFDA). Huh-7s were then serum starved and treated with 100 ng/ml cytokines for 1 hr. Huh-7s were then co-cultured with Celltracker Red (CTR)/CMTPX-labelled live, primary human CD4$^+$ T cells. Cells were cultured in the presence of cytokines, for 3 hr, fixed with MeOH, and then imaged by confocal microscopy using a Zeiss LSM 880 microscope. Graph shows the quantification of the number of captured live CD4$^+$ T cells per 100 Huh-7 cells for each cytokine treatment. Numbers were obtained using 5 fields of view (FOV), taken from three independent experiments (N=3). Statistics were derived from a two-tailed, unpaired Student's t-test when comparing other treatments to the control. Error bars represent the SEM. IFN-γ – interferon-gamma; IL – interleukin; TGF-β – tumour growth factor-beta. Data set was partially acquired from work conducted by Nuffield Foundation work experience student, Sophie Rouvray.

5.3 Hepatocyte internalisation of CD4$^+$ T cells was distinct to entosis

Entosis is the homotypic internalisation of a live epithelial cell by another and prominent process in CICS formation (183-185). Live capture of CD4$^+$ by hepatocytes may bear some similarities to this process. This section will aim to compare the capture of live CD4$^+$ T cells by hepatocytes to entosis.

5.3.1 Capture of live CD4$^+$ T cells was inhibited by macropinocytosis and actin remodelling inhibitors but unaffected by an inhibitor of entosis

Entosis can be identified by its sensitivity to the ROCK inhibitor, H-1152 (183, 311). To investigate if the activity of ROCK is associated with live CD4$^+$ T cell capture by hepatocytes, I attempted to perturb CD4$^+$ T cell capture using H-1152. To ensure that Huh-7 hepatomas were susceptible to H-1152, I assessed its ability to inhibit more frequent activities of ROCK. ROCK phosphorylates and activates LIM kinase, which subsequently phosphorylates the actin-binding protein (ABP), cofilin, and increases the stability of filamentous actin (312). This ultimate phosphorylation of cofilin was shown to be susceptible to H-1152 treatment (313). Therefore, Huh-7s and live, primary CD4$^+$ T cells were treated with 10 µM H-1152 for 1 hr. Cells were also treated with previously used inhibitors; cytochalasin D was again used as a positive control, as inhibition of actin polymerisation has been reported to prevent entosis (194, 314). Furthermore, as membrane blebs have been reported for cells conducting macropinocytosis as well as ruffles, cells were also treated with inhibitors of this process, EIPA and blebbistatin. Levels of total and cofilin and phosphorylated cofilin (P-cofilin) in cell lysates were then determined by western blotting (**Fig. 5Fi**). Total cofilin was unaffected by inhibitor treatment. However, all cells displayed substantial reductions in P-cofilin in response to inhibitors.

With the knowledge that Huh-7 cells were susceptible to H-1152 treatment, Huh-7 cells were co-cultured with live, primary $CD4^+$ T cells in the presence of H-1152 and the other tested inhibitors (**Fig. 5Fii**). As expected, live $CD4^+$ T cell capture was almost totally ablated by cytochalasin D treatment. Contrasting to reports on the mechanism of entosis, inhibition of ROCK by H-1152 did not reduce live $CD4^+$ cell capture by Huh-7s. In contrast, significant decreases in $CD4^+$ T cell capture by Huh-7s were seen in response to treatment with EIPA and blebbistatin. Inhibition by EIPA was comparable to that seen from cytochalasin D treatment. As H-1152 failed to inhibit hepatocyte capture of live $CD4^+$ T cells, it would suggest that this live $CD4^+$ T cell capture by hepatocytes bears molecular differences to entosis.

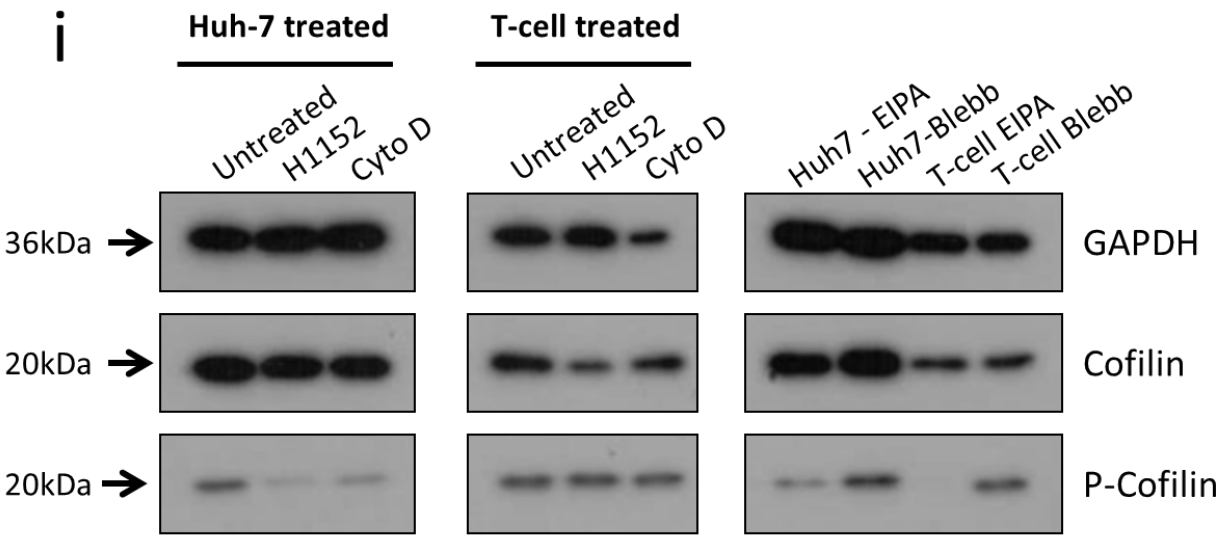
i
Huh-7 treated
T-cell treated
Untreated
H1152
Cyto D
Untreated
H1152
Cyto D
Huh7 - EIPA
Huh7-Blebb
T-cell EIPA
T-cell Blebb
36kDa
GAPDH
20kDa
Cofilin
20kDa
P-Cofilin

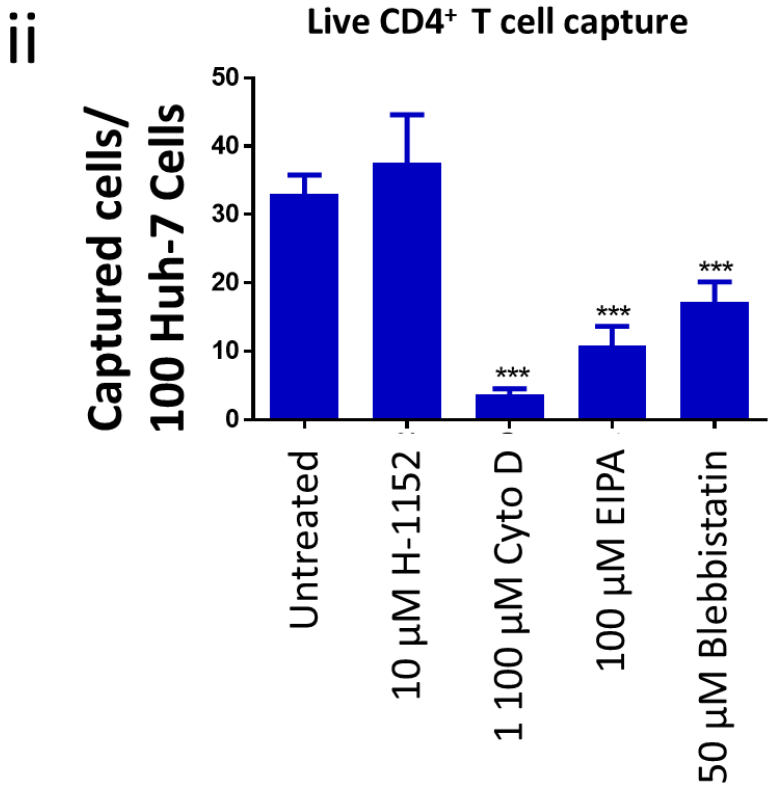
ii
Live CD4+ T cell capture
Captured cells/ 100 Huh-7 Cells
50
40
30
20
10
0
***
***
***
Untreated
10 µM H-1152
1 100 µM Cyto D
100 µM EIPA
50 µM Blebbistatin

Figure 5F: Capture of live CD4$^+$ T cells by hepatomas was unaffected by inhibitors of entosis but was reduced by those inhibiting macropinocytosis and cytoskeletal rearrangements. (i) Western blot showing expression levels of cofilin and phosphorylated cofilin (P-cofilin) in Huh-7 hepatomas and primary human CD4$^+$ T cells following treatment with molecular inhibitors. Cells were treated with 10 µM H-1152, 1 µM cytochalasin D, 100 µM 5-(N-Ethyl-N-isopropyl) amiloride (EIPA) or 50 µM blebbistatin for 1 hr. Inhibitors were diluted in serum-free media. Cells were then lysed, and their lysates were resolved by SDS-polyacrylamide gel electrophoresis (SDS-PAGE). Bands were then transferred to PVDF membranes via western blotting. Membranes were then blotted for cofilin and P-cofilin. Membranes were also blotted for GAPDH as a loading control. **(ii)** Huh-7 hepatomas seeded in 24-well plates on glass coverslips were fluorescently labelled and treated with inhibitors at concentrations indicated above for 1 hr. Huh-7s were then co-cultured with alternatively-labelled, live, primary CD4$^+$ T cells, in the presence of inhibitors, for 3 hr. Cells were then fixed with MeOH, and then imaged by confocal microscopy using a Zeiss LSM 880 microscope. The number of captured CD4$^+$ T cells per 100 Huh-7 cells was then quantified for each treatment. Numbers were derived from three experimental repeats (N=3), using 5 fields of view (FOV) per repeat. *** - p≤0.001. Statistics were derived from a two-tailed, unpaired Student's t-test when comparing other treatments to the control. Error bars represent the SEM. GAPDH - glyceraldehyde 3-phosphate dehydrogenase; cyto D – cytochalasin D; blebb – blebbistatin.

5.3.2 Vesicles containing live CD4$^+$ T cells in hepatocytes associated with β-catenin but not with E-cadherin.

An early observation in the developing concept of entosis was the requisite for CICSs created in this way to associate with β-catenin and E-cadherin (183). Other studies have used these observations to identify entosis in other cell types. To elucidate whether captured live CD4$^+$ T cells possessed this characteristic, Huh-7 cells were stained by immunofluorescence for E-cadherin (**Fig. 5G**) and β-catenin (**Fig. 5Hi**) following co-culture with primary CD4$^+$ T cells. Cells were then imaged using confocal microscopy. Images were also 3D volume rendered to show the distribution of the probed molecules in relation to the internalised CD4$^+$ T cell. Huh-7 cells stained positively for both proteins with little positivity present when using an isotype matched control (IMC) (**Fig. A2)**. The membranes of vesicles containing live CD4$^+$ cells were enriched with β-catenin (**Fig. 5Hi**). However, these vesicles did not associate with E-cadherin (**Fig. 5G**).

To confirm the presence of β-catenin on vesicles containing live lymphocytes, and to confirm the specificity of the antibody used, tissues from 'normal' donor livers were stained for β-catenin by IHC (**Fig 5Hii**). The expected 'chicken-wire' structure of junctional β-catenin was visible in between hepatocytes which verifies the accuracy of this antibody. In addition, several circular intracytoplasmic structures within hepatocytes document were documented. Taken together, thesis data imply that the activity of β-catenin may be involved with the capture of live $CD4^+$ T cells by hepatocytes.

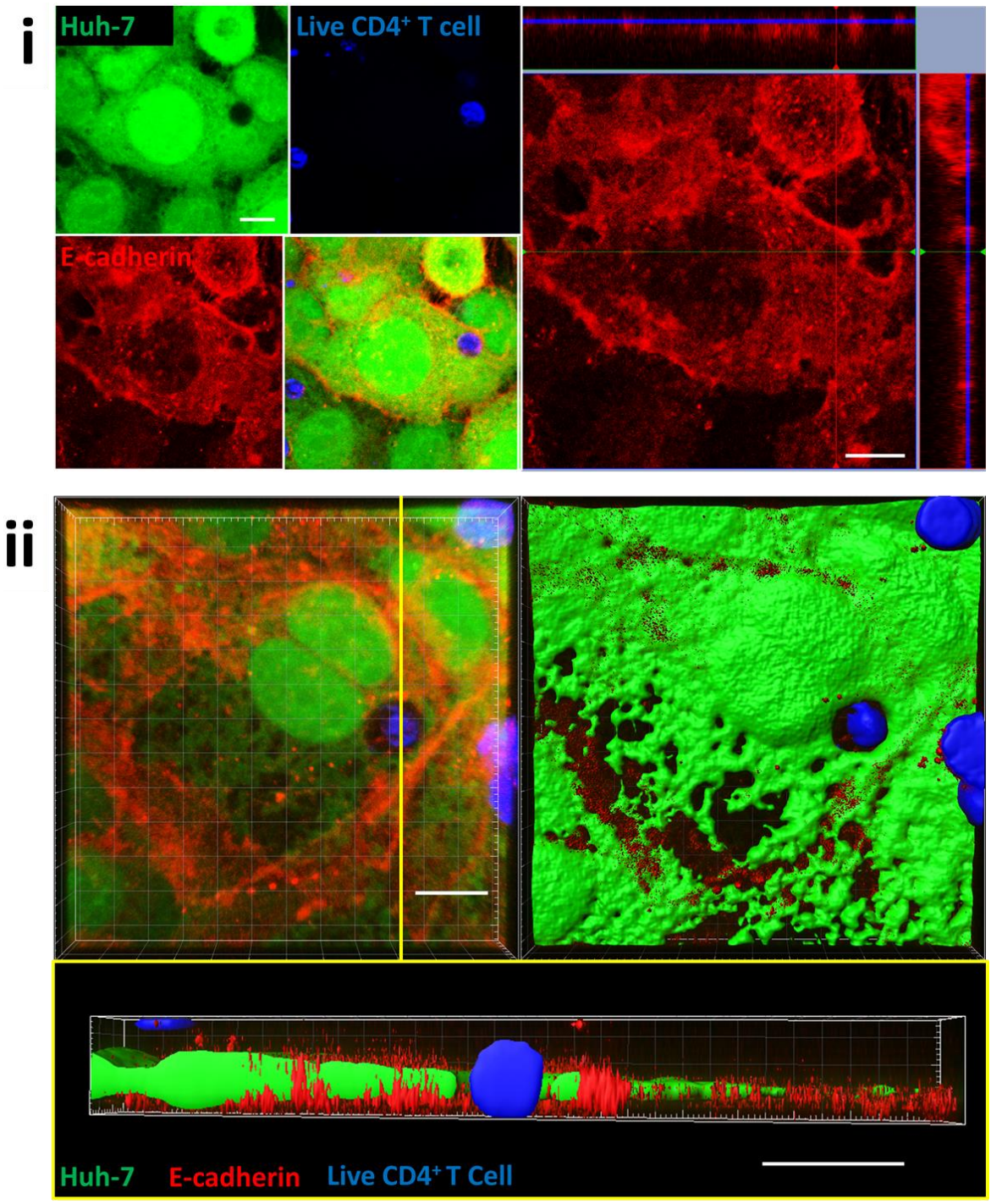
i
Huh-7
Live CD4+ T cell
E-cadherin
ii
Huh-7
E-cadherin
Live CD4+ T Cell

Figure 5G: Vesicles containing captured live CD4$^+$ T cells did not associate with E-cadherin within Huh-7 hepatomas. Huh-7 seeded in 24-well plates on glass coverslips were fluorescently labelled with Cell Tracker Green (CTG/ CMFDA). Huh-7s were then co-cultured with primary human CD4$^+$ T cells, labelled with Cell Tracker Violet (CTV/BMQC) for 3 hr. Cells were then fixed with 3.7% formaldehyde and stained for E-cadherin via immunofluorescence (shown in red). Cells were then imaged by confocal microscopy using a Zeiss LSM 880, in which Z-stacks were acquired. Images were also 3D volume rendered using Bitplane IMARIS software. **(i)** Confocal micrograph with orthographical view showing a Huh-7 hepatoma (green) containing internalised live CD4$^+$ T cell (blue). **(ii)** Confocal micrograph together with 3D-rendered images. Bottom panel shows cross-section made using a plane which cuts through the internalised T cell, as indicated by yellow line on the left panel. Images are representative of 3 experimental repeats. Scale bars represent 10 µm. Isotype-matched control can be found in the appendix, section A.2.2, **Figure. A2ii.**

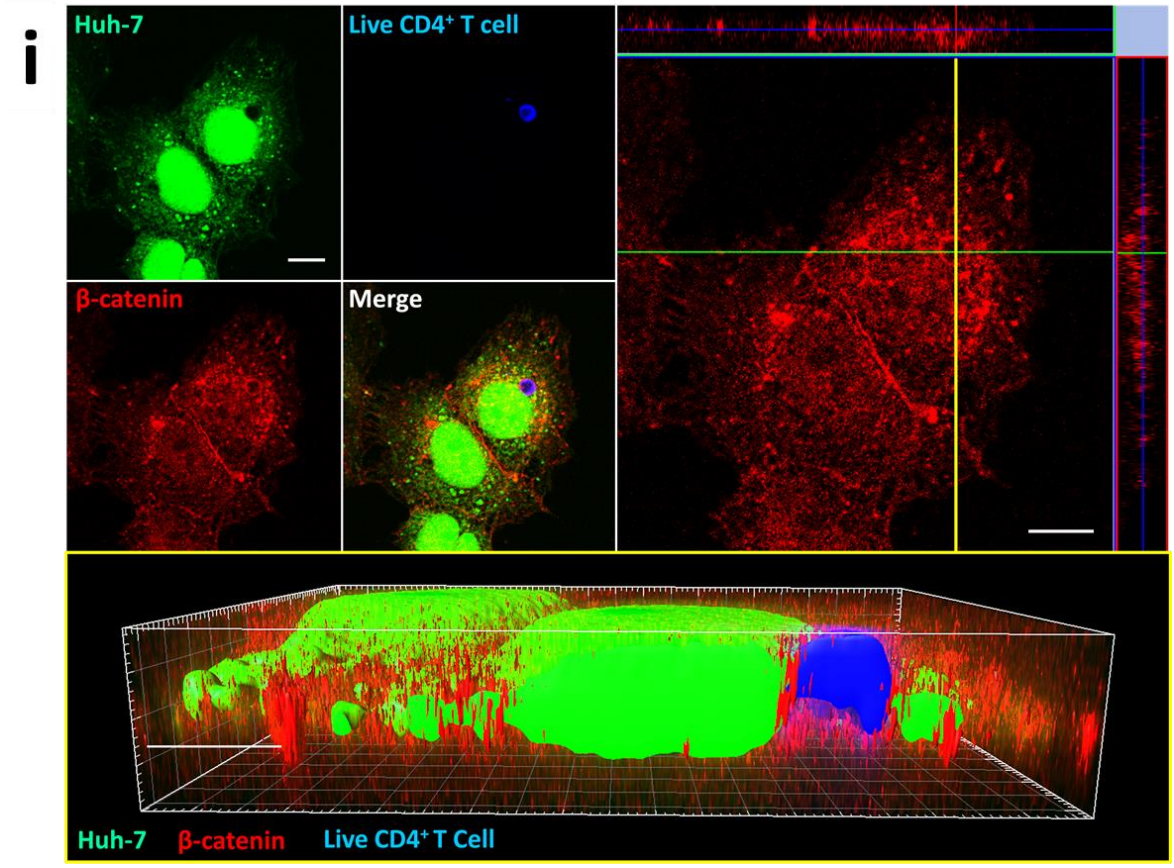
i
Huh-7
Live CD4+ T cell
β-catenin
Merge
Huh-7 β-catenin Live CD4+ T Cell

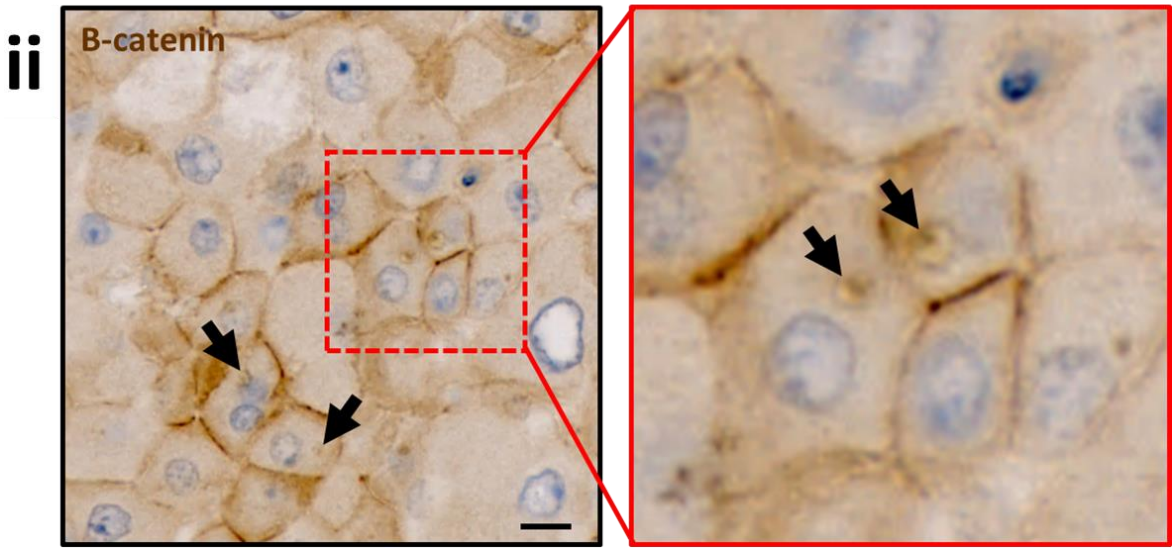
ii
B-catenin

Figure 5H: Captured live CD4$^+$ T cells associated with β-catenin within Huh-7 hepatomas *in vitro* and possibly in hepatocytes *in vivo*. Scale bars represent 10 μm. Huh-7 seeded in 24-well plates on glass coverslips were fluorescently labelled with Cell Tracker Green (CTG/CMFDA). Huh-7s were then co-cultured with primary human CD4$^+$ T cells, labelled with Cell Tracker Violet (CTV/BMQC) for 3 hr. Cells were then fixed with 1% paraformaldehyde and stained for β-catenin via immunofluorescence (shown in red). Cells were then imaged by confocal microscopy using a Zeiss LSM 880, in which Z-stacks were acquired. Images were also 3D volume rendered using Bitplane IMARIS software. **(i)** Confocal micrograph with orthographical view showing a Huh-7 hepatoma (green) containing internalised live CD4$^+$ T cell (blue). Bottom panel shows cross-section made using a plane which cuts through the internalised T cell, as indicated by yellow line on the right panel. Images are representative of 3 experimental repeats. **(ii)** Immunohistochemistry (IHC) staining of paraffin-embedded normal donor liver tissue for β-catenin (brown). Tissues were counterstained with Mayers haematoxylin nuclear stain (blue). Black arrows indicate hepatocytes containing large, positively stained vesicles. Isotype-matched stains for both procedures can be found in the appendix, section A.2.2, **Figures A2i and A3.**

5.4 Vesicles containing captured human T-regulatory cells within hepatomas acidified more frequently than non-T regulatory cells

Although Entosis and other processes of live cell capture are often termed as 'non-apoptotic' forms of cell death, not all CICSs are destined for lysosomal degradation. Some reports suggest that cells can survive within their host and sometimes even escape their captors (184). In relation, previous data in our lab showed that only 20% of captured CD4$^+$ T cells enter acidic compartments in hepatocytes. In addition, *in vivo* observations made in our lab across multiple liver diseases suggested that hepatocytes preferentially engulf cells expressing forkhead box P3 (FOXP3), a transcription factor that arbitrarily denotes human T regulatory cells (Tregs)(161), compared to other T cell subsets. Hepatocytes may process internalised Tregs differently compared to non-regulatory sub-types (non-Tregs). To address this, total CD4$^+$ T cells were isolated from PBMCs and then Tregs were separated from non-Treg cells based on high CD25 and low CD127 expression. Both Tregs and non-Tregs were then labelled and co-cultured for with Huh-7 cells 24 hr, in presence of pHrodo red dextran, a pH indicator which fluoresces red in acidic cellular compartments. Cells were then labelled

with a membrane dye, CellMask Deep Red and imaged live using confocal microscopy (**Fig. 5I**). Fully internalised cells were identified through the absence of CellMask labelling (**Fig. 5Ii**). The percentage of internalised cells, both Treg and non-Treg, within acidic compartments was then determined (**Fig. 5Iii**). Almost three-times as many Tregs compared to non-Tregs were found within acidic compartments; a mean of 60% internalised Tregs were positively stained for pHrodo red compared to around 20% for non-Tregs. This showed that captured Tregs were more likely enter acidic compartments than non-Tregs.

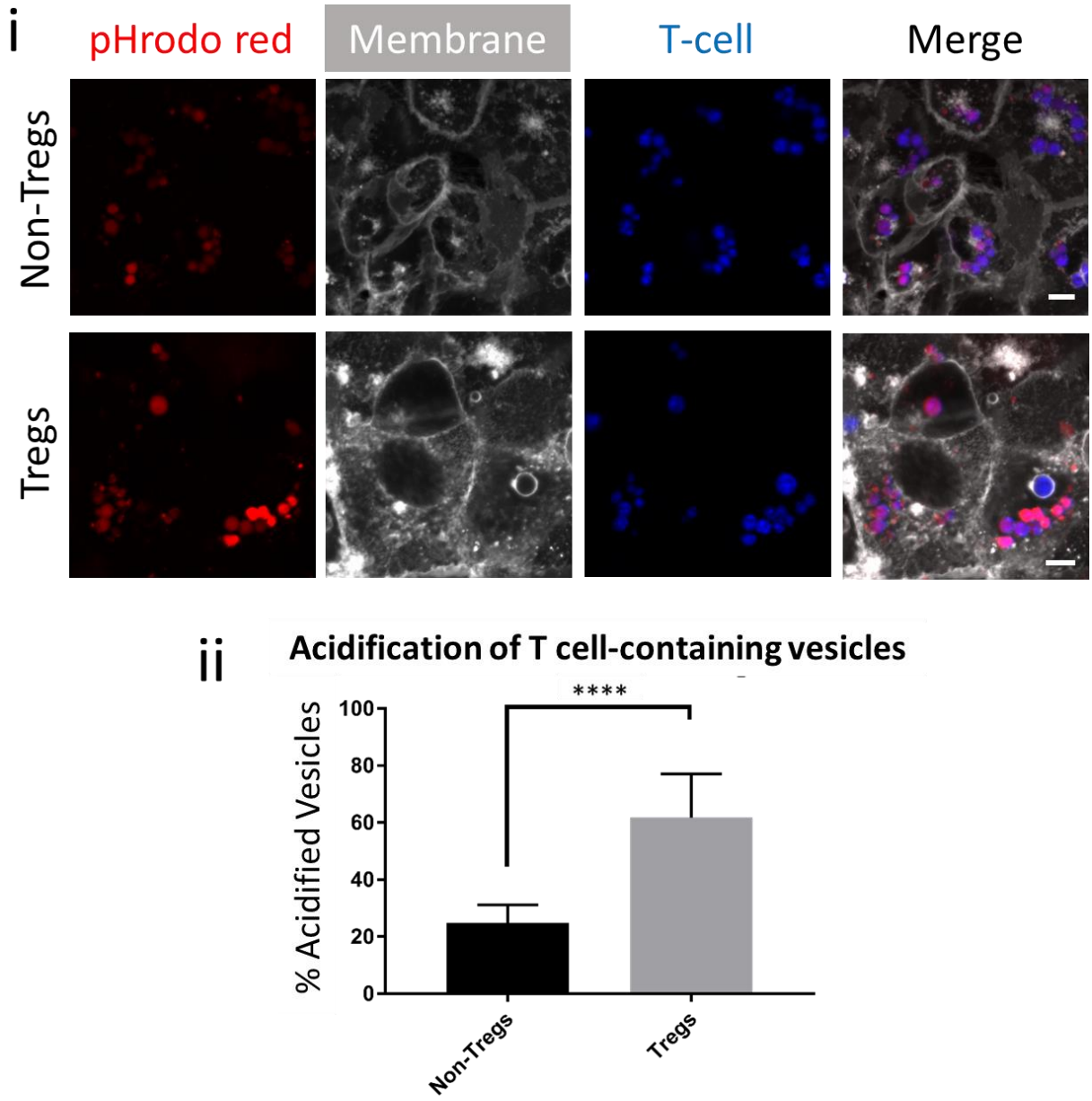

Figure 5I: Tregs acidified within hepatomas more frequently that non-Tregs *in vitro*. Huh-7 hepatomas were seeded in glass-bottomed 24-well plates and allowed to adhere for 24 hr. Primary $CD25^{+}$, $CD125^{lo}$ T regulatory cells (Tregs) were isolated from donor peripheral blood mononuclear cells (PBMCs) using a Stemcell™ magnetic negative-selection kit. The separated cells were recovered and designated as non-Tregs. These were fluorescently labelled with Cell Tracker Violet (CTV)/ bromomethyl derivative of coumarin (BMQC) and then co-cultured in equal numbers with Huh-7 cells for 24 hr in presence of the pH sensing reagent, pHrodo red dextran (red in acidic conditions). Cell membranes were then labelled with CellMask membrane (grey) and then cells were then imaged live using a Zeiss 780 confocal microscope. **(i)** Representative confocal micrographs of CellMask -labelled Huh-7 hepatomas co-cultured with fluorescent-labelled $CD4^{+}$ T cells (violet). **ii)** Quantification of acidified vesicles in Huh-7s containing Treg or non-Tregs. Numbers were derived three experimental repeats (N=3) from 5 fields of view (FOV) per experiment. **** - $p \leq 0.0001$. Statistics were derived from a two-tailed, unpaired Students t-test. Errors represent the SEM. Data in this figure was supplemented by work conducted by visiting PhD student, Xiaoyan Li.

5.5 Chapter summary

Table 6: Summary of all new discoveries presented in chapter 5.

1. Efferocytosis of dead cells by hepatomas involved the formation of membrane ruffles. In contrast, live CD4$^+$ T cell capture involved membrane bleb formation and was less frequent than efferocytosis.
2. Live CD4$^+$ T cell capture by hepatomas was unaffected by an inhibitor of entosis or by cytokines but was susceptible to macropinocytosis inhibitors.
3. Hepatoma vesicles containing live CD4$^+$ T cells did not associate with E-cadherin or SCARF2 *in vitro.*
4. Vesicles containing live CD4$^+$ T cells associated with β-catenin in hepatomas *in vitro* and in hepatocytes *in vivo.*
5. Vesicles containing T regulatory cells acidified more frequently than those containing non-Tregs.

5.6 Discussion

5.6.1 Live CD4$^+$ T cell capture by hepatocytes is a unique and distinct process

5.6.1.1 Live CD4$^+$ T cell capture by hepatocytes is not efferocytosis

Our lab previously described a novel phenomenon whereby CD4$^+$ T lymphocytes are singled-out and engulfed by hepatocytes. Scanning electron microscopy revealed that this processed involved the formation of membrane blebs at the surface of the engulfing hepatocyte (**Fig. 5B**). This contrasted with the ruffles that were formed during efferocytosis and implies that different cytoskeletal rearrangements are required of hepatocytes for the internalisation of live CD4$^+$ T cells to those induced for efferocytosis.

Time-lapse fluorescence microscopy showed that the capture of live CD4$^+$ T cells was also shown to have a slower kinetic than efferocytosis of apoptotic and head-killed cell (**Fig. 5C**).

Of note, the number of Huh-7 cells containing live cells steadily decreased after 9 hr incubation. The reason for this was unclear, but may be related to several observed fates of CICSs (184). One possibility is a portion of captured cells were digested throughout the course of the experiment. T cells may also have been released from Huh-7 cells. It was not likely that the latter would be captured when imaging the cells every 0.5 hr. More frequent imaging times, as well as beginning the experiment at an earlier point may provide more information to the dynamics of Huh-7 interactions with $CD4^+$ T cells. This would also provide more information on the dynamics of hepatocyte efferocytosis. The number of heat-killed cells found within the Huh-7 cells did not change throughout the experiment. This is likely because of heat-killed cell saturation during the pre-incubation period.

Finally, immunofluorescence staining revealed that vesicles containing these cells did not associate with SCARF2 (**Fig. 5D**) as previously described for hepatocyte efferosomes. This implies that $CD4^+$ T cells are recognised or internally processed through distinct to mechanism to dead cells. Taken together, these data demonstrate that live $CD4^+$ T cell capture is not a case of mistaken identity, and that hepatocytes do not accidentally capture live T cells, believing they are dead.

5.6.1.2 Is live $CD4^+$ T cell capture affected by cytokines?

Another way in which live capture of $CD4^+$ T cells differed from efferocytosis was its response to cytokines. Huh-7 cells co-cultured with live, primary human $CD4^+$ T cells in the presence of different cytokines showed no variation in their capacity to conduct this process (**Fig. 5E**). However, this is unlikely to be a true representation of this process. Compared to studying efferocytosis, this process has the added complication of involving a live T cell that can also respond to cytokines as well as the Huh-7s. $CD4^+$ T cells also encompass a wide variety of subtypes with different effector functions [**Fig. 1C** (165)]. Each subtype of $CD4^+$ T cells

displays individual responses to cytokine stimulation and also produce their own repertoire of cytokines, based on their role in immunology (315). Therefore, using a mixed population of $CD4^+$ T cells was unlikely to provide informative results. Cytokine stimulation may also alter T cell permissiveness to internalisation by hepatomas. This is supported by previous observations made in our lab in which Tregs were more frequently found within hepatocyte cytoplasmic spaces *in vivo* compared to other subtypes. Specific responses of Huh-7 cells and T cells could not be separated with this approach. This experiment could be improved by pre-treating either Huh-7 cells or T cells with cytokines prior to their co-culture, ensuring that all stimuli are removed prior to this. Isolation of individual subtypes, as performed in later experiments concerned with Treg internalisation, may also allow more accurate and detailed conclusions to be drawn from this type of experiment.

5.6.1.3 Live $CD4^+$ T cell capture was distinct to entosis

This process was also shown not to share all qualities of CICSs formed through entosis; it was not perturbed by ROCK inhibition (**Fig. 5F**) as with entosis (183) and immunofluorescence staining showed that vesicles containing live $CD4^+$ T cells did not associate with E-cadherin (**Fig. 5G**). This was confirmed by 3D volume rendering of these stains. These observations suggest that alternative cell-cell interactions may be utilised for this process when compared with entosis. This is conceivable as entosis generally involves cells with similar polarities, whereby the cell with less-well established adhesion junctions often becomes the internalised cell. This has been reported in both epithelial cells (188) and non-adherent cancer cells (202, 203). The latter was shown to be dictated by E-cadherin expression. Comparatively, $CD4^+$ T cells are circulatory and have different migratory habits to hepatocytes. Therefore, they would have alternative capacities for forming cell-cell junctions. In conclusion, these results collectively demonstrate that this activity of live $CD4^+$ T cell capture by hepatocytes is a novel example of a CICS, which is unique to the liver.

5.6.1.4 Similarities of CD4$^+$ T cell capture by hepatocytes to macropinocytosis

Although it was shown that Huh-7 cells did not require the activity of ROCK to capture live CD4$^+$ T cells, this process was susceptible to inhibition by cytochalasin D (**Fig. 5F**). This suggested that cytoskeletal rearrangements within the hepatocyte are necessary for live cell capture. It also implies an active role for the hepatocyte to physically engulf the live T cell. Alternatively, this process could also have been a form of T cell invasion into the hepatocyte. In addition, this process was also susceptible to macropinocytosis inhibitors, EIPA and blebbistatin. This is the only similarity which this process has shared with efferocytosis. In support of this observation, macropinocytosis has been reported to be identifiable by both membrane ruffles and blebs (234). This would suggest that although live cell capture by hepatocytes is a distinct process to efferocytosis, some of their intracellular molecular machinery may be shared. Further exploration into the molecular processes that regulate live CD4$^+$ T cell capture will be required to validate further similarities of this process to macropinocytosis.

5.6.2 What is the purpose of CD4$^+$ T cell capture by hepatocytes?

An explanation as to why the capture of live CD4$^+$ T cells by hepatocytes has been preserved in the liver remains uncertain. Some situations in which lymphocytes are cannibalised are conducted to prevent the initiation of an immune response. Melanoma cells have been reported to cannibalise CD8$^+$ T cells, which was reported to prolong the survival of these tumour cells (182). It is likely that hepatocytes capture T cells to assist with immune modulation and maintaining immunotolerance within the liver. As only a small proportion of total captured CD4$^+$ T cells acidify, it is unlikely that this process is a form of population control. Perhaps hepatocytes can limit the activation of T cells by relocating them within their own cytoplasm. They may also be able to change the activity of cells which they engulf.

Profiling $CD4^+$ T cell transcriptomes and secretomes before and after their internalisation into hepatocytes may provide insights into the requirement of this process for the liver. This is assuming that T cells can be activated from within the hepatocytes.

The internalisation of these T cell by hepatocytes may also act as a somewhat forceful method to retain T cell populations within the liver. Certain stimuli may also dictate their release from hepatocytes. This is related to the observed gradual decrease in the number of hepatocytes that contained live $CD4^+$ T cells after 9 hrs incubation (**Fig. 5Cii**), which may imply that these cells were released. Similar scenarios of leukocyte-based cell-in-cell structure release have been reported (184, 190, 196). As to what causes this process in hepatocytes is uncertain. Thymocytes internalised by thymic nurse cells were released as a result of poor recognition of self-antigens (190). This was a method of ensuring the survival of non-autoreactive T cells. It is not certain as to whether a similar internal checkpoint exists within hepatocytes, or to what might determine the release of $CD4^+$ T cells. As hepatocytes can respond to inflammatory stimulators via TLRs and cytokine receptors (48), similar stimulation may dictate the release of T cells. This would allow hepatocytes to respond to inflammatory insults by quickly deploying T cells, reducing the time taken for resolution and the need for further T cell recruitment. It is also likely that these T cells will have not been activated using co-stimulatory molecules and would only remain active for a shorter amount of time as previously described for $CD8^+$ T cells (66). Treatments of hepatocytes/hepatomas in possession of live $CD4^+$ with inflammatory stimuli would help to validate this theory. Although cytokine stimulation did not alter the capacity of the hepatocytes to engulf live $CD4^+$ T cells *in vitro*, (**Fig. 5E**), it may encourage the release of T cells which have already been internalised.

5.6.3 How do hepatocytes recognise and internalise $CD4^+$ T cells?

Insights into the molecular machinery behind $CD4^+$ T cells capture by hepatocytes are still lacking. The experiments described in this chapter involving ineffective treatments of Huh-7 hepatomas with inhibitors of entosis imply that this process is distinct. Previous work in our lab showed that hepatocytes can distinguish $CD4^+$ T cells for engulfment from other types of lymphocyte (**Fig. 5A**). This would suggest that hepatocytes can recognise these cells through some form of intercellular interaction. This recognition is likely to be reciprocated by the $CD4^+$ T cell. This is implied by the slow rate of internalisation (**Fig. 5C**) and the formation of blebs on the surface of actively engulfing hepatomas (**Fig. 5B**). In contrast to speedy efferocytosis, the hepatocyte must negotiate a live, actively moving T cell into its cytoplasm. As such, the two cells are likely to directly communicate to allow this. The proteins involved in forming this interaction must be present on all subsets of $CD4^+$ T cells but absent on other lymphocytes, as other lymphocyte types were not observed to enter hepatocytes. This reduces the likelihood that immune response-specific signalling is used. Although hepatocytes can express MHC-II, this is not done constitutively (64). It is thus unlikely that an immunological synapse is formed between hepatocyte and T cell to facilitate their internalisation. Whether this interaction occurs intracellularly instead is still not certain. This has been reported in thymic nurse cells, which present self-antigens in MHC complexes to immature thymocytes (190). Initial contacts between hepatocytes and T cells are likely to be reminiscent of the primary interactions associated with lymphocyte recruitment. Blockade of ICAM-1, for example, has been shown to reduce of frequency of phagocytosis of live $CD4^+$ and $CD8^+$ T cells, and thymocytes by haemophagocytic macrophages (175). In agreement with this, our lab previously found that treatment of hepatomas with ICAM1-blocking antibodies reduced T cell capture by hepatocytes following short co-cultures, but not after

incubations longer than 60 min. This implies a role for molecules involved with lymphocyte tethering in the initial binding of T cells to hepatocytes but not for their complete internalisation. How the hepatocyte negotiates the T cell into its cytoplasm following its initial binding is still unknown.

Understanding the process of live T cell capture by hepatocytes is difficult without knowing the form of endocytosis through which they are internalised. I observed that blebs formed on the surface of hepatomas that were actively engulfing live T cells. As stated earlier, the formation of these blebs have been reported for cells conducting macropinocytosis (234) and live $CD4^+$ T cells capture was susceptible to inhibitors of this process. This suggests that this process may be related to macropinocytosis, although the exact mechanical cascades involved are lacking. Certain aspects of these are likely to be shared by hepatocyte efferocytosis which was also susceptible to inhibition by EIPA. Similar parallels between efferocytosis and live cell capture have been described previously. The universal 'don't eat me' signal for apoptotic cell capture, CD47, has been shown to aid both leukemic cell survival, as well as donor T cell survival in models of graft vs host disease (92, 136, 176). Both pathways may also converge on the autophagy pathways as also described for entosis (206). Further dissection of the initiating events for both live and dead cell capture are needed before both processes can separated on a molecular level.

Perhaps related processes involving molecular scavenging are repurposed either for T cell capture or retention. One example involves the metabolism of lipids. Hepatocytes possess several receptors, including class B receptors CD36 and SR-B1, involved in scavenging lipids like LDLs, HDLs and cholesterol (316-318). This helps to control their available levels in the liver and potentially convert them to bile acids. A recent publication may suggest that this process could be exploited for T cell dissolution and capture. Surls *et al*, described how

membrane levels of cholesterol could alter the activity of $CD4^+$ T cells (319). Increased cholesterol was shown to increase the resting population of rest $CD4^+$ T cells, but not $CD8^+$ T cells. Furthermore, these T cells were more likely to differentiate into T_H1 cells. In agreement with these findings, it was also shown that cholesterol starvation of mice caused a decrease in T cell proliferation (320). Lipid sensing by hepatocytes through scavenger receptors could be an initiating event for engulfing overactive or overpopulating T cells. In relation to this, increases in cell membrane cholesterol were reported to act as negative regulator of CICS formation (321). Liver-infiltrating T cells are likely to alter their membrane composition in a lipid-rich environment like the liver. As such, high lipid content may be a signal for hepatocytes to internalise these cells and prevent/reduce their inflammatory activity. In relation to this, our lab previously observed that hepatomas infected with HCV could not internalise live T cells. This virus infects hepatocytes through interactions with SR-B1 (322). This receptor may be downregulated after viral infection to prevent subsequent virion particle binding, which would concomitantly reduce their capacity for live $CD4^+$ capture. This has been reported for its co-receptor for viral entry, CD81 (323). Increased lipidation of T cells before co-culture with hepatocyte cell lines could be used to verify this theory. This still does not explain the preference of hepatocytes to engulf Tregs cells, as Surls *et al* reported that $FOXP3^+$ activity was not altered by increased membrane cholesterol. Other, possibly synergistic processes which may explain this are discussed below.

5.6.4 Why do T-regulatory acidify within hepatocytes?

Tregs are the major cell type responsible for dampening inflammatory responses. This has brought them a lot of attention as potential therapeutics for inflammatory disease, including those within the liver (163). The immunotolerant environment of the liver, however, presents complications in the necessity of Tregs in this organ. Many regulatory mechanisms

are already in place in liver to limit the duration of inflammatory responses, such as the increased induction of lymphocyte apoptosis and their short-term activation by hepatocytes (9, 66). Immunotolerance in the liver is, thus, not achieved by an abundance of Tregs. This may provide explanations as why Tregs captured by hepatomas entered acidic compartments of their host more frequently than non-Tregs (**Fig. 5I**). Even so, it would be counter-intuitive to delete local Tregs when aiming to maintain an immunotolerant environment. Additionally, even though these observations were made using hepatomas, it is unlikely that this preference for deleting Tregs is a tumour-specific observation, as Tregs are often beneficial for tumours to avoid immune detection (324-326).

One possible reason for the potential deletion of Tregs would be as an additional process of immune control within the liver. Were the ratio of Treg : non-Tregs to skew in the liver, potentially through increased preservation of T-regulatory cells, it may become impossible for an adequate immune response to be mounted, rendering the liver 'immunoblind'. This may shed light on the role of this observed deletion of Tregs by hepatocytes. Hepatocytes may possess an intrinsic capability of limiting the number of available Tregs within parenchymal regions. Coupled with the lower tendency of hepatocytes to kill non-Treg cells, hepatocytes may control the potential of the liver to mount an immune response. Not only do hepatocytes reduce the viability of activated pro-inflammatory cells, but by capturing and deleting Tregs, they ensure that the liver can mount an immune response altogether. This may also provide some insight into the absence of cytokine sensitivity of live cell capture. Although the capacity of hepatocytes to capture live cells was unaffected by cytokine stimulation, be it pro-inflammatory or anti-inflammatory, such treatments may skew the fates of already internalised cells. This may reduce the frequency of Treg acidification,

potentially increasing the livers capacity for raising an anti-inflammatory response, presuming that Tregs are released or still able to function from within hepatocytes.

Preferential acidification of vesicles containing Tregs suggested that Tregs could be differentially recognised or processed by hepatocytes. This implies the presence of an intracellular decision-making mechanism for the trafficking of certain Tregs to acidic compartments. The molecular mechanisms of how this is conducted remain a mystery. An internal mechanism of sensing T cell subsets must be present within the hepatocyte. One investigation reported that increased activity and stability of Tregs was associated with higher intracellular expression of β-catenin (327). Overexpression of β-catenin in Tregs, even in $FOXP3^-$ cells, was associated with lower activity of effector T cells. Although this was hypothesised to be mostly endowed through overactive Wnt signalling pathway, increased total β-catenin expression would also increase the pool available for cell junction formation. *In vitro* immunofluorescence staining revealed that β-catenin associated with internalised live $CD4^+$ T cells (**Fig. 5Hi**). Further, *in vivo* IHC staining revealed β-catenin-positive intracellular structure within hepatocytes which were of a comparable size to lymphocytes (**Fig. 5Hii**). Interactions involving membranal β-catenin may therefore dictate which cells become internalised. This may represent yet another aspect of liver biology that contributes to immune regulation.

Chapter 6: General Discussion

6.1 How hepatocyte cell-in-cell structures effect general hepatocyte function

6.1.1 Efferocytosis and hepatocyte activity

Hepatocytes form 80% of the human liver and conduct most of it's functions. Furthermore, they are significantly involved with immune responses within the liver and contribute to the immunotolerance in the liver (48). In relation to this, I have now shown that hepatocytes play further immunological roles in the liver, by engulfing both dying cells and live $CD4^+$ T helper cells. How hepatocytes balanced their wide variety of functions is difficult to interpret. Efferocytosis commonly alters the immunological activity of phagocytes (328), so it would be intuitive that a transcriptional alteration also occurs in hepatocytes. However, due to the speed and frequency at which hepatocytes clear dying cells, particularly necrotic cells, it is unlikely that such a drastic phenotypic change would occur within hepatocytes. Otherwise, in the presence of large sheets of necrosis (329) which are associated with liver disease (1), many proximal live hepatocytes would be unable to function. In support of this, I showed that hepatocytes became multinucleate by clearing dead cells originating from both chemical and physical injury (APAP and *ex vivo* cauterisation respectively) (**Fig. 4D+4G**). It is thus unlikely that the capacity of hepatocytes to clear dead cells is affected by their zonation within the liver. Overall, besides providing nutrients to the hepatocyte, efferocytosis is unlikely to drastically alter hepatocyte biology to the same extent as in other cells.

6.1.2 Live CD4$^+$ T cell capture and hepatocyte function

Although efferocytosis is unlikely to alter hepatocyte biology, the same may not be true for live CD4$^+$ T cell capture. It was observed that not all internalised cells enter acidic compartments within the hepatocyte (**Fig. 5I)**. Moreover, these cells do not exhibit other signs of stress once they're captured and do not appear to die through other means. This would imply that internalised T cells are not always 'starved'. Related to this, our lab has observed, through membrane labelling, that small, non-acidic vesicles derived from the hepatocyte were trafficked to the internalised T cell. This implies that the hepatocytes invest internal resources to either communicate with the internalised T cell or promote its survival. This may detract from the other functions of hepatocyte if much of its cytoskeletal trafficking network is directed towards internalised T cells. Comparable mechanisms of molecular parasitism have been reported by the invading bacterial species, *Chlamydia Trachomatis*, which usurps the endosomal trafficking proteins of a host macrophage (330).

Changes caused to hepatocyte activity by internalising T cells are likely to be reciprocated with alterations to T cell behaviour. It is still not clear as to whether T cells remain active from within hepatocytes. This entails whether a T cells' receptors are available to possible agonists from within their vesicular enclosure. As such, it is not certain as to whether T cells could be activated from with a hepatocyte. Furthermore, it would be of interest to observed whether T cells can secrete cytokines into the hepatocyte cytoplasm. Would this propagate immune signalling within the hepatocyte, or would be they continue to be secreted by the hepatocyte itself? Time-lapse imaging of T cell-specific, fluorescently tagged cytokines may be required to investigate this notion, by tracking cytokines in internalised CD4$^+$ T cells.

Furthermore, it would be of interest to assess how zonation alters hepatocyte capacity for live $CD4^+$ T cell internalisation. It is likely that periportal hepatocytes are more likely to capture T cells, as these hepatocytes make first contact with infiltrating lymphocytes. Hepatocytes in this zone also possess a higher metabolic rate (3, 40), which would be likely to facilitate the cytoskeletal rearrangements for capturing a live cell. In support of this, cancer cells generally exhibit higher metabolic rates then their normal counterparts, which facilitates their ability to capture their neighbours by Entosis (201, 203, 331). As such, more metabolically active hepatocytes may be more successful in capturing $CD4^+$ T cells.

Specific activities may be directly altered by accommodating an internalised cell. Hepatocytes are the major stores of lipids within the liver. These are stored in relatively large droplets that are often enlarged in patients with fatty diets, which is known as steatosis (332). Hepatocytes containing internalised cells may not be able to store large quantities of lipids. In relation, T cells may be altered if internalised by hepatocytes which already possess reasonable lipid stores. Such lipids may incorporate into the T cells membrane and alter their behaviour, as lipid content has been linked to alterations in Teff activity (319, 320). However, it is unlikely that hepatocytes which possess giant lipid droplets associated with steatosis will have cytoplasmic space to house live $CD4^+$ T cells. This would likely increase T cell population in the parenchyma which may contribute to the associated increased inflammation.

6.2. Mechanisms of cell-in-cell structures in the liver

6.2.1 How do hepatocytes know what they're eating? – Treg vs Non-Treg

6.2.1.1 Possible role of autophagy in captured live cell processing

The mechanisms which underlie the recognition and capture of $CD4^+$ T cells by hepatocytes are lacking. Equally, it is uncertain as to how these cells are trafficking within the hepatocyte on their capture. Results described in this thesis showed that not all engulfed T cells entered acidic compartments within the hepatocyte (**Fig. 5I**). Treg cells, however, were more likely to acidify than non-Tregs. It is likely that there is some form of checkpoint present within the hepatocyte which prevents certain internalised live cells from fusing with lysosomes. A candidate for this checkpoint is when a live cell-containing vesicle converges on the autophagy pathway. This was described in breast cancer cell entosis, whereby internalised cells were transiently labelled with LC3-II (111). This recruitment required the presence of Phosphatidylinositol 3-phosphate (Pi_3P) for the recruitment of downstream autophagy proteins possessing FYVE domains and was subsequently followed by lysosomal fusion. PI_3P formed at phagosomes was reported as a requirement for autolysosome formation (333). Of note, PI_3P has been shown to promote the activity of the K^+ channel, $K_{Ca}3.1$, which has been linked to T naïve cell proliferation (334, 335). Such systems may therefore be employed by hepatocytes to specifically target overly proliferating T cells for LC3-II-mediated lysosomal degradation. Further understanding into the differences in signalling lipids between Tregs and non-Tregs, during different stages of activation, will be required to potentially confirm this role of PI_3P and hepatocyte-derived LC3-II.

Autophagy is frequently active within hepatocytes and is required for the mobilised lipid droplets stored within them (336). Such lipid droplets were also shown to co-localise with

LC3 and lysosomal protein, LAMP1, in the same investigation. Notably, acute increases in hepatocyte lipid-content were shown to activate autophagy-related lipid depletion, or lipophagy, whereas chronic exposure associated with a high-fat diet was inhibitory. The entry of T cells into hepatocytes may therefore trigger autophagy through similar mechanisms, derived from increases in cytosolic lipid content. Were this to be accurate, hepatocytes may be less likely to deploy lysosomes to internalised T cells in fatty livers. Observations of lipid-rich hepatocytes containing T cells may prove useful in proving this concept.

6.2.1.2 Mimicry of intracellular parasitism

Another possibility for the observed differences in the treatment of Tregs by hepatocytes is that Teffs possess some sort of 'don't kill me' signal which is inefficiently expressed by Tregs. This is not likely to be related to the don't-eat me signal, CD47, which prevents the engulfment of cells (176). As both Tregs and non-Tregs can be engulfed, it more likely to be a protein which prevents lysosomal fusion. Many intracellular pathogens, such as *Chlamydia* or *Listeria*, achieve this through manipulation of the actin cytoskeleton through which the lysosomes are trafficked upon (337). Perhaps T cells can manipulate the hepatocyte cytoskeletal network, with non-Tregs being more adept at this process. This is dependent on whether hepatocyte or T cell is in control of the captured cells fate. Real-time imaging of hepatocyte cell lines with fluorescently-labelled actin may provide insights into the spatiotemporal organisation of cytoskeletal rearrangements induced by T cell capture.

6.2.1.3 Survivability of $CD4^+$ T cell subsets

The differences in survival between Tregs and Teffs may not be due to their internal recognition by hepatocytes whatsoever. Perhaps Treg themselves possess deficits in autophagy and are simply not well accustomed to situations of starvation. Related to this,

internalised breast cancer cells were shown to upregulate autophagy up entry into neighbouring cells (111). Inhibition of autophagy resulted in the starvation of the captured cell and death through apoptosis. Although captured T cells may obtain resources from their hosts, they would still be required to recycle internal structures to promote their survival once they were separated from the extracellular environment. Tregs may be unable to do this as efficiently as non-Tregs, which may predispose them more to apoptosis and subsequent degradation by the hepatocyte. Importantly, it was reported that Tregs require autophagy more than other $CD4^+$ lineages to promote their survival, but also to maintain FOXP3 expression (338). Treg-specific deletions of *Atg7* were associated with reduced viability of these cells, as well as an expansion of Teffs (338, 339). This implies that Treg cells may be addicted to autophagy pathways and drain internal resources faster than they can replenished by the hepatocyte. Tregs may therefore be less-well prepared for separation from the extracellular environment that non-Tregs. It was not clear from the experiments described in this thesis as to the processes through with captured $CD4^+$ T cells died. Analysis of changes in phenotype and caspase activation will be needed to confirm this possibility. Overall, further research into the role of autophagy in T cell capture by hepatocytes is likely to elucidate numerous molecular aspects of this process. This may provide further insight into the possible molecular explanations for why Tregs are more likely to acidify than non-Tregs.

6.2.2 Differences and similarities between live and dead cell capture

The observations made in this project have provided some insight into separating efferocytosis from live cell capture in hepatocytes (**Fig. 6A**). The processes are phenotypically different, using different membranal structures with which to internalise their cargo (**Fig. 5B**). Efferocytosis was also shown to occur more frequently and at a faster rate than $CD4^+$ T

cell capture (**Fig. 5C**). It was also observed that hepatocyte efferosomes were enriched with SCARF2, a phenomenon which was absent from vesicles containing live cells. Although the exact involvement of SCARF2 in hepatocyte efferocytosis if not clear, its absence from vesicles containing live T cells implies that hepatocytes can distinguish dead cells from live cells. Together, with the use of alternative membrane structures and differences in capture rates, it is clear that these processes are distinct and separate. What's more, the presence of SCARF2 at intracellular structures within hepatocytes could be used to specifically identify efferosomes *in vivo*. Conversely, I showed that increased expression of β-catenin at similar structures can denote internalised $CD4^+$ T cells. Although these molecular differences are currently only superficial, they are sufficient to deviate them as separate processes.

These mechanistic and spatiotemporal differences between live and dead cell capture are likely related to their purposes within the liver. I observed that efferocytosis was a rapid process, especially with the clearance of necrotic cells, where Huh-7 cells were saturated within 1.5 hr co-culture (**Fig. 5C**). This rapid onset of efferocytosis would be necessary in preventing the accumulation of dying cells, both in homeostasis and disease. Further, although the distribution of SCARF2 was altered under inflammatory circumstances, its expression appeared to be constitutive.

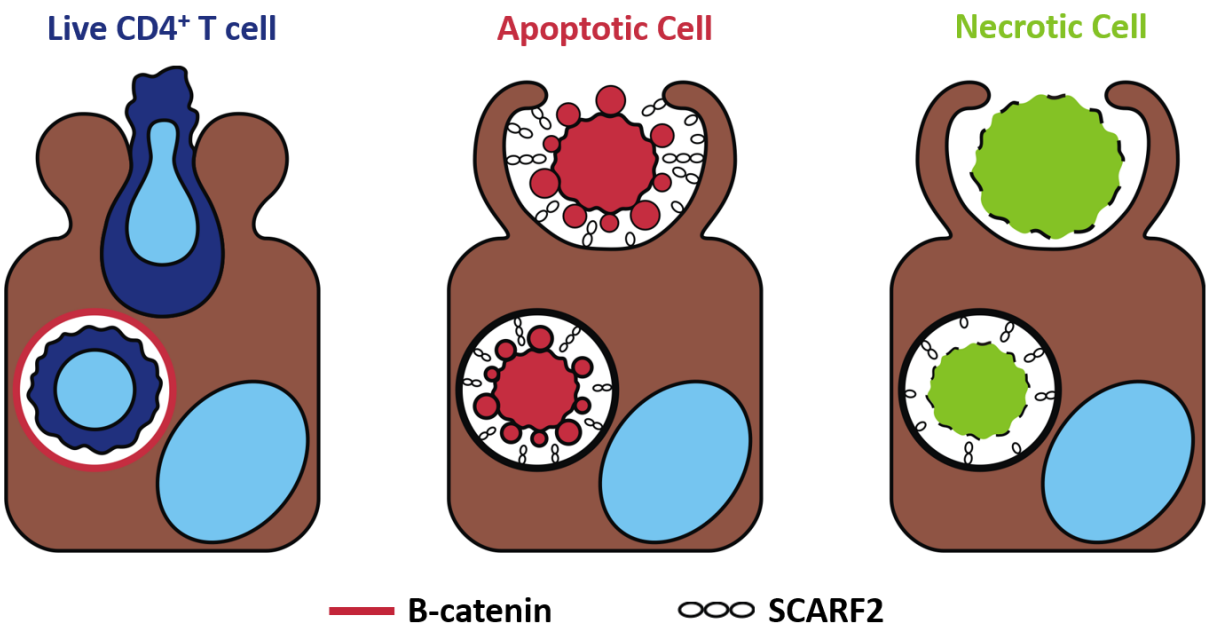

Figure 6A: The differences between live CD4$^+$ T cell capture and efferocytosis by hepatocytes uncovered from this project. Hepatocytes (brown) form blebs when live CD4$^+$ T cells (dark blue) are internalised. The vesicle containing the fully internalised T cell associated with β-catenin. In contrast, the capture of both apoptotic (red) and necrotic (green) cells was concurrent with the formation of membrane ruffles on the hepatocyte membrane. Both types of dead cells associate with hepatocyte scavenger receptor family f, class 2 (SCARF2) when fully internalised. Adhered apoptotic cells were also shown to associate with SCARF2 prior to their internalisation. Details behind the exact roles of β-catenin and SCARF2 in these processes are still lacking.

As several different ligands have been reported for the related receptor, SCARF1 (130, 145), it is likely that SCARF2 may contribute to hepatocyte uptake of several molecules, given its constitutive expression. This system would allow hepatocytes to be primed for dead cell clearance without the continuous expression of a specialised receptor. Hepatocytes can therefore respond swiftly upon encountering dead cells as they do not require transcriptional alterations. Whether this situation is the same for $CD4^+$ T cell capture is uncertain. Although β-catenin is also constitutively expressed in the liver, it does not possess the same diversity of binding partners as SCARF2 has, in the way of potential ligands, and is mostly required for adhesion junctions. From these potential binding partners, I showed that E-cadherin is not involved in this process. Moreover, although its involvement in $CD4^+$ capture is not known, its activity is heavily influenced by Wnt signalling (340). It is thus likely that signalling events will be required for changing the distribution of β-catenin prior to T cell capture. Requiring such fulfilment would limit the number of T cells which can be captured by hepatocytes at any given time, allowing some to patrol the parenchyma. Alternatively, requiring alterations in signal transduction may also limit the number of hepatocytes which are capable of T cell capture. Hepatoma cultures with limited differentiation are heterogeneous and not all cells internalised T cells during time-lapse experiments. In relation to this, hepatocyte zonal distribution in the liver is dictating by Wnt signalling (36, 40). Perhaps periportal hepatocytes are more efficient hunters of $CD4^+$ T cells than pericentral hepatocytes and are tasked with controlling the traffic of these cells as they drain through the parenchyma. Analysing the frequency of CICSs across these zones may provide insight to this notion.

Of note, the staining procedures used in this investigation do not distinguish the cellular ownership of β-catenin. As such, it is unknown as to whether T cell or hepatocyte-derived β-catenin is associated with the capture process. Cell-specific labelling may be required to determine the specific interactions. The requirement for these interactions and the time taken to establish them are likely what dictate the lower frequency of live cell capture, compared to efferocytosis.

6.3 Cell-in-cell structures and drug discovery

6.3.1 Manipulating T cell capture in chronic liver disease

It is likely that $CD4^+$ capture by T cells contributes to immune regulation of the liver. As such, it may be possible to manipulate this process for therapeutic benefit (**Fig. 6B**). It is not certain however as to how preventing or encouraging this process would affect liver. The most beneficial application of manipulating this process would most likely be aimed at manipulating the availability of Tregs in the liver. It was shown that this subtype was more frequently acidified by hepatocytes (**Fig. 5I**). Preventing this acidification or their initial capture could increase their viability in liver and consequently promote resolution of inflammatory responses. This presumes that they are unchanged following their internalisation by hepatocytes. However, if using global inhibitors of $CD4^+$ T cell capture (such as EIPA), pro-inflammatory non-Tregs would also be less likely to be captured by hepatocytes. Their persistence in the parenchyma would increase the likelihood of developing inflammatory responses. Although this may be beneficial at early stages of disease pathogenesis, it would counteract the concurrent increased viability of Tregs. Further understanding into how hepatocytes distinguish Tregs from Teffs may provide

opportunities to therapeutically target the capture or release of individual $CD4^+$ T cell subsets.

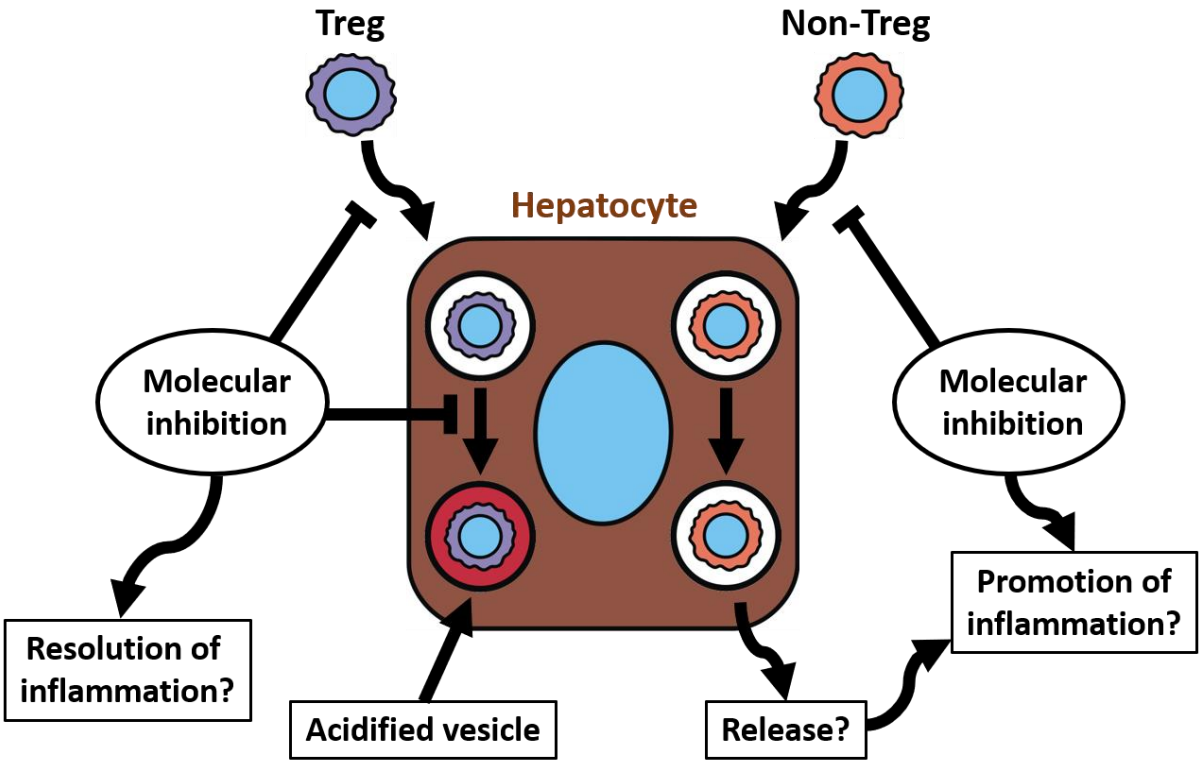

Figure 6B: The consequences of manipulating Treg and non-Treg capture by hepatocytes. Hepatocytes can engulf live $CD4^+$ T cells**.** This work has shown that a specific anti-inflammatory subset of these cells, T regulatory cells (Tregs) are more likely to enter acidic compartments of the hepatocyte and be killed compared to non-Tregs. As reported for other types of cell-in-cell structure, unacidified non-Tregs may be released from there host cells, allowing them to contribute to inflammatory responses. Inhibiting the formation of these cell-in-cell structures could have profound consequences for liver immune response. Inhibiting the capture or acidification of Tregs could promote their survival in the liver and promote resolution of inflammatory response. Conversely, inhibiting non-Treg capture by hepatocytes may have the opposite effect and increase the likelihood of developing inflammation. Further understanding into the molecular processes which dictate the capture of $CD4^+$ T cells and the selective acidification of Tregs is required to the validate these possibilities.

6.3.2 Cell-in-cell structures – a new therapeutic target for hepatocellular carcinoma

One of the major findings of this project was the consistent and reproducible increase in multinucleation in hepatocytes caused by efferocytosis (**Chapter 4**). This provides a further source for the frequent binucleate hepatocytes witnessed within the liver besides seemingly-random cytokinesis failure (275, 341). Exactly what this means for the liver is still not entirely certain. Some have stated that increased ploidy can be beneficial for the liver by providing residence from tumorigenesis and the potential for genetic diversity amongst hepatocytes (298, 299). However, increased ploidy could also provide an advantage for tumour cells. Gaining further mutations increases the likelihood of further dysregulation of proliferation pathways, and of metastasis. This outcome has been described for other cancers which gained increases in ploidy (265, 270, 272). In the liver, the risk of developing HCC is increased throughout end-stage, regardless of aetiology (342, 343). Besides the genetically instability from certain viral infections (344), the reason for this is not certain. Chronic liver disease (CLD) is also synonymous with wide-spread cell dead throughout the liver (1). As such, continuous efferocytosis by hepatocytes may be a risk factor for oncogenesis associated with CLD. Reducing hepatocyte efferocytosis may therefore be of therapeutic benefit for managing the risk of developing HCC. Although this could increase the risk of apoptotic cells progressing to secondary necrosis, many other cells in the liver are capable of efferocytosis and could compensate, including Kupffer cells, BEC and infiltrating macrophages (1). Once these mechanisms of how hepatocytes recognise dead cells are better understood, they could be therapeutically targeted specifically, sparing the activity of other phagocytes, and removing the requirement for broader inhibitors like EIPA.

It is also likely that increased efferocytosis would not be the only contributor for increased multinucleation in tumours. It is likely that the $CD4^+$ T cells would also be engulfed by

hepatomas. Some of these cells were shown not to be digested by Huh-7 hepatomas (**Fig. 5C**). As such, they might persist longer within hepatocytes *in vivo* and also prevent cytokinesis and induce multinucleation. This would also have the added benefit of preventing the liver from mounting an immune response against the tumour. As cancer cells often acquire the ability to engulf their neighbours upon transformation due to increased cytoskeletal malleability (185), it is also likely that hepatomas could engulf live cells more readily than normal cells. Taken together, reducing the number of T cell capture by both hepatocytes and hepatomas may be efficacious for controlling tumour growth both by limited their level of genetic instability and increasing the number of available effector $CD4^+$ T cells to mount immune responses against the tumour. Overall, limiting the creation of CICSs in the liver could be beneficial both in reducing the risk of oncogenesis, and managing the growth of already established tumours.

6.3.3 How hepatocyte efferocytosis contributes to disease

This project has the revealed the adeptness of hepatocytes to engulf dying cells. Although their capacity for this was described a long time ago, little work has been conducted in its contribution to liver disease pathogenesis. The inability of phagocytes to clear dying cells has been described in a multitude of other diseases (125, 128, 152, 345). It is thus likely that defects in hepatocyte efferocytosis may be related to forms of chronic liver disease. This is likely the case for many diseases whose initiating events are not well understood, particularly for autoimmune diseases. These largely include primary biliary cholangitis (PBC), primary sclerosing cholangitis (PSC) and autoimmune hepatitis (AIH), whose molecular causalities are unknown. As a result, there are currently no mouse models for these diseases. Many autoimmune diseases are caused through the production of self-recognising antibodies, which can develop upon immune recognition of dead cell components,

particularly from apoptotic blebs (78, 156). It is difficult to fathom diminished efferocytosis within the liver, as almost all tissue-forming cells have been reported to clear dead cells (1, 143, 346-348). It is more likely that certain diseases may be associated with defects in efferocytosis at a cell-specific level. Defects in BEC efferocytosis by contribute to the pathogenesis of PBC, for example (156). Further understanding into the markers of hepatocyte efferocytosis, as well as its effects on hepatocyte biology may therefore prove useful in understanding the pathogenesis of these diseases.

In other liver diseases whose pathogeneses are better understood, the contribution of efferocytosis is easier to observe and comprehend. Both acute and chronic forms of diseases are commonly associated with necrotic lesions (1). Furthermore, lymphocytes recruited to the liver during inflammation are more prone to apoptosis in the liver (24). As such, there is a high burden of dead cell clearance in the diseased liver. Hepatocyte efferocytosis is likely to be increased in diseased livers, on the verge of exasperation. This was exemplified by the upregulation and translocation of SCARF2 that was observed both in diseased livers and cytokine-treated hepatomas (**Fig 3K+3L**). As SCARF2 associated with vesicles containing both apoptotic and necrotic cells (**Fig. 3I**), it would thus seem that efferocytosis is increased in the hepatocytes under inflammatory conditions to promote resolution and repair. Manipulation and prolongation of efferocytosis may therefore be of therapeutic benefit. Investigations into the effects of SCARF2 knockout on liver disease pathogenesis would aid to understand its role in the liver and potentially measure the necessity of hepatocyte efferocytosis in controlling disease pathogenesis.

6.3.4 Cell-in-cell structures and liver regeneration

The liver is unique amongst other internal organs with its ability to regenerate following injury. However, this ability is often compromised in patients with chronic liver disease and is difficult to induce experimentally. Furthermore, the exact signals which switch off the hepatocytes capacity to regenerate are not fully understood. It was recently reported that efferocytosis by macrophages caused increased liver regeneration in mice, through the STAT3-IL10 signalling pathway (45). In relation to this, IHC staining suggested that efferocytosis increased the frequency of Ki67 on hepatocytes in APAP-treated mice and injured *ex vivo* human tissue (**Fig 4I**). Moreover, efferocytosis also caused a reduction in hepatocyte p21 expression in cauterised *ex vivo* human liver tissues (**Fig. 4K**). This suggests that efferocytosis could promote liver regeneration. This must also be an efferocytosis-specific event, as EIPA-treated tissues failed to show the same alterations in p21 and Ki67 in human tissues. Dying cells therefore may be an important factor in promoting liver regeneration.

This is a cogent observation, with the liver promoting its own repair in response to injury. It is likely that regeneration is not limited to hepatocytes which have captured dying cells. Otherwise the hepatocytes lost during injury would not be replenished if all proliferating cells failed cytokinesis. Of interest, it appears that hepatocytes can promote their own genetic diversity with this system; efferocytosis induces the hepatocyte to enter the cell cycle but also prevents it from dividing, promoting multinucleation. Other hepatocytes not conducting efferocytosis are likely the cells to be charged with regeneration. It is likely that soluble factors are also involved in this promote of hepatocyte proliferation in response to dying cells. Efferocytosis has been reported to invoke transcriptional alterations in macrophages, and subsequently promote the secretion of anti-inflammatory cytokines

(155). It is thus more likely that dead cell capture alters the hepatocyte secretome which ultimately induces neighbouring hepatocytes to divide. Cytokine and growth factor profiling of efferocytosing hepatocytes will prove useful in understanding this in the future.

6.4 Conclusions and prospects

This project has unearthed a novel and likely important aspect of hepatocyte biology in the form of cell-in-cell structures (CICSs). Here, I have described and contrasted the mechanism of efferocytosis by a hepatocyte, to their unique ability to specifically capture live $CD4^+$ T cells (Fig 6B). Both processes share phenotypic aspects of macropinocytosis, although utilising distinct cytoskeletal structures. Each occur at different rates and subsequently formed vesicles associate with different membranal proteins; efferosomes with SCARF2 and live $CD4^+$ T cell-containing vesicles with β-catenin. Efferocytosis can be both beneficial and detrimental to liver biology; frequent efferocytosis represents another form of immune regulation within the liver and may be necessary for promoting regeneration. It represents a mechanism by which the liver can alter its own genetic diversity through hepatocyte multinucleation. Uncontrolled efferocytosis and increased multinucleation, however, may be associated with the development of HCC. In contrast, the novel action of $CD4^+$ T cell capture is infrequent and mechanistically different to a major process of CICS formation, entosis. Hepatocytes can also distinguish between $CD4^+$ T cell subsets, as shown by the preferential acidification of Tregs *in vitro*. Such a process is likely to contribute to the immune regulation in the liver. Mechanistic details for both for both CICS-forming processes are still lacking, including methods of recognition, the sequential events involved in internal processing and the transcriptional consequences for the hepatocyte. Both events are likely to be prominent events occurring throughout liver disease. As such, a greater understanding of both

processes will likely improve our knowledge of pathogenesis across all liver diseases and hopefully provide new platforms for therapeutic intervention.

Appendix

A.1 Isotyped- matched control (IMC) stains

The following figures display immunofluorescence or immunohistochemistry stains using IMC controls corresponding to specific stains used within this thesis that were not present within the main figures.

A.1.1 Chapter 3 IMCs

This section contains all IMCs for immunofluorescence stains performed in Chapter 3 that were not included in primary figures.

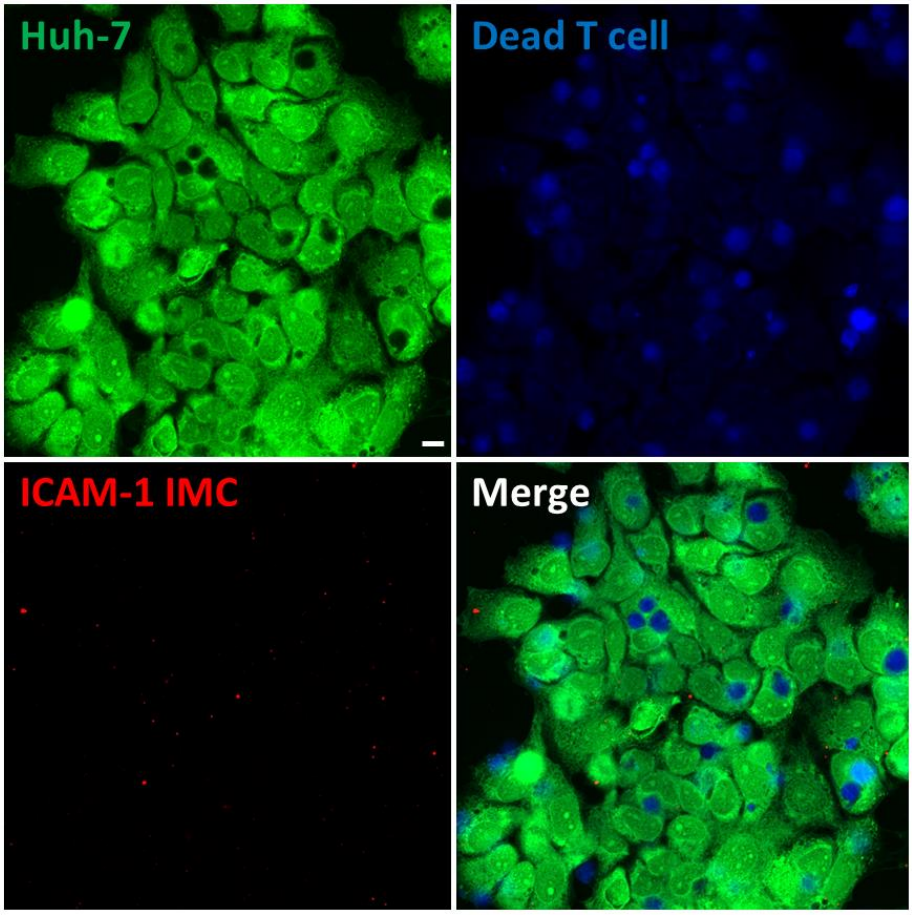

Figure A1: Isotyped matched control (IMC) immunofluorescence staining of efferocytosing Huh-7 cells for ICAM-1. Huh-7 seeded in 24-well plates on glass coverslips were fluorescently labelled with Cell Tracker Green (CTG)/ Chloromethylfluorescein diacetate (CMFDA). Huh-7s were then co-cultured with primary human $CD4^+$ T cells, labelled with Cell Tracker Violet (CTV)/ bromomethyl derivative of coumarin (BMQC) for 3 hr. Cells were then fixed with MeOH formaldehyde and stained by immunofluorescence using an anti-intercellular adhesion moledule 1 (ICAM-1) antibody, or a mouse IgG1 IMC (shown here) via immunofluorescence (shown in red). Cells were then imaged by confocal microscopy using a Zeiss LSM 880, in which Z-stacks were acquired. Scale bars represent 10 µm. Corresponding stain: **Figure. 3E.**

A.1.2 Chapter 5 IMCs

This section contains all IMCs for immunofluorescence and immunohistochemistry stains performed in Chapter 5 that were not included in primary figures.

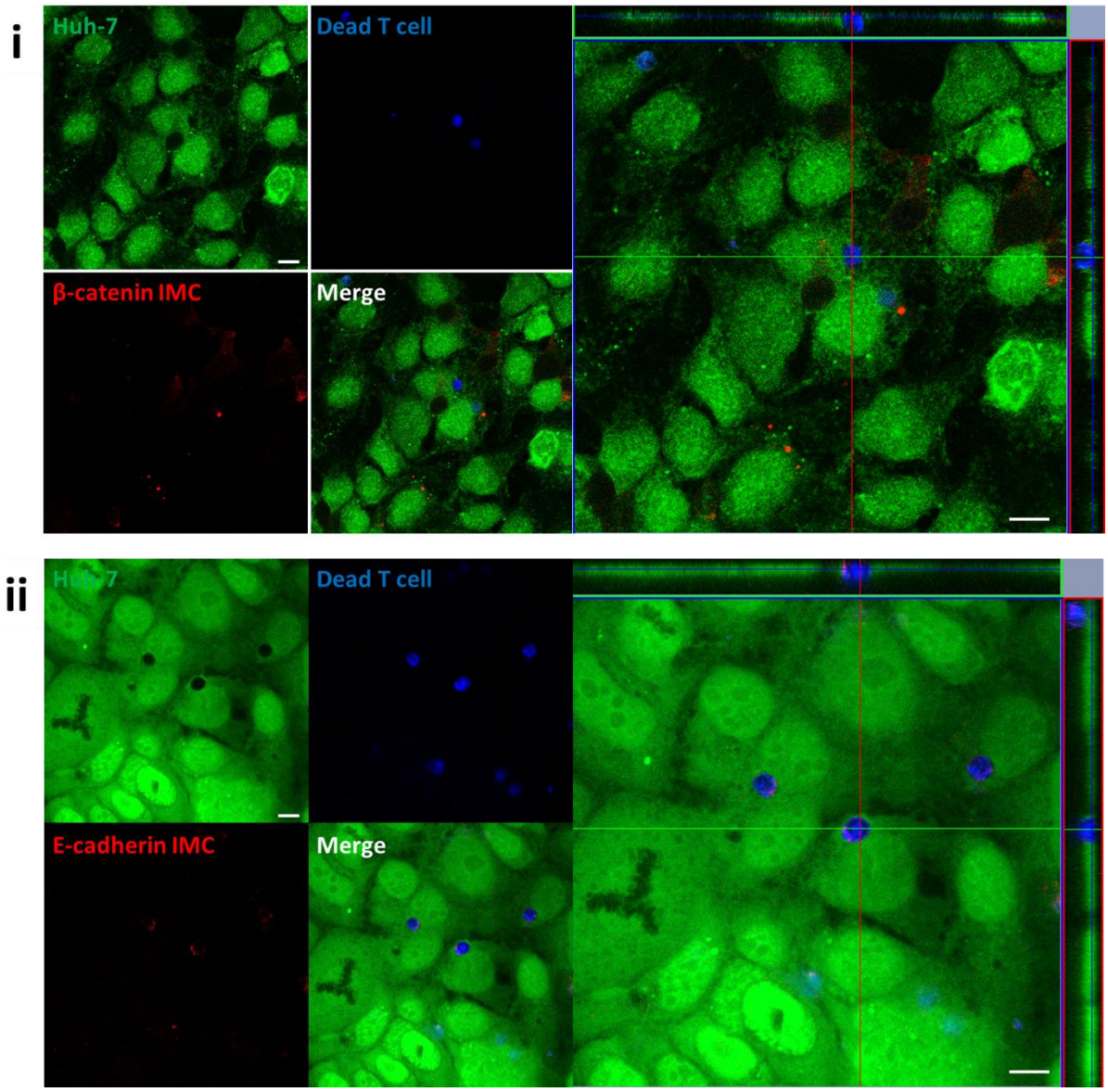

Figure A2: Vesicles containing captured live CD4$^+$ T cells did not associate with E-cadherin within Huh-7 hepatomas. Huh-7 seeded in 24-well plates on glass coverslips were fluorescently labelled with Cell Tracker Green (CTG)/ Chloromethylfluorescein diacetate (CMFDA). Huh-7s were then co-cultured with primary human CD4$^+$ T cells, labelled with Cell Tracker Violet (CTV)/ bromomethyl derivative of coumarin (BMQC) for 3 hr. Cells were then fixed with 3.7% formaldehyde and stained for E-cadherin, β-catenin or corresponding IMCs (shown here) via immunofluorescence (shown in red). Cells were then imaged by confocal microscopy using a Zeiss LSM 880, in which Z-stacks were acquired. Scale bars represent 10 μm **(i)** IMC staining for β-catenin using a mouse IgG1 antibody. Corresponding stain: **Figure 5Hi (ii)** IMC staining for E-cadherin using a mouse IgG2a antibody. Corresponding stain: **Figure 5G**.

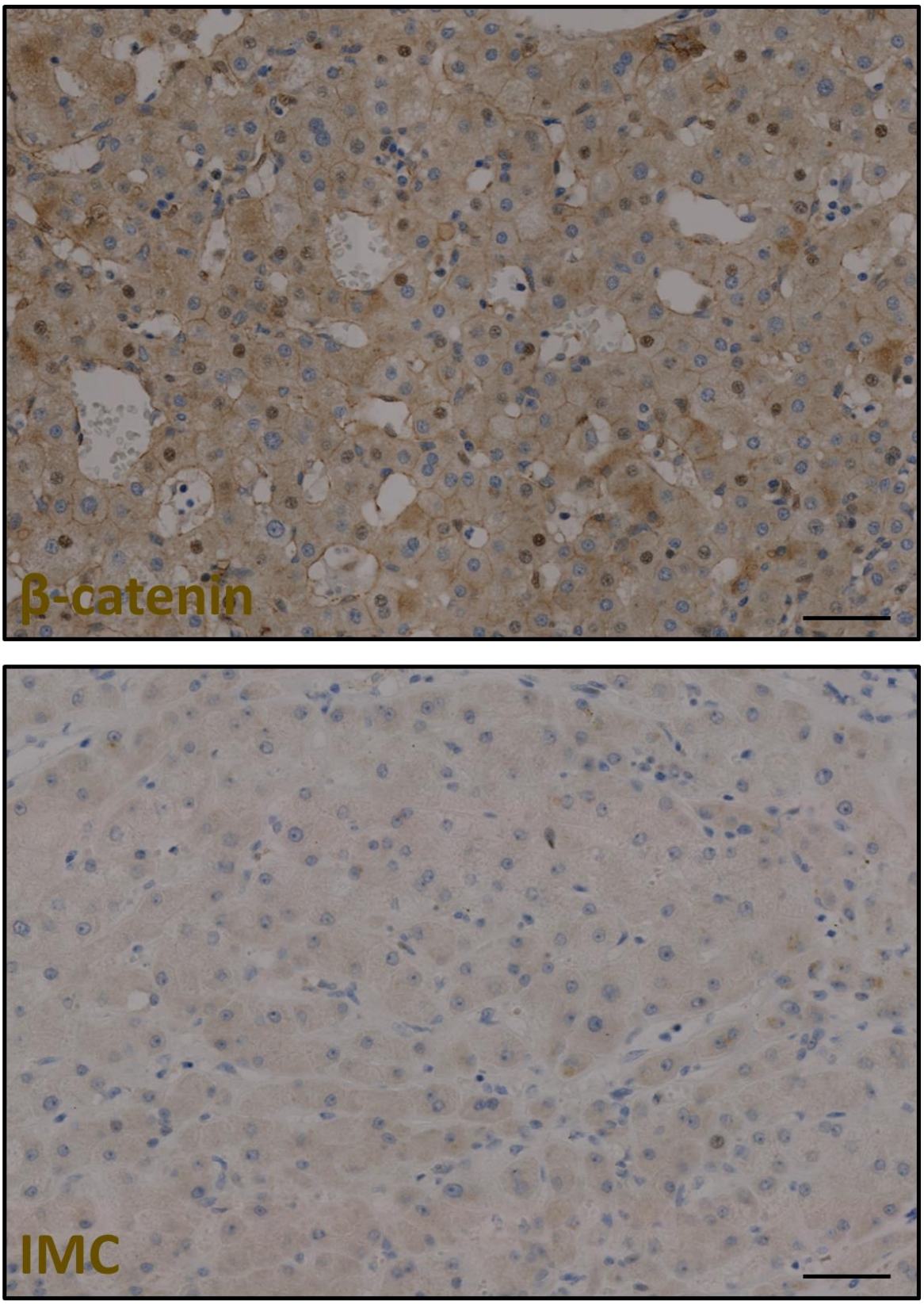

Figure A3: Isotyped matched control (IMC) immunohistochemistry staining of donor human liver for β-catenin. Immunohistochemistry (IHC) staining of paraffin-embedded normal donor liver tissue for β-catenin IMC (Mouse IgG1 - brown). Tissues were counterstained with Mayers haematoxylin nuclear stain (blue). Scale bars represent 100 µm. Corresponding stain: **Figure 5Hii**.

Bibliography

1. Davies SP, Reynolds GM, Stamataki Z. Clearance of Apoptotic Cells by Tissue Epithelia: A Putative Role for Hepatocytes in Liver Efferocytosis. Frontiers in immunology. 2018;9:44.
2. Abdel-Misih SR, Bloomston M. Liver anatomy. The Surgical clinics of North America. 2010;90(4):643-53.
3. Si-Tayeb K, Lemaigre FP, Duncan SA. Organogenesis and development of the liver. Developmental cell. 2010;18(2):175-89.
4. Lalor PF, Adams DH. The liver: a model of organ-specific lymphocyte recruitment. Expert Rev Mol Med. 2002;4(2):1-16.
5. Lalor PF, Lai WK, Curbishley SM, Shetty S, Adams DH. Human hepatic sinusoidal endothelial cells can be distinguished by expression of phenotypic markers related to their specialised functions in vivo. World J Gastroenterol. 2006;12(34):5429-39.
6. Lalor PF, Shields P, Grant A, Adams DH. Recruitment of lymphocytes to the human liver. Immunol Cell Biol. 2002;80(1):52-64.
7. Shetty S, Lalor PF, Adams DH. Lymphocyte recruitment to the liver: molecular insights into the pathogenesis of liver injury and hepatitis. Toxicology. 2008;254(3):136-46.
8. Shetty S, Weston CJ, Oo YH, Westerlund N, Stamataki Z, Youster J, et al. Common lymphatic endothelial and vascular endothelial receptor-1 mediates the transmigration of regulatory T cells across human hepatic sinusoidal endothelium. Journal of immunology (Baltimore, Md : 1950). 2011;186(7):4147-55.
9. Crispe IN. Hepatic T cells and liver tolerance. Nature reviews Immunology. 2003;3(1):51-62.
10. Crispe IN. Immune tolerance in liver disease. Hepatology (Baltimore, Md). 2014;60(6):2109-17.
11. Ezzelarab M, Thomson AW. Tolerogenic dendritic cells and their role in transplantation. Seminars in immunology. 2011;23(4):252-63.
12. Matta BM, Raimondi G, Rosborough BR, Sumpter TL, Thomson AW. IL-27 production and STAT3-dependent upregulation of B7-H1 mediate immune regulatory functions of liver plasmacytoid dendritic cells. Journal of immunology (Baltimore, Md : 1950). 2012;188(11):5227-37.
13. Liu H, Bakthavatsalam R, Meng Z, Li Z, Li W, Perkins JD, et al. PD-L1 signal on liver dendritic cells is critical for Foxp3(+)CD4(+)CD25(+) Treg and liver tolerance induction in mice. Transplantation proceedings. 2013;45(5):1853-5.
14. Wu K, Kryczek I, Chen L, Zou W, Welling TH. Kupffer cell suppression of CD8+ T cells in human hepatocellular carcinoma is mediated by B7-H1/programmed death-1 interactions. Cancer Res. 2009;69(20):8067-75.
15. Zhang M, Xu S, Han Y, Cao X. Apoptotic cells attenuate fulminant hepatitis by priming Kupffer cells to produce interleukin-10 through membrane-bound TGF-beta. Hepatology (Baltimore, Md). 2011;53(1):306-16.
16. Higashitani K, Kanto T, Kuroda S, Yoshio S, Matsubara T, Kakita N, et al. Association of enhanced activity of indoleamine 2,3-dioxygenase in dendritic cells with the induction of regulatory T cells in chronic hepatitis C infection. Journal of gastroenterology. 2013;48(5):660-70.

17. Yan ML, Wang YD, Tian YF, Lai ZD, Yan LN. Inhibition of allogeneic T-cell response by Kupffer cells expressing indoleamine 2,3-dioxygenase. World J Gastroenterol. 2010;16(5):636-40.
18. Fallarino F, Grohmann U, Hwang KW, Orabona C, Vacca C, Bianchi R, et al. Modulation of tryptophan catabolism by regulatory T cells. Nature immunology. 2003;4(12):1206-12.
19. Mezrich JD, Fechner JH, Zhang X, Johnson BP, Burlingham WJ, Bradfield CA. An interaction between kynurenine and the aryl hydrocarbon receptor can generate regulatory T cells. Journal of immunology (Baltimore, Md : 1950). 2010;185(6):3190-8.
20. Crispe IN. Liver antigen-presenting cells. Journal of hepatology. 2011;54(2):357-65.
21. Bertolino P, Bowen DG, McCaughan GW, Fazekas de St Groth B. Antigen-specific primary activation of CD8+ T cells within the liver. Journal of immunology (Baltimore, Md : 1950). 2001;166(9):5430-8.
22. Sun Z, Wada T, Maemura K, Uchikura K, Hoshino S, Diehl AM, et al. Hepatic allograft-derived Kupffer cells regulate T cell response in rats. Liver transplantation : official publication of the American Association for the Study of Liver Diseases and the International Liver Transplantation Society. 2003;9(5):489-97.
23. Rosin A, Doljanski L. Erythrocytes in the cytoplsm and nuclei of liver cells. Br J Exp Pathol. 1944;25(4):111-5.
24. Crispe IN, Dao T, Klugewitz K, Mehal WZ, Metz DP. The liver as a site of T-cell apoptosis: graveyard, or killing field? Immunological reviews. 2000;174:47-62.
25. Crispe IN, Huang L. Neonatal, moribund and undead T cells: the role of the liver in T cell development. Seminars in immunology. 1994;6(1):39-41.
26. Huang L, Soldevila G, Leeker M, Flavell R, Crispe IN. The liver eliminates T cells undergoing antigen-triggered apoptosis in vivo. Immunity. 1994;1(9):741-9.
27. Crispe IN. Death and destruction of activated T lymphocytes. Immunologic research. 1999;19(2-3):143-57.
28. John B, Crispe IN. Passive and active mechanisms trap activated CD8+ T cells in the liver. Journal of immunology (Baltimore, Md : 1950). 2004;172(9):5222-9.
29. Huang L, Sye K, Crispe IN. Proliferation and apoptosis of B220+CD4-CD8-TCR alpha beta intermediate T cells in the liver of normal adult mice: implication for lpr pathogenesis. International immunology. 1994;6(4):533-40.
30. Guguen-Guillouzo C, Guillouzo A. General review on in vitro hepatocyte models and their applications. Methods Mol Biol. 2010;640:1-40.
31. Michalopoulos GK. Liver regeneration. Journal of cellular physiology. 2007;213(2):286-300.
32. Fausto N, Campbell JS. The role of hepatocytes and oval cells in liver regeneration and repopulation. Mechanisms of development. 2003;120(1):117-30.
33. Tannuri AC, Tannuri U, Coelho MC, Santos NA, Mello ES. Experimental models of hepatectomy and liver regeneration using newborn and weaning rats. Clinics (Sao Paulo, Brazil). 2007;62(6):757-62.
34. Sakamoto T, Liu Z, Murase N, Ezure T, Yokomuro S, Poli V, et al. Mitosis and apoptosis in the liver of interleukin-6-deficient mice after partial hepatectomy. Hepatology (Baltimore, Md). 1999;29(2):403-11.
35. Hijmans BS, Grefhorst A, Oosterveer MH, Groen AK. Zonation of glucose and fatty acid metabolism in the liver: mechanism and metabolic consequences. Biochimie. 2014;96:121-9.

36. Burke ZD, Tosh D. The Wnt/beta-catenin pathway: master regulator of liver zonation? BioEssays : news and reviews in molecular, cellular and developmental biology. 2006;28(11):1072-7.
37. Leu JI, Crissey MA, Craig LE, Taub R. Impaired hepatocyte DNA synthetic response posthepatectomy in insulin-like growth factor binding protein 1-deficient mice with defects in C/EBP beta and mitogen-activated protein kinase/extracellular signal-regulated kinase regulation. Mol Cell Biol. 2003;23(4):1251-9.
38. Rabes HM. Kinetics of hepatocellular proliferation as a function of the microvascular structure and functional state of the liver. Ciba Foundation symposium. 1977(55):31-53.
39. Birchmeier W. Orchestrating Wnt signalling for metabolic liver zonation. Nat Cell Biol. 2016;18(5):463-5.
40. Planas-Paz L, Orsini V, Boulter L, Calabrese D, Pikiolek M, Nigsch F, et al. The RSPO-LGR4/5-ZNRF3/RNF43 module controls liver zonation and size. Nat Cell Biol. 2016;18(5):467-79.
41. Haruyama T, Ajioka I, Akaike T, Watanabe Y. Regulation and significance of hepatocyte-derived matrix metalloproteinases in liver remodeling. Biochemical and biophysical research communications. 2000;272(3):681-6.
42. Webber EM, Wu JC, Wang L, Merlino G, Fausto N. Overexpression of transforming growth factor-alpha causes liver enlargement and increased hepatocyte proliferation in transgenic mice. The American journal of pathology. 1994;145(2):398-408.
43. Meijer C, Wiezer MJ, Diehl AM, Schouten HJ, Schouten HJ, Meijer S, et al. Kupffer cell depletion by CI2MDP-liposomes alters hepatic cytokine expression and delays liver regeneration after partial hepatectomy. Liver. 2000;20(1):66-77.
44. Abshagen K, Eipel C, Kalff JC, Menger MD, Vollmar B. Loss of NF-kappaB activation in Kupffer cell-depleted mice impairs liver regeneration after partial hepatectomy. American journal of physiology Gastrointestinal and liver physiology. 2007;292(6):G1570-7.
45. Campana L, Starkey Lewis PJ, Pellicoro A, Aucott RL, Man J, O'Duibhir E, et al. The STAT3-IL-10-IL-6 Pathway Is a Novel Regulator of Macrophage Efferocytosis and Phenotypic Conversion in Sterile Liver Injury. Journal of immunology (Baltimore, Md : 1950). 2018;200(3):1169-87.
46. Fausto N. Liver regeneration. Journal of hepatology. 2000;32(1 Suppl):19-31.
47. Greenbaum LE, Cressman DE, Haber BA, Taub R. Coexistence of C/EBP alpha, beta, growth-induced proteins and DNA synthesis in hepatocytes during liver regeneration. Implications for maintenance of the differentiated state during liver growth. The Journal of clinical investigation. 1995;96(3):1351-65.
48. Crispe IN. Hepatocytes as Immunological Agents. Journal of immunology (Baltimore, Md : 1950). 2016;196(1):17-21.
49. Zhou Z, Xu MJ, Gao B. Hepatocytes: a key cell type for innate immunity. Cellular & molecular immunology. 2016;13(3):301-15.
50. He XS, Nanda S, Ji X, Calderon-Rodriguez GM, Greenberg HB, Liang TJ. Differential transcriptional responses to interferon-alpha and interferon-gamma in primary human hepatocytes. Journal of interferon & cytokine research : the official journal of the International Society for Interferon and Cytokine Research. 2010;30(5):311-20.
51. Castell JV, Gomez-Lechon MJ, David M, Hirano T, Kishimoto T, Heinrich PC. Recombinant human interleukin-6 (IL-6/BSF-2/HSF) regulates the synthesis of acute phase proteins in human hepatocytes. FEBS letters. 1988;232(2):347-50.
52. Bode JG, Albrecht U, Haussinger D, Heinrich PC, Schaper F. Hepatic acute phase proteins--regulation by IL-6- and IL-1-type cytokines involving STAT3 and its crosstalk with NF-kappaB-dependent signaling. European journal of cell biology. 2012;91(6-7):496-505.

53. Zhang N, Ahsan MH, Purchio AF, West DB. Serum amyloid A-luciferase transgenic mice: response to sepsis, acute arthritis, and contact hypersensitivity and the effects of proteasome inhibition. Journal of immunology (Baltimore, Md : 1950). 2005;174(12):8125-34.
54. Uhlar CM, Whitehead AS. Serum amyloid A, the major vertebrate acute-phase reactant. European journal of biochemistry. 1999;265(2):501-23.
55. Vodovotz Y, Liu S, McCloskey C, Shapiro R, Green A, Billiar TR. The hepatocyte as a microbial product-responsive cell. Journal of endotoxin research. 2001;7(5):365-73.
56. Galloway E, Shin T, Huber N, Eismann T, Kuboki S, Schuster R, et al. Activation of hepatocytes by extracellular heat shock protein 72. American journal of physiology Cell physiology. 2008;295(2):C514-20.
57. Foy E, Li K, Sumpter R, Jr., Loo YM, Johnson CL, Wang C, et al. Control of antiviral defenses through hepatitis C virus disruption of retinoic acid-inducible gene-I signaling. Proceedings of the National Academy of Sciences of the United States of America. 2005;102(8):2986-91.
58. Ishikawa H, Barber GN. STING is an endoplasmic reticulum adaptor that facilitates innate immune signalling. Nature. 2008;455(7213):674-8.
59. Guo F, Tang L, Shu S, Sehgal M, Sheraz M, Liu B, et al. Activation of Stimulator of Interferon Genes in Hepatocytes Suppresses the Replication of Hepatitis B Virus. Antimicrobial agents and chemotherapy. 2017;61(10).
60. Wu J, Meng Z, Jiang M, Pei R, Trippler M, Broering R, et al. Hepatitis B virus suppresses toll-like receptor-mediated innate immune responses in murine parenchymal and nonparenchymal liver cells. Hepatology (Baltimore, Md). 2009;49(4):1132-40.
61. Liu Y, Li J, Chen J, Li Y, Wang W, Du X, et al. Hepatitis B virus polymerase disrupts K63-linked ubiquitination of STING to block innate cytosolic DNA-sensing pathways. Journal of virology. 2015;89(4):2287-300.
62. Ferreon JC, Ferreon AC, Li K, Lemon SM. Molecular determinants of TRIF proteolysis mediated by the hepatitis C virus NS3/4A protease. J Biol Chem. 2005;280(21):20483-92.
63. Yu S, Chen J, Wu M, Chen H, Kato N, Yuan Z. Hepatitis B virus polymerase inhibits RIG-I- and Toll-like receptor 3-mediated beta interferon induction in human hepatocytes through interference with interferon regulatory factor 3 activation and dampening of the interaction between TBK1/IKKepsilon and DDX3. The Journal of general virology. 2010;91(Pt 8):2080-90.
64. Herkel J, Jagemann B, Wiegard C, Lazaro JF, Lueth S, Kanzler S, et al. MHC class II-expressing hepatocytes function as antigen-presenting cells and activate specific CD4 T lymphocyutes. Hepatology (Baltimore, Md). 2003;37(5):1079-85.
65. Chen M, Tabaczewski P, Truscott SM, Van Kaer L, Stroynowski I. Hepatocytes express abundant surface class I MHC and efficiently use transporter associated with antigen processing, tapasin, and low molecular weight polypeptide proteasome subunit components of antigen processing and presentation pathway. Journal of immunology (Baltimore, Md : 1950). 2005;175(2):1047-55.
66. Bertolino P, Trescol-Biemont MC, Rabourdin-Combe C. Hepatocytes induce functional activation of naive CD8+ T lymphocytes but fail to promote survival. European journal of immunology. 1998;28(1):221-36.
67. Bertolino P, Trescol-Biemont MC, Thomas J, Fazekas de St Groth B, Pihlgren M, Marvel J, et al. Death by neglect as a deletional mechanism of peripheral tolerance. International immunology. 1999;11(8):1225-38.
68. Muhlbauer M, Fleck M, Schutz C, Weiss T, Froh M, Blank C, et al. PD-L1 is induced in hepatocytes by viral infection and by interferon-alpha and -gamma and mediates T cell apoptosis. Journal of hepatology. 2006;45(4):520-8.

69. Levy G, Bomze D, Heinz S, Ramachandran SD, Noerenberg A, Cohen M, et al. Long-term culture and expansion of primary human hepatocytes. Nature Biotechnology. 2015;33:1264.
70. Block GD, Locker J, Bowen WC, Petersen BE, Katyal S, Strom SC, et al. Population expansion, clonal growth, and specific differentiation patterns in primary cultures of hepatocytes induced by HGF/SF, EGF and TGF alpha in a chemically defined (HGM) medium. J Cell Biol. 1996;132(6):1133-49.
71. Olsavsky KM, Page JL, Johnson MC, Zarbl H, Strom SC, Omiecinski CJ. Gene expression profiling and differentiation assessment in primary human hepatocyte cultures, established hepatoma cell lines, and human liver tissues. Toxicology and applied pharmacology. 2007;222(1):42-56.
72. Liu K, Shi Y, Guo XH, Ouyang YB, Wang SS, Liu DJ, et al. Phosphorylated AKT inhibits the apoptosis induced by DRAM-mediated mitophagy in hepatocellular carcinoma by preventing the translocation of DRAM to mitochondria. Cell Death Dis. 2014;5:e1078.
73. Bressac B, Galvin KM, Liang TJ, Isselbacher KJ, Wands JR, Ozturk M. Abnormal structure and expression of p53 gene in human hepatocellular carcinoma. Proceedings of the National Academy of Sciences of the United States of America. 1990;87(5):1973-7.
74. Hsu IC, Tokiwa T, Bennett W, Metcalf RA, Welsh JA, Sun T, et al. p53 gene mutation and integrated hepatitis B viral DNA sequences in human liver cancer cell lines. Carcinogenesis. 1993;14(5):987-92.
75. Blight KJ, McKeating JA, Rice CM. Highly permissive cell lines for subgenomic and genomic hepatitis C virus RNA replication. Journal of virology. 2002;76(24):13001-14.
76. Michailidis E, Pabon J, Xiang K, Park P, Ramanan V, Hoffmann HH, et al. A robust cell culture system supporting the complete life cycle of hepatitis B virus. Scientific reports. 2017;7(1):16616.
77. Arandjelovic S, Ravichandran KS. Phagocytosis of apoptotic cells in homeostasis. Nature immunology. 2015;16(9):907-17.
78. Franz S, Herrmann K, Furnrohr BG, Sheriff A, Frey B, Gaipl US, et al. After shrinkage apoptotic cells expose internal membrane-derived epitopes on their plasma membranes. Cell death and differentiation. 2007;14(4):733-42.
79. Poon IK, Hulett MD, Parish CR. Molecular mechanisms of late apoptotic/necrotic cell clearance. Cell death and differentiation. 2010;17(3):381-97.
80. Green DR, Oguin TH, Martinez J. The clearance of dying cells: table for two. Cell death and differentiation. 2016;23(6):915-26.
81. Ravichandran KS. Beginnings of a good apoptotic meal: the find-me and eat-me signaling pathways. Immunity. 2011;35(4):445-55.
82. Medina CB, Ravichandran KS. Do not let death do us part: 'find-me' signals in communication between dying cells and the phagocytes. Cell death and differentiation. 2016;23(6):979-89.
83. Elliott MR, Chekeni FB, Trampont PC, Lazarowski ER, Kadl A, Walk SF, et al. Nucleotides released by apoptotic cells act as a find-me signal to promote phagocytic clearance. Nature. 2009;461(7261):282-6.
84. Gude DR, Alvarez SE, Paugh SW, Mitra P, Yu J, Griffiths R, et al. Apoptosis induces expression of sphingosine kinase 1 to release sphingosine-1-phosphate as a "come-and-get-me" signal. FASEB journal : official publication of the Federation of American Societies for Experimental Biology. 2008;22(8):2629-38.
85. Truman LA, Ford CA, Pasikowska M, Pound JD, Wilkinson SJ, Dumitriu IE, et al. CX3CL1/fractalkine is released from apoptotic lymphocytes to stimulate macrophage chemotaxis. Blood. 2008;112(13):5026-36.

86. Li MO, Sarkisian MR, Mehal WZ, Rakic P, Flavell RA. Phosphatidylserine receptor is required for clearance of apoptotic cells. Science (New York, NY). 2003;302(5650):1560-3.
87. Penberthy KK, Ravichandran KS. Apoptotic cell recognition receptors and scavenger receptors. Immunological reviews. 2016;269(1):44-59.
88. Salvayre R, Auge N, Benoist H, Negre-Salvayre A. Oxidized low-density lipoprotein-induced apoptosis. Biochimica et biophysica acta. 2002;1585(2-3):213-21.
89. Sambrano GR, Steinberg D. Recognition of oxidatively damaged and apoptotic cells by an oxidized low density lipoprotein receptor on mouse peritoneal macrophages: role of membrane phosphatidylserine. Proceedings of the National Academy of Sciences of the United States of America. 1995;92(5):1396-400.
90. Gregory CD, Devitt A, Moffatt O. Roles of ICAM-3 and CD14 in the recognition and phagocytosis of apoptotic cells by macrophages. Biochem Soc Trans. 1998;26(4):644-9.
91. Marques-da-Silva C, Burnstock G, Ojcius DM, Coutinho-Silva R. Purinergic receptor agonists modulate phagocytosis and clearance of apoptotic cells in macrophages. Immunobiology. 2011;216(1-2):1-11.
92. Jaiswal S, Jamieson CH, Pang WW, Park CY, Chao MP, Majeti R, et al. CD47 is upregulated on circulating hematopoietic stem cells and leukemia cells to avoid phagocytosis. Cell. 2009;138(2):271-85.
93. Tsai RK, Discher DE. Inhibition of "self" engulfment through deactivation of myosin-II at the phagocytic synapse between human cells. J Cell Biol. 2008;180(5):989-1003.
94. Flusberg DA, Sorger PK. Surviving apoptosis: life-death signaling in single cells. Trends in cell biology. 2015;25(8):446-58.
95. Lawrence T, Willoughby DA, Gilroy DW. Anti-inflammatory lipid mediators and insights into the resolution of inflammation. Nature reviews Immunology. 2002;2(10):787-95.
96. Trump BF, Berezesky IK, Chang SH, Phelps PC. The pathways of cell death: oncosis, apoptosis, and necrosis. Toxicologic pathology. 1997;25(1):82-8.
97. Schwegler M, Wirsing AM, Dollinger AJ, Abendroth B, Putz F, Fietkau R, et al. Clearance of primary necrotic cells by non-professional phagocytes. Biol Cell. 2015.
98. Brouckaert G, Kalai M, Krysko DV, Saelens X, Vercammen D, Ndlovu MN, et al. Phagocytosis of necrotic cells by macrophages is phosphatidylserine dependent and does not induce inflammatory cytokine production. Mol Biol Cell. 2004;15(3):1089-100.
99. Hirt UA, Leist M. Rapid, noninflammatory and PS-dependent phagocytic clearance of necrotic cells. Cell death and differentiation. 2003;10(10):1156-64.
100. Ellis RE, Jacobson DM, Horvitz HR. Genes required for the engulfment of cell corpses during programmed cell death in Caenorhabditis elegans. Genetics. 1991;129(1):79-94.
101. Hedgecock EM, Sulston JE, Thomson JN. Mutations affecting programmed cell deaths in the nematode Caenorhabditis elegans. Science (New York, NY). 1983;220(4603):1277-9.
102. Reddien PW, Horvitz HR. CED-2/CrkII and CED-10/Rac control phagocytosis and cell migration in Caenorhabditis elegans. Nat Cell Biol. 2000;2(3):131-6.
103. Wu YC, Horvitz HR. C. elegans phagocytosis and cell-migration protein CED-5 is similar to human DOCK180. Nature. 1998;392(6675):501-4.
104. Gumienny TL, Brugnera E, Tosello-Trampont AC, Kinchen JM, Haney LB, Nishiwaki K, et al. CED-12/ELMO, a novel member of the CrkII/Dock180/Rac pathway, is required for phagocytosis and cell migration. Cell. 2001;107(1):27-41.
105. Park D, Tosello-Trampont AC, Elliott MR, Lu M, Haney LB, Ma Z, et al. BAI1 is an engulfment receptor for apoptotic cells upstream of the ELMO/Dock180/Rac module. Nature. 2007;450(7168):430-4.

106. Gillooly DJ, Simonsen A, Stenmark H. Phosphoinositides and phagocytosis. The Journal of Cell Biology. 2001;155(1):15-8.
107. Araki N, Johnson MT, Swanson JA. A role for phosphoinositide 3-kinase in the completion of macropinocytosis and phagocytosis by macrophages. The Journal of Cell Biology. 1996;135(5):1249-60.
108. Vieira OV, Botelho RJ, Rameh L, Brachmann SM, Matsuo T, Davidson HW, et al. Distinct roles of class I and class III phosphatidylinositol 3-kinases in phagosome formation and maturation. J Cell Biol. 2001;155(1):19-25.
109. Schlam D, Bagshaw RD, Freeman SA, Collins RF, Pawson T, Fairn GD, et al. Phosphoinositide 3-kinase enables phagocytosis of large particles by terminating actin assembly through Rac/Cdc42 GTPase-activating proteins. Nature communications. 2015;6:8623.
110. Vieira OV, Bucci C, Harrison RE, Trimble WS, Lanzetti L, Gruenberg J, et al. Modulation of Rab5 and Rab7 Recruitment to Phagosomes by Phosphatidylinositol 3-Kinase. Molecular and Cellular Biology. 2003;23(7):2501-14.
111. Florey O, Kim SE, Sandoval CP, Haynes CM, Overholtzer M. Autophagy machinery mediates macroendocytic processing and entotic cell death by targeting single membranes. Nat Cell Biol. 2011;13(11):1335-43.
112. Martinez J, Almendinger J, Oberst A, Ness R, Dillon CP, Fitzgerald P, et al. Microtubule-associated protein 1 light chain 3 alpha (LC3)-associated phagocytosis is required for the efficient clearance of dead cells. Proceedings of the National Academy of Sciences of the United States of America. 2011;108(42):17396-401.
113. Florey O, Overholtzer M. Autophagy proteins in macroendocytic engulfment. Trends in cell biology. 2012;22(7):374-80.
114. Parnaik R, Raff MC, Scholes J. Differences between the clearance of apoptotic cells by professional and non-professional phagocytes. Curr Biol. 2000;10(14):857-60.
115. Wood W, Turmaine M, Weber R, Camp V, Maki RA, McKercher SR, et al. Mesenchymal cells engulf and clear apoptotic footplate cells in macrophageless PU.1 null mouse embryos. Development (Cambridge, England). 2000;127(24):5245-52.
116. Juncadella IJ, Kadl A, Sharma AK, Shim YM, Hochreiter-Hufford A, Borish L, et al. Apoptotic cell clearance by bronchial epithelial cells critically influences airway inflammation. Nature. 2013;493(7433):547-51.
117. Penberthy KK, Juncadella IJ, Ravichandran KS. Apoptosis and engulfment by bronchial epithelial cells. Implications for allergic airway inflammation. Annals of the American Thoracic Society. 2014;11 Suppl 5:S259-62.
118. Han CZ, Juncadella IJ, Kinchen JM, Buckley MW, Klibanov AL, Dryden K, et al. Macrophages redirect phagocytosis by non-professional phagocytes and influence inflammation. Nature. 2016;539(7630):570-4.
119. Ryeom SW, Sparrow JR, Silverstein RL. CD36 participates in the phagocytosis of rod outer segments by retinal pigment epithelium. Journal of cell science. 1996;109 (Pt 2):387-95.
120. Irschick EU, Sgonc R, Bock G, Wolf H, Fuchs D, Nussbaumer W, et al. Retinal pigment epithelial phagocytosis and metabolism differ from those of macrophages. Ophthalmic research. 2004;36(4):200-10.
121. Mellen MA, de la Rosa EJ, Boya P. The autophagic machinery is necessary for removal of cell corpses from the developing retinal neuroepithelium. Cell death and differentiation. 2008;15(8):1279-90.

122. Nandrot EF, Anand M, Almeida D, Atabai K, Sheppard D, Finnemann SC. Essential role for MFG-E8 as ligand for alphavbeta5 integrin in diurnal retinal phagocytosis. Proceedings of the National Academy of Sciences of the United States of America. 2007;104(29):12005-10.
123. Caberoy NB, Zhou Y, Li W. Tubby and tubby-like protein 1 are new MerTK ligands for phagocytosis. Embo j. 2010;29(23):3898-910.
124. Sexton DW, Blaylock MG, Walsh GM. Human alveolar epithelial cells engulf apoptotic eosinophils by means of integrin- and phosphatidylserine receptor-dependent mechanisms: a process upregulated by dexamethasone. The Journal of allergy and clinical immunology. 2001;108(6):962-9.
125. Lee CS, Penberthy KK, Wheeler KM, Juncadella IJ, Vandenabeele P, Lysiak JJ, et al. Boosting Apoptotic Cell Clearance by Colonic Epithelial Cells Attenuates Inflammation In Vivo. Immunity. 2016;44(4):807-20.
126. Lu Z, Elliott MR, Chen Y, Walsh JT, Klibanov AL, Ravichandran KS, et al. Phagocytic activity of neuronal progenitors regulates adult neurogenesis. Nat Cell Biol. 2011;13(9):1076-83.
127. Poon IK, Lucas CD, Rossi AG, Ravichandran KS. Apoptotic cell clearance: basic biology and therapeutic potential. Nature reviews Immunology. 2014;14(3):166-80.
128. Szondy Z, Garabuczi É, Joós G, Tsay GJ, Sarang Z. Impaired Clearance of Apoptotic Cells in Chronic Inflammatory Diseases: Therapeutic Implications. Frontiers in immunology. 2014;5:354.
129. Weinger JG, Brosnan CF, Loudig O, Goldberg MF, Macian F, Arnett HA, et al. Loss of the receptor tyrosine kinase Axl leads to enhanced inflammation in the CNS and delayed removal of myelin debris during experimental autoimmune encephalomyelitis. Journal of neuroinflammation. 2011;8:49.
130. Ramirez-Ortiz ZG, Pendergraft WF, 3rd, Prasad A, Byrne MH, Iram T, Blanchette CJ, et al. The scavenger receptor SCARF1 mediates the clearance of apoptotic cells and prevents autoimmunity. Nature immunology. 2013;14(9):917-26.
131. Bosurgi L, Bernink JH, Delgado Cuevas V, Gagliani N, Joannas L, Schmid ET, et al. Paradoxical role of the proto-oncogene Axl and Mer receptor tyrosine kinases in colon cancer. Proceedings of the National Academy of Sciences of the United States of America. 2013;110(32):13091-6.
132. Tian L, Choi SC, Murakami Y, Allen J, Morse HC, 3rd, Qi CF, et al. p85alpha recruitment by the CD300f phosphatidylserine receptor mediates apoptotic cell clearance required for autoimmunity suppression. Nature communications. 2014;5:3146.
133. Tian L, Choi SC, Lee HN, Murakami Y, Qi CF, Sengottuvelu M, et al. Enhanced efferocytosis by dendritic cells underlies memory T-cell expansion and susceptibility to autoimmune disease in CD300f-deficient mice. Cell death and differentiation. 2016;23(6):1086-96.
134. Hodge S, Hodge G, Scicchitano R, Reynolds PN, Holmes M. Alveolar macrophages from subjects with chronic obstructive pulmonary disease are deficient in their ability to phagocytose apoptotic airway epithelial cells. Immunol Cell Biol. 2003;81(4):289-96.
135. Vandivier RW, Fadok VA, Hoffmann PR, Bratton DL, Penvari C, Brown KK, et al. Elastase-mediated phosphatidylserine receptor cleavage impairs apoptotic cell clearance in cystic fibrosis and bronchiectasis. The Journal of clinical investigation. 2002;109(5):661-70.
136. Chao MP, Alizadeh AA, Tang C, Jan M, Weissman-Tsukamoto R, Zhao F, et al. Therapeutic antibody targeting of CD47 eliminates human acute lymphoblastic leukemia. Cancer Res. 2011;71(4):1374-84.

137. Majeti R, Chao MP, Alizadeh AA, Pang WW, Jaiswal S, Gibbs KD, Jr., et al. CD47 is an adverse prognostic factor and therapeutic antibody target on human acute myeloid leukemia stem cells. Cell. 2009;138(2):286-99.
138. Kojima Y, Volkmer JP, McKenna K, Civelek M, Lusis AJ, Miller CL, et al. CD47-blocking antibodies restore phagocytosis and prevent atherosclerosis. Nature. 2016;536(7614):86-90.
139. Krysko DV, D'Herde K, Vandenabeele P. Clearance of apoptotic and necrotic cells and its immunological consequences. Apoptosis : an international journal on programmed cell death. 2006;11(10):1709-26.
140. Ji H, Liu Y, Zhang Y, Shen XD, Gao F, Busuttil RW, et al. T-cell immunoglobulin and mucin domain 4 (TIM-4) signaling in innate immune-mediated liver ischemia-reperfusion injury. Hepatology (Baltimore, Md). 2014;60(6):2052-64.
141. Tacke F. Targeting hepatic macrophages to treat liver diseases. Journal of hepatology. 2017;66(6):1300-12.
142. Canbay A, Taimr P, Torok N, Higuchi H, Friedman S, Gores GJ. Apoptotic body engulfment by a human stellate cell line is profibrogenic. Laboratory investigation; a journal of technical methods and pathology. 2003;83(5):655-63.
143. Rong GH, Yang GX, Ando Y, Zhang W, He XS, Leung PS, et al. Human intrahepatic biliary epithelial cells engulf blebs from their apoptotic peers. Clinical and experimental immunology. 2013;172(1):95-103.
144. Lee SJ, Park SY, Jung MY, Bae SM, Kim IS. Mechanism for phosphatidylserine-dependent erythrophagocytosis in mouse liver. Blood. 2011;117(19):5215-23.
145. Patten DA, Kamarajah SK, Rose JM, Tickle J, Shepherd EL, Adams DH, et al. SCARF-1 promotes adhesion of CD4(+) T cells to human hepatic sinusoidal endothelium under conditions of shear stress. Scientific reports. 2017;7(1):17600.
146. Soji T, Murata Y, Ohira A, Nishizono H, Tanaka M, Herbert DC. Evidence that hepatocytes can phagocytize exogenous substances. The Anatomical record. 1992;233(4):543-6.
147. Dini L, Autuori F, Lentini A, Oliverio S, Piacentini M. The clearance of apoptotic cells in the liver is mediated by the asialoglycoprotein receptor. FEBS letters. 1992;296(2):174-8.
148. Triantafyllou E, Pop OT, Possamai LA, Wilhelm A, Liaskou E, Singanayagam A, et al. MerTK expressing hepatic macrophages promote the resolution of inflammation in acute liver failure. Gut. 2017.
149. Wang X, Bu HF, Zhong W, Asai A, Zhou Z, Tan XD. MFG-E8 and HMGB1 are involved in the mechanism underlying alcohol-induced impairment of macrophage efferocytosis. Molecular medicine (Cambridge, Mass). 2013;19:170-82.
150. Casey CA, McVicker BL, Donohue TM, Jr., McFarland MA, Wiegert RL, Nanji AA. Liver asialoglycoprotein receptor levels correlate with severity of alcoholic liver damage in rats. Journal of applied physiology (Bethesda, Md : 1985). 2004;96(1):76-80.
151. Wu CT, Davis PA, Luketic VA, Gershwin ME. A review of the physiological and immunological functions of biliary epithelial cells: targets for primary biliary cirrhosis, primary sclerosing cholangitis and drug-induced ductopenias. Clinical & developmental immunology. 2004;11(3-4):205-13.
152. Czaja AJ. Targeting apoptosis in autoimmune hepatitis. Digestive diseases and sciences. 2014;59(12):2890-904.
153. Fox CK, Furtwaengler A, Nepomuceno RR, Martinez OM, Krams SM. Apoptotic pathways in primary biliary cirrhosis and autoimmune hepatitis. Liver. 2001;21(4):272-9.
154. Henson PM, Hume DA. Apoptotic cell removal in development and tissue homeostasis. Trends in immunology. 2006;27(5):244-50.

155. N AG, Bensinger SJ, Hong C, Beceiro S, Bradley MN, Zelcer N, et al. Apoptotic cells promote their own clearance and immune tolerance through activation of the nuclear receptor LXR. Immunity. 2009;31(2):245-58.
156. Ana L, Carlo S, Pietro I, Mauro P, L. CR, R. MI, et al. Apotopes and the biliary specificity of primary biliary cirrhosis. Hepatology (Baltimore, Md). 2009;49(3):871-9.
157. Poralla T, Treichel U, Lohr H, Fleischer B. The asialoglycoprotein receptor as target structure in autoimmune liver diseases. Semin Liver Dis. 1991;11(3):215-22.
158. Raphael I, Nalawade S, Eagar TN, Forsthuber TG. T cell subsets and their signature cytokines in autoimmune and inflammatory diseases. Cytokine. 2015;74(1):5-17.
159. Laidlaw BJ, Craft JE, Kaech SM. The multifaceted role of CD4(+) T cells in CD8(+) T cell memory. Nature reviews Immunology. 2016;16(2):102-11.
160. Singh B, Schwartz JA, Sandrock C, Bellemore SM, Nikoopour E. Modulation of autoimmune diseases by interleukin (IL)-17 producing regulatory T helper (Th17) cells. The Indian journal of medical research. 2013;138(5):591-4.
161. Fontenot JD, Gavin MA, Rudensky AY. Foxp3 programs the development and function of CD4+CD25+ regulatory T cells. Nature immunology. 2003;4(4):330-6.
162. Roncarolo MG, Gregori S. Is FOXP3 a bona fide marker for human regulatory T cells? European journal of immunology. 2008;38(4):925-7.
163. Singer BD, King LS, D'Alessio FR. Regulatory T Cells as Immunotherapy. Frontiers in immunology. 2014;5:46.
164. Levine AG, Mendoza A, Hemmers S, Moltedo B, Niec RE, Schizas M, et al. Stability and function of regulatory T cells expressing the transcription factor T-bet. Nature. 2017;546(7658):421-5.
165. Swain SL, McKinstry KK, Strutt TM. Expanding roles for CD4(+) T cells in immunity to viruses. Nature reviews Immunology. 2012;12(2):136-48.
166. Dahan S, Roth-Walter F, Arnaboldi P, Agarwal S, Mayer L. Epithelia: lymphocyte interactions in the gut. Immunological reviews. 2007;215:10.1111/j.600-065X.2006.00484.x.
167. Hammad H, Lambrecht Bart N. Barrier Epithelial Cells and the Control of Type 2 Immunity. Immunity.43(1):29-40.
168. Woodruff PG, Boushey HA, Dolganov GM, Barker CS, Yang YH, Donnelly S, et al. Genome-wide profiling identifies epithelial cell genes associated with asthma and with treatment response to corticosteroids. Proceedings of the National Academy of Sciences of the United States of America. 2007;104(40):15858-63.
169. Kirby JA, Rajasekar MR, Lin Y, Proud G, Taylor RM. Interaction between T lymphocytes and kidney epithelial cells during renal allograft rejection. Kidney international Supplement. 1993;39:S124-8.
170. Gregerson DS, Heuss ND, Lew KL, McPherson SW, Ferrington DA. Interaction of retinal pigmented epithelial cells and CD4 T cells leads to T-cell anergy. Investigative ophthalmology & visual science. 2007;48(10):4654-63.
171. Cruickshank SM, McVay LD, Baumgart DC, Felsburg PJ, Carding SR. Colonic epithelial cell mediated suppression of CD4 T cell activation. Gut. 2004;53(5):678-84.
172. Olivares-Villagomez D, Algood HM, Singh K, Parekh VV, Ryan KE, Piazuelo MB, et al. Intestinal epithelial cells modulate CD4 T cell responses via the thymus leukemia antigen. Journal of immunology (Baltimore, Md : 1950). 2011;187(8):4051-60.
173. Campeau JL, Salim SY, Albert EJ, Hotte N, Madsen KL. Intestinal epithelial cells modulate antigen-presenting cell responses to bacterial DNA. Infection and immunity. 2012;80(8):2632-44.
174. Akitake-Kawano R, Seno H, Nakatsuji M, Kimura Y, Nakanishi Y, Yoshioka T, et al. Inhibitory role of Gas6 in intestinal tumorigenesis. Carcinogenesis. 2013;34(7):1567-74.

175. Ishidome T, Yoshida T, Hanayama R. Induction of Live Cell Phagocytosis by a Specific Combination of Inflammatory Stimuli. EBioMedicine. 2017;22:89-99.
176. Blazar BR, Lindberg FP, Ingulli E, Panoskaltsis-Mortari A, Oldenborg PA, Iizuka K, et al. CD47 (integrin-associated protein) engagement of dendritic cell and macrophage counterreceptors is required to prevent the clearance of donor lymphohematopoietic cells. The Journal of experimental medicine. 2001;194(4):541-9.
177. Janka GE. Familial and acquired hemophagocytic lymphohistiocytosis. Annual review of medicine. 2012;63:233-46.
178. Billiau AD, Roskams T, Van Damme-Lombaerts R, Matthys P, Wouters C. Macrophage activation syndrome: characteristic findings on liver biopsy illustrating the key role of activated, IFN-gamma-producing lymphocytes and IL-6- and TNF-alpha-producing macrophages. Blood. 2005;105(4):1648-51.
179. Grom AA, Horne A, De Benedetti F. Macrophage activation syndrome in the era of biologic therapy. Nature reviews Rheumatology. 2016;12(5):259-68.
180. Baxter AE, Russell RA, Duncan CJ, Moore MD, Willberg CB, Pablos JL, et al. Macrophage infection via selective capture of HIV-1-infected CD4+ T cells. Cell host & microbe. 2014;16(6):711-21.
181. Benseler V, Warren A, Vo M, Holz LE, Tay SS, Le Couteur DG, et al. Hepatocyte entry leads to degradation of autoreactive CD8 T cells. Proceedings of the National Academy of Sciences of the United States of America. 2011;108(40):16735-40.
182. Lugini L, Matarrese P, Tinari A, Lozupone F, Federici C, Iessi E, et al. Cannibalism of live lymphocytes by human metastatic but not primary melanoma cells. Cancer Res. 2006;66(7):3629-38.
183. Overholtzer M, Mailleux AA, Mouneimne G, Normand G, Schnitt SJ, King RW, et al. A nonapoptotic cell death process, entosis, that occurs by cell-in-cell invasion. Cell. 2007;131(5):966-79.
184. Overholtzer M, Brugge JS. The cell biology of cell-in-cell structures. Nat Rev Mol Cell Biol. 2008;9(10):796-809.
185. Krajcovic M, Johnson NB, Sun Q, Normand G, Hoover N, Yao E, et al. A non-genetic route to aneuploidy in human cancers. Nat Cell Biol. 2011;13(3):324-30.
186. Sun Q, Cibas ES, Huang H, Hodgson L, Overholtzer M. Induction of entosis by epithelial cadherin expression. Cell research. 2014;24(11):1288-98.
187. Wen S, Shang Z, Zhu S, Chang C, Niu Y. Androgen receptor enhances entosis, a non-apoptotic cell death, through modulation of Rho/ROCK pathway in prostate cancer cells. Prostate. 2013;73(12):1306-15.
188. Durgan J, Tseng YY, Hamann JC, Domart MC, Collinson L, Hall A, et al. Mitosis can drive cell cannibalism through entosis. eLife. 2017;6.
189. Krishna S, Overholtzer M. Mechanisms and consequences of entosis. Cellular and molecular life sciences : CMLS. 2016;73(11-12):2379-86.
190. Philp D, Pezzano M, Li Y, Omene C, Boto W, Guyden J. The binding, internalization, and release of thymocytes by thymic nurse cells. Cellular immunology. 1993;148(2):301-15.
191. Webb O, Kelly F, Benitez J, Li J, Parker M, Martinez M, et al. The identification of thymic nurse cells in vivo and the role of cytoskeletal proteins in thymocyte internalization. Cellular immunology. 2004;228(2):119-29.
192. Li Y, Sun X, Dey SK. Entosis allows timely elimination of the luminal epithelial barrier for embryo implantation. Cell Rep. 2015;11(3):358-65.
193. Garanina AS, Khashba LA, Onishchenko GE. Stages of Cell Cannibalism--Entosis--in Normal Human Keratinocyte Culture. Biochemistry Biokhimiia. 2015;80(11):1469-77.

194. Sottile F, Aulicino F, Theka I, Cosma MP. Mesenchymal stem cells generate distinct functional hybrids in vitro via cell fusion or entosis. Scientific reports. 2016;6:36863.
195. Ahmed N, Yang P, Huang Y, Chen H, Liu T, Wang L, et al. Entosis Acts as a Novel Way within Sertoli Cells to Eliminate Spermatozoa in Seminiferous Tubule. Frontiers in physiology. 2017;8:361.
196. Larsen TE. Emperipolesis of granular leukocytes within megakaryocytes in human hemopoietic bone marrow. American journal of clinical pathology. 1970;53(4):485-9.
197. Centurione L, Di Baldassarre A, Zingariello M, Bosco D, Gatta V, Rana RA, et al. Increased and pathologic emperipolesis of neutrophils within megakaryocytes associated with marrow fibrosis in GATA-1(low) mice. Blood. 2004;104(12):3573-80.
198. Bobik R, Dabrowski Z. Emperipolesis of marrow cells within megakaryocytes in the bone marrow of sublethally irradiated mice. Annals of hematology. 1995;70(2):91-5.
199. Tavassoli M. Modulation of megakaryocyte emperipolesis by phlebotomy: megakaryocytes as a component of marrow-blood barrier. Blood cells. 1986;12(1):205-16.
200. Sierro F, Tay SS, Warren A, Le Couteur DG, McCaughan GW, Bowen DG, et al. Suicidal emperipolesis: a process leading to cell-in-cell structures, T cell clearance and immune homeostasis. Current molecular medicine. 2015;15(9):819-27.
201. Sharma N, Dey P. Cell cannibalism and cancer. Diagnostic cytopathology. 2011;39(3):229-33.
202. Kroemer G, Perfettini JL. Entosis, a key player in cancer cell competition. Cell research. 2014;24(11):1280-1.
203. Sun Q, Luo T, Ren Y, Florey O, Shirasawa S, Sasazuki T, et al. Competition between human cells by entosis. Cell research. 2014;24(11):1299-310.
204. Krajcovic M, Overholtzer M. Mechanisms of ploidy increase in human cancers: a new role for cell cannibalism. Cancer Res. 2012;72(7):1596-601.
205. Duncan AW. Aneuploidy, polyploidy and ploidy reversal in the liver. Seminars in cell & developmental biology. 2013;24(4):347-56.
206. Green DR, Levine B. To be or not to be? How selective autophagy and cell death govern cell fate. Cell. 2014;157(1):65-75.
207. Krajcovic M, Krishna S, Akkari L, Joyce JA, Overholtzer M. mTOR regulates phagosome and entotic vacuole fission. Mol Biol Cell. 2013;24(23):3736-45.
208. Florey O, Gammoh N, Kim SE, Jiang X, Overholtzer M. V-ATPase and osmotic imbalances activate endolysosomal LC3 lipidation. Autophagy. 2015;11(1):88-99.
209. Qu X, Zou Z, Sun Q, Luby-Phelps K, Cheng P, Hogan RN, et al. Autophagy gene-dependent clearance of apoptotic cells during embryonic development. Cell. 2007;128(5):931-46.
210. Heckmann BL, Boada-Romero E, Cunha LD, Magne J, Green DR. LC3-Associated Phagocytosis and Inflammation. Journal of molecular biology. 2017;429(23):3561-76.
211. Abe Y, Hines IN, Zibari G, Pavlick K, Gray L, Kitagawa Y, et al. Mouse model of liver ischemia and reperfusion injury: method for studying reactive oxygen and nitrogen metabolites in vivo. Free radical biology & medicine. 2009;46(1):1-7.
212. Dixon LJ, Barnes M, Tang H, Pritchard MT, Nagy LE. Kupffer cells in the liver. Compr Physiol. 2013;3(2):785-97.
213. Alper CA, Johnson AM, Birtch AG, Moore FD. Human C'3: evidence for the liver as the primary site of synthesis. Science (New York, NY). 1969;163(3864):286-8.
214. Xu W, Roos A, Schlagwein N, Woltman AM, Daha MR, van Kooten C. IL-10-producing macrophages preferentially clear early apoptotic cells. Blood. 2006;107(12):4930-7.
215. Korns D, Frasch SC, Fernandez-Boyanapalli R, Henson PM, Bratton DL. Modulation of macrophage efferocytosis in inflammation. Frontiers in immunology. 2011;2:57.

216. Szondy Z, Sarang Z, Kiss B, Garabuczi E, Koroskenyi K. Anti-inflammatory Mechanisms Triggered by Apoptotic Cells during Their Clearance. Frontiers in immunology. 2017;8:909.
217. Dalton SR, Wiegert RL, Baldwin CR, Kassel KM, Casey CA. Impaired receptor-mediated endocytosis by the asialoglycoprotein receptor in ethanol-fed mice: implications for studying the role of this receptor in alcoholic apoptosis. Biochemical pharmacology. 2003;65(4):535-43.
218. Canton J, Neculai D, Grinstein S. Scavenger receptors in homeostasis and immunity. Nature reviews Immunology. 2013;13(9):621-34.
219. Ishii J, Adachi H, Aoki J, Koizumi H, Tomita S, Suzuki T, et al. SREC-II, a new member of the scavenger receptor type F family, trans-interacts with SREC-I through its extracellular domain. J Biol Chem. 2002;277(42):39696-702.
220. Anastasio N, Ben-Omran T, Teebi A, Ha KC, Lalonde E, Ali R, et al. Mutations in SCARF2 are responsible for Van Den Ende-Gupta syndrome. American journal of human genetics. 2010;87(4):553-9.
221. Migliavacca MP, Sobreira NL, Antonialli GP, Oliveira MM, Melaragno MI, Casteels I, et al. Sclerocornea in a patient with van den Ende-Gupta syndrome homozygous for a SCARF2 microdeletion. American journal of medical genetics Part A. 2014;164a(5):1170-4.
222. Janko C, Munoz L, Chaurio R, Maueroder C, Berens C, Lauber K, et al. Navigation to the graveyard-induction of various pathways of necrosis and their classification by flow cytometry. Methods Mol Biol. 2013;1004:3-15.
223. Song AS, Najjar AM, Diller KR. Thermally induced apoptosis, necrosis, and heat shock protein expression in 3D culture. Journal of biomechanical engineering. 2014;136(7).
224. Roberts KM, Rosen A, Casciola-Rosen LA. Methods for inducing apoptosis. Methods in molecular medicine. 2004;102:115-28.
225. Ruegg UT, Burgess GM. Staurosporine, K-252 and UCN-01: potent but nonspecific inhibitors of protein kinases. Trends Pharmacol Sci. 1989;10(6):218-20.
226. Feng G, Kaplowitz N. Mechanism of staurosporine-induced apoptosis in murine hepatocytes. American journal of physiology Gastrointestinal and liver physiology. 2002;282(5):G825-34.
227. Nakabayashi H, Taketa K, Miyano K, Yamane T, Sato J. Growth of human hepatoma cells lines with differentiated functions in chemically defined medium. Cancer Res. 1982;42(9):3858-63.
228. Aden DP, Fogel A, Plotkin S, Damjanov I, Knowles BB. Controlled synthesis of HBsAg in a differentiated human liver carcinoma-derived cell line. Nature. 1979;282(5739):615-6.
229. Knowles BB, Howe CC, Aden DP. Human hepatocellular carcinoma cell lines secrete the major plasma proteins and hepatitis B surface antigen. Science (New York, NY). 1980;209(4455):497-9.
230. Qiu G-H, Xie X, Xu F, Shi X, Wang Y, Deng L. Distinctive pharmacological differences between liver cancer cell lines HepG2 and Hep3B. Cytotechnology. 2015;67(1):1-12.
231. Kusaba M, Nakao K, Goto T, Nishimura D, Kawashimo H, Shibata H, et al. Abrogation of constitutive STAT3 activity sensitizes human hepatoma cells to TRAIL-mediated apoptosis. Journal of hepatology. 2007;47(4):546-55.
232. Liu P, Menon K, Alvarez E, Lu K, Teicher BA. Transforming growth factor-beta and response to anticancer therapies in human liver and gastric tumors in vitro and in vivo. International journal of oncology. 2000;16(3):599-610.
233. Elliott MR, Ravichandran KS. The Dynamics of Apoptotic Cell Clearance. Developmental cell. 2016;38(2):147-60.
234. Mercer J, Helenius A. Virus entry by macropinocytosis. Nat Cell Biol. 2009;11(5):510-20.

235. Mercer J, Schelhaas M, Helenius A. Virus entry by endocytosis. Annual review of biochemistry. 2010;79:803-33.
236. Mercer J, Knebel S, Schmidt FI, Crouse J, Burkard C, Helenius A. Vaccinia virus strains use distinct forms of macropinocytosis for host-cell entry. Proceedings of the National Academy of Sciences of the United States of America. 2010;107(20):9346-51.
237. Shu S, Liu X, Korn ED. Blebbistatin and blebbistatin-inactivated myosin II inhibit myosin II-independent processes in Dictyostelium. Proceedings of the National Academy of Sciences of the United States of America. 2005;102(5):1472-7.
238. West MA, Bretscher MS, Watts C. Distinct endocytotic pathways in epidermal growth factor-stimulated human carcinoma A431 cells. J Cell Biol. 1989;109(6 Pt 1):2731-9.
239. Koivusalo M, Welch C, Hayashi H, Scott CC, Kim M, Alexander T, et al. Amiloride inhibits macropinocytosis by lowering submembranous pH and preventing Rac1 and Cdc42 signaling. The Journal of Cell Biology. 2010;188:547-63.
240. Aderem A, Underhill DM. Mechanisms of phagocytosis in macrophages. Annual review of immunology. 1999;17:593-623.
241. Vieira OV, Botelho RJ, Rameh L, Brachmann SM, Matsuo T, Davidson HW, et al. Distinct roles of class I and class III phosphatidylinositol 3-kinases in phagosome formation and maturation. The Journal of Cell Biology. 2001;155(1):19-26.
242. May JA, Ratan H, Glenn JR, Losche W, Spangenberg P, Heptinstall S. GPIIb-IIIa antagonists cause rapid disaggregation of platelets pre-treated with cytochalasin D. Evidence that the stability of platelet aggregates depends on normal cytoskeletal assembly. Platelets. 1998;9(3-4):227-32.
243. Flannagan RS, Jaumouille V, Grinstein S. The cell biology of phagocytosis. Annual review of pathology. 2012;7:61-98.
244. Tuncer C, Oo YH, Murphy N, Adams DH, Lalor PF. The regulation of T-cell recruitment to the human liver during acute liver failure. Liver Int. 2013;33(6):852-63.
245. Hubscher SG, Adams DH. ICAM-1 expression in normal liver. Journal of clinical pathology. 1991;44(5):438-9.
246. Edmondson R, Broglie JJ, Adcock AF, Yang L. Three-Dimensional Cell Culture Systems and Their Applications in Drug Discovery and Cell-Based Biosensors. Assay and Drug Development Technologies. 2014;12(4):207-18.
247. Schyschka L, Sanchez JJ, Wang Z, Burkhardt B, Muller-Vieira U, Zeilinger K, et al. Hepatic 3D cultures but not 2D cultures preserve specific transporter activity for acetaminophen-induced hepatotoxicity. Archives of toxicology. 2013;87(8):1581-93.
248. Sainz B, TenCate V, Uprichard SL. Three-dimensional Huh7 cell culture system for the study of Hepatitis C virus infection. Virology Journal. 2009;6:103-.
249. Saito Y, Nishio K, Ogawa Y, Kimata J, Kinumi T, Yoshida Y, et al. Turning point in apoptosis/necrosis induced by hydrogen peroxide. Free radical research. 2006;40(6):619-30.
250. Fujimoto LM, Roth R, Heuser JE, Schmid SL. Actin assembly plays a variable, but not obligatory role in receptor-mediated endocytosis in mammalian cells. Traffic (Copenhagen, Denmark). 2000;1(2):161-71.
251. Millan J, Hewlett L, Glyn M, Toomre D, Clark P, Ridley AJ. Lymphocyte transcellular migration occurs through recruitment of endothelial ICAM-1 to caveola- and F-actin-rich domains. Nat Cell Biol. 2006;8(2):113-23.
252. Yang M, Liu J, Piao C, Shao J, Du J. ICAM-1 suppresses tumor metastasis by inhibiting macrophage M2 polarization through blockade of efferocytosis. Cell Death Dis. 2015;6:e1780.
253. Roy J, Audette M, Tremblay MJ. Intercellular adhesion molecule-1 (ICAM-1) gene expression in human T cells is regulated by phosphotyrosyl phosphatase activity.

Involvement of NF-kappaB, Ets, and palindromic interferon-gamma-responsive element-binding sites. J Biol Chem. 2001;276(18):14553-61.
254. Lemke G, Burstyn-Cohen T. TAM receptors and the clearance of apoptotic cells. Annals of the New York Academy of Sciences. 2010;1209:23-9.
255. Tong L, Tergaonkar V. Rho protein GTPases and their interactions with NFκB: crossroads of inflammation and matrix biology. Bioscience Reports. 2014;34(3):e00115.
256. Murphy JE, Tacon D, Tedbury PR, Hadden JM, Knowling S, Sawamura T, et al. LOX-1 scavenger receptor mediates calcium-dependent recognition of phosphatidylserine and apoptotic cells. The Biochemical journal. 2006;393(Pt 1):107-15.
257. Albert ML, Kim JI, Birge RB. alphavbeta5 integrin recruits the CrkII-Dock180-rac1 complex for phagocytosis of apoptotic cells. Nat Cell Biol. 2000;2(12):899-905.
258. Callahan MK, Halleck MS, Krahling S, Henderson AJ, Williamson P, Schlegel RA. Phosphatidylserine expression and phagocytosis of apoptotic thymocytes during differentiation of monocytic cells. J Leukoc Biol. 2003;74(5):846-56.
259. Borisenko GG, Matsura T, Liu SX, Tyurin VA, Jianfei J, Serinkan FB, et al. Macrophage recognition of externalized phosphatidylserine and phagocytosis of apoptotic Jurkat cells--existence of a threshold. Archives of biochemistry and biophysics. 2003;413(1):41-52.
260. Oka K, Sawamura T, Kikuta K, Itokawa S, Kume N, Kita T, et al. Lectin-like oxidized low-density lipoprotein receptor 1 mediates phagocytosis of aged/apoptotic cells in endothelial cells. Proceedings of the National Academy of Sciences of the United States of America. 1998;95(16):9535-40.
261. Ichimura T, Asseldonk EJ, Humphreys BD, Gunaratnam L, Duffield JS, Bonventre JV. Kidney injury molecule-1 is a phosphatidylserine receptor that confers a phagocytic phenotype on epithelial cells. The Journal of clinical investigation. 2008;118(5):1657-68.
262. Brempelis KJ, Crispe IN. Infiltrating monocytes in liver injury and repair. Clinical & translational immunology. 2016;5(11):e113.
263. Sexton DW, Al-Rabia M, Blaylock MG, Walsh GM. Phagocytosis of apoptotic eosinophils but not neutrophils by bronchial epithelial cells. Clinical and experimental allergy : journal of the British Society for Allergy and Clinical Immunology. 2004;34(10):1514-24.
264. Florey O, Krajcovic M, Sun Q, Overholtzer M. Entosis. Curr Biol. 2010;20(3):R88-9.
265. Fujiwara T, Bandi M, Nitta M, Ivanova EV, Bronson RT, Pellman D. Cytokinesis failure generating tetraploids promotes tumorigenesis in p53-null cells. Nature. 2005;437(7061):1043-7.
266. Pinto AE, Andre S, Soares J. Short-term significance of DNA ploidy and cell proliferation in breast carcinoma: a multivariate analysis of prognostic markers in a series of 308 patients. Journal of clinical pathology. 1999;52(8):604-11.
267. Sun HS, Wilde A, Harrison RE. Chlamydia trachomatis inclusions induce asymmetric cleavage furrow formation and ingression failure in host cells. Mol Cell Biol. 2011;31(24):5011-22.
268. Schroeder F, Kinden DA. Measurement of phagocytosis using fluorescent latex beads. Journal of biochemical and biophysical methods. 1983;8(1):15-27.
269. Danes BS, De Angelis P, Traganos F, Melamed MR. Tetraploidy in cultured dermal fibroblasts from patients with heritable colon cancer. Dis Markers. 1988;6(3):151-61.
270. Olaharski AJ, Sotelo R, Solorza-Luna G, Gonsebatt ME, Guzman P, Mohar A, et al. Tetraploidy and chromosomal instability are early events during cervical carcinogenesis. Carcinogenesis. 2006;27(2):337-43.
271. Ganem NJ, Storchova Z, Pellman D. Tetraploidy, aneuploidy and cancer. Current opinion in genetics & development. 2007;17(2):157-62.

272. Lv L, Zhang T, Yi Q, Huang Y, Wang Z, Hou H, et al. Tetraploid cells from cytokinesis failure induce aneuploidy and spontaneous transformation of mouse ovarian surface epithelial cells. Cell Cycle. 2012;11(15):2864-75.
273. Rochlin K, Yu S, Roy S, Baylies MK. Myoblast fusion: when it takes more to make one. Dev Biol. 2010;341(1):66-83.
274. Vignery A. Macrophage fusion: molecular mechanisms. Methods Mol Biol. 2008;475:149-61.
275. Duncan AW, Taylor MH, Hickey RD, Hanlon Newell AE, Lenzi ML, Olson SB, et al. The ploidy conveyor of mature hepatocytes as a source of genetic variation. Nature. 2010;467(7316):707-10.
276. Hsu SH, Delgado ER, Otero PA, Teng KY, Kutay H, Meehan KM, et al. MicroRNA-122 regulates polyploidization in the murine liver. Hepatology (Baltimore, Md). 2016;64(2):599-615.
277. Gentric G, Maillet V, Paradis V, Couton D, L'Hermitte A, Panasyuk G, et al. Oxidative stress promotes pathologic polyploidization in nonalcoholic fatty liver disease. The Journal of clinical investigation. 2015;125(3):981-92.
278. McGill MR, Sharpe MR, Williams CD, Taha M, Curry SC, Jaeschke H. The mechanism underlying acetaminophen-induced hepatotoxicity in humans and mice involves mitochondrial damage and nuclear DNA fragmentation. The Journal of clinical investigation. 2012;122(4):1574-83.
279. Weinberg MS, Nicolson S, Bhatt AP, McLendon M, Li C, Samulski RJ. Recombinant adeno-associated virus utilizes cell-specific infectious entry mechanisms. Journal of virology. 2014;88(21):12472-84.
280. Salaspuro M. Use of Enzymes for the Diagnosis of Alcohol-Related Organ Damage. Enzyme. 1987;37:87-107.
281. Laing RW, Bhogal RH, Wallace L, Boteon Y, Neil DAH, Smith A, et al. The Use of an Acellular Oxygen Carrier in a Human Liver Model of Normothermic Machine Perfusion. Transplantation. 2017;101(11):2746-56.
282. Laing RW, Mergental H, Yap C, Kirkham A, Whilku M, Barton D, et al. Viability testing and transplantation of marginal livers (VITTAL) using normothermic machine perfusion: study protocol for an open-label, non-randomised, prospective, single-arm trial. BMJ open. 2017;7(11):e017733.
283. Duncan AW, Dorrell C, Grompe M. Stem cells and liver regeneration. Gastroenterology. 2009;137(2):466-81.
284. Duncan AW, Hickey RD, Paulk NK, Culberson AJ, Olson SB, Finegold MJ, et al. Ploidy reductions in murine fusion-derived hepatocytes. PLoS genetics. 2009;5(2):e1000385.
285. Scholzen T, Gerdes J. The Ki-67 protein: from the known and the unknown. Journal of cellular physiology. 2000;182(3):311-22.
286. Sherr CJ. Mammalian G1 cyclins. Cell. 1993;73(6):1059-65.
287. Herbig U, Jobling WA, Chen BP, Chen DJ, Sedivy JM. Telomere shortening triggers senescence of human cells through a pathway involving ATM, p53, and p21(CIP1), but not p16(INK4a). Mol Cell. 2004;14(4):501-13.
288. Khang SK, Lee SS, Cho KJ, Ha HJ. Cytologic Features of Well Differentiated Hepatocellular Carcinoma. J Pathol Transl Med. 1997;8(1):1-10.
289. Mukherjee A, Misra S, Howlett NG, Karmakar P. Multinucleation regulated by the Akt/PTEN signaling pathway is a survival strategy for HepG2 cells. Mutation research. 2013;755(2):135-40.

290. Saha SK, Parachoniak CA, Ghanta KS, Fitamant J, Ross KN, Najem MS, et al. Mutant IDH inhibits HNF-4alpha to block hepatocyte differentiation and promote biliary cancer. Nature. 2014;513(7516):110-4.
291. de Boer YS, van Nieuwkerk CM, Witte BI, Mulder CJ, Bouma G, Bloemena E. Assessment of the histopathological key features in autoimmune hepatitis. Histopathology. 2015;66(3):351-62.
292. Herzog D, Soglio DB, Fournet JC, Martin S, Marleau D, Alvarez F. Interface hepatitis is associated with a high incidence of late graft fibrosis in a group of tightly monitored pediatric orthotopic liver transplantation patients. Liver transplantation : official publication of the American Association for the Study of Liver Diseases and the International Liver Transplantation Society. 2008;14(7):946-55.
293. Vergani D, Mackay IR, Mieli-Vergani G. Chapter 61 - Hepatitis. The Autoimmune Diseases (Fifth Edition). Boston: Academic Press; 2014. p. 889-907.
294. Mercapide J, Anzanello F, Rappa G, Lorico A. Relationship between tumor cell invasiveness and polyploidization. PloS one. 2012;7(12):e53364.
295. Yu Y, Ping J, Chen H, Jiao L, Zheng S, Han Z-G, et al. A comparative analysis of liver transcriptome suggests divergent liver function among human, mouse and rat. Genomics. 2010;96(5):281-9.
296. Mestas J, Hughes CC. Of mice and not men: differences between mouse and human immunology. Journal of immunology (Baltimore, Md : 1950). 2004;172(5):2731-8.
297. Gentric G, Desdouets C. Polyploidization in liver tissue. The American journal of pathology. 2014;184(2):322-31.
298. Duncan AW, Hanlon Newell AE, Bi W, Finegold MJ, Olson SB, Beaudet AL, et al. Aneuploidy as a mechanism for stress-induced liver adaptation. The Journal of clinical investigation. 2012;122(9):3307-15.
299. Zhang S, Zhou K, Luo X, Li L, Tu HC, Sehgal A, et al. The Polyploid State Plays a Tumor-Suppressive Role in the Liver. Developmental cell. 2018;44(4):447-59.e5.
300. Kim SH, Jeon Y, Kim HS, Lee JK, Lim HJ, Kang D, et al. Hepatocyte homeostasis for chromosome ploidization and liver function is regulated by Ssu72 protein phosphatase. Hepatology (Baltimore, Md). 2016;63(1):247-59.
301. Celton-Morizur S, Desdouets C. Liver physiological polyploidization: MicroRNA-122 a key regulator. Clinics and research in hepatology and gastroenterology. 2017;41(2):123-5.
302. Horiguchi N, Ishac EJN, Gao B. Liver regeneration is suppressed in alcoholic cirrhosis: Correlation with decreased STAT3 activation. Alcohol (Fayetteville, NY). 2007;41(4):271-80.
303. Maiwal R, Kumar A, Sarin SK. Liver Regeneration During Acute-on-Chronic Liver Failure Using Growth Factors: In Vivo or Ex Vivo Indulgence of Bone Marrow? Gastroenterology. 2013;145(4):901-4.
304. Tsochatzis EA, Bosch J, Burroughs AK. Liver cirrhosis. The Lancet. 2014;383(9930):1749-61.
305. Chen C, Lou T. Hypoxia inducible factors in hepatocellular carcinoma. Oncotarget. 2017;8(28):46691-703.
306. McKeown SR. Defining normoxia, physoxia and hypoxia in tumours-implications for treatment response. The British journal of radiology. 2014;87(1035):20130676.
307. Koivusalo M, Welch C, Hayashi H, Scott CC, Kim M, Alexander T, et al. Amiloride inhibits macropinocytosis by lowering submembranous pH and preventing Rac1 and Cdc42 signaling. J Cell Biol. 2010;188(4):547-63.
308. Shetty S, Weston CJ, Adams DH, Lalor PF. A flow adhesion assay to study leucocyte recruitment to human hepatic sinusoidal endothelium under conditions of shear stress. J Vis Exp. 2014(85).

309. Canton I, Battaglia G. Endocytosis at the nanoscale. Chemical Society reviews. 2012;41(7):2718-39.
310. Patel PC, Harrison RE. Membrane ruffles capture C3bi-opsonized particles in activated macrophages. Mol Biol Cell. 2008;19(11):4628-39.
311. Martins I, Raza SQ, Voisin L, Dakhli H, Law F, De Jong D, et al. Entosis: The emerging face of non-cell-autonomous type IV programmed death. Biomedical journal. 2017;40(3):133-40.
312. Maekawa M, Ishizaki T, Boku S, Watanabe N, Fujita A, Iwamatsu A, et al. Signaling from Rho to the actin cytoskeleton through protein kinases ROCK and LIM-kinase. Science (New York, NY). 1999;285(5429):895-8.
313. Zhang Z, Ottens AK, Larner SF, Kobeissy FH, Williams ML, Hayes RL, et al. Direct Rho-associated kinase inhibition [correction of inhibiton] induces cofilin dephosphorylation and neurite outgrowth in PC-12 cells. Cellular & molecular biology letters. 2006;11(1):12-29.
314. Garanina AS, Kisurina-Evgenieva OP, Erokhina MV, Smirnova EA, Factor VM, Onishchenko GE. Consecutive entosis stages in human substrate-dependent cultured cells. Scientific reports. 2017;7(1):12555.
315. Golubovskaya V, Wu L. Different Subsets of T Cells, Memory, Effector Functions, and CAR-T Immunotherapy. Cancers. 2016;8(3):36.
316. Rhainds D, Brissette L. The role of scavenger receptor class B type I (SR-BI) in lipid trafficking: Defining the rules for lipid traders. The International Journal of Biochemistry & Cell Biology. 2004;36(1):39-77.
317. Acton S, Rigotti A, Landschulz KT, Xu S, Hobbs HH, Krieger M. Identification of scavenger receptor SR-BI as a high density lipoprotein receptor. Science (New York, NY). 1996;271(5248):518-20.
318. Koonen DP, Jacobs RL, Febbraio M, Young ME, Soltys CL, Ong H, et al. Increased hepatic CD36 expression contributes to dyslipidemia associated with diet-induced obesity. Diabetes. 2007;56(12):2863-71.
319. Surls J, Nazarov-Stoica C, Kehl M, Olsen C, Casares S, Brumeanu T-D. Increased Membrane Cholesterol in Lymphocytes Diverts T-Cells toward an Inflammatory Response. PloS one. 2012;7(6):e38733.
320. Chyu KY, Lio WM, Dimayuga PC, Zhou J, Zhao X, Yano J, et al. Cholesterol lowering modulates T cell function in vivo and in vitro. PloS one. 2014;9(3):e92095.
321. Ruan B, Zhang B, Chen A, Yuan L, Liang J, Wang M, et al. Cholesterol inhibits entotic cell-in-cell formation and actomyosin contraction. Biochemical and biophysical research communications. 2018;495(1):1440-6.
322. Bartosch B, Vitelli A, Granier C, Goujon C, Dubuisson J, Pascale S, et al. Cell entry of hepatitis C virus requires a set of co-receptors that include the CD81 tetraspanin and the SR-B1 scavenger receptor. J Biol Chem. 2003;278(43):41624-30.
323. Ke P-Y, Chen SSL. Active RNA Replication of Hepatitis C Virus Downregulates CD81 Expression. PloS one. 2013;8(1):e54866.
324. Ward ST, Li KK, Hepburn E, Weston CJ, Curbishley SM, Reynolds GM, et al. The effects of CCR5 inhibition on regulatory T-cell recruitment to colorectal cancer. British journal of cancer. 2015;112(2):319-28.
325. Danke NA, Koelle DM, Yee C, Beheray S, Kwok WW. Autoreactive T cells in healthy individuals. Journal of immunology (Baltimore, Md : 1950). 2004;172(10):5967-72.
326. Ha T-Y. The Role of Regulatory T Cells in Cancer. Immune Network. 2009;9(6):209-35.
327. Ding Y, Shen S, Lino AC, Curotto de Lafaille MA, Lafaille JJ. Beta-catenin stabilization extends regulatory T cell survival and induces anergy in nonregulatory T cells. Nature medicine. 2008;14(2):162-9.

328. Angsana J, Chen J, Liu L, Haller CA, Chaikof EL. Efferocytosis as a regulator of macrophage chemokine receptor expression and polarization. European journal of immunology. 2016;46(7):1592-9.
329. Majno G, Joris I. Apoptosis, oncosis, and necrosis. An overview of cell death. The American journal of pathology. 1995;146(1):3-15.
330. Sun HS, Eng EW, Jeganathan S, Sin AT, Patel PC, Gracey E, et al. Chlamydia trachomatis vacuole maturation in infected macrophages. J Leukoc Biol. 2012;92(4):815-27.
331. Sun Q, Huang H, Overholtzer M. Cell-in-cell structures are involved in the competition between cells in human tumors. Molecular & cellular oncology. 2015;2(4):e1002707.
332. Mashek DG, Khan SA, Sathyanarayan A, Ploeger JM, Franklin MP. Hepatic lipid droplet biology: Getting to the root of fatty liver. Hepatology (Baltimore, Md). 2015;62(3):964-7.
333. Ellson CD, Anderson KE, Morgan G, Chilvers ER, Lipp P, Stephens LR, et al. Phosphatidylinositol 3-phosphate is generated in phagosomal membranes. Current Biology. 2001;11(20):1631-5.
334. Srivastava S, Li Z, Lin L, Liu G, Ko K, Coetzee WA, et al. The phosphatidylinositol 3-phosphate phosphatase myotubularin- related protein 6 (MTMR6) is a negative regulator of the Ca2+-activated K+ channel KCa3.1. Mol Cell Biol. 2005;25(9):3630-8.
335. Ghanshani S, Wulff H, Miller MJ, Rohm H, Neben A, Gutman GA, et al. Up-regulation of the IKCa1 potassium channel during T-cell activation. Molecular mechanism and functional consequences. J Biol Chem. 2000;275(47):37137-49.
336. Singh R, Kaushik S, Wang Y, Xiang Y, Novak I, Komatsu M, et al. Autophagy regulates lipid metabolism. Nature. 2009;458(7242):1131-5.
337. Sarantis H, Grinstein S. Subversion of Phagocytosis for Pathogen Survival. Cell host & microbe. 2012;12(4):419-31.
338. Wei J, Long L, Yang K, Guy C, Shrestha S, Chen Z, et al. Autophagy enforces functional integrity of regulatory T cells by coupling environmental cues and metabolic homeostasis. Nature immunology. 2016;17(3):277-85.
339. Le Texier L, Lineburg KE, Cao B, McDonald-Hyman C, Leveque-El Mouttie L, Nicholls J, et al. Autophagy-dependent regulatory T cells are critical for the control of graft-versus-host disease. JCI Insight. 2016;1(15):e86850.
340. Valenta T, Hausmann G, Basler K. The many faces and functions of beta-catenin. Embo j. 2012;31(12):2714-36.
341. Duncan AW, Hanlon Newell AE, Smith L, Wilson EM, Olson SB, Thayer MJ, et al. Frequent aneuploidy among normal human hepatocytes. Gastroenterology. 2012;142(1):25-8.
342. Forner A, Llovet JM, Bruix J. Hepatocellular carcinoma. The Lancet. 2012;379(9822):1245-55.
343. Spiliopoulou P, Millar J, Bamford C, Bisset L, Evans J. P-243Undiagnosed chronic liver disease (CLD) in patients presenting with Hepatocellular Carcinoma (HCC). Annals of Oncology. 2016;27(Suppl 2):ii70-ii.
344. Aravalli RN, Steer CJ, Cressman ENK. Molecular mechanisms of hepatocellular carcinoma. Hepatology (Baltimore, Md). 2008;48(6):2047-63.
345. Wermeling F, Chen Y, Pikkarainen T, Scheynius A, Winqvist O, Izui S, et al. Class A scavenger receptors regulate tolerance against apoptotic cells, and autoantibodies against these receptors are predictive of systemic lupus. The Journal of experimental medicine. 2007;204(10):2259-65.

346. Karikoski M, Marttila-Ichihara F, Elima K, Rantakari P, Hollmen M, Kelkka T, et al. Clever-1/stabilin-1 controls cancer growth and metastasis. Clinical cancer research : an official journal of the American Association for Cancer Research. 2014;20(24):6452-64.
347. Park SY, Jung MY, Kim HJ, Lee SJ, Kim SY, Lee BH, et al. Rapid cell corpse clearance by stabilin-2, a membrane phosphatidylserine receptor. Cell death and differentiation. 2008;15(1):192-201.
348. Faubion WA, Gores GJ. Death receptors in liver biology and pathobiology. Hepatology (Baltimore, Md). 1999;29(1):1-4.